Glycomaterials: From Synthesis of Glycoconjugates to Potential Biomedical Applications

Sany Chea

Kumulative Dissertation

zur Erlangung des akademischen Grades
"doctor rerum naturalium"
(Dr. rer. nat.)
in der Wissenschaftsdisziplin "Polymerchemie"

eingereicht an der
Mathematisch-Naturwissenschaftlichen Fakultät
Institut für Chemie
der Universität Potsdam
und
Fraunhofer Institut für Angewandte Polymerforschung

Ort und Tag der Disputation: Potsdam, 14.12.2022

I certify that the content presented within this report is my own original work based on the research I performed using only the means and source materials as noted therein.
This thesis was not submitted to another examination board in this or other countries. There were no unsuccessful examination processes.

Sany Chea

1st Reviewer: Prof. Dr. Alexander Böker
2nd Reviewer: Prof. Dr. Andreas Taubert
3rd Reviewer: Prof. Dr. Rainer Haag

Published online on the
Publication Server of the University of Potsdam:
https://doi.org/10.25932/publishup-57424
https://nbn-resolving.org/urn:nbn:de:kobv:517-opus4-574240

Acknowledgements

This thesis would not have come about without the support of several people, whom I would like to thank herewith. First and foremost, I would like to thank Univ.- Prof. Dr. rer. nat. A. Böker, who gave me the opportunity as my doctoral supervisor and supported me from the beginning whenever I needed it. My thanks also go to Univ.- Prof. Dr. rer. nat. A. Taubert, who acted as my second supervisor and to Univ.- Prof. Dr. rer. nat. R. Haag for taking on the 3rd reviewer.

I would especially like to thank Dr. Ruben R. Rosencrantz, who taught me a lot, but above all supported me at all times. He always had an open ear for me when it came to professional and personal challenges and was able to support me by sharing his experiences.

I would like to say a big thank you to Kristin Schade, who accompanied me every day in the lab and relieved me of many (sometimes annoying) tasks.

Thanks to the other members of Department 4.1 for the lively exchange and the support with certain questions. In particular, I want to thank Dr. Sophia Rosencrantz for the nice conversations and the great coordination of a project, as well as Karina Wolf for the relaxed evenings.

I am grateful to Jo Sing Tang, with whom I was able to share my office for the entire time. I really enjoyed the active interaction on a professional, as well as on a personal level.

My thanks go to my former office colleagues Dr. Chris Gäbert and Dr. Magnus Schwieters, with whom I had a lot of laughs, but also a lot of tears. Initial collegial meetings for lunch turned into more intensive moments over time, which we spent as friends outside of work.

I would also like to thank Gregor Ziegler, Khac Toan Nguyen, Kimia Amir-Moazami, Marc Safferthal and Lucas Tepper, who faced me with new challenges as Master's students, Bachelor's students and HiWis and thus shaped my development.

The lab was a great place to work and I would like to thank my colleagues Dr. Stefan Reinicke, Dr. Martin Reifarth, Dr. Marcel Sperling, Falko Rottke, Dr. Marc Zimmermann, Thilo Fischer, Richard Grobe, Cihan Baydaroglu and Pınar Akarsu for the pleasant atmosphere in the lab.

I would also like to thank the other members of FB4: Dr. Maria Mathieu-Gädke, Dr. Uli Glebe, Dr. Xiaolin Dai-Glebe, Johannes Martin, Yannic Müllers, Dr. Dmitry Grigoriev, Marion Stage, Mareike Andro, Dr. Hannes Hinneburg and Ulrike Döring.

Of course, I would also like to thank all the other colleagues who have accompanied me on this journey.

Furthermore, I thank Angela Krtitschka, Dr. Ines Starke, Sylvia Fürstenberg and Sascha Prentzel from the University of Potsdam, as well as Dr. Erik Wischerhoff, Dr. Andreas Bohn, Minh Thu Tran and Dr. Melanie Bartel from Fraunhofer IAP for their support in carrying out the analytical methods NMR, GPC, MS and SEM.

I want to thank my family and friends for their encouragement, energy and happiness. Thanks to Felix Haase, without him I probably wouldn't have managed the whole thing.

Abbreviations

A	Adenine
ACVA/ABCVA	4,4-Azobis(4-cyanovaleric acid)
AFM	Atomic force microscopy
AIBN	Azobisisobutyronitrile
APMA	*N*-(3-Aminopropyl)methacrylamide
ASF	Asialofetuin
ATP	Adenosine triphosphate
ATRP	Atom transfer radical polymerization
BAIB	Bis(acetoxy)iodobenzene
BSA	Bovine serum albumin
BTH	2,6-Di-*tert*-butyl-4-methylphenol
C	Cytidine
Cal B	*Candida Antarctica Lipase B*
CDG	Congenital disorder of glycolysation
CDMT	2-Chloro-4,6-dimethoxy-1,3,5-triazine
ConA	Concavalin A
CPADB	4-Cyano-4-(phenylcarbonothioylthio)pentanoic acid
CRD	Carbohydrate recognition domain
CTA	Chain transfer agent
CuAAC	Copper-catalyzed azide-alkyne cycloaddition
d	Doublet
DCC	*N*,*N*'-Dicyclohexylcarbodiimide
DIPEA	*N*,*N*-Diisopropylethylamine
DLS	Dynamic light scattering
DMA	Dimethylacetamide
DMAP	4-Dimethylaminopyridine
DMC	2-Chloro-1,3-dimethylimidazolinium chloride

DMF	Dimethylformamide
DMPU	*N*,*N*′-Dimethylpropyleneurea
DMSO	Dimethyl sulfoxide
DNA	Deoxyribonucleic acid
DoE	Design of experiments
E. coli	*Escherichia coli*
ECL	*Erythrina cristagalli*
EDC	1-Ethyl-3-(3-dimethylaminopropyl)carbodiimide
ee	Enantiomeric excess
EGDMA	Ethylene glycol dimethacrylate
EHEC	Enterohemorrhagic *E. coli*
ELISA	Enzyme-linked immunosorbent assay
EtOH	Ethanol
FAD	Flavin adenine dinucleotide
FimH	Type 1 fimbriae
FRP	Free radical polymerization
Fuc	Fucose
FucMAm	Fucose-methacrylamide
G	Guanosine
Gal	Galactose
GalNAc	*N*-Acetylgalactosamine
Glc	Glucose
GlcA	Glucuronic acid
GlcNAc	*N*-Acetylglucosamine
GNA	*Galanthus nivalis* agglutinin
GSD	Global spectral deconvolution
GSII	*Griffonia simplicifolia II*
HATU	1-[Bis(dimethylamino)methylene]-1H-1,2,3-triazolo[4,5-b]pyridinium 3-oxide hexafluorophosphate

HOMO	Highest occupied molecular orbital
HPMA	*N*-(2-Hydroxypropyl)methacrylamide
HSV	*Herpes Simplex Virus*
IAV	*Influenza A viruses*
iC-COOH	2',3'-*O*-Isopropylidene-5'-carboxy cytidine
iG-COOH	2',3'-*O*-Isopropylidene-5'-carboxy guanosine
IgG	Immunoglobulin
Lac	Lactose
LacMAm	Lactose-methacrylamide
LCA	*Lens culinaris* agglutinin
LCST	Lower critical solution temperature
LG	Leaving group
LUMO	Lowest unoccupied molecular orbital
m	Multiplett
m/z	Mass-to-charge ratio
MBA	Methylenebis(acrylamide)
MCPyV	*Merkel Cell Polyomavirus*
Mel	Melibiose
MelMAm	Melibiose-methacrylamide
MeOH	Methanol
MLR	Multiple linear regression
MO	Molecule orbital
MW	Microwave
NAD	Nicotinamide adenine dinucleotide
NeuAc	*N*-Acetylneuraminic acid
NHS	*N*-Hydroxysuccinimide
NiPAm	*N*-Isopropylacrylamide
NMM	*N*-Methylmorpholine

NMP	Nitroxide-mediated polymerization
OVAT	One-variable-at-a-time
PA	*Pseudomonas aeruginosa*
PBS	Polybutylene succinate
PEG	Polyethylene glycol
PEO	Poly(ethylene oxide)
PHEMA	Poly(hydroxyethyl methacrylate)
pHPMA	Poly-*N*-(2-hydroxypropyl)methacrylamide
piCPMA	2',3'-*O*-Isopropylidene-5'-propylmethacrylamide cytidine
piGPMA	2',3'-*O*-Isopropylidene-5'-propylmethacrylamide guanosine
PLA	Polylactic acid
PNA	Peanut agglutinin
PNiPAm	Poly(*N*-isopropylacrylamide)
PSA	*Pisum sativum* agglutinin
PVME	Poly(vinyl methyl ether)
q	Quartett
quin	Quintett
RAFT	Reversible addition-fragmentation chain-transfer
RCA_{120}	*Ricinus communis* agglutinin
RDRP	Reversible-deactivation polymerization
RI	Refractive index
RNA	Ribonucleic acid
ROMP	Ring-opening metathesis polymerization
ROP	Ring-opening polymerization
rt	Room temperature
s	Singlet
SDS	Sodium dodecyl sulfate
SEM	Scanning electron microscopy

t	Triplett
T	Thymine
***t*-BuOH**	*tert*-Butanol
TEMPO	(2,2,6,6-Tetramethylpiperidin-1-yl)oxyl
TGA	Thermogravimetric analysis
THF	Tetrahydrofuran
UCST	Upper critical solution temperature
UEA I	*Ulex europaeus* agglutinin I
UV	Ultraviolet
UV-Vis	Ultraviolet-visible
Xyl	Xylose

Formular Signs

q	Charge
δ	Chemical shift
c	Concentration
K_D	Dissociation constant
$\overrightarrow{F_{el}}$	Electrical force
ΔE	Energy difference
D_h	Hydrodynamic diameter
$\overrightarrow{F_L}$	Lorentz force
B_0	Magnetic field
μ	Magnetic moment
M_w	Mass average molar mass
M_n	Number average molar mass
PDI	Polydispersity index
J	Spin-spin coupling
T	Temperature
t	Time
V	Volume

Publications, Posters and Talks

Publications

Optimization of the Microwave Assisted Glycosylamines Synthesis Based on a Statistical Design of Experiments Approach; Jo Sing Julia Tang, Kristin Schade, Lucas Tepper, Sany Chea, Gregor Ziegler and Ruben R. Rosencrantz; *Molecules* **2020**, *25*, 5121; DOI: 10.3390/molecules25215121

Functional Glyco-Nanogels for Multivalent Interaction with Lectins; Jo Sing Julia Tang, Sophia Rosencrantz, Lucas Tepper, Sany Chea, Stefanie Klöpzig, Anne Krüger-Genge, Joachim Storsberg and Ruben R. Rosencrantz; *Molecules* **2019**, *24*, 1865; DOI: 10.3390/molecules24101865

Protection group-free synthesis of α-mannopyranosyl methacrylamide; Sany Chea, Gregor Ziegler, Ruben R. Rosencrantz; In preparation

Microwave-assisted synthesis of 5'-*O*-methacryloylcytidine using the immobilized lipase Novozym 435; Sany Chea, Khac Toan Nguyen and Ruben R. Rosencrantz; *Molecules* **2022**, *27*, 4112; DOI: 10.3390/molecules27134112

Synthesis and self-assembly of cytidine- and guanosine-based copolymers; Sany Chea, Kristin Schade, Stefan Reinicke, Regina Bleul, and Ruben R. Rosencrantz; *Polym. Chem.* **2022**; **13**, 5058; DOI: 10.1039/d2py00615d; Front Cover accepted.

Patent

Thermoresponsives Polymersystem basierend auf Nucleobase-Interaktion; Raphael Thiermann, Regina Bleul, Ruben R. Rosencrantz, Sany Chea; DE10 2022 202 099.5

Conference poster

Development of novel glycopolymer coatings for adherent cell cultivation; Sany Chea, Sophia Rosencrantz, Lucas Tepper, Alena Palkowitz, Lena Thoring, Stefan Kubick, Ruben R. Rosencrantz; Polydays 2019, Berlin, September 11 – 13, 2019

Talks

Targeting the heat of cancer cells for therapy; Bionnale (Speed Lecture Award 2020), Berlin, October 6, 2020

Sugar for treatment against COVID-19; Women in Science, University of Potsdam, online, February 11, 2021

Table of Content

1 Abstract

The importance of carbohydrate structures is enormous due to their ubiquitousness in our lives. The development of so-called glycomaterials is the result of this tremendous significance. These are not exclusively used for research into fundamental biological processes, but also, among other things, as inhibitors of pathogens or as drug delivery systems. This work describes the development of glycomaterials involving the synthesis of glycoderivatives, -monomers and -polymers. Glycosylamines were synthesized as precursors in a single synthesis step under microwave irradiation to significantly shorten the usual reaction time. Derivatization at the anomeric position was carried out according to the methods developed by Kochetkov and Likhorshetov, which do not require the introduction of protecting groups. Aminated saccharide structures formed the basis for the synthesis of glycomonomers in β-configuration by methacrylation. In order to obtain α-Man-based monomers for interactions with certain α-Man-binding lectins, a monomer synthesis by Staudinger ligation was developed in this work, which also does not require protective groups. Modification of the primary hydroxyl group of a saccharide was accomplished by enzyme-catalyzed synthesis. Ribose-containing cytidine was transesterified using the lipase Novozym 435 and microwave irradiation. The resulting monomer synthesis was optimized by varying the reaction partners. To create an amide bond instead of an ester bond, protected cytidine was modified by oxidation followed by amide coupling to form the monomer. This synthetic route was also used to isolate the monomer from its counterpart guanosine. After obtaining the nucleoside-based monomers, they were block copolymerized using the RAFT method. Pre-synthesized pHPMA served as macroCTA to yield cytidine- or guanosine-containing block copolymer. These isolated block copolymers were then investigated for their self-assembly behavior using UV-Vis, DLS and SEM to serve as a potential thermoresponsive drug delivery system.

1 Kurzfassung

Die Bedeutung von Kohlenhydratstrukturen ist immens, da sie in unserem Leben allgegenwärtig sind. Die Entwicklung sogenannter Glykomaterialien ist das Ergebnis dieser großen Bedeutung. Diese werden nicht nur zur Erforschung grundlegender biologischer Prozesse eingesetzt, sondern unter anderem auch als Hemmstoffe für Krankheitserreger oder als Wirkstofftransportsysteme. Die vorliegende Arbeit beschreibt die Entwicklung von Glycomaterialien durch die Synthese von Glycoderivaten, -monomeren und -polymeren. Glycosylamine wurden als Vorstufen in einem einzigen Syntheseschritt unter Mikrowellenbestrahlung synthetisiert, um die übliche Reaktionszeit deutlich zu verkürzen. Die Derivatisierung an der anomeren Position wurde nach den von Kochetkov und Likhorshetov entwickelten Methoden durchgeführt, die keine Einführung von Schutzgruppen erfordern. Die aminierten Saccharidstrukturen bildeten die Grundlage für die Synthese von Glycomonomeren in β-Konfiguration durch Methacrylierung. Um α-Man-basierte Monomere für Interaktionen mit bestimmten α-Man-bindenden Lektinen zu erhalten, wurde in dieser Arbeit eine Monomersynthese durch Staudinger-Ligation entwickelt, die ebenfalls keine Schutzgruppen erfordert. Die Modifizierung der primären Hydroxylgruppe eines Saccharids wurde durch enzymkatalysierte Synthese erreicht. Ribosehaltiges Cytidin wurde mit Hilfe der Lipase Novozym 435 und Mikrowellenbestrahlung umgeestert. Die resultierende Monomersynthese wurde durch Variation der Reaktionspartner optimiert. Um eine Amidbindung anstelle einer Esterbindung zu erzeugen, wurde geschütztes Cytidin durch Oxidation und anschließende Amidkupplung modifiziert, um das Monomer zu bilden. Dieser Syntheseweg wurde auch zur Isolierung des Monomers aus seinem Gegenstück Guanosin verwendet. Nach der Gewinnung der nukleosidbasierten Monomere wurden diese mit Hilfe der RAFT-Methode blockcopolymerisiert. Vorsynthetisiertes pHPMA diente als MakroCTA, um Cytidin- oder Guanosin-haltige Blockcopolymere zu erhalten. Diese isolierten Blockcopolymere wurden dann mit UV-Vis, DLS und SEM auf ihr Selbstorganisationsverhalten untersucht, um als potenzielles thermoresponsives Drug-Delivery-System zu dienen.

2 Introduction

Sugar structures, also called glycans, are found everywhere. This makes them the most abundant organic molecules on Earth with crucial functions; be it glucose (Glc) as an energy supplier, sucrose in sweets or cellulose as cotton for textile processing.[1,2,3]

Today's zeitgeist focuses in particular on sustainability. Developments in recent years regarding synthetic waste have greatly increased the market for sustainably labeled biodegradable artificial products.[4] Bioplastics already present on the market include polylactic acid (PLA)- based plastics. PLA is sourced from renewable sugar-based raw materials. Due to their ubiquity, carbohydrates in biomasses also play a major role in the field of renewable energy.[5,6] Research results indicate that carbohydrates from renewable biomass may be a suitable high-density hydrogen carrier for clean energy storage. So far, sugar structures from biomasses have in fact been used as a renewable energy source themselves.[7,8] Biomasses contain high energy content and are not as limited compared to fossil resources. Liquid fuels are already being added to gasoline blends to reduce the consumption of restricted fossil fuels. This is possible via a production of ethanol as biofuel by catalysis of sugar molecules.[9,10] Furan derivatives, which are also derived from lignocellulose in biomass, have a higher energy density than ethanol and are being discussed as an alternative to bioethanol. By suitable catalysis, a clean fuel with low pollution emissions can therefore be obtained.[6,11] The utilization of sugar in the energy sector was inspired by nature. As glycogen in bacteria and animals or starch in plants, sugars are of great importance as biological fuel stores and biosynthetic starting materials.[12,13,14]

Pure Glc or breaking down starch into Glc from food is metabolized as an energy source.[15] As a nutrient, sugar is in nearly all foods, whether in natural or processed food. Besides the best-known table sugar sucrose, there is Glc or fructose, which is contained in honey, fruits and vegetables. The slight sweetness of milk is owed to the disaccharide lactose (Lac).[16,17] However, they are not only sources of energy and thus an indispensable part of our diet, but also contribute significantly to the formation of structure and protection, for example as cellulose in the cell walls of plants or as chitin in the exoskeleton of arthropods.[18,19] This stability-giving property was the basis for the development of protective encapsulation systems for drugs in the pharmaceutical industry.[20,21] For example, starch is often used as a vegan alternative to gelatin to contain active ingredients.[22,23] Sugar structures can not only serve as a protective capsule for the active compound, but can also be the drug itself. Heparin, for instance,

is prescribed as an anticoagulant drug for the prevention and treatment of thrombosis and occlusive diseases of the veins and arteries, while D-mannose (Man) is used as a competitive inhibitor to prevent and treat urinary tract infections caused by *Escherichia coli* (*E. coli*).[24,25]

The polysaccharide hyaluronic acid has gained popularity as a lip filler or wrinkle smoothing agent in cosmetic surgery. The glycoprotein collagen is also used as an anti-aging agent for direct injection or as an admixture in creams, as it is a constituent of our skin.[26] The main function of collagen is to provide structure and is located in white inelastic fibers of tendons, ligaments, cartilage and bones, among others.[27] Glycoproteins and glycolipids are, as the name suggests, glycan structures attached to the respective biomolecules. Without this glycosylation, proteins and lipids cannot function properly in some cases. For example, glycans, as part of the glycocalyx, densely coat every living cell with glycosylated proteins and lipids or the cell wall in plants, which are needed for any kind of interaction, be it with other cells, active substances or organisms.[28] Carbohydrates are bound to most cellular and secreted proteins, which can affect protein function. Glycolipids are mainly participating in the process of immune response and cell-cell interactions.[29,30] Thus, they are responsible for blood group classification by communicating the interaction of the cell with its environment. This division into blood groups is based on the determination of the oligosaccharide bound to a specific glycolipid on the surface of the red blood cells.[31] Along with desoxyribonucleic acid (DNA) /ribonucleic acid (RNA) and proteins, glycans therefore belong to one of the main classes of biopolymers that even contain carbohydrate structures or whose activity is based on glycans. Incorporated into our RNA and DNA as the monosaccharide ribose or related desoxyribose forming the backbone, they are involved in transmitting and storing genetic information. They are also commonly found as important structures of coenzymes such as adenosine triphosphate (ATP), nicotinamide adenine dinucleotide (NAD) or flavin adenine dinucleotide (FAD), which have vital roles in our metabolism pathways.[32,33] Even though sugar is a crucial key to life, it may be involved in diseases. The common disease diabetes mellitus, for example, describes a metabolic disorder of carbohydrates. Due to the lack of the polypeptide hormone insulin, the patient suffers from hyperglycemia, an increase in blood sugar level. Congenital disorder of glycosylation (CDG) is characterized by dysfunction of a wide variety of organs and is the result of defects or a deficiency of glycosylation to tissue proteins or lipids.[34,35]

It is thus evident that sugar structures are found in abundance and form the basis for our life in many ways.

3 State of the Art

3.1 Glycoscience

The science of carbohydrates is one of the oldest fields of research and has long been underrated. Emil Fischer's impressive findings on the stereochemistry of Glc were recognized with a Nobel Prize, thus laying the first building block for further research with and on sugars, focused on their role as energy storage and supplier.[36] In recent years, however, glycoscience has become one of the most valuable disciplines in the field of life science and material science due to its diversity mentioned above. The omnipresence of carbohydrates leads to applications from medical/ pharmaceutical matters as drugs or drug vehicle, for use in the energy sector as fuel to biofunctional materials like biocompatible implantable medical devices.[37,38,39,40,41]

Due to their high complexity, codes and symbols were assigned to monosaccharides for simplification. The term glycan refers to any sugar or assembly of sugars, whether in free form or attached to another molecule. Carbohydrate or saccharide is a more general term, which includes monosaccharides, oligosaccharides, polysaccharides and their derivatives. Covalently attached glycan units to a non-carbohydrate moiety like protein or lipid are described as glycoconjugates.

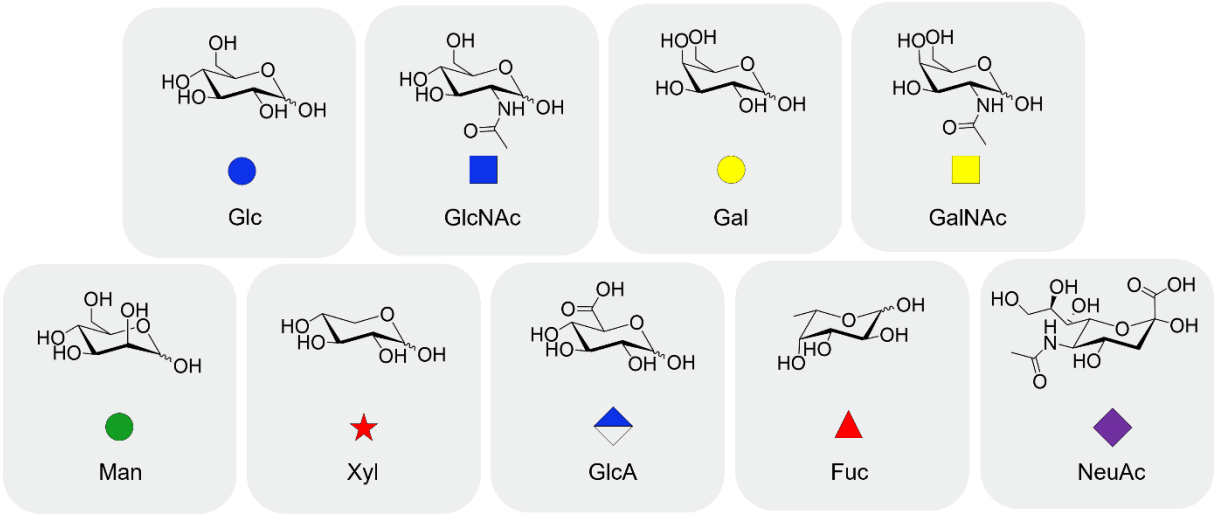

Figure 1. Major monosaccharides in vertebrates: Glc, *N*-acetylglucosamine (GlcNAc), galactose (Gal), *N*-acetylgalactosamine (GalNAc), Man, xylose (Xyl), glucuronic acid (GlcA), fucose (Fuc), *N*-acetylneuraminic acid (NeuAc).

Nine major monosaccharides were identified as building blocks for most abundant glycans in vertebrates (Figure 1). These monosaccharides are linked through glycosidic bond

to form complex glycans, found on the surface of every living cell, among other places. They are involved in important biological processes such as immune response, cellular and pathogen recognition, as well as fertilization.[29,42,43]

3.1.1 Glycochemistry

Figure 2. From monosaccharide to polysaccharide.

In terms of a molecular context, sugars are defined as (poly)hydroxylated carbon chains with aldehyde, ketone or their hydrolyzed functional groups and are classified in three major groups depending on the degree of polymerization: sugars, oligosaccharides and polysaccharides. Short structures such as monosaccharides and disaccharides belong to the group of sugars. Structures increased to three to nine units, linked by glycosidic bonds, are categorized as oligosaccharides and above that the term polysaccharides is used (Figure 2).[44]

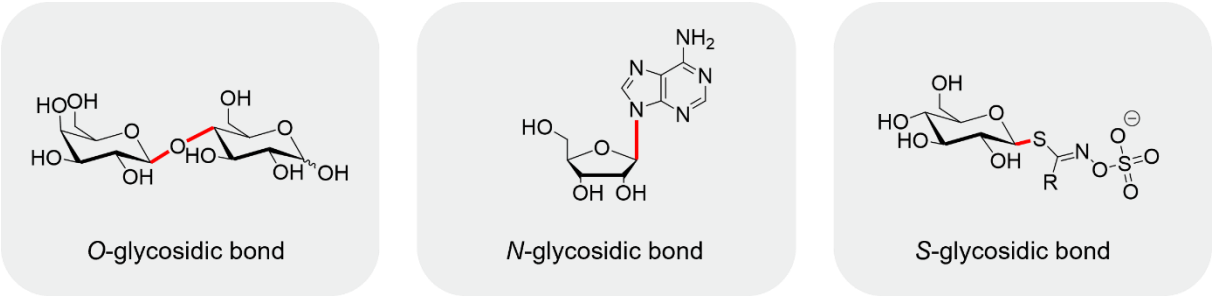

Figure 3. Examples of *O*-glycosidic bond (Lac), *N*-glycosidic bond (adenosine) and *S*-glycosidic bond (glucosinolate).

The glycosidic linkage is a result of a dehydration reaction after losing a hydroxyl group from one monosaccharide and a hydrogen atom from the other carbohydrate or another molecule. Depending on the atom found between the two linked species, the bond is referred as an *O*-, *N*- or *S*-glycosidic bond with different lability towards hydrolysis (Figure 3). The most common naturally present polysaccharides are linked by an *O*, while nucleosides in our genetic information have an *N*-glycosidic linkage. The anomeric center leads to either an α- or β-glycosidic binding.[45]

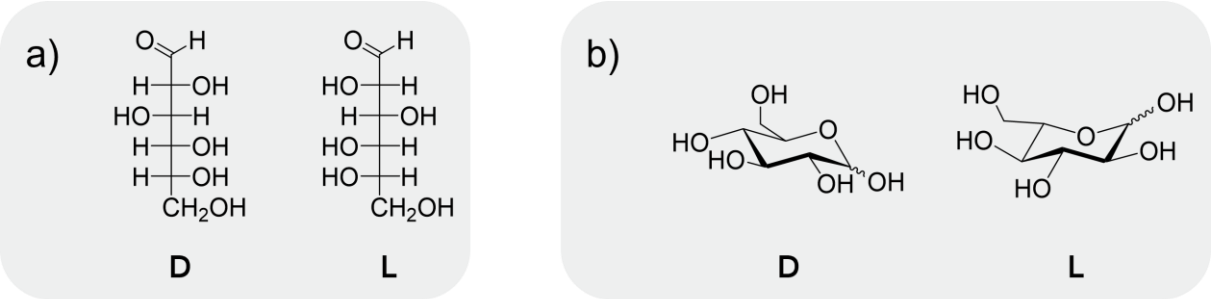

Figure 4. D- and L- configuration of Glc in a) Fischer projection and b) chair conformation.

The asymmetry of carbohydrates leads to two possible configurations, D and L, depending on the orientation of asymmetric carbon atom farthest from the carbonyl group in the standard Fischer projection (Figure 4a). The preferred conformation is usually the more stable five- or six-ring in chair conformation, called furanose or pyranose, respectively (Figure **4**b).

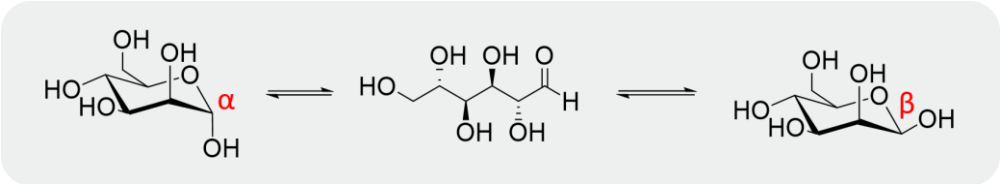

Scheme 1. Mutarotation of Man from α- to β- configuration.

Among other things, they can be classified into sugar alcohols, sugar acids, amino sugars, deoxy sugars and more. They are exhibiting an isomerism in which the aldehyde or ketone group of the open monosaccharide chain reacts with a hydroxyl group of another carbon atom. This formation of a hemiacetal or hemiketal leads to a heterocyclic ring with an oxygen atom between two carbon atoms. This is a reversible equilibrium reaction and results in two anomers due to the anomeric carbon as the stereogenic center. The α anomer refers to hydroxyl groups in axial position, whereas β anomers implies the opposite, hydroxyl groups in equatorial position (Scheme 1).[46,47]

3.1.2 Glycobiology

Glycobiology research focuses on the investigation of sugar-mediated biological interactions combined with the design of inhibitors. As so-called glycoconjugates, glycosylated biomolecules are involved in essential biological functions including cell-cell interaction and

the recognition of viruses, bacteria and other pathogens as foreign bodies. Insights into these functions are the basis for the development of glyco-drugs that can influence targeted biological processes.[29,42,43]

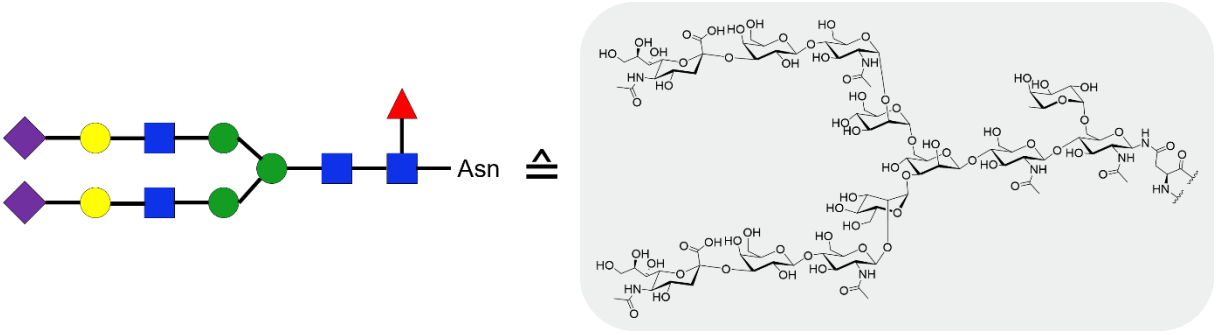

Figure 5. Complex biantennary glycan structure of human endogenous immunoglobulin (IgG).

Besides nucleic acids, proteins and lipids, glycans play an enormously important role in storage of information due to their high complexity. Such complex information stores are conceivable considering the large variety of regio- and stereoisomers that arise in highly branched biopolymers starting from monosaccharides. Glycans cover every living cell as dense and complex layers to control biological processes by interacting with proteins. This wide variety of monosaccharide structures leads to a lining up resulting in an individual “glycocode” to store necessary information with a high capacity. For example, compared to peptide dendrimers, their glycosylated forms can store more information related to complexity, biological activity or structural variability. Unlike peptide bonds, which are in a linear structure due to their defined sequence, glycans achieve higher diversity by anomeric configuration, glycosidic linkage position, sugar ring size and branching of the oligomers (Figure 5). Decoding of this glycocode was performed much later compared to those of peptides and nucleotides due to the more challenging and time-consuming structure determination of glycans. However, this diversity and thus complexity ensures that glycans have a higher information potential than nucleic acids and proteins.[48]

Figure 6. Crystallographic structure of a tetramer of the lectin concavalin A (ConA).[49]

The protein class lectins plays a key role in this process, as they are capable of reading the information code by interacting with carbohydrate structures through high specificity (Figure 6). They mostly include at least two binding sites, referred to as either di- or polyvalent, which can detect free sugar molecules, as well as glycoconjugates. These proteins are vital for many biological processes and are therefore found in all biological systems. Processes like cell adhesion, cell agglutination or cell recognition via lock-key-principle are attributed to lectins. The recognition takes place through reversible binding by a combination of hydrophobic stacking, van der Waals interactions and hydrogen bond interactions of the numerous hydroxyl groups of the sugar units with the amino acids of lectins. In addition, high specificity via metal coordination of divalent ions like Ca^{2+} or Mn^{2+} is common. The presence of these ions leads to the coordination of specific amino acid residues in the carbohydrate recognition domain (CRD) to specifically bind the hydroxyl groups of the carbohydrate structures.[50,51]

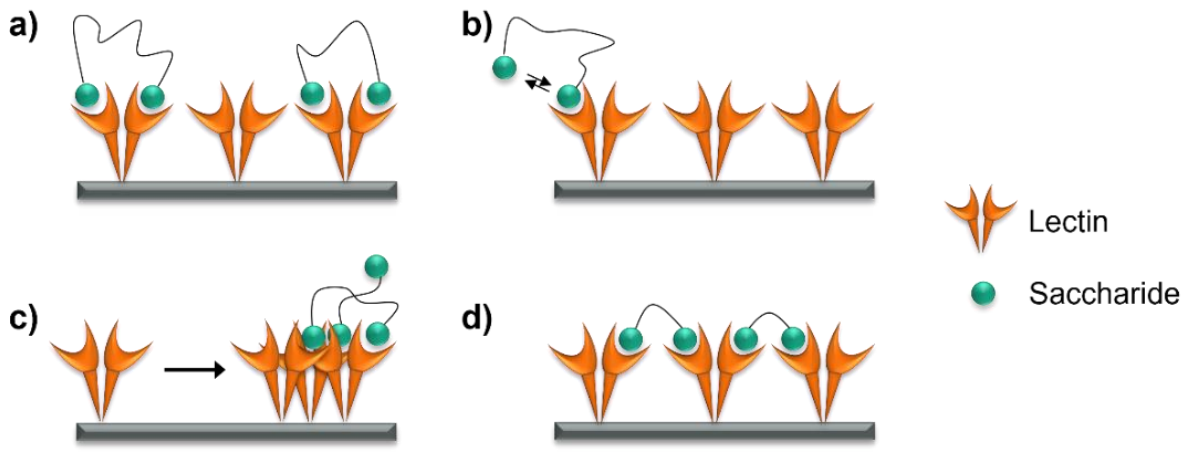

Figure 7. Multivalency mechanisms divided into a) chelation, b) rebinding, c) clustering and d) aggregation.

The binding affinities are enhanced by the multivalency or cluster glycoside effect[52] as the highly specific interaction of lectins and carbohydrates are usually weak. The term multivalency describes a reversible, non-covalent attachment of multiple receptors of one type (e.g. lectins) to multiple ligands of another species (e.g. sugar ligands). One prominent, visible example is the burdock with its several small hooks, which can adhere to fleece surface. Lectins are inherently multivalent receptors, as they feature more than one binding site and interact with copies of a monovalent ligand simultaneously. The glycocalyx, for example, the glycan coating of cellular surfaces, shows this behavior of carbohydrates and their multiple interactions. A higher complexity of the interactions can be achieved by using additional binding partners in this recognition process. Influencing the avidity, i.e. the final affinity in a multivalent system, by a mechanism can be inter- or intramolecular or a combination of both at the same time. These mechanisms of the multivalent effect involve receptor chelating, statistical rebinding, clustering and aggregation (Figure 7).[53,54] These lectin-glycan interactions are of central importance, as they are involved in fundamental processes, such as signal transduction, host-pathogen recognition, infection, fertilization and tissue adhesion. The multiple involvement in biological events leads to the design of glyco-related drugs that intervene in the process. Thus, carbohydrate research requires the basic understanding of lectins in their function and specificity.[29,30,42,43]

3.2 Glycomaterials

The ubiquity of glyco-structures and especially the recognition of lectins to trigger biological interactions led to a great interest in carbohydrate-containing materials. Methods to isolate synthetic polysaccharides are plentiful, but they are associated with drawbacks. On account of the similar chemical composition of the respective monosaccharides due to the many hydroxyl groups, the synthesis of polysaccharides from them requires a time-consuming introduction of protecting group chemistry. Advanced techniques, such as automated solid phase synthesis, allow isolation of short oligosaccharides in low yield, while more easily synthesized glycoclusters show insufficient valency towards lectins.[55,56,57] The application of glycopolymers instead as mimics of natural glycoconjugates can overcome these limitations. These can be synthesized in a defined manner with high molecular weight and simultaneously high yield. Furthermore, they show increased binding affinity to lectins as receptors on cell surfaces, since they offer a larger number of ligands and therefore trigger the effect of multivalency.[58,59]

3.2.1 Synthesis of Synthetic Glycoconjugates

3.2.1.1 Glycopolymers

Natural glycoconjugates can be mimicked by glycopolymers as multivalent ligands, which bear repeating units of monosaccharides and/or oligosaccharides as pendant groups. This imitation allows us the development of new materials or to gain insights into recognition processes in which naturally occurring lectins are involved. The larger the monovalent polysaccharide, the more problematic its solubility, as can be observed in the example of cellulose. The use of glycopolymers as multivalent ligands can circumvent this, as their solubility is often enhanced. The individual saccharides are held in place by a synthetic backbone to form glycopolymers, unlike polysaccharides in which glycosidic bonds between the single saccharide take over this task. The similarity of the many alcohol groups to each other poses a challenge for the synthesis of polysaccharides, glycoproteins and -lipids. In addition, these hydroxyl groups are relatively unreactive and thus derivatization is only possible after activation. Synthesized polysaccharides, glycoproteins and -lipids can be obtained by chemical or enzymatic reactions. Suitable polymerization techniques of glycostructures, however, allow the isolation of materials with controlled sugar amount and polymer length in different

architectures. These include linear glycopolymers, glycodendrimers and spherical glycopolymers like vesicles, micro- and nanoparticles, as well as micelles. Not only the glycopolymer morphology influences the lectin-glycopolymer-interaction, but also properties including molecular weight, polymer rigidity or the density of carbohydrate structures.[60,61] The potential application of glycopolymers allows for broad development in areas, such as protein and bacterial detection, viral inhibition, tissue engineering or surface modification. [62,63,64,65]

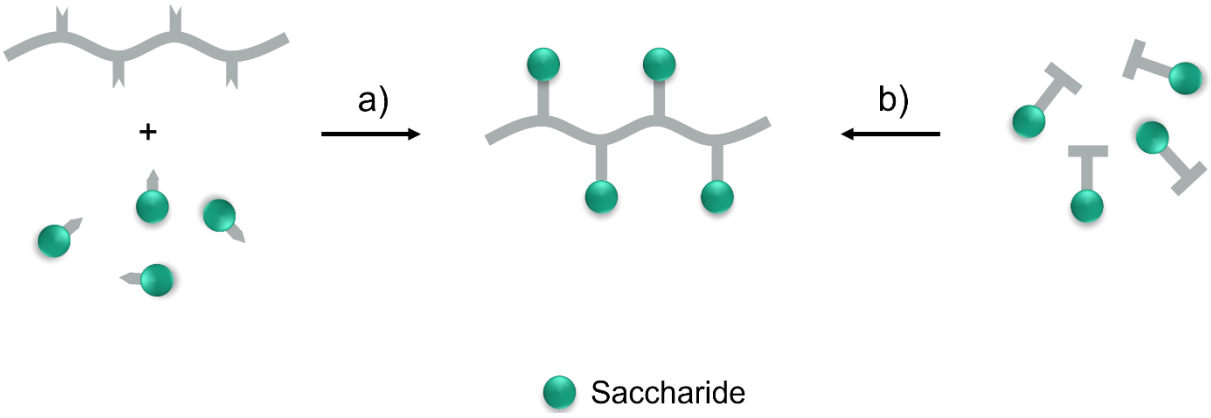

Scheme 2. Synthesis of glycopolymers via a) post-polymerization modification or b) direct polymerization of glycomonomers.

Glycopolymers can be synthesized either by addition of carbohydrate structures to existing polymers via post-polymerization modification or by direct polymerization techniques of glycomonomers previously synthesized (Scheme 2).

3.2.1.1.1 Post-Polymerization Modification

Existing or previously synthesized polymers can be derivatized with sugar structures via conjugation of the reactive functional groups. This method is suitable to isolate glycopolymers, which cannot be prepared from direct polymerization of monomers due to low tolerance to functional groups during polymerization. In addition, this method is applicable for glycomonomers, which tend to self-polymerize during purification attempts. This approach enables the attachment of sugar structures without tedious protection and deprotection steps.

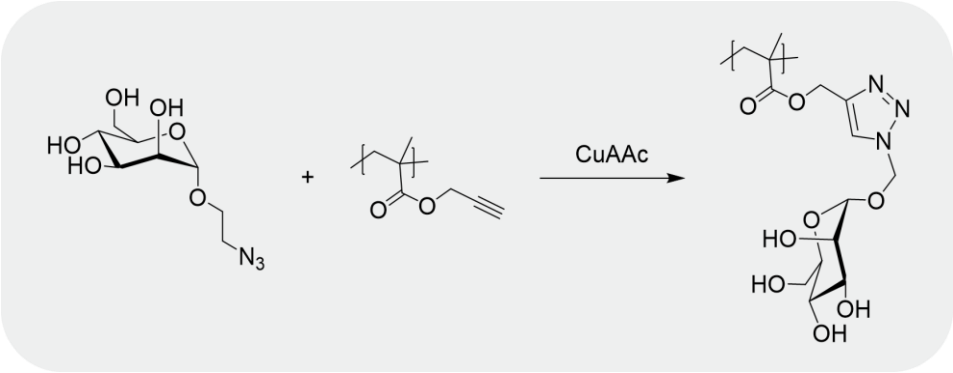

Scheme 3. Synthesis of Man-based glycopolymer via azide-alkyne Huisgen cycloaddition.

Click chemistry is due to its advantages one of the most common and valuable methods for post-glycosylation of polymers. Included chemical reactions are stable towards most functional groups and water, are stereospecific, as well as generating low byproducts, while having a high efficiency. The classical click reaction, known as copper-catalyzed azide-alkyne cycloaddition (CuAAC), allows the linkage of azide-functionalized sugars to a polymer backbone containing alkyne functional groups or, inversely, the coupling of alkyne sugars to azide-bearing polymers. This 1,3-dipolar cycloaddition occurs via the formation of a 5-membered heteroatom ring. Double hydrophilic block glycopolymer for self-assembly studies via coordination and hydrogen bonds was synthesized this way. Therefore, the polyethylene glycol (PEG)-based, propargyl-containing parent blockcopolymer was isolated using the reversible addition-fragmentation chain-transfer (RAFT) polymerization technique. For the counterpart, Man or Gal were converted to the azide derivative without the need of protection and deprotection steps. The resulting Man or Gal azide were coupled to the propargyl functionality using a Cu(II) catalyst with the addition of the reducing agent sodium ascorbate by producing Cu(I) in situ (Scheme 3).[66,67] Alternatively, a Cu(I) species can be used directly to connect azide functionalized sugars with a propargyl containing polymer, which was isolated after the removal of the prior introduced trimethylsilyl protection group.[68,69] Unlike CuAAC, thiol click reactions do not require metal catalysts, while they also have high efficiency and no sensitivity to water and oxygen.

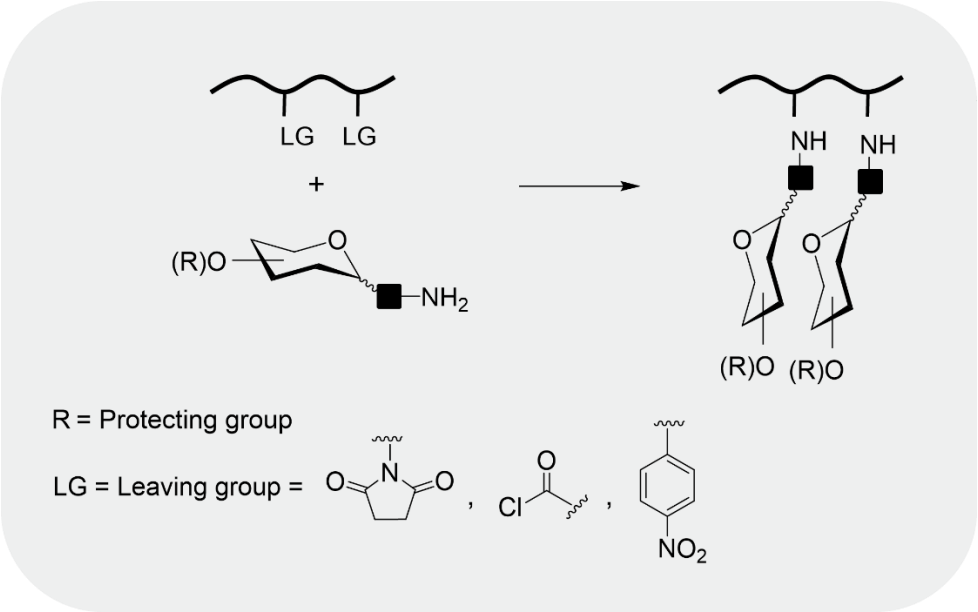

Scheme 4. Synthesis of glycopolymers via amidation.

Aminosaccharides can be directly attached to a parent polymer without the use of protecting groups due to the increased nucleophilicity of the amine group relative to the alcohol functional groups. Instead of natural amino sugars, such as glucosamine, galactosamine or mannosamine, amine-functionalized saccharides synthesized via chemical reactions can be used. Post-modification via an amide linkage is only feasible with polymers having active carbonyl functionalities, such as *N*-hydroxysuccinimide (NHS) esters, anhydrides, *p*-nitrophenyl carbonate or carboxylic acids (Scheme 4).[70,71,72,73] Conversely, the amine functionality may be pendant to the polymer, which then attacks the sugar molecule via reductive amination.[74,75]

3.2.1.1.2 Polymerization of Glycomonomers

A wide variety of polymerization techniques allows the isolation of glycopolymers from monomers with carbohydrate moieties. These can be categorized into two principal groups of radical polymerizations, free radical polymerization (FRP) and reversible-deactivation polymerization (RDRP). In addition, synthesis of glycopolymers is also possible via living anionic polymerization, photopolymerization, ring-opening polymerization (ROP) or ring-opening metathesis polymerization (ROMP), among others.[76,77,78,79,80,81]

The most commonly used approach for glycopolymerization is conventional FRP due to the advantages of scalability, low tolerance to impurities, commercial availability of

initiators, low costs, as no deactivators or catalysts are necessary, and a wide range of reaction temperatures and solvents. The use of highly polar solvents, such as water, dimethyl sulfoxide (DMSO) or methanol, are recommended due to the solubility of the polar glycomonomers and the resulting polymers. Unprotected, as well as with protecting groups modified glycomonomers, were polymerized in this polymerization way.[82,83,84]

The disadvantages in terms of controlling the molecular weight and thus the molecular weight distribution can be reduced by using RDRP techniques, including atom transfer radical polymerization (ATRP), RAFT and nitroxide-mediated polymerization (NMP). They all represent an outstanding method to isolate glycopolymers with functional terminals, polymer architecture, a controlled targeted molecular weight and a narrow molecular weight distribution, therefore a lower polydispersity can be achieved. ATRP enables the polymerization at low temperatures, which is beneficial for glycomonomers and the resulting polymers with lability towards high temperatures. Due to its high tolerance to functional groups, the application of ATRP is particularly popular in the polymerization of unprotected carbohydrate monomers. It requires an initiator in the form of an alkyl halide and a transition metal complex as a catalyst.[85,86] The use of toxic copper ions or other transition metal complexes, as catalysts is necessary for ATRP and therefore not suitable in the development of biomedical applications, as purification must be done with the highest degree of care. Furthermore, surfaces can be modified accordingly by surface-initiated ATRP. For instance, glycopolymer brushes have been placed on surfaces to develop biointerfaces.[87,88]

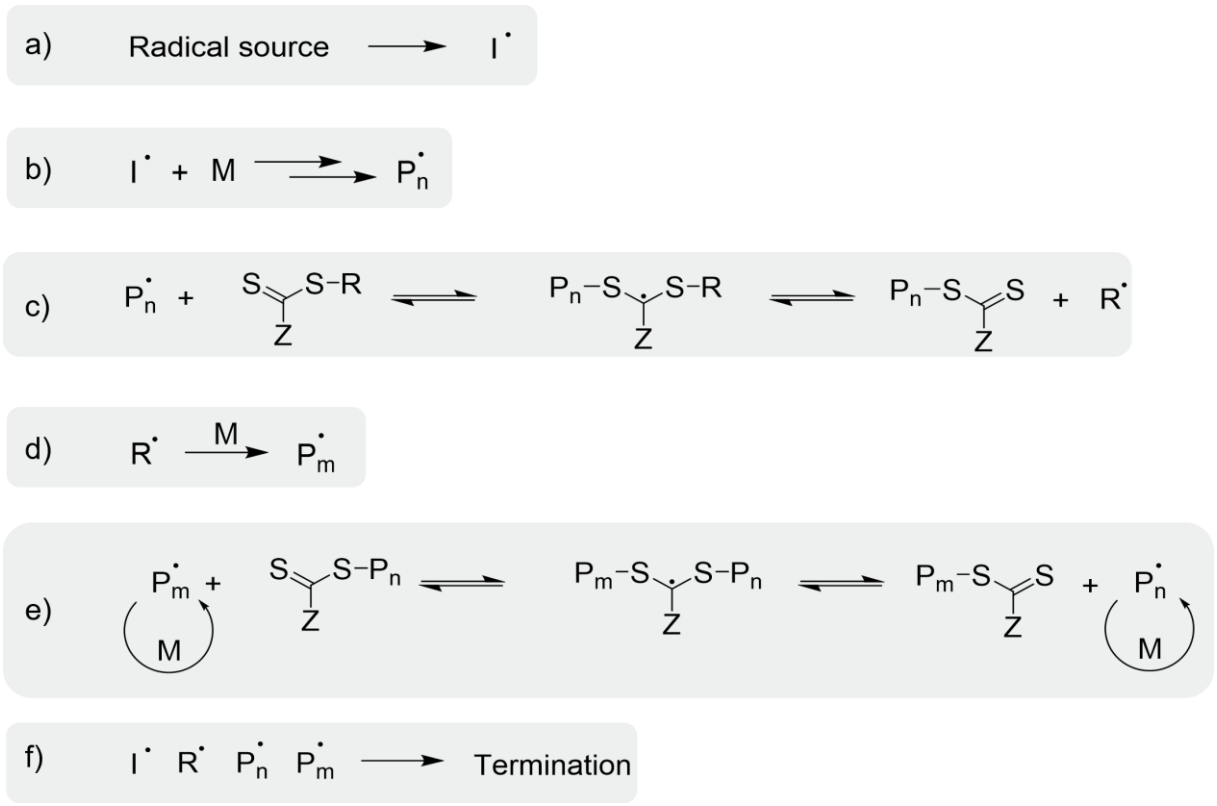

Scheme 5. Proposed mechanism of RAFT polymerization: a) radical formation, b) initiation, c) equilibrium between active and dormant species, d) re-initiation by formation of P_m•, e) equilibrium between active and dormant species and f) termination reaction.

RAFT polymerization is economical in its handling and thus a popular method for the synthesis of glycopolymers. This technique has similar advantages to ATRP, except that instead of using metal catalysts for polymerization mediation, RAFT also requires a chain transfer agent (CTA), also called a RAFT agent. It consists of an R- and a Z-functional end group, which must be selected carefully in advance. Its control is based on reversible chain transfer reactions in which growing radical chains are added to the RAFT agents. The resulting radical intermediate fragments to different sides due to the agent structure, so that in turn an agent and a radical for propagation are formed back. Thus, the probability of propagation is evenly distributed among all chains. The average chain length of the polymer formed is proportional to the RAFT agent concentration, as well as the reaction conversion. Common initiators, such as azobisisobutyronitrile (AIBN) or 4,4-azobis(4-cyanovaleric acid) (ACVA), are used for initiation and thus initial chain growth (Scheme 5). Decomposition into two fragments (I•) results in reaction with the monomer resulting in propagating radical polymer (P_n•). CTAs, typically dithiocarbamate-, trithiocarbonate- or dithioester-based molecules drive the formation of adduct radical through the actively growing chain P_n•. Pre-equilibrium is set by the cleavage of R•, which forms another active polymer chain P_m• from M again as an actively propagating

radical. Subsequently, $P_m^{\bullet}$ attaches to the functional chain end-group, which leads to equilibrium between active and dormant species. Since these are conventional free radical reactions, the occurrence of termination reactions cannot be prevented. The reaction of two radically reactive forms leads to a dead polymer.

This polymerization method enabled the synthesis of numerous glycopolymers, such as GlcNAc- and *N*-acetylmannosamine-containing polymers, that equip tumor cells and elicit an increased immune response.[89] Furthermore, this technique was used to polymerize a fructose-based glycopolymer, which enhanced the potential of multiwalled carbon nanotubes in cancer therapy.[90]

NMP is not as common in the synthesis of glycopolymers compared to ATRP and RAFT, as the latter modern polymerization techniques are more convenient to perform. High reaction temperatures and a polymerization initiation by a homolytic cleavage of alkoxyamine are the reason for the lower reports of NMP-mediated glycopolymers.

3.2.1.2 Glycomonomers

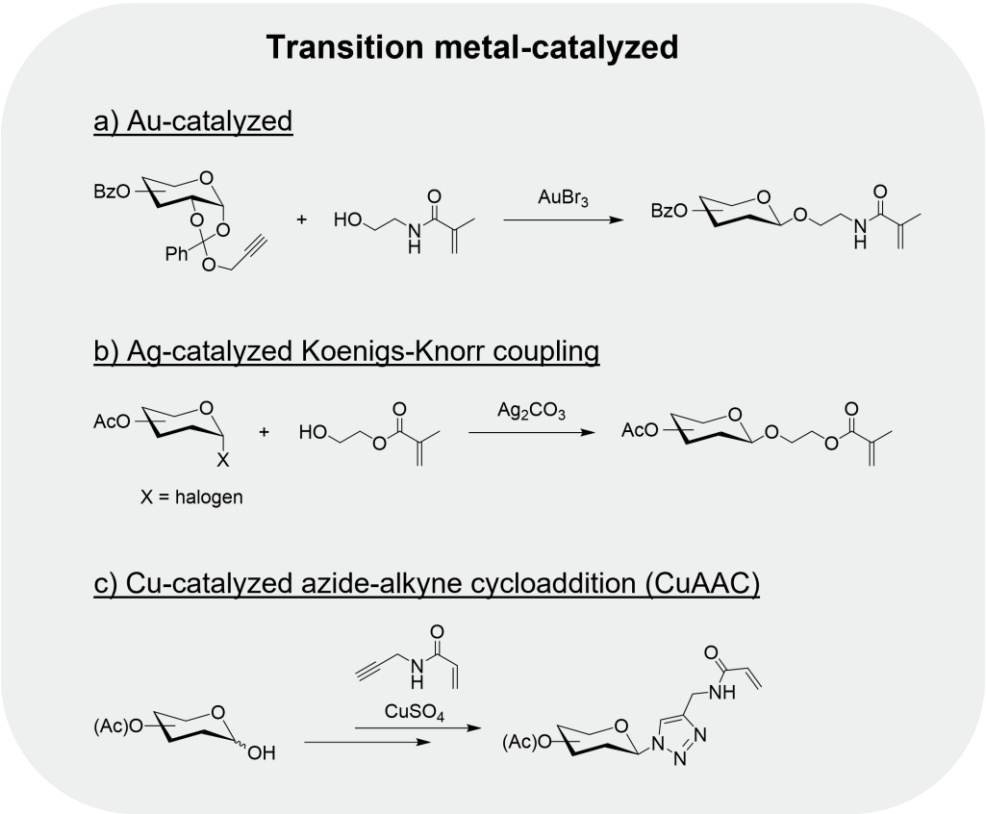

Scheme 6. Transition metal-catalyzed synthesis of glycomonomers.

Polymerizations require the prior synthesis of glycomonomers. Transition metal-catalyzed synthesis is a common method to introduce polymerizable groups into carbohydrate molecules at the anomeric position. Au(III) ions activate anomeric alkynes, which resulted in the formation of Gal-, Man- and Glc-based acrylamides (Scheme 6a).[83,91] Pre-synthesized glycosyl halides can be derivatized with a polymerizable functional group via the Koenigs-Knorr glycosylation mechanism using Ag(I) salts as the catalyst (Scheme 6b).[87,92] In addition, the most famous representative in click-chemistry, CuAAC, enables the synthesis of glycomonomers by combining an azide functionality with alkynes (Scheme 6c).[93,94] However, due to the presence of transition metals, metal-catalyzed glycosylation can only be used for subsequent biomedical materials after these have been thoroughly removed.

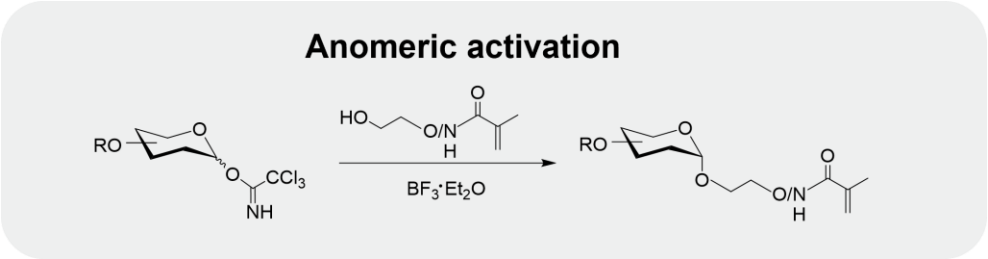

Scheme 7. Synthesis of glycomonomer via anomeric activation.

Moreover, activation of the sugar anomeric position with trichloroacetimidate leads to the isolation of glycomonomers (Scheme 7).[95,96] Both methods of glycosylation, metal-catalyzed and anomeric activation, require the introduction of protecting groups, which prolongs the synthetic route of glycomonomers.

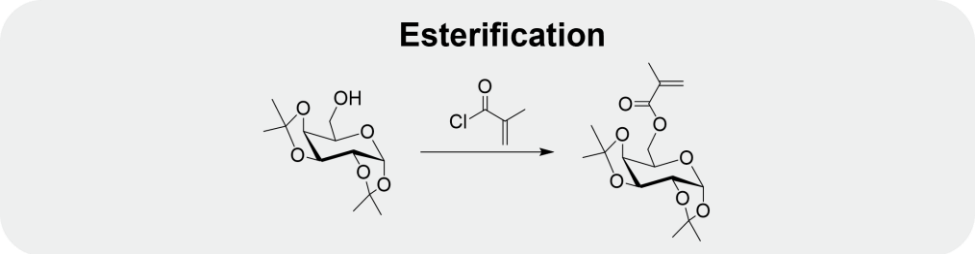

Scheme 8. Synthesis of Gal-bearing glycomonomer via esterification.

A simple synthesis route to isolate a glycomonomer is the etherification or esterification. These methods allow a selective modification on different C positions of the saccharide, depending on the hydroxyl group protecting strategies and saccharides. By leaving one hydroxyl group unprotected, this targeted hydroxyl group can be etherified or esterified, which can react with a halogenated acceptor molecule under basic conditions (Scheme 8).[97,98,99,100]

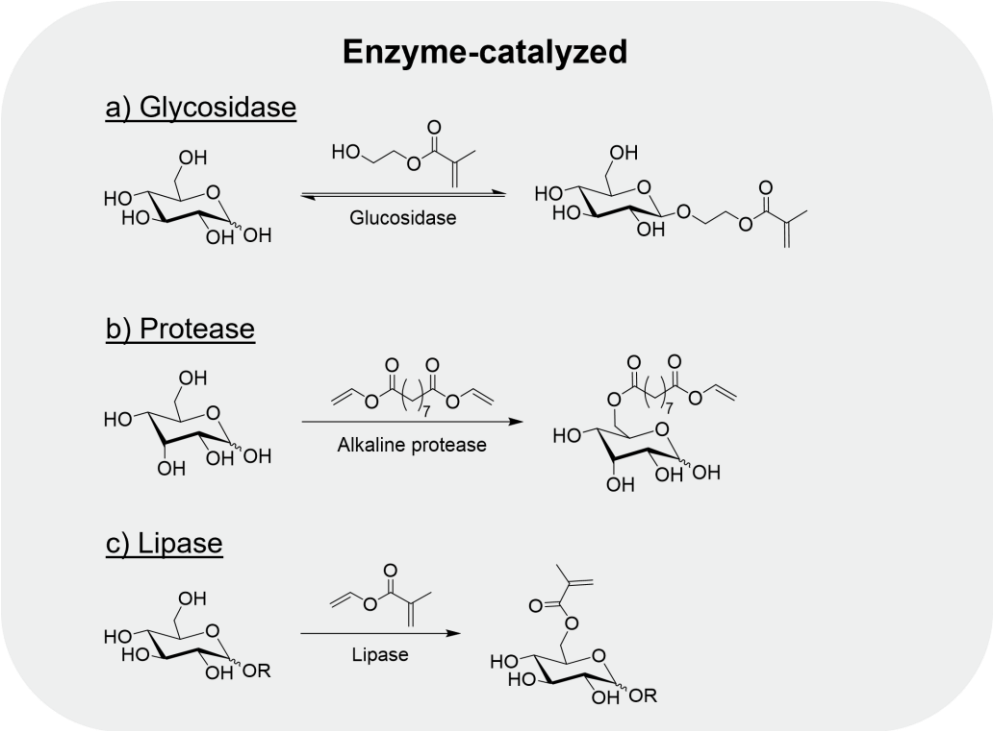

Scheme 9. Synthesis of glycomonomers via enzyme catalysis.

The employment of hydrolases, such as glycosidases, proteases and lipases, enable esterification without the use of protecting groups, which is why interest in biocatalysis related to glycomonomer syntheses has increased in recent years. Hydrolases (EC 3) belong to the class of enzymes, which promotes the bond cleavage of for example esters, peptides or glycosides by hydrolysis. Glycosidases, proteases and lipases can not only catalyze hydrolysis reactions, but also the formation of ester-, amide- and glycosidic bonds.[101] The particular advantage of biocatalysis is that the enzymes are non-toxic, as well as biodegradable, and operate even under mild reaction conditions. These environmentally friendly properties need to be considered in terms of green chemistry. Nevertheless, reaction conditions with enzymes must be precisely adjusted in pH and temperature, which makes the use of biocatalyst challenging to achieve high yields.

Glycosidases are used to introduce a polymerizable group to the sugar in its anomeric C1 position by forming a glycosyl-enzyme intermediate (Scheme 9a). Pure anomeric products in α- or β-configuration depend on the enzyme type. As glycosidase hydrolyzes oligosaccharides in the presence of water, this method is only applicable for the isolation of glycomonomers with a monosaccharide moiety. Small amounts of water are necessary to increase the solubility of the carbohydrate and to preserve the enzyme activity.[102,103,104]

Proteases were used to generate glycomonomers via a transesterification mechanism with divinyl esters. The regioselectivity of this chemoenzymatic transesterification depends on the saccharide type. Compared to the utilization of glycosidase with usual reaction times of 24 h, protease-catalyzed synthesis has a longer reaction time up to several days.[105,106] Lipases are enzymes, which play a significant physiological role by converting triglycerides into free fatty acids and glycerol. Most of them possess a lid domain to shield the active site from the environment. They act at the interface between hydrophilic and hydrophobic domains, whereby the water content influences the enantioselectivity. Lipases catalyzes mainly hydrolysis, transesterification and esterification reactions, depending on the reaction equilibrium. The equilibrium can be affected by using organic solvents, water concentration and soluble substrates. Immobilization on suitable insoluble, hydrophobic polymer supports, improves the stability and activity of lipases.[107] In addition, using hydrophobic supporting materials, such as acrylic resin beads, is a common method for shifting the preferred catalyzed reaction towards esterification. Novozym 435 is a commercially available isoform B of *Candida antarctica* (Cal B) lipase with a microporous acrylic polymer resin, which comes with a spherical pearl morphology. Its active site consists of a Ser-His-Asp triad. High efficiency allows the conversion with less by-products. Like proteases, lipases can perform in organic solvents like dimethylformamide (DMF), acetonitrile or butanone. Lipase-catalyzed glycomonomer syntheses are highly regioselective, as the esterification of primary alcohols is favored. This leads to a functionalization of pyranoses in the C6 position and of furanoses in the C5 position (Scheme 9c).[102,108]

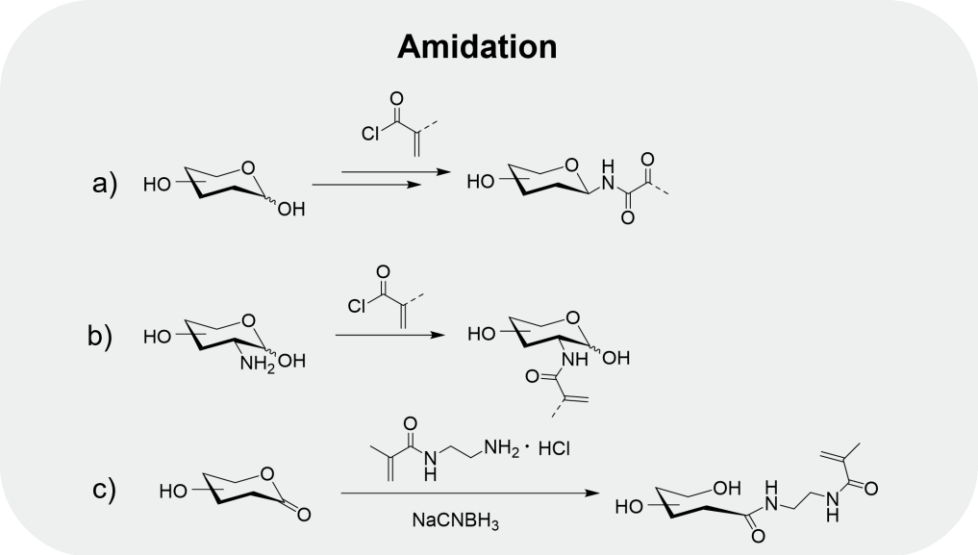

Scheme 10. Synthesis of glycomonomer via amidation.

However, since ester compounds tend to hydrolyze in the presence of water, isolation of glycomonomers via amide bond formation is preferred. This can also be accomplished without the use of protection groups by amidation, which belongs to the nucleophilic acyl substitution reactions. This reaction requires on one hand a nucleophile, in this case an amine, and on the other hand an electrophile with a good leaving group of an acyl derivative, such as acid halides, anhydrides or esters. The resulting product is the substitution of the leaving group by the nucleophile (Scheme 10a). An acceleration of this amidation reaction can be achieved by performing the reaction under acidic or basic conditions, which makes the carbonyl derivative more electrophilic or the amine more nucleophilic, respectively. A drug delivery system for hepatocellular carcinoma therapy was prepared by collaborative assembly of the active agent doxorubicin and Gal-bearing diblock glycopolymer.[109] The needed galactosyl monomer was prepared in a two-step synthesis without the introduction of protecting groups. For this purpose, galactose was derivatized via the Likhorshertov amination reaction and subsequently with acryloyl chloride via a substitution mechanism.

The use of commercially available amino-saccharides like glucosamine hydrochloride enables the synthesis of 2-deoxy-2-methacrylamido-D-glucose by coupling with methacryloyl chloride in the presence of Et_3N for future bone tissue engineering (Scheme 10b).[110]

The saccharide derivative can not only act as the nucleophile, but also as the electrophile in an acyl substitution reaction. The C1 position of the sugar can be modified by oxidation to a lactone, which results in a formation of an electrophilic carbonyl position, followed by a

nucleophilic attack of a polymerizable amine (Scheme 10c). The use of protecting groups in this method is not necessary as well.[111,112]

3.2.2 Application

3.2.2.1 Principal Investigation of Carbohydrate-Lectin Interactions

A big research field in glycobiology is the evaluation of reversible interactions of lectins with carbohydrates. Glycopolymers are most commonly used as synthetic polymers with sugar pendant groups to investigate carbohydrate-lectin interactions. By mimicking natural glycoconjugates, glycopolymers can interact with lectins in biological recognition processes due to their high binding affinity and specificity to sugar molecules. Using the RAFT polymerization technique, Gal-based copolymers were synthesized with a biotin pendant moiety leading to the preparation of subsequent gold nanoparticles due to biocompatibility, low cytotoxicity and simple functionalization reasons.[113] Recognition investigations were performed with the lectins Jacalin from *Artocarpus intergrifolia* and *Ricinus communis* agglutinin (RCA_{120}) from castor bean. RCA_{120} interacts with Gal, and therefore also Lac residues. GlcNAc and LacNAc functionalized PEG-based microgels were prepared by applying a radical polymerization mechanism.[114] Prepared microgel networks showed colloidal behavior and contain a swollen molecular structure in the presence of water. Multivalent binding interactions were indicated after evaluating the high binding affinities to the corresponding lectins *Griffonia simplicifolia II* (GSII) and *Erythrina cristagalli* (ECL). Binding activities with ConA were studied by isolating SiO_2 nanoparticles with Man moieties using the RAFT polymerization technique.[96] This required the synthesis of a suitable monomer from Man, which was achieved by the introduction and removal of acetylic protecting groups. These results contribute, among others, to the development of biomaterials from glyco-bearing polymers with increased efficiency for biomedical engineering or application in general.

3.2.2.2 Pathogen Inhibition

Based on carbohydrate-lectin interaction studies, multivalent glycopolymers have great potential as inhibitors to prevent infections of host cells caused by pathogens. The multivalency of these materials leads to a cluster glycoside effect, resulting in an enhancement of the molecular interactions with lectins, cells, bacteria and viruses. Cell infection with pathogens is

triggered by their interaction with sugar structures found on the surface of potential host cells. Pathogens achieve adhesion through their own lectins. By competing with these sugar-recognition domains, synthetic derivatives including sugar moieties can act as inhibitors to prevent cell infection. Sialyllactose-based polystyrene was prepared by amination of sialyllactose and subsequent substitution to styrene, followed by polymerization.[115] The synthesized glycopolymer showed inhibition of hemagglutination of *Influenza A viruses* (IAV) with significantly increased activity compared to the oligosaccharide itself. In addition, different viruses can be trapped by the glycopolymer that is adsorbed on a polystyrene surface. Gal- and Man-bearing glycopolymers were isolated using RAFT polymerization technique and were tested as competitive inhibitors for viruses with various glycan functionalities like *Herpes Simplex Virus* (HSV), *Merkel Cell Polyomavirus* (MCPyV) and IAV.[116] Copolymerization with poly(*N*-isopropylacrylamide) (PNiPAm) lead to a glycopolymer with lower critical solution temperature (LCST) behavior.[117] Binding activities to *E. coli* and ConA depends on the LCST due to coil-to-globule transition of the glycopolymer. At temperatures above LCST, binding to ConA is weaker. In addition, steric shielding is accomplished by the formation of microphases of the temperature-dependent copolymer, resulting in enhanced inhibition of *E. coli*.

3.2.2.3 Drug Delivery

For controlled drug delivery in terms of time, location and concentration, numerous obstacles must be overcome. Low solubility, non-specific toxicity, enzymatic and environmental degradation, rapid clearance rates from the body and other biological barriers require the development of suitable drug carrier systems. The interactions between carbohydrates and lectins can be exploited to target the drug to the desired location in the body. High uptake to specific cell lines and the low cytotoxicity render glycopolymers excellent candidates for drug delivery. Hydrophobic drugs, like doxorubicin for tumor therapy, can be easily encapsulated by glyco-containing block copolymers with a hydrophobic part resulting in self-assembly to nanoparticles. A fluorescence active polymeric nanogel from glucosamine was used to load doxorubicin by adding the drug molecule to a redox responsive cross-linker.[118] The glycopolymer was isolated after using RAFT polymerization technique, followed by a post-modification with the carbohydrate via click chemistry. Biological experiments revealed that the obtained nanogel was not cytotoxic, while it showed anticancer activities over various cell

lines. As the previously mentioned example, the property of the glycopolymer can be changed by using suitable copolymers making it, for example, thermoresponsive and thus programmable. A pH- and temperature-sensitive block copolymer of PNiPAm and poly(acryloyl glucosamine) was synthesized and evaluated a for potential drug targeting and drug delivery applications.[119] The fully dissolved polymer changed to a micellar structure above the LCST of PNiPAm, which degraded at an acidic pH of 2. To achieve sustained drug release, a double hydrophilic and at the same time thermoresponsive glycopolymer of Gal was developed.[120] The glycopolymer was synthesized using a chemo-enzymatic procedure and free radical copolymerization. After varying the molar fraction of the Gal monomer in the polymerization process, a LCST of 32 to 40 °C was obtained. The desired nanofibers were developed using electrospinning, which showed appropriate cytocompatibility towards HeLa cells and recognition of peanut agglutinin (PNA). These results indicate targeted and temperature regulated drug release.

4 Methods

4.1 Microwave (MW) Irradiation

MWs are electromagnetic waves with frequencies of 300 MHz to 300 GHz and thus have a wavelength between 1 m and 1 mm. The electromagnetic energy has been increasingly used in synthetic settings over the last 30 years. It found application in organic, organometallic, inorganic and peptide synthesis, as well as in catalysis, materials science, nanotechnology and polymer chemistry.[121,122,123,124,125,126,127,128,129]

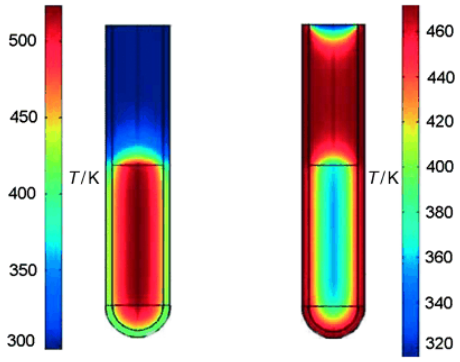

Figure 8. Differences in the inverse temperature gradients when heating with MW irradiation (left) and in an oil bath (right).[127]

Due to the steady heat distribution, the reaction yield can be increased in shorter time, especially for organic syntheses when compared to conventional heating with an oil bath. Heat compensation by conventional heating produces a temperature gradient from the outside to the inside resulting in a longer temperature transfer starting on the surface of the glassware. In comparison, using MW irradiation enables a contact-free internal heat supply due to rotational and vibrational motions of the molecules, which leads to a safer, more precise and more efficient way of heating (Figure 8). This phenomenon is referred to as dielectric heating by MW and has the effect of inducing the absorption of MW energy by substances, such as solvents or reagents, and converting it into heat. MWs interact with molecules in two ways, dipolar polarization and ionic conduction. In the presence of MW frequencies, the ions or dipoles of the sample align in the applied oscillating field. The ionic or dipole field tries to realign with the altering electric field, causing energy loss in the form of heat due to molecular friction and dielectricity. Ionic conduction describes the collision of ions in the sample with neighboring molecules or atoms in a similar way during oscillation.[122,126,130,131]

Before the advantages of MW effects become beneficial, the reactions often have to be optimized in a time-consuming process. Another point is that MW heating is associated with numerous properties of compounds due to dipolar polarization and ionic conduction. For example, the permittivity and thus the dielectric constant and the magnetic loss tangent matter, limiting the choice of solvent to be used to polar solvents. Hence, already improved synthesis reactions must be redesigned and optimized when they are carried out in the MW reactor, which is initially very time-consuming. In addition, the penetration depth decreases with larger volume, making upscaling of a reaction non-transferable and thus requiring optimization experiments to be carried out again.[132,133]

4.2 Liquid Chromatography (LC)

Chromatography describes the process of separating a mixture of substances by different distribution of its individual components. In this process, various substances are transported in the mobile phase on a stationary phase. Interactions between the sample, the mobile phase and the stationary phase lead to different onward transport speeds, so that individual substances are separated from each other. The stationary phase is the phase that interacts with the individual substances of a sample mixture and does not move, i.e., as the name implies, it remains stationary. In the LC method, this stationary phase is usually solid. The mobile phase is the moving phase into which the crude substance mixture is introduced at the beginning of the separation system. Mobile phases in LC are also called eluents and differ in their elution capacity, which leads to different retention times and selectivity.[134,135,136,137]

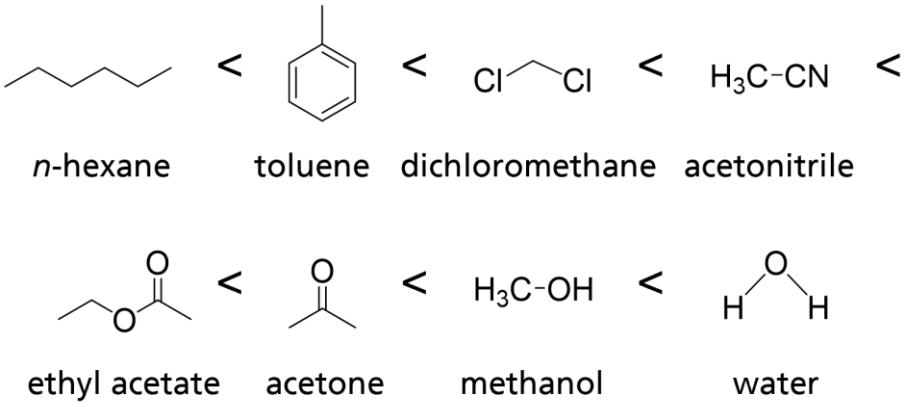

Figure 9. Elutropic series of solvents for normal-phase chromatography with silica gel.

Solvents as eluents are sorted into an elutropic series according to increasing elution strength (Figure 9). This represents the solvent's ability to transport a compound. The retention time refers to the total time required for a substance to pass through the stationary phase. Interactions with the stationary phase lead to a delayed flow of individual analytes of the sample mixture into the mobile phase and thus to an influence on the retention time.[138,139]

4.2.1 (Preparative) High-Performance Liquid Chromatography (HPLC)

Besides manual column chromatography for the purification of crude products, preparative HPLC is also an established separation method. This has the benefits in terms of reproducibility and automation. In this method, the compound mixture to be separated is pumped in the mobile phase through a separation column containing the stationary phase. The detection is usually realized with a UV detector. Since the amount of sample which can be separated into its individual substances depends on the column volume, manual column chromatography is recommended when the amount to be purified is high. The greater the sample quantity required to be separated into its individual substances, the larger the column volume must be. This leads to high acquisition costs, therefore manual column chromatography is recommended for quantities in the gram range.[140,141,142]

The reversed-phase (RP) HPLC method is the most common technique and is applied in sugar chemistry for the isolation of polar carbohydrate-containing derivatives. A non-polar stationary phase, e.g. a modified C18 silica gel column, is used so that the elution strength of the mobile phase decreases with increasing polarity. Mixtures of water and acetonitrile are often used as eluents. In this manner, polar compounds, in this case glyco derivatives are obtained with lower retention times as compared to manual column chromatography.[143,144,145]

4.2.2 Size Exclusion Chromatography (SEC)

Compared to the LC methods mentioned above, SEC separates sample mixtures based on their size, caused by different diffusion volumes for molecules of different sizes. The stationary phase usually consists of porous polymers into which smaller molecules can enter. This leads to an increase in the diffusion volume available for them and a prolongation of the retention time. Accordingly, small molecules are more strongly retained than large ones.

Consequentially, large molecules flow faster through the chromatography column while smaller molecules elute later. Refractive index (RI) and UV are often used for detection. With the help of standard substances, the molecular masses can be determined after suitable calibration. In polymer chemistry, SEC is a popular method for calculating the various weighted average molecular masses, such as M_n and M_w, as well as polydispersity. However, the results are relative, as they depend on standard substances that have only a rough similarity to the analyzed substance.[146,147]

4.3 Nuclear Magnetic Resonance (NMR) Spectroscopy

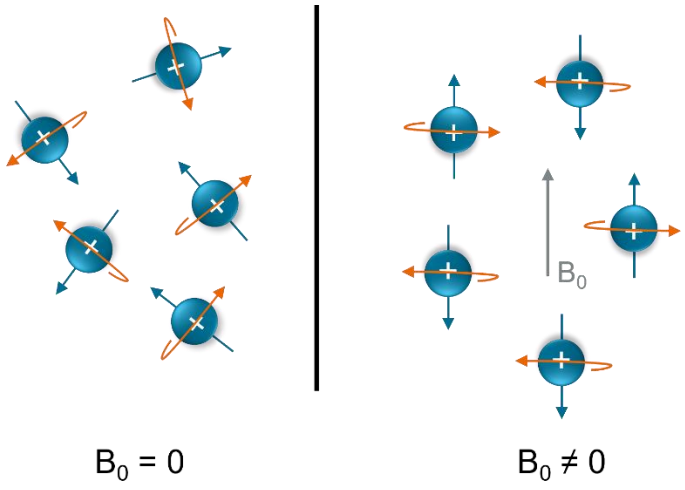

Figure 10. Arrangement of the nucleons without (left) and with applied magnetic field (right).

NMR spectroscopy is indispensable in organic synthesis chemistry to determine the chemical structure of a substance. This method is used to investigate the electronic environment of the individual atoms and their interactions with neighboring atoms. It is therefore based on the behavior of magnetically active atomic nuclei under the influence of a strong external magnetic field. The nuclear components (protons and neutrons) of atoms have both a spin (intrinsic angular momentum) and a magnetic moment μ of their own since they generate a magnetic field through their electrical and rotating charges.[148,149,150]

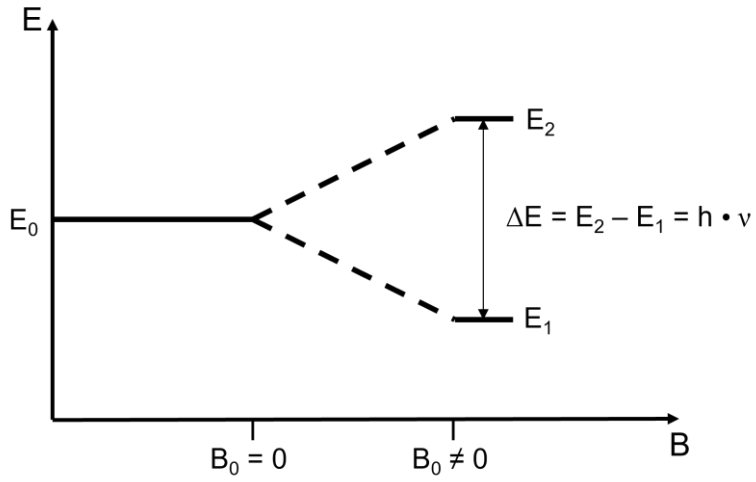

Figure 11. Zeeman splitting.

In the ground state nuclear magnetic moments are aligned randomly. When an external magnetic field (B_0) is applied, the magnetic moments arrange as shown in Figure 10. This leads to a cancellation of the degeneration of the nuclei and the magnetic moment takes on two different orientations and thus splits to two different energies with an energy difference called Zeeman splitting (Figure 11). If a high frequency electromagnetic alternating field corresponds exactly to the energy difference ΔE, resonance occurs between the irradiated alternating field and the nuclei. The nuclei are shielded from the external magnetic field to various degrees by the electron shell of the atoms, as the electron density has an influence on the effective field strength. An example is neighboring atoms which affect the splitting of nuclear energy levels through inductive or mesomeric effects. By changing the chemical environment and thus the structure of a molecule, there is a shift in the resonance frequency of the nucleus under consideration. This chemical shift allows conclusions to be drawn about the molecular structure. Thus, the number of NMR-active nuclei and the bonding states can be determined in order to identify functional groups, single and multiple bonds, as well as the number and type of bonding partners. However, the analysis of large, non-symmetrical molecules is limited by overlapping peaks.[151,152,153]

4.4 Electrospray Ionization Mass Spectrometry (ESI-MS)

MS is a suitable method for determining the mass of molecules and thus contributes to structural elucidation. However, it is not able to separate optical and geometric isomers. Furthermore, hydrocarbons that form similar ions cannot be identified. In MS, the molecule

under investigation is transferred to the gas phase in the so-called desorption and is subsequently ionized. Ionization is the process of removing electrons from an atom or molecule, usually creating a positively charged ion (cation). For the herein described projects, the electrospray method was used to generate ions. In electrospray ionization, the sample solution is passed through a metal capillary and a voltage is applied at the capillary tip. This leads to the formation of an electric field between the capillary and a counter electrode, which enters the sample solution. The electrons of the sample move electrophoretically to the counter electrode and an excess of similarly charged ions forms at the tip of the capillary. These repel each other and are released from the capillary as a fine aerosol.[154,155]

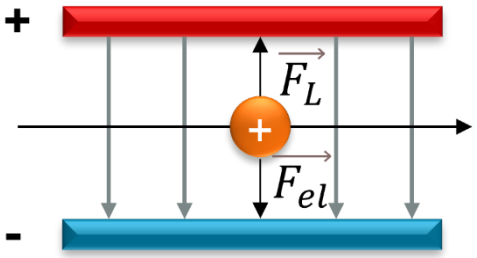

Figure 12. Ionized particles between plate capacitors.

The resulting ions are then accelerated by an electric field and passed to the analyzer, which arranges them according to their mass-to-charge ratio (m/z). The analyzer, which consists of a plate capacitor and a magnetic field, ensures that the ions have the same direction and speed. For the particles to fly straight through, the Lorentz force ($\overrightarrow{F_L}$) and the electrical force ($\overrightarrow{F_{el}}$) acting upwards and downwards respectively, must equalize each other (Figure 12). Consequentially, the mass of a particle can be calculated by knowing its charge q.[156,157]

4.5 Ultraviolet-Visible (UV-Vis) Spectroscopy

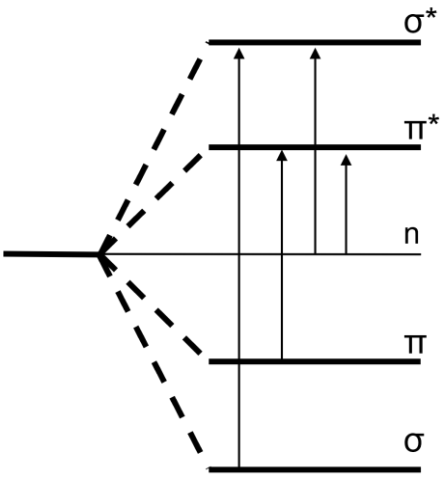

Figure 13. Molecule orbital (MO) diagram.

Samples that absorb in the UV-vis range, such as chromophores, can be analyzed with UV-Vis spectroscopy. It is based on measuring the absorption of visible and UV light by unsaturated organic sample where valence electrons of σ and π bonds become excited. According to the diagram of MO, the orbitals divide into a binding and an antibinding orbital when they overlap (Figure 13). Usually, the electrons fill the binding σ and π orbitals, while the antibinding σ* and π* orbital remains empty. In the case of an excitation, these electrons rise to the antibinding orbital. The necessary energy difference to excite an electron from the highest occupied molecular orbital (HOMO) into the lowest unoccupied molecular orbital (LUMO) is the excitation energy. Therefore, the molecule can only be excited with a certain wavelength as the absorption only takes place when the irradiated wavelength corresponds to excitation energy. In the case of UV as radiation source, the $\pi \rightarrow \pi^*$ transitions are in range compared to the $\sigma \rightarrow \sigma^*$ transitions which would require more energy due to the larger splitting of binding and antibinding orbitals. The presence of an electron in an antibinding orbital has consequences on the molecule and leads to a relaxation of the chemical bond affected. Normally, the electron immediately returns to the ground state, but further relaxation processes can be triggered that lead to bond breaks. The transmission or extinction spectrum thus enables the identification and quantitative determination of analytes. The wavelength-dependent information is obtained, among other things, by selecting and scanning the wavelength of the incident light in front of the sample with a double-beam spectrometer. The transmission spectrum results from the ratio of the spectral intensity of the transmitted and incident light, while the extinction spectrum is the logarithmic reciprocal of the transmission. The basis for photometry is Lambert-Beer law,

which describes the attenuation of the radiation intensity in relation to the initial intensity when passing through a medium with an absorbing substance as a function of the concentration of the absorbing substance and the layer thickness.[158,159,160]

4.6 Dynamic Light Scattering (DLS)

The hydrodynamic radius (r_h) of macromolecules can be determined using the DLS analysis method. In this method, the scattered light of a laser is detected on a dissolved or suspended sample. In the presence of particles, light is scattered in all directions according to the principle of Rayleigh scattering, which then interferes with each other via different scattering centers. Rayleigh scattering states the elastic scattering of electromagnetic waves by small molecules. Coherent and monochromatic laser light ensures small fluctuations in the scattering intensity of this generated interference, since the distances between the scattering centers constantly change due to Brownian molecular motion. A closer examination of the time scale of the fluctuations allows the determination of the velocity of the particles in the solution. Through an automated non-linear adjustment of the autocorrelation function according to the method of least squares, the translational diffusion coefficient (D) can be determined.

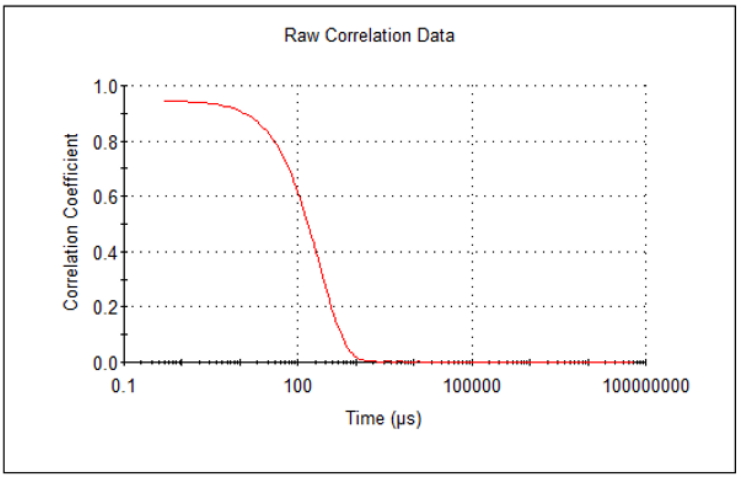

Figure 14. Typical correlation curve of a monodisperse sample.

The autocorrelation function specifies the observed time-dependent fluctuations of the light scattering intensity (Figure 14). The typical correlation curve of a monodisperse sample is linear and almost constant at the beginning. Since the correlation curve describes how long a particle remains in the same place, this linearity means that the particle is in the same place as before. Later, an exponential decrease of the function can be observed, which is due to the

movement of the particle. If there is no similarity with the initial location of the particle, the correlation function again shows a linear behaviour, which is referred to as the baseline in the curve. After determining D, r_h can be calculated using the Stokes-Einstein relation (eq. 1), which describes the correlation between the particle size and the velocity of the particles. k_b describes the Boltzmann's constant, T the temperature in K and η the viscosity of the solvent.[161,162,163]

$$r_H = \frac{k_B T}{6\pi\eta D} \quad (1)$$

5 Motivation and Outline

From the previous subchapters, the importance of sugar structures in our lives and in our environment is evident. These natural glycoconjugates, which cover every living cell, are involved in essential biological functions like cell-cell interactions or the recognition of viruses, bacteria and other pathogens. The mimicking of these difficult-to-synthesise glycoconjugates by glycopolymers enables the development and design of novel biofunctional and biomedical materials. Not only can carbohydrate-containing structures be utilized to investigate and regulate biological processes, but they can also be used as polymeric coatings or materials themselves for functional tasks, such as drug delivery, tissue engineering or medication. However, the development of these glycomaterials is challenging due to the high polarity and diversity of sugar structures. For this reason, this work focuses on the development of synthetic pathways for glycostructures.

More specifically, the work focused on the synthesis of glycomonomers, the precursors for carbohydrate-based materials. The focus was on a simple implementation and the employment of as few synthesis steps as possible. This was mainly accomplished by refraining from the introduction of protection groups. The syntheses were partly supported by microwave irradiation and/or enzyme catalysis. Selected synthesized monomers were then polymerized using the radical polymerization technique for lectin-sugar binding studies or to generate a thermoresponsive material for potential drug delivery.

The synthesis of glycopolymers for lectin-sugar binding studies only allows derivatization of the anomeric position to ensure recognition by the lectins. Also, depending on the lectin being used, control of stereoselectivity is relevant. For this purpose, two different synthetic routes for the preparation of glycomonomers are discussed. The first synthetic pathway presented led to the formation of β-glycomonomers, which is completed in two reaction steps. The first reaction step is a microwave-assisted amination according to the mechanism of Kochetkov and Likhorshetov (Chapter 7). The advantage of these ammonium salt-based method is the derivatization of the carbohydrates without protection groups. The synthesis of glycomonomers and resulting glycopolymers as inhibitors of pathogens is subsequently reported in detail (Chapter 8). The alternative synthetic route for the preparation of an alpha-glycomonomer is described in Chapter 9. For this purpose, Staudinger ligation was used, which requires the synthesis of a suitable triphenylphosphine derivative. To develop a potential drug delivery system, Chapter 10 discusses the syntheses of nucleoside-containing

monomers. The combination of MW irradiation and immobilized lipase enables the synthesis of cytidine-based monomers without the introduction of protection groups. Alternatively, a synthetic route for the isolation of cytidine- and complementary guanosine-containing monomers by oxidation and subsequent amide coupling is presented, which is only viable with acetonide protecting groups (Chapter 11). After polymerization of these nucleoside monomers using the RAFT method, the self-assembly behavior of the respective block copolymers was investigated. The closing discussion refers to the entirety of all individual manuscripts (Chapter 12). It places the individual results in an overall context that fit into the current state of knowledge on the topic. This work therefore investigates synthetic routes of glycoderivatives to glycopolymers that can potentially function as biofunctional materials.

6 Contribution Statement of Publications

This doctoral thesis is based on following scientific publications. Numbering of chapters, figures, schemes and tables, as well as font styles, page settings and general style are adjusted to this work.

1. "Optimization of the Microwave Assisted Glycosylamines Synthesis Based on a Statistical Design of Experiments Approach" (Chapter 7)[164]

Jo Sing Julia Tang, Kristin Schade, Lucas Tepper, **Sany Chea**, Gregor Ziegler and Ruben R. Rosencrantz

Molecules **2020**, *25*, 5121

DOI: 10.3390/molecules2521512

Own contribution: planning and implementation of several amination reactions including their molecular characterization by NMR spectroscopy.

Data from Ref. 164 with permission from MDPI.

2. "Functional Glyco-Nanogels for Multivalent Interaction with Lectins" (Chapter 8)[165]

Jo Sing Julia Tang, Sophia Rosencrantz, Lucas Tepper, **Sany Chea**, Stefanie Klöpzig, Anne Krüger-Genge, Joachim Storsberg and Ruben R. Rosencrantz

Molecules **2019**, *24*, 1865

DOI: 10.3390/molecules24101865

Own contribution: research, planning and implementation of the synthesis of the fucosyl monomer and precursor including their molecular characterization by NMR spectroscopy and ESI-MS spectrometry.

Data from Ref. 165 with permission from MDPI.

3. "Protection group-free synthesis of α-mannopyranosyl methacrylamide" (Chapter 9)

Sany Chea, Gregor Ziegler, Ruben R. Rosencrantz

In preparation

Own contribution: research, design, planning of compound syntheses; performance of preliminary experiments; molecular characterization by NMR spectroscopy and ESI-MS spectrometry; conceptualization and writing of the manuscript.

4. "Microwave-assisted synthesis of 5'-*O*-methacryloylcytidine using the immobilized lipase Novozym 435" (Chapter 10)[166]

Sany Chea, Khac Toan Nguyen and Ruben R. Rosencrantz

Molecules **2022**, *27*, 4112

DOI: 10.3390/molecules27134112

Own contribution: research, design, planning of compound syntheses; performance of preliminary experiments; molecular characterization by NMR spectroscopy and ESI-MS spectrometry; conceptualization, writing and revision of the manuscript.

Data from Ref. 166 with permission from MDPI.

5. "Synthesis and self-assembly of cytidine- and guanosine-based copolymers" (Chapter 11)[168]

Sany Chea, Kristin Schade, Stefan Reinicke, Regina Bleul, and Ruben R. Rosencrantz

Polym. Chem. **2022,** *13*, 5058

DOI: 10.1039/d2py00615d

Own contribution: research, design, planning and implementation of compound syntheses; molecular characterization by NMR and UV-Vis spectroscopy, ESI-MS spectrometry and DLS; conceptualization, writing and revision of the manuscript.

Reproduced from Ref. 168 with permission from the Royal Society of Chemistry.

7 Optimization of the Microwave Assisted Glycosylamines Synthesis Based on a Statistical Design of Experiments Approach

7.1 Abstract

Glycans carry a vast range of functions in nature. Utilizing their properties and functions in form of polymers, coatings or glycan derivatives for various applications makes the synthesis of modified glycans crucial. Since amines are easy to modify for subsequent reactions, we investigated regioselective amination conditions of different saccharides. Amination reactions were performed according to Kochetkov and Likhoshertov and accelerated by microwave irradiation. We optimized the synthesis of glycosylamines for *N*-acetyl- D-galactosamine, D-lactose, D-glucuronic acid and L-fucose using the design of experiments (DoE) approach. DoE enables efficient optimization with limited number of experimental data. A DoE software generated a set of experiments where reaction temperature, concentration of carbohydrate, nature of aminating agent and solvent were investigated. We found that the synthesis of glycosylamines significantly depends on the nature of the carbohydrate and on the reaction temperature. There is strong indication that high temperatures are favored for the amination reaction.

7.2 Introduction

Glycosylation is a crucial modification of biomolecules involved in almost all biological processes.[167,169,170,171,172] Glycans may act as scaffolds for mechanical stabilization, as cell-surface coating, enabling cellular crosstalk and have various functions including in diseases.[173,174,175,176,177,178] Especially for the latter, potent inhibitors of glycan-binding proteins (lectins) are sought after, as well as glycan scaffolds for trapping pathogens.[179,180,181] For all examples, the glycans may be chemically modified and presented in polymers,[182,183,184] on surfaces,[185,186,187,188] on nanoparticles[189,190,191] or as (multivalent) glycan derivatives[192,193,194,195] with increased binding affinity.[52,196,197] Prerequisites for this are straight forward chemical processes that yield regioselective modifications of glycans without hampering the natural recognition processes. For this, very diverse chemical routes have been employed which can be roughly distinguished between protecting group dependent and

protecting group free or even enzymatic routes.[103,198,199,200] Protecting group free routes in general require less synthesis steps, but the reaction conditions and purification must be elaborated carefully. However, we utilized a protecting group free process to regioselectively insert an amino group into saccharides at the C1 position which was subsequently modified into a methacrylamide to generate glycopolymers.[165,201] From literature and our work, amination seems a rather robust process, but it turned out that chosen reaction conditions influence the yield substantially. Interestingly, this effect was diverse for different carbohydrates. This amination was introduced by Kochetkov and later modified by Likhoshertov.[202,203,204,205] The Kochetkov reaction is performed with ammonium carbonate whereas the amination according to Likhoshertov employs ammonium carbamate as the aminating agent. Significant advantages of these methods are enabling of protecting group free synthesis routes, the regioselectivity and the applicability on various oligosaccharides with only few and cost-efficient reagents. Essentially, a saccharide is stirred in solvent with an excess amount of amination agent. It is a straightforward approach to regioselectively insert a single functional group into various glycans and enables subsequent coupling to generate glycoconjugates. The Kochetkov amination is further facilitated by employing the advantageous features of microwave assisted synthesis. The reaction can be tremendously accelerated by microwave irradiation, shortening the initial reaction time of 5 d to 90 min.[185,206] Moreover, the use of microwave irradiation allows the tenfold reduction of the amount of ammonium salt, facilitating homogeneous suspending of starting material and purification.[206] To the best of our knowledge, the amination according to Likhoshertov has not been performed under microwave irradiation yet. Here, we investigate this synthesis using microwave irradiation as well. As the syntheses have a broad substrate scope and are only a one-step procedure, they seem a very worthwhile approach to yield glycan derivatives for follow-up functionalization to achieve glycomonomers, biosensor coatings and others. We chose a statistical approach to efficiently determine the optimal amination conditions of saccharides and to study the use of design of experiment (DoE) for optimization of glycochemistry reactions.

Design of experiments is a valuable tool to limit the amount of data needed to find optimal experimental conditions. Any method to optimize a synthesis of interest starts by identifying the parameters of the reaction, namely, temperature, concentration or reaction time. In a classical optimization setting, all but one parameter are kept constant at a time, and the result of the experiment, such as yield or purity, is improved. This strategy, referred to as “one-variable-at-a-time” (OVAT), can be unnecessarily labor-intensive and fails to capture

correlations between the input parameters. If these input factors influence each other strongly, OVAT might not find the true optimum of the experimental conditions and the result depends on the initial reaction conditions selected.[207] To circumvent this obstacle, we use a statistical design of experiments approach as an alternative to the OVAT method. DoE aims to evenly sample all possible values for the input parameters and find a mathematical relationship between them and the outcome of the experiment. Although it has been known since the early 1900s, it has only recently found wide-spread application.[208,209,210,211,212,213,214] DoE was previously employed to optimize synthetic procedures with a small number of experiments.[213,214,215,216,217,218] A successful application of DoE guides the selection of further experiments and allows the localization of most promising sets of features. It has become increasingly accessible to researchers through the advent of user-friendly software options such as MODDE or JMP.

Contrary to former studies, where amination was mostly optimized for one specific carbohydrate,[185,206,219] we show the significance of and possible interactions between selected parameters for each respective saccharide, as the yield and optimal reaction conditions are strongly determined by the nature of chosen saccharide.[185,203,206,219,220,221] For instance, Likhoshertov et al. yielded 81 % aminated D-glucuronic acid, while the amination of L-fucose resulted in a yield of 52 % with the same reaction conditions.[203] By utilizing the DoE software MODDE, we optimized the reaction conditions for four selected saccharides: *N*-acetyl-D-galactosamine (GalNAc), D-lactose (Lac), D-glucuronic acid (GlcA) and L-fucose (Fuc). These saccharides are important for biomolecular interactions on the one hand and, on the other, they resemble an overview of the most common chemical properties of non-modified glycans, such as *N*-acetyl glycans, disaccharides, uronic acids and desoxy-glycans.

7.3 Results and Discussion

7.3.1 Optimizing the Amination of Oligosaccharides

We optimized the synthesis of glycosylamines using a statistical DoE approach. As our synthesis route, we chose the amination methods of Kochetkov and Likhoshertov assisted by microwave irradiation (Scheme 11).

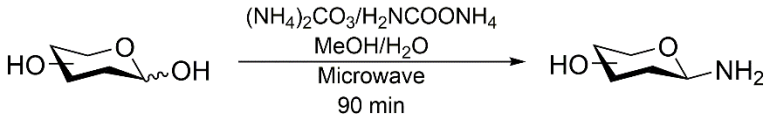

Scheme 11. Protecting group free and microwave-assisted synthesis route for amination of free saccharides according to Kochetkov and Likhoshertov in methanol or water with a 5-fold excess of ammonium salt.

To promote an equal distribution of microwave irradiation for all experiments, the volume of solvent was kept constant. We chose to vary reaction temperature, concentration of starting material, solvent and ammonium salt as our quantitative and qualitative parameters (Table 1). Ranges of temperature and concentration were set to 30 – 60 °C and 10 – 100 mg/mL, respectively, as the conditions of previous studies mostly lie within these ranges. Former studies showed successful amination of saccharides in water, dimethyl sulfoxide and methanol.[185,202,206,219,221,222,223,224] We tested water and methanol as solvent, since they are more readily removed by evaporation than dimethyl sulfoxide. In addition, ammonium salts and unmodified oligosaccharides generally dissolve better in water than in organic solvents, which might be beneficial for reaction and yield. The other qualitative parameters are the aminating agents ammonium carbonate and ammonium carbamate.

Table 1. Reaction conditions and yields of amination. Highest yields are indicated by underscores.

Exp No	T (°C)	(mg/mL)	Salt	Solvent	Yield (%)			
					Am-I $GalNAcNH_2$	Am-II $LacNH_2$	Am-III $GlcANH_2$	Am-IV $FucNH_2$
01	60	10	$(NH_4)_2CO_3$	MeOH	<u>64.2</u>	<u>83.6</u>	7	60.5
02	30	100	$(NH_4)_2CO_3$	MeOH	53.7	33	0.9	12.4
03	60	100	$(NH_4)_2CO_3$	MeOH	42.2	68	33.6	21.8
04	30	40	$(NH_4)_2CO_3$	MeOH	43.1	46.4	2.1	45
05	40	10	$(NH_4)_2CO_3$	MeOH	30.9	20.8	1.6	25
06	30	10	$H_2NCOONH_4$	MeOH	33.6	11.8	3.3	42.6
07	60	10	$H_2NCOONH_4$	MeOH	51.6	81.4	12	<u>69.8</u>
08	30	100	$H_2NCOONH_4$	MeOH	44.9	27.4	3	32.4
09	60	100	$H_2NCOONH_4$	MeOH	41.9	79.2	23.6	38.8
10	45	55	$H_2NCOONH_4$	MeOH	57.4	79.7	53.1	26
11	30	10	$(NH_4)_2CO_3$	H_2O	39.1	16.7	16.8	16.2
12	60	10	$(NH_4)_2CO_3$	H_2O	27.3	26.2	35.7	18.2
13	30	100	$(NH_4)_2CO_3$	H_2O	26.5	11.5	37.3	9
14	60	70	$(NH_4)_2CO_3$	H_2O	37.8	42.4	54.6	10.3
15	50	100	$(NH_4)_2CO_3$	H_2O	20.4	44.3	51.9	8.4
16	30	10	$H_2NCOONH_4$	H_2O	41.2	8.8	18.3	6.9
17	60	100	$H_2NCOONH_4$	H_2O	50.5	30.2	46.8	12.4
18	30	70	$H_2NCOONH_4$	H_2O	29.4	13.5	47.8	8.7
19	60	40	$H_2NCOONH_4$	H_2O	44.2	21.5	44.4	17.1
20	50	10	$H_2NCOONH_4$	H_2O	30	20.1	46.1	11.1
21	40	100	$H_2NCOONH_4$	H_2O	34.4	24.7	40.3	8.7
22a	45	55	$H_2NCOONH_4$	H_2O	17	32.5	77.7	33.3
22b	45	55	$H_2NCOONH_4$	H_2O	20.4	74.1	77	41.8
22c	45	55	$H_2NCOONH_4$	H_2O	18	62.5	<u>81.6</u>	31.2

We tested the optimization conditions on four chosen saccharides: (I) *N*-acetyl-D-galactosamine (GalNAc), (II) D-lactose (Lac), (III) D-glucuronic acid (GlcA) and (IV) L-fucose (Fuc) (Figure 15).

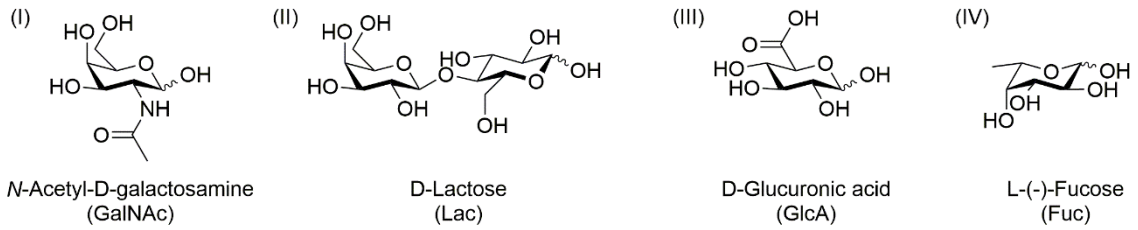

Figure 15. Mono- and disaccharides chosen for the optimization of amination reactions.

The products were not isolated but solvents were fully and ammonium salts were partially or mostly removed under high vacuum. We determined the yields by ^1H NMR spectroscopy in deuterium oxide. Here, the peak of the anomeric proton of glycosylamine was

analyzed in relation to a known peak that both starting material and glycosylamine share, for example, the methyl moiety of GalNAc/GalNAcNH$_2$. NMR spectroscopy offers fast and easy analysis without requiring the isolation of products and is sufficient for the optimization process. However, it is known that glycosylamines can hydrolyze in D_2O which could distort the actual yield. The hydrolysis rate is decreased with higher pH value.[222] Experiments performed with high amounts of aminating agents can lead to residuals of them after drying and therefore to higher pH values. Due to the basic conditions, less hydrolysis might occur which does not distort the yield as much as experiments performed with low amounts of ammonium salts.

We used the DoE software MODDE to design a set of experiments with varied reaction parameters for optimization. MODDE provides a summary of fit with four values which estimate how well the respective model works. R^2 indicates how well the model fits the data and should be of large value for a good model. An R^2 of 0.5 presents a model with rather low significance. The prediction value Q^2 estimates the predictive power of the model and is the most sensitive indication. Here, a value above 0.1 represents a significant model whereas a value above 0.5 expresses a good model. However, Q^2 should not deviate from R^2 by more than 0.3. A model validity of 1.0 represents a perfect model. If the model validity is below 0.25, there are indications of statistically significant problems with the model. Values above 0.25 show that the model error is in the same range as the pure experimental error. The reproducibility value represents the experimental error according to the deviation of responses of repeated experiments and should be above 0.25. MODDE displays a coefficient plot where the significance of chosen factors and their interactions is shown (Supporting Information). We removed non-significant terms from the model.

7.3.2 Design of Experiment Approach

The amination of GalNAc was investigated, as this saccharide is not only a model compound for 2-*N*-acetylated sugars, but also an important saccharide in mucin-like *O*-glycosylation. In the experimental set for GalNAc, we recognized the data of the experiments Am-I-06 and Am-I-10 (Table 1) as outliers and removed them from the model. The summary of fits of GalNAc (Figure 16a) presents an R^2 value of 0.80 and a Q^2 value of 0.50, which indicates a good model. The model validity of 0.27 is rather low; the reproducibility displays a very good value of 0.98. The model validity might be low due to the great reproducibility value.

Overall, this model of GalNAc is significant. Significant terms according to MODDE are temperature, concentration, both aminating agents ammonium carbonate and carbamate, the solvents methanol and water and the quadratic term of temperature × temperature, concentration × concentration, ammonium carbonate × water, ammonium carbamate × methanol and ammonium carbamate × water (Figure 16b). The 4D contour plot represents predicted response values as a function of chosen (and significant) factors. Figure 16c shows the yield as a function of concentration (Y-axis) and temperature (X-axis) for both ammonium salts and both solvents, respectively. According to this, temperature and concentration greatly influence the yield. Ammonium carbonate affects the yield only when different solvents are compared. Amination with ammonium carbamate is similar in both water and methanol. We found that the highest yield (64.2 %) is achieved at the highest chosen temperature (60 °C) and at the lowest tested concentration (10 mg/mL) with ammonium carbonate and methanol. MODDE calculated optimized conditions with exactly the same reaction conditions and a predicted yield of 54.7 %. The predicted yield differs from the achieved one by more than the error deviation; additionally, the calculated optimized yield is lower than the highest yield achieved. This indicates statistical problems of this model. Considering the quantity of varied parameters, a rather small set of experiments has been conducted. A larger number of experiments can improve the model. Since the experimental conditions with methanol and ammonium carbonate proved to be superior, we suggest the collecting of additional data for mentioned condition to further improve the model and optimize the amination conditions for GalNAc.

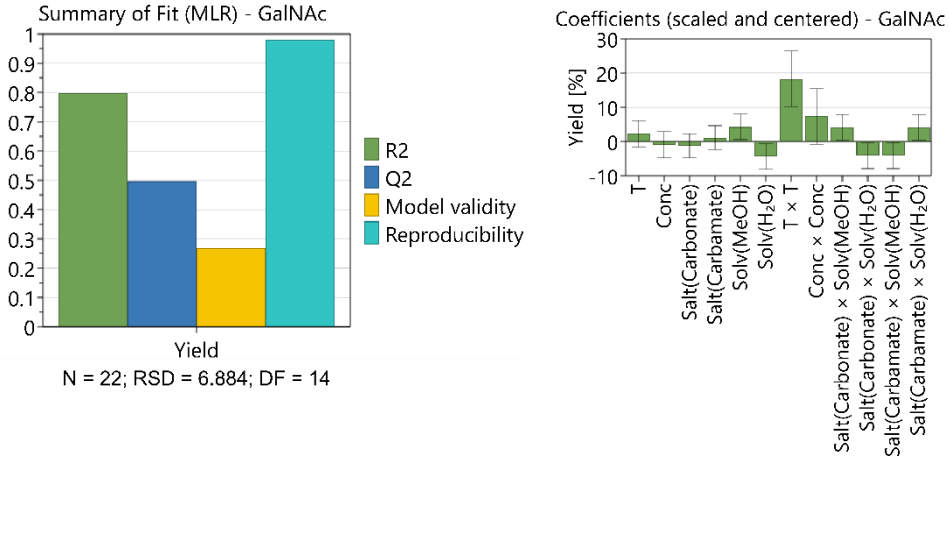

(a) **(b)**

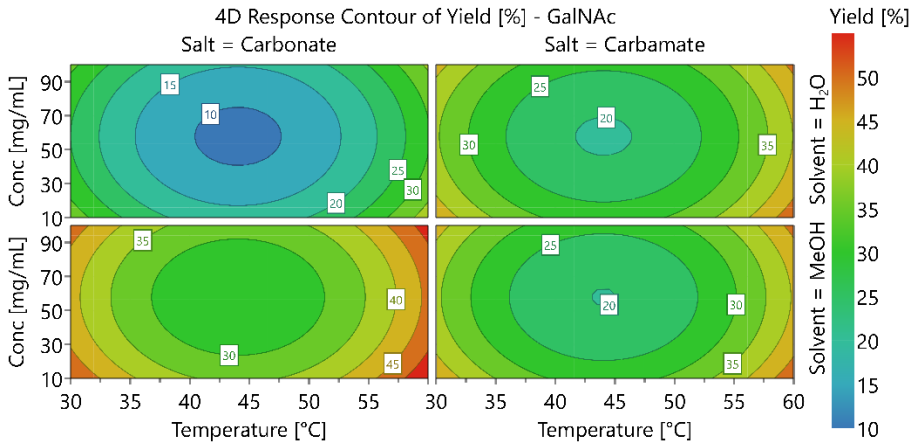

(c)

Figure 16. Plots of the model for GalNAc generated by MODDE: (a) Summary of fit shows a rather low significance of the model; (b) plot of coefficient values for scaled and centered factors shows significant factors according to the model; (c) the 4D response contour plot of yield predicts yields of amination in dependence on qualitative and quantitative factors.

Next, we investigated the reaction of Lac, which is our model compound for disaccharides and also an important ligand for lectins, mostly due to the terminal Gal residue. The summary of fits of the model for Lac shows good values with R^2 = 0.75 and Q^2 = 0.59 (Figure 17a). It has an excellent model validity of 0.97 and a low reproducibility of 0.29. Thus, we understand the model for Lac has high significance. Significant terms are temperature, concentration, the solvents methanol and water, the quadratic term of concentration × concentration, temperature × methanol and temperature × water (Figure 17b). Hence, the

amination of Lac is less dependent on the nature of ammonium salt than on the other factors. The 4D response contour plot for Lac shows that the yield increases with rising temperature and with a concentration converging at 58.3 mg/mL (Figure 17c). We can clearly observe a strong dependence of the yield on temperature and less on concentration. Furthermore, the plot indicates that temperatures above 60 °C may lead to even better yields. Surprisingly, the solvent methanol is by far superior to water even though the solubility of Lac is poor in methanol. We conclude that the solubility of a saccharide is not a determining factor for the amination according to Kochetkov and Likhoshertov. As well as for GalNAc, we obtained the highest yield for Lac (83.6 %) at the highest temperature (60 °C) and the lowest concentration (10 mg/mL) with ammonium carbonate and methanol. Calculated optimized conditions for Lac are a temperature of 60 °C and a concentration of 58 mg/mL with ammonium carbonate and methanol. After conducting the optimized experiment, we could indeed increase the yield to 91.1 %. The deviation from the predicted yield of 100.4 % lies within the experimental error. The prediction lies above 100 %, as solely the target was set to 100 % and not the maximum (the maximum cannot equal the target in MODDE). Overall, the DoE approach successfully improved the yield of aminated Lac.

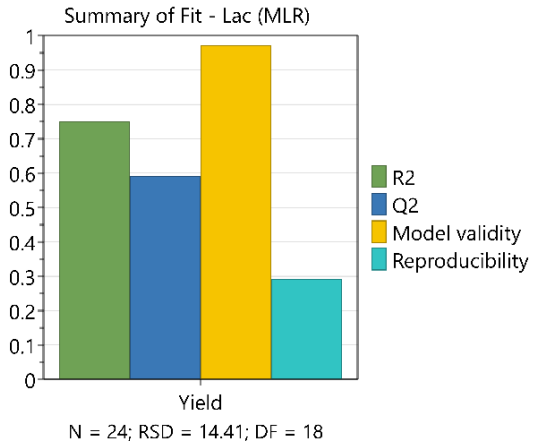

(a)

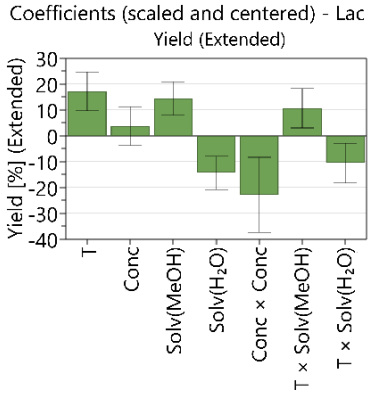

(b)

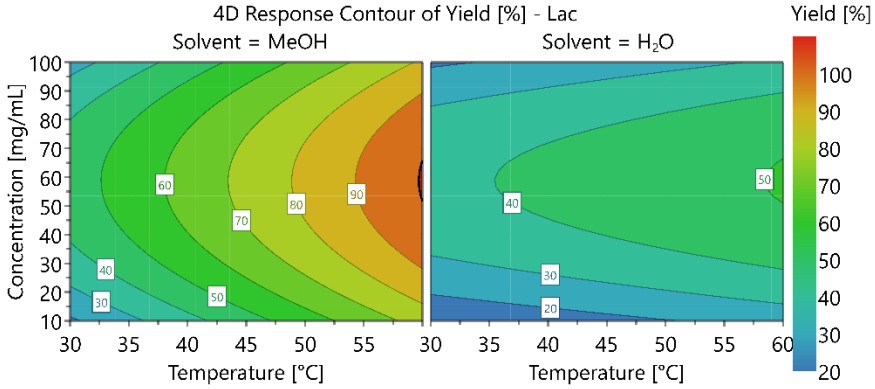

(c)

Figure 17. Plots of the model for Lac generated by MODDE: (a) Summary of fit represents a good model; (b) plot of coefficient values for scaled and centered factors shows significant factors according to the model; (c) the 4D response contour plot of yield predicts yields of amination in dependence on qualitative and quantitative factors.

GlcA is a uronic acid and therefore our model compound for this class of saccharides. After amination a zwitter-ionic compound is produced. In humans, GlcA is mostly found in glucosaminoglycans. The summary of fits for GlcA displays excellent values of $R^2 = 0.94$ and $Q^2 = 0.84$ (Figure 18a). In comparison, the model validity is rather low (0.39) which may be due to the high reproducibility value of 0.99 and not due to a real lack of fit. Significant terms for GlcA are temperature, concentration, both aminating agents ammonium carbonate and

ammonium carbamate, the solvents methanol and water, the quadratic term of temperature × temperature, concentration × concentration, temperature × methanol, temperature × water, concentration × ammonium carbonate and concentration × ammonium carbamate (Figure 18b). The amination of GlcA seems strongly dependent on temperature, concentration and choice of solvent. Interestingly, for GlcA further factors are significant including the nature of ammonium salt and its dependency on the concentration. From the 4D contour plot (Figure 18c), it is evident that water works better than methanol for the amination of GlcA. Regarding the aminating agent, ammonium carbamate appears to be the preferred choice. In experiments, the highest yield (81.6 %) was achieved at 45 °C, 55 mg/mL with ammonium carbamate in water. Optimized reactions conditions are 47 °C, 59 mg/mL, ammonium carbamate and water with a predicted yield of 73.8 %. The optimized experimental conditions resulted in a yield of 60.3 %. The predicted yield is lower than the highest yield found in previous experiments and, furthermore, does not correlate to the yield found. This hints at statistical problems of the model even though the prediction value Q^2 was very good. Moreover, in this model yields above 73.8 % are not achievable although Ghadban et al. did attain yields of up to 89 %.[219] We suggest a larger set of experiments and a wider range of reaction parameters for the reaction conditions with water and ammonium carbamate to improve the model.

Our model compound for desoxy-sugars is 6-desoxy galactose, better known as Fuc. Fuc-based derivatives could, for example, be important for inhibiting the formation of *Pseudomonas aeruginosa* biofilms. Additionally, it is a very abundant sugar in human milk oligosaccharides. The summary of fits for Fuc presents a good R^2 value of 0.67 and a Q^2 value of 0.40 (Figure 19a). The model validity is 0.57 and the reproducibility has a high value of 0.90. Thus, this is a model of lower significance. Although the histogram of the Fuc experiments exhibits positive skewness (Supplementary Materials), no transformation was performed, as the model for Fuc produced better values than without transformation. MODDE displays the significant terms temperature, concentration, both salts ammonium carbonate and carbamate, the solvents methanol and water, the square term of temperature × concentration, temperature × methanol, temperature × water, concentration × methanol and concentration × water (Figure 19b). Thus, the amination of Fuc greatly depends on temperature, concentration and nature of solvent. Furthermore, the choice of ammonium salt and the influence of temperature and concentration on the solvents affect the yield, too. In the 4D contour plot of yield (Figure 19c), when comparing the solvents, we see that overall methanol leads to higher yields. Water seems to work poorly for the amination of Fuc. Regarding the aminating agent, the highest yield is

obtained with ammonium carbamate. Yield increases with rising temperature and decreasing concentration. Hence, a further increase of the temperature and decrease of the concentration might improve the yield. We obtained the highest yield of 69.8 % at 60 °C and 10 mg/mL with ammonium carbamate and methanol. Optimized amination conditions for Fuc are the exact reaction conditions with a predicted yield of 63.4 %. The predicted yield is lower than the already obtained yield but lies within the experimental error. This still indicates a flawed model, which correlates to the rather low prediction value Q^2. However, the optimized reaction conditions coincide with the performed conditions with the best result. To further optimize the amination of Fuc, the model should be improved by producing more data of experiments where methanol is used as the solvent.

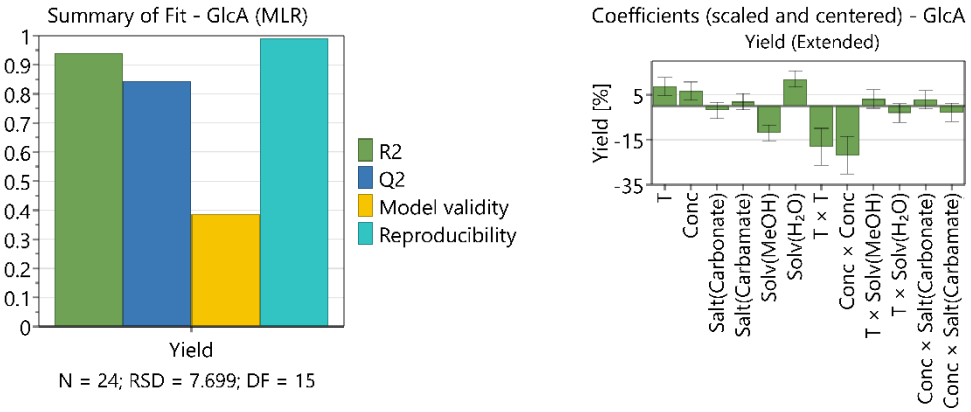

(a) **(b)**

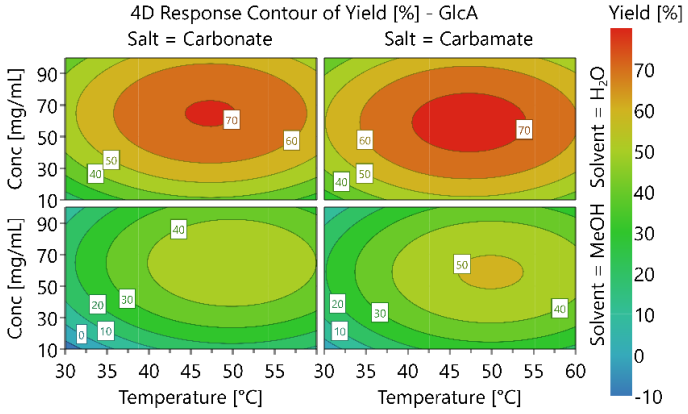

(c)

Figure 18. Plots of the model for GlcA generated by MODDE: (a) Summary of fit represents a good model; (b) plot of coefficient values for scaled and centered factors show significant factors according to the model; (c) the 4D response contour plot of yield predicts yields of amination in dependence on qualitative and quantitative factors.

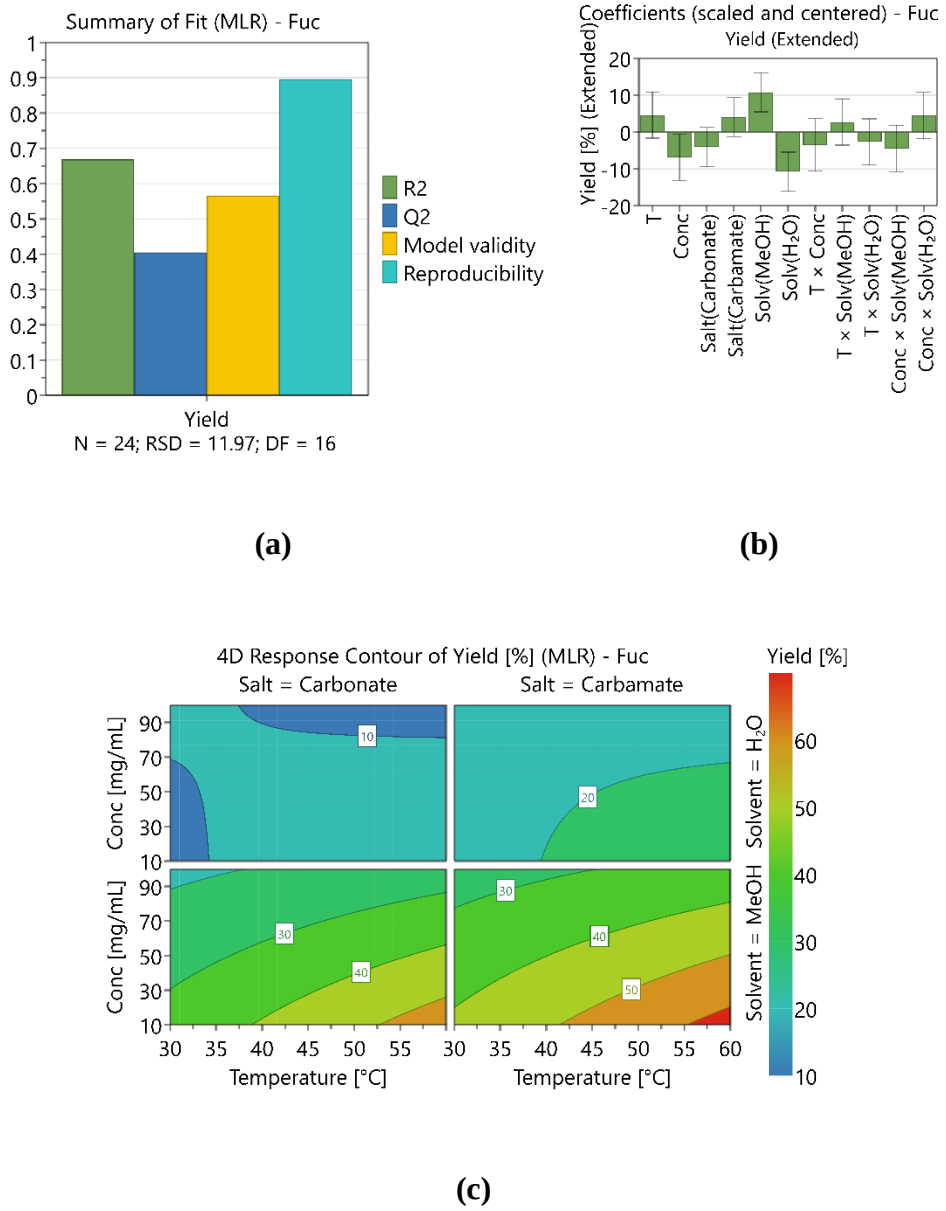

Figure 19. Plots of the model for Fuc generated by MODDE: (a) Summary of fit shows a lower significance of the model; (b) plot of coefficient values for scaled and centered factors show significant factors according to the model; (c) the 4D response contour plot of yield predicts yields of amination in dependence on qualitative and quantitative factors.

Overall, for the amination of carbohydrates according to the Kochetkov and Likhoshertov method, the reaction temperature has the most significant influence on the yield. The contour plots of MODDE indicate that higher yields are achievable at temperatures above 60 °C. In contrast, according to Bejugam et al. higher temperatures generally lead to an increased formation of side products and, therefore, lower yields.[206] Side products, such as dimers, were not analyzed but as such would usually not disturb subsequent reactions like, for example, (meth-)acrylations.[165,201] Though colorations of yellow and reddish brown were

observed after reaction at temperatures above 50 °C, this did not seem to diminish the yield of glycosylamines. Concentration of saccharide does affect the yield but not strongly. Surprisingly, suspension of highly concentrated reactions did not necessarily decrease the yield even though thorough stirring was not always possible; microwave irradiation and excess amount of ammonium salt was enough to aminate the saccharides in the suspension. Choice of solvent also influences the yield and depends on the nature of saccharide. Contrary to our expectation, methanol seems to be the superior solvent for amination of saccharides except for GlcA. The poor solubility of saccharides and aminating agents in methanol shows no negative influence on the yield. In conclusion, the solubility of starting material does not seem to affect the amination. A possible explanation is that the temperature and microwave irradiation are enough to dissolve, aminate, or both, the saccharides in methanol. Moreover, water can lead to hydrolysis and hence decrease the actual yield during purification or analysis. Regarding the first-time use of microwave assisted amination according to Likhoshertov, good yields of up to 81.6 % could be obtained within 90 min as opposed to the 4 – 48 h from the traditional procedure.[203] Thus, microwave irradiation allows a great reduction of reaction time for the amination according to Likhoshertov, too. Generally, the nature of aminating agent can have an influence depending on selected saccharide, solvent, or both. This shows that both microwave-assisted syntheses work equally well as amination reaction for oligosaccharides and is not surprising since both ammonium salts are volatile and generate ammonia. Furthermore, we repeated experiment Am-I-01 (Table 1) with a 33-fold batch size in a 1 L PTFE vessel, as its reaction conditions lead to the highest yield achieved. In this way we investigated the scalability of the process in principle. The initial yield of 64 % dropped significantly even if the reaction time was doubled. No amine was found in NMR spectrum and only little amine was found by TLC. This may be due to different distribution of microwave irradiation in the larger volume, which could be another parameter for future investigations. However, we can also conclude that alterations of microwave distribution can be one of the reasons why yields from different publications and our yields may differ.

The DoE approach enabled a reduced number of experiments; however, if the model is insufficient, more experiments have to be conducted to improve the model. Predictions of the software support the direction of future experiments, namely, which solvent or aminating agent to use. We suggest additional experiments with higher reaction temperatures to further optimize the amination of saccharides. We consider investigating the reaction time to be worthwhile as well.

7.4 Materials and Methods

7.4.1 Materials

All chemicals were purchased from commercial sources. Water was double deionized by a Milli-Q purification system (18.2 MΩ·cm, Millipore Quantum TEX, Darmstadt, Germany). *N*-Acetyl-D-galactosamine (GalNAc; ≥ 9 9%, Carbosynth, Comptun, UK), D-lactose monohydrate (Lac; ≥ 96 %, Carbosynth), D-glucuronic acid (GlcA; ≥98%, Carbosynth), L-fucose (Fuc; ≥ 98 %, Carbosynth), ammonium carbamate ($H_2NCOONH_4$; 99 %, Aldrich, Steinheim, Germany), ammonium carbonate ($(NH_4)_2CO_3$; ≥ 30.5 % NH_3, extra pure, Carl Roth, Karlsruhe, Germany), methanol (MeOH; ≥ 98.8 %, VWR, Darmstadt, Germany), deuterium oxide (D_2O; 99.9 %, Deutero, Kastellaun, Germany) were used as received.

7.4.2 Methods

7.4.2.1 Design of Experiments (DoE)

The software MODDE version 12.1 (Sartorius Stedim Data Analytics AB, Malmö, Sweden) for generation and evaluation of statistical experimental designs was used to optimize synthesis conditions. We selected concentration of saccharide (Conc) and reaction temperature (T) as quantitative factors. The aminating agents (Salt) and solvents (Solv) represented our qualitative factors. We investigated the yield of the respective glycosylamine as response and set 100 % yield as target. We chose the D-optimal design (with highest G-efficiency) and quadratic model to generate a set of experiments for optimization. This set includes two replicates for testing reproducibility. The models were fitted with multiple linear regression (MLR) analysis.

7.4.2.2 Nuclear Magnetic Resonance (NMR)

^{1}H NMR spectra were recorded on a Bruker Neo Avance 400 MHz spectrometer (Bruker, Ettlingen, Germany) to identify the glycosylamines and determine their yields. We measured all spectra in D_2O. Yields of the respective glycosylamines were determined by evaluating the ratio between the integral of proton signals, that both starting material and glycosylamine share, and the integral that is solely specific to the respective glycosylamine. In

case of $GalNAcNH_2$, we examined the ratio between the integral of the methyl group proton signal of GalNAc/$GalNAcNH_2$ (H-7; 3 H) and the integral of the anomeric proton signal of the $GalNAcNH_2$ (n H; yield of glycosylamine = n × 100%). For $LacNH_2$, the ratio between the integral of the proton peak H-7 (1 H) and the integral of the anomeric proton signal of $LacNH_2$ (n H). As peaks of the anomeric proton of GlcA and its amination product overlap, we performed global spectral deconvolution (GSD) for analysis. The integral of the peaks of the protons H-2 to H-5 (4 H) were compared with the integral of the anomeric proton signal of $GlcANH_2$ (n H). The yield of $FucNH_2$ was determined by analyzing the ratio between the integral of the methyl group proton signal H-6 (3 H) and the integral of the anomeric proton peak of $FucNH_2$ (n H).

7.4.2.3 Electrospray Ionization Mass Spectrometry (ESI-MS)

ESI-MS spectra were recorded on a PerkinElmer Flexar SQ 300 MS (Rodgau, Germany). We dissolved samples in acetonitrile/water mixture (50:50) with 0.1 % formic acid. The measurements were performed at 300 °C with a flow rate of 15 μL min^{-1}.

7.4.2.4 Synthesis of Glycosylamines

Amination of saccharides were performed in a START 1500 rotaPREP microwave reactor (MLS GmbH, Leutrich, Germany). The respective saccharide is charged in a 50 mL-glass vessel and stirred with solvent. Afterwards, the ammonium salt is added under stirring and the reaction vessel is transferred to the microwave reactor. We set the reaction time to 90 min. The heating phase to our desired reaction temperature was set to 5 min. Volume of solvent was constantly 8 mL to ensure equal distribution of microwave irradiation for every experiment. We varied reaction temperature, concentration of saccharide, solvent and aminating agent according to Table 1. The last experiment is repeated three times in total for testing reproducibility. After reaction, samples prepared in MeOH were first concentrated by rotary evaporation at 40 °C and 300 mbar, followed by complete drying under high vacuum over several days or until most of the ammonium salt is removed. Aqueous reaction mixtures were lyophilized after reaction for several days or until most of the ammonium salt is removed. We yielded (hygroscopic) β-glycosylamines and stored them in nitrogen atmosphere at 4 °C.

The numbering of experiments starts with “Am” for amination, followed by the designated roman numeral of saccharide, GalNAc (I), Lac (II), GlcA (III)and Fuc (IV), and ends with the number of experiment. For example, Am-IV-03 refers to the amination of Fuc with the reaction conditions of experiment number 03. Experiments with optimized reaction conditions generated by MODDE carry the experiment number 0 (Table 2).

Table 2. Optimized reaction conditions and yields generated by MODDE.

Exp No	T (°C)	(mg/mL)	Salt	Solvent	Predicted Yield (%)	Found Yield (%)
Am-I-0/-01	60	10	$(NH_4)_2CO_3$	MeOH	54.7	64.2
Am-II-0	60	58	$(NH_4)_2CO_3$	MeOH	100.4	91.1
Am-III-0	47	59	$H_2NCOONH_4$	H_2O	73.8	60.3
Am-IV-0/-07	60	50	$H_2NCOONH_4$	MeOH	63.4	69.8

7.5 Conclusions

We optimized amination conditions for *N*-acetyl-D-galactosamine, D-lactose, D-glucuronic acid and L-(−)-fucose using DoE approach. Additionally, we showed that the acceleration of the amination according to Likhoshertov is possible by microwave irradiation. It is very apparent that optimized reaction conditions for one saccharide do not apply in the same way for other saccharides. Due to the relatively small number of experiments most models were lacking to some extent. However, the DoE approach supported the direction of which reaction parameters are worth further testing, including their quantitative and qualitative ranges or properties, respectively. The model for the amination of Lac provided a great improvement of yield. We observed strong indication that high temperatures are preferable for the amination. For future experiments, we suggest additional data of experiments with our found, most beneficial conditions to improve the models, testing of reaction time and of elevated temperatures.

7.6 Acknowledgments

We thank Angela Krtitschka from the University of Potsdam for enabling measurements of NMR spectra and Sophia Rosencrantz from Fraunhofer IAP for reviewing the manuscript.

8 Functional Glyco-Nanogels for Multivalent Interaction with Lectins

8.1 Abstract

Interactions between glycans and proteins have tremendous impact in biomolecular interactions. They are important for cell–cell interactions, proliferation and much more. Here, we emphasize the glycan-mediated interactions between pathogens and host cells. *Pseudomonas aeruginosa*, responsible for a huge number of nosocomial infections, is especially the focus when it comes to glycan-derivatives as pathoblockers. We present a microwave assisted protecting group free synthesis of glycomonomers based on lactose, melibiose and fucose. The monomers were polymerized in a precipitation polymerization in the presence of NiPAm to form crosslinked glyco-nanogels. The influence of reaction parameters like crosslinker type or stabilizer amount was investigated. The gels were characterized in lectin binding studies using model lectins and showed size and composition-dependent inhibition of lectin binding. Due to multivalent presentation of glycans in the gel, the inhibition was clearly stronger than with unmodified saccharides, which was compared after determination of the glycan loading. First studies with *Pseudomonas aeruginosa* revealed a surprising influence on the secretion of virulence factors. Functional glycogels may be in the future potent alternatives or adjuvants for antibiotic treatment of infections based on glycan interactions between host and pathogen.

8.2 Introduction

A vast number of pathogens utilize glycan-mediated interactions for cell invasion and their actual pathogenicity.[225,226] Well known examples are enterohemorrhagic *E. coli* (EHEC) with its shiga-like toxin,[227] *Clostridium difficile* with its glycan binding Toxin A,[228,229] *Vibrio cholera* [230] and others. Several small molecules based on sugars, as well as larger glycoclusters have been synthesized as patho-blocking agents for fighting these microbes or their toxins.[231,232,233]

A key point for strong glycan-mediated interactions is the multivalent presentation of glycan ligands inducing the ‘cluster glycoside effect’.[196,234, 235] Good choices for multivalent glycostructures are so called glycopolymers.[52,236,237,238] These are polymers with pendent

glycan groups attached to a polymeric backbone. Glycopolymers have been shown to enable very high binding avidities with lectins resulting in K_D values in the nanomolar range.[239] Multivalency is crucial for good interactions between glycans and lectins and may increase binding strength in orders of magnitude. Examples of the usage of glycopolymers are biosensor surfaces for lectin binding studies or as mannose-based scavenging material for *E. coli*.[239,240,241,242,243]

Recently, polymeric gels containing glycans were synthesized[244] via a microfluidic set-up to yield lactose containing gels with good binding to appropriate lectins.[245] Micro-, nano- or hydrogels in general can be considered as very promising systems for lectin binding. This is mainly due to their swollen "waterlike" state, their biocompatibility, the large internal volume and their potential multivalent presentation mode with incorporated glycans.[246,247] A very often used monomer for nanogel synthesis is NiPAm (*N*-isopropylacrylamide), which yields thermoresponsive polymers and enables precipitation polymerization of uniform gel particles.[248,249] PNiPAm (Poly(*N*-isopropylacrylamide)) shows a lower critical solution temperature (LCST) of about 32 °C. Below this temperature, gel particles are considered swollen and rather fuzzy, whereas above the LCST the particles become more defined, smaller and more rigid due to denser packaging. While NiPAm itself is considered cytotoxic, PNiPAm is reported to be biocompatible and non-toxic to cells.[250,251,252] The thermoresponsive properties of PNiPAm enable the batch synthesis of gels via precipitation polymerization preventing the usage of organic solvents compared to, e.g., emulsion polymerization.

Pseudomonas aeruginosa (PA) is an opportunistic pathogen rated as critical by the WHO list indicating for which strain new antibiotics are urgently needed.[253,254] Interestingly, PA utilizes two lectins (LecA and LecB) as virulence factors.[255,256] Many glycan derivatives were synthesized as patho-blocking agents.[257,258] However, the number of reports on glycopolymeric multivalent structures for lectin inhibition is rather limited. Potent glycomaterials must comprise a sufficient multivalent mode of ligand presentation. For PA, it was shown that multivalent ligands based on glycooligomers, dendrimers or as peptide derivatives are superior to the monovalent species.[259,260,261,262,263] This stands also for other lectins: Here, increase of affinity over several orders of magnitude by multivalent ligand presentation is known.[52]

We here describe for the first time the synthesis of different glycogel species containing either lactose (Galβ1,4Glc-), melibiose (Galα1,6Glc-) or fucose. The glycans were chosen as

readily available, naturally occurring structures, with the latter two known to act as ligand for LecA and LecB.[264,265] By enabling multivalent presentation in the gel, we expect to circumvent the necessity of introducing modifications to monovalent glycans increasing their affinity. The gels were synthesized in a batch process via precipitation polymerization utilizing NiPAm and lactose, melibiose or fucose glycomonomers in the presence of crosslinker and surfactant for stabilization. In this study, we focus on the influence of synthesis parameters on the inhibition potential of the gels and determined the presence or absence of a multivalent effect compared to monovalent, soluble sugars. Ability of lectin inhibition was screened by an enzyme-linked immunosorbent assay (ELISA)-type approach with fluorescently labeled plant lectins as model lectins. Ultimately, we tested in a preliminary study the influence of the gels on the growth of PA.

In the future, glycan-based soft matter can be a good way to yield biocompatible yet strong pathoblockers for medical applications. Glycoscavengers can be used for numerous different pathogens and be a promising alternative to antibiotic treatment with minimal selection pressure avoiding acquirement of resistances.

8.3 Results and Discussion

8.3.1 Synthesis of Glycomonomers

For the synthesis of glycomonomers with a polymerizable moiety at the C1 position we chose a protecting group free microwave-assisted Kochetkov-amination with subsequent reaction with methacryloylchloride (Scheme 12).[185,206,219,221]

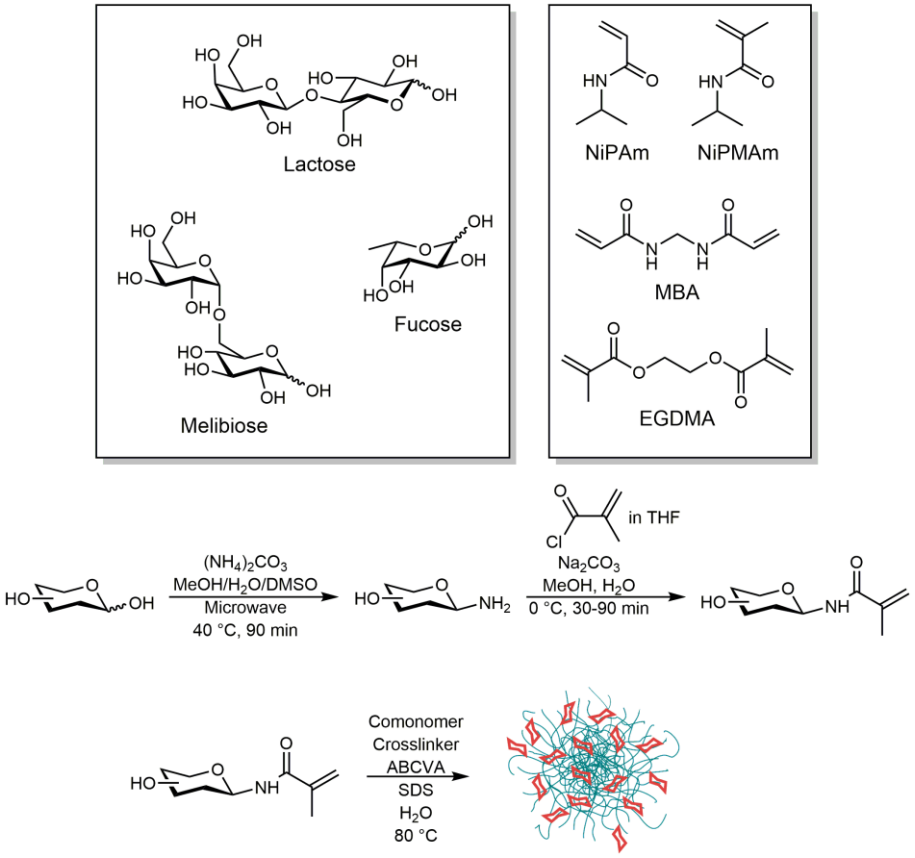

Scheme 12. Lactose, melibiose and fucose were converted via a protecting group free synthesis utilizing microwave irradiation to the respective methacrylamides. The monomers were used for the synthesis of glyco-nanogels in a precipitation polymerization in the presence of comonomer *N*-isopropylacrylamide (NiPAm) or *N*-isopropylmethacrylamide (NiPMAm) and crosslinker methylenebis(acrylamide) (MBA) or ethylene glycol dimethacrylate (EGDMA).

Modification of the saccharides at C1 postion should not affect the biological recognition of the sugar by lectins. The disaccharides lactose and melibiose, as well as the monosaccharide fucose were used as starting material and converted to the respective methacrylamides MelMAm (melibiose-methacrylamide), LacMAm (lactose-methacrylamide) and FucMAm (fucose-methacrylamide) (Scheme 12). The overall yields ranged from 18 % to 75 %, which is sufficient for the production of nanogels. The compounds were identified by

NMR spectroscopy and ESI-MS (Figure 55 – Figure 63, Supporting Information). Advantages of the synthesis are the usage of cheap starting materials, the intact cyclization of the reducing sugar and the regioselectivity for the C1 position. However, it must be noted that the β-anomer is strongly favored as reaction product. For melibiose and lactose, we do not expect any drawbacks regarding this, but β-fucose is a rather rare compound and may not be recognized by typical fucose binding lectins like *Ulex europaeus* agglutinin I (UEA I). However, it is reported that LecB binding can be inhibited to some extent by fucosylamine, which is in fact 1-amino-β-L-fucose and the intermediate of our synthesis route.[257,265,266]

8.3.2 Synthesis of Glycogels

8.3.2.1 Free-Radical Precipitation Polymerization

We evaluated two different procedures for the preparation of the glycogels: Inverse emulsion polymerization and free-radical precipitation polymerization with NiPAm and NiPMAm. The yields of the emulsion polymerization turned out to be not sufficient for subsequent analysis in lectin-assays or tests with PA (yields were below 5 %, data not shown). We assume a slow propagation and deactivation by the glycomonomers resulting in these low yields. The syntheses via free-radical precipitation polymerization in contrast gave a sufficient yield of up to 75 % compared to the initially used amount of monomer and crosslinker. Furthermore, conducting the reaction in water gives the advantage of bypassing the poor solubility of the unprotected glycomonomers in organic solvents and enabling a "green" route avoiding potentially toxic solvents. Hence, we synthesized all gels presented here by free-radical precipitation polymerization in water. The reaction temperature was chosen to be 80 °C, as this is above the LCST of PNiPAm/PNiPMAm, as well as above the 10 h half-life decomposition temperature of the water soluble azoinitiator 4,4′-azobis(4-cyanovaleric acid) (ABCVA). The freeze-dried glycogels were hygroscopic and TGA analysis revealed an equilibrium water content of about 10 %. Throughout the text the gels carrying melibiose are labeled "MG", gels with lactose are labeled "LG" and fucose containing gels are labelled "FG". Gels without sugar serve as comparative sample and negative control for the bioassays and are labelled with "G".

8.3.2.2 Comonomer and Crosslinker

Since the glycopolymer itself does not precipitate in water upon chain propagation, we required comonomers which are water soluble and exhibit a LCST as a polymer. Furthermore, the different monomers should have similar reaction kinetics in order to form a hydrogel with evenly distributed glycosides to the greatest extent possible. As the glycomonomers are methacrylamides, we selected the methacrylamide NiPMAm and ethylene glycol dimethacrylate (EGDMA) and compared the performance to the acrylamide NiPAm and *N*,*N*′-methylenebis(acrylamide) (MBA) as comonomer and crosslinker, respectively. Interestingly, PNiPMAm glycogels (MG-7) proved to be unsuitable for binding assays, as the pure PNiPMAm nanogel (G-3) itself seems to influence the lectin binding (see Section 8.3.3). Hence, no reliable lectin binding data can be produced with PNiPMAm gels and we omitted these gels. Gels containing PNiPAm showed clearly better suitability for the lectin assays. The type of crosslinker (MBA vs. EGDMA) had no significant influence on the yield but for glycogels synthesized with NiPAm and EGDMA (MG-8), binding studies with lectins showed less inhibition potentials (see Section 8.3.3) than glycogels produced with NiPAm and MBA. Thus, we chose for the syntheses of glycogels NiPAm as the comonomer enabling the precipitation polymerization, and MBA as crosslinker. We assume that for good inhibition performance, a core-shell-like gel morphology is appreciated where the core is built up by the non-glycosylated monomers, surrounded by a glycan-shell. This can be achieved most likely by using the fast polymerizing acrylamides NiPAm and MBA together with the rather slow methacrylamide glycomonomers.

8.3.2.3 PNiPAm Glycogels

Typically, when PNiPAm nanogels particles are formed by precipitation polymerization, the reaction solution turns turbid. The turbidity depends on the concentration and size of the particles. For the glycogels, we observed a strikingly lower turbidity during reaction. This indicates that the gels were not only consisting of NiPAm but the glycomonomer could be incorporated into the polymers as well. We assume that the glyco-comonomer interferes with the complete collapse of PNiPAm and forms a fuzzy shell-like structure around a PNiPAm core. In scanning electron microscopy (SEM), as well as in atomic force microscopy (AFM) images, we can find spherical particles (see Supporting Information). Hence, we achieved glycogel particles and not free polymers. From dynamic light scattering (DLS)

measurements and SEM images, we observe high polydispersity in contrast to the excellent monodispersity of pure PNiPAm nanogels (Figure 20). Due to the hydrophobic propyl moiety of NiPAm, the polymer precipitates above its LCST when the hydrophobic interactions dominate. The glycomonomers exhibit a high hydrophilicity. This property may counteract the hydrophobic interactions of NiPAm which could explain the high polydispersity. As the gels do not dissolve in water independently of the surrounding temperature, we can assume that the products are crosslinked networks and not free copolymer chains.

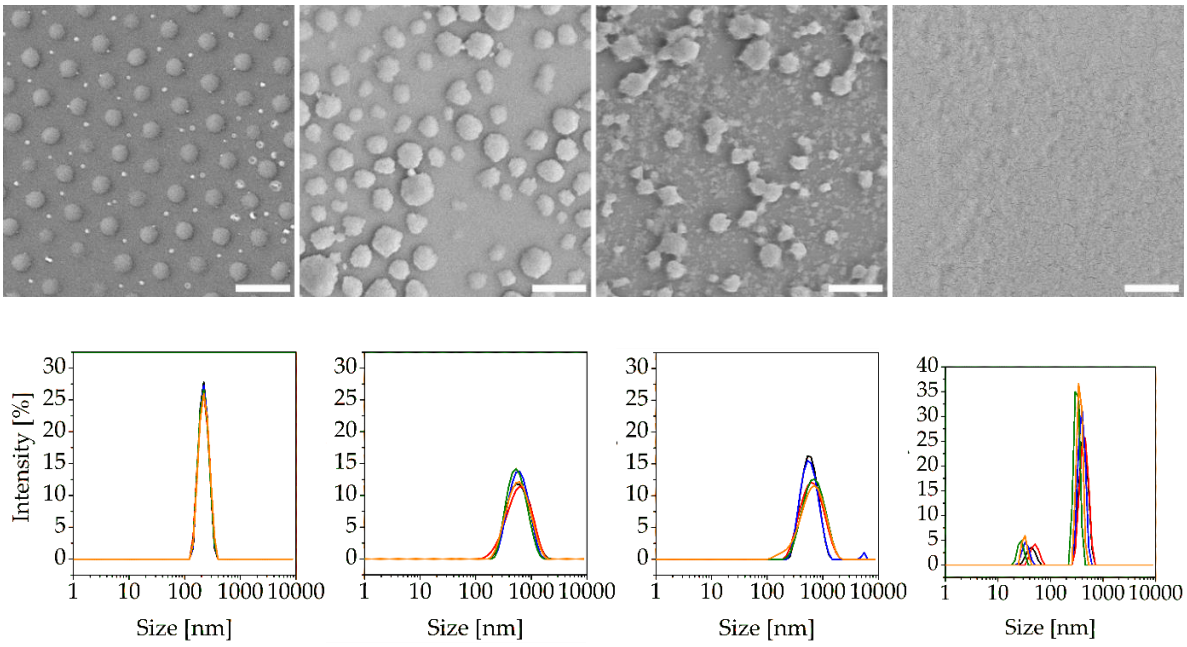

Figure 20. Scanning electron microscopy (SEM) images and dynamic light scattering (DLS) size distribution by intensity (at 50 °C) of different nanogels: (a) monodisperse PNiPAm nanogel particles G-1 synthesized with 0.2 mM SDS; (b) glycogel MG-1 synthesized with 0.4 mM SDS; (c) MG-2 synthesized with 2.0 mM SDS; (d) glycogel MG-3 synthesized with 4.0 mM SDS. Scale bars represent 1 µm.

We used SDS in order to stabilize the gels during reaction. At similar surfactant concentrations, the sizes of the glycogels are larger than the size of the PNiPAm nanogels (Figure 20), which may be related to the fuzzy glyco-shell, which tends to swell in aqueous media independent of the surrounding temperature. Furthermore, with increasing surfactant concentration, the size of the glycogels do not evidently become smaller and their monodispersity does not increase either (Table 3). Typically, increased concentrations of stabilizer in precipitation polymerizations lead to smaller diameters.[267] The effect of SDS

seems to be diminished in the case of glycogels. Surprisingly, high concentrations of SDS appear to even increase the polydispersity. We assume that the hydrophilic property of the glycomonomers counteracts the formation of monodisperse and uniform particles. A possible explanation is that the hydrophilic part of the surfactant and the hydrophilic glycomonomer repel each other, which disturbs the formation of stabilizing SDS-corona around the growing gel particles. Therefore, a high amount of SDS may cause the glycosyl moiety to distribute and scatter in the water instead of letting formed polymer chains immediately collapse into a coil in between the surfactants.

Table 3. Gels synthesized with varied sodium dodecyl sulfate (SDS) concentrations.

Gel	**c(SDS) [mM]**	**Yield [%]**	**D_h(50 °C) [nm]**	**PDI [%]**
G-1	0.2	-	218	2.54
MG-1	0.4	67	507	21.2
MG-2	2.0	67	554	26.4
MG-3	4.0	43	1084	56.6

Temperature-dependent DLS measurements show that some glycogels still retain some of the thermoresponsiveness of PNiPAm. It has to be noted that the hydrodynamic diameter (D_h) of the glycogels is not reliable as the polydispersity index (PDI) is quite high. However, we can observe a trend where the PDI decreases at 50 °C as well as the averaged hydrodynamic diameter (Table 4).

Table 4. Hydrodynamic diameters (D_h) and polydispersity index (PDI) of nanogels.

Gel	D_h (20 °C) [nm]	PDI [%]	D_h (50 °C) [nm]	PDI [%]
G-1	406	4.30	218	2.54
G-2	101	9.10	54.2	12.9
MG-0	143	30.3	103	23.0
MG-1	669	29.7	507	21.2
MG-2	678	40.7	554	26.4
MG-3	1084	56.6	1084	56.6
MG-4	474	31.5	488	20.4
MG-5	651	22.4	569	18.7
MG-6	436	66.6	328	27.9

This comes in agreement with the typical behavior of PNiPAm nanogels. Their hydrodynamic diameter decreases with increasing temperature as they collapse. Their PDI usually improves at temperatures above the LCST since the collapsed particles with the defined surface border are easier to measure via DLS than swollen, soft nanogels with their fuzzy surface and dangling polymer chains. Though, we do not observe a defined LCST for the glycogels (see Figure 21).

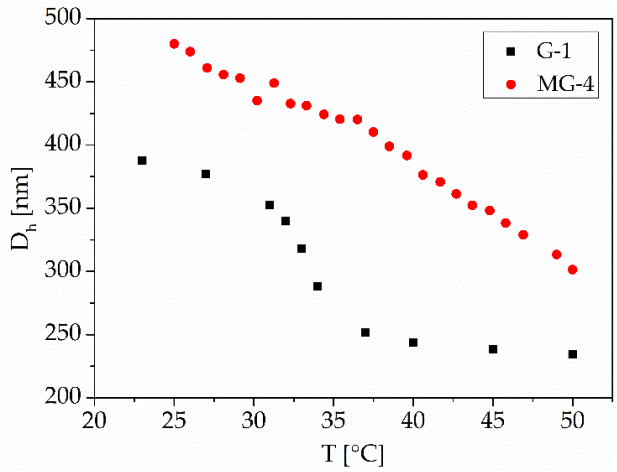

Figure 21. Temperature-dependent analysis of the hydrodynamic diameter of PNiPAm nanogel G-1 and melibiose glycogel MG-4 using DLS. While still thermoresponsive to some extent, no distinct lower critical solution temperature (LCST) can be detected for the glycogels (MG-4).

8.3.2.4 Initiation of the Polymerization

Generally, the synthesis of pure PNiPAm nanogels require only little amounts of initiator (0.25 mol%).[268] By using a mixture of NiPAm and MelMAm, 0.25 mol% of initiator seems to be insufficient as the reaction mixture stays clear. This is even the case with the fourfold amount of ABCVA (1 mol%). This indicates that no crosslinked networks are formed or that the polymerization is not taking place or being inhibited somehow. Therefore, we fed an additional amount initiator after two hours to the reaction mixture (Table 5, MG-1). It is also possible to use an even higher amount of the initiator from the beginning to start the reaction (MG-4). For better comparison with previously synthesized gels, we continued with the method mentioned first with an initiator feed. Preceding equilibration of the reaction mixture at the reaction temperature, as often executed for PNiPAm nanogels,[267] does not lead to significantly better binding performance (MG-5). The method of reaction start does not significantly affect the yield, hydrodynamic diameter nor the polydispersity. Thus, we synthesized the rest of the glycogels without temperature equilibration.

Table 5. Glycogels synthesized with three different methods of reaction start.

Glycogel	X_1(ABCVA) [mol%]	X_2(ABCVA) [mol%]	Yield [%]	D_h (50 °C) [nm]	PDI [%]
MG-1	1.0	2.0	67	507	21.2
MG-4	3.0	-	61	488	20.4
MG-5	3.0	-	66	569	18.7

8.3.2.5 Glycogels with Various Crosslinking Densities

The crosslinking density generally influences the morphology of PNiPAm nanogels such as deformability, softness and swelling ability.[268] Here, we compare glycogels based on different saccharides and the influence of the crosslinker amount. The highest yield of 75 % related to the initial amount of total monomer was achieved with LacMAm and 5 mol% crosslinker resulting in glycogel LG-1 (Table 6). Similar synthesis with MelMAm and 5 mol% crosslinker gained 29 % less yield (MG-6; 46 %). For melibiose glycogels, the highest yield was achieved with 10 mol% of crosslinker (MG-2; 67 %). Comparable synthesis with FucMAm and 5 mol% crosslinker also achieved lower yields of 56 % (FG-1). When changing the crosslinking density from 5 to 10 mol% (FG-2), the yields dropped to 33 %. It has to be noted

that during synthesis the fucose glycogels precipitated more readily than the other glycogels and tend to aggregate during reaction. Here, we filtered off the large, aggregated sediments before freeze-drying. We assume that higher amounts of crosslinker lead to more aggregation. This is consistent with the low yield of FG-2. It is strongly evident how differently various crosslinker amounts and various saccharides influence the precipitation polymerization, even though LacMAm and MelMAm are both disaccharides. Melibiose exhibits a higher water solubility than lactose, indicating a stronger negative influence on the precipitation behavior of the gels. Therefore, in case of melibiose glycogels, higher amounts of crosslinker might be necessary in order to gain higher yields since MBA reacts faster than NiPAm and, thus, does not slow down the reaction. Fucose, however, carries a non-polar methyl-group which can reestablish a more PNiPAm-like precipitation behavior, hence, the reaction solution turned turbid faster. Besides, the higher hydrophobicity of fucose might be a cause for the aggregation during synthesis.

Table 6. Comparison of glycogels with different saccharides and crosslinker amounts.

Glycogel	X(MBA) [mol%]	Yield [%]	D_h(50°C) [nm]	PDI [%]
LG-1	5.0	67	507	21.2
MG-6	5.0	46	488	20.4
MG-2	10	66	569	18.7
FG-1	5.0	56	643	51.7
FG-2	10	33	548	65.0

8.3.2.6 Amount of incorporated Carbohydrates in Glycogels

We determined the amount of incorporated glycomonomer by a phenol-sulfuric acid assay and studied how it is influenced by synthesis parameters and type of sugar (Table 7). The assay revealed the total carbohydrate content of the gel and was calibrated with the free sugars. When the same type of glycomonomer is used, the amount of incorporated sugar is not strongly influenced by different synthesis parameters such as the amount of stabilizer, crosslinker and initiator, the type of comonomer and crosslinker and the method of initiation. Hence, the sugar content is very similar, independent of glycogel size and crosslinking density. This means that the incorporation of the glycan is solely controlled by the polymerization kinetics of the monomer and not dramatically affected by the actual reaction parameters. On the other hand, a

striking difference in sugar content is observed when different glycomonomers are examined. On average, the fucose glycogel contains the highest sugar amount with a calculated incorporation of up to 70 % of the initially used glycomonomer, followed by lactose (up to 40 %) and melibiose (up to 25 %) glycogel. This coincides with the before mentioned fast reaction of FucMAm as it is more hydrophobic and therefore might react similar to and with NiPAm in contrast to the very hydrophilic lactose and melibiose glycomonomers.

Table 7. Amount of incorporated glycomonomer in the glycogels.

Glycogel	Sugar Content [µmol/mg]	Averaged Sugar Content for Each Glycomonomer Type [µmol/mg]	Theoretical Sugar Content [a] [µmol/mg]	Yield of Incorporated Glycomonomer [b] [%]
LG-1	0.43 ± 0.03	0.41 ± 0.03	1.12	38.3 ± 2.7
LG-2	0.39 ± 0.01		1.16	33.7 ± 0.9
MG-0	0.24 ± 0.02	0.26 ± 0.05	1.16	20.8 ± 1.7
MG-1	0.29 ± 0.06		1.14	25.4 ± 5.3
MG-2	0.28 ± 0.02		1.14	24.5 ± 1.8
MG-3	0.23 ± 0.04		1.14	22.8 ± 3.5
MG-4	0.20 ± 0.05		1.14	18.1 ± 4.5
MG-5	0.26 ± 0.05		1.11	23.5 ± 4.5
MG-6	0.26 ± 0.02		1.12	23.1 ± 1.8
MG-7	0.27 ± 0.02		1.06	25.5 ± 1.9
MG-8	0.28 ± 0.04		1.14	24.5 ± 3.5
FG-1	0.94 ± 0.19	0.98 ± 0.16	1.43	65.6 ± 13
FG-2	1.01 ± 0.13		1.43	70.5 ± 9.1

[a] Theoretical amount of incorporated glycomonomer if complete turn-over of all relevant components is considered. [b] Measured sugar content divided by theoretical sugar content.

8.3.3 Inhibition Studies with Plant Lectins

The aim of this study is to synthesize glycogels with full functionality in means of glycan binding. Therefore, it is important to prove the accessibility of the saccharide units for lectins. For screening the synthesized glycogels, we chose three plant lectins as representatives for melibiose, lactose and fucose binding lectins, respectively—Jacalin,[269] *Erythrina cristagalli* lectin (ECL)[270] and *Ulex europaeus* agglutinin I (UEA I).[271] In ELISA-type

inhibition assays, the nanogels were applied as inhibitors for lectin binding to an immobilized ligand.

First of all, we investigated lectin binding to standard glycoproteins asialofetuin (ASF) and thyroglobulin. ECL and Jacalin bind sufficiently to ASF, whereas for UEA I binding α-fucose residues are necessary. This could be found neither on ASF nor on thyroglobulin (data not shown). As mucins contains fucose units, porcine stomach mucin was tested and found to possess ligands for UEA I. The binding curves of UEA I on mucin as well as of the other two lectins on ASF are shown in Figure 22a. These binding signals are glycan mediated because inhibition with the appropriate sugar was proven (Figure 22b).

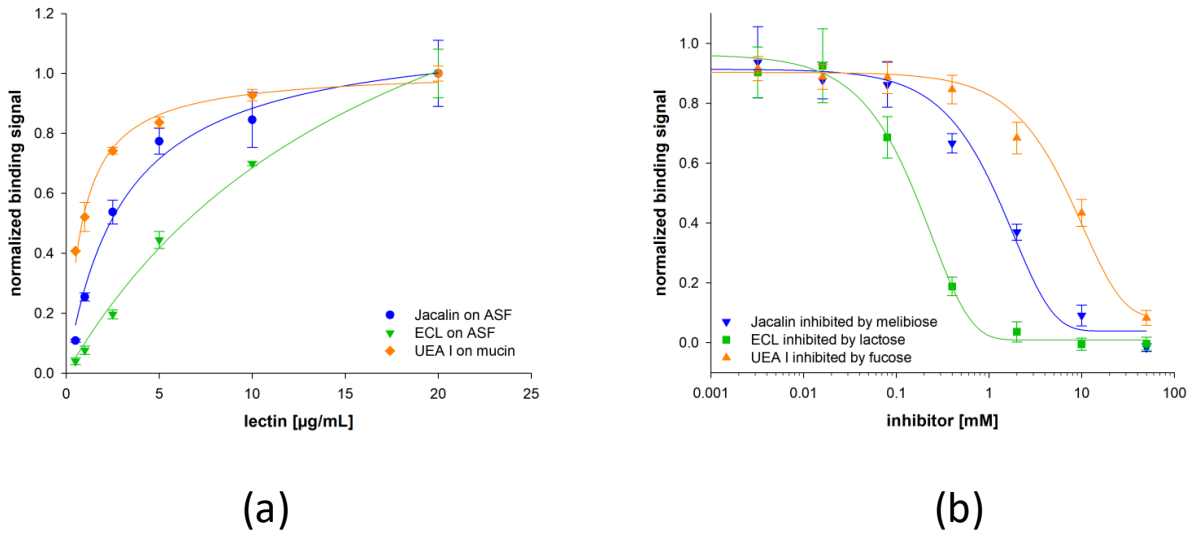

Figure 22. Binding and inhibition of chosen plant lectins to immobilized glycoproteins. (a) The lectins Jacalin and *Erythrina cristagalli* lectin (ECL) show binding to immobilized asialofetuin (ASF), whereas *Ulex europaeus* agglutinin I (UEA I) binds to immobilized mucin from porcine stomach. (b) The three lectins bind glycan mediated and are inhibitable by appropriate saccharides. Typical inhibition curves are shown for Jacalin inhibited by melibiose, ECL inhibited by lactose and UEA I inhibited by fucose.

A set of melibiose containing nanogels was synthesized with different synthesis conditions. The majority of these glycogels inhibited the binding of Jacalin to ASF indicating functional melibiose presentation. The SDS amount during the synthesis had a small influence on the inhibition potential of the glycogels. An increasing amount of SDS seemed to weaken the lectin binding (Figure 23a). However, we tested if this is an effect caused by the denaturing properties of SDS and incomplete removal during dialysis. It turned out that the lectin binding is not affected by SDS at concentrations around 0.1% (data not shown), which represents the

highest amount used during synthesis. The initiation method of polymerization is irrelevant for lectin binding, as the inhibition curves for MG-1, MG-4 and MG-5 in Figure 23b are nearly identical. The type of crosslinker as well as the monomer type have the strongest influence. If NiPMAm was used for nanogel synthesis, no lectin inhibition was measured but an elevated binding signal occurred (Figure 23c). This phenomenon was observed for the NiPMAm control G-3 as well as for the melibiose-NiPMAm gel MG-7. Potentially, the lectin interacts with the nanogel somehow but is further able to bind ASF. In general, PNiPMAm as well as PNiPAm are reported to show rather low unspecific protein adsorption.[272] MG-8 has again a NiPAm backbone but EGDMA as crosslinker instead of MBA. EGDMA and MBA exhibit different reaction kinetics which can lead to different sizes and structures in the gel as shown in previous studies with PNiPAm microgels.[273] The change to EGDMA had a negative influence on the functionality and led to weak inhibitory potency as well as incomplete inhibition (Figure 23c and Figure 24). Comparing the glycogels, regarding their size, a positive effect was seen with smaller gels (Figure 23d). MG-4 with approximately 500 nm D_h showed slightly better inhibition than MG-1 with approximately 700 nm. But the highest inhibitory potency among all melibiose nanogels had MG-0 that was the smallest by far (approximately 150 nm D_h). The smaller the particle, the larger the surface and that means, in this case, a higher density of glycans. We found the highest multivalent effect of these smallest nanogels reaching an IC50 value of 0.05 mg/mL which is a threefold higher inhibition value than the average of all larger nanogels (see Figure 24).

Noticeably, in the presence of glycogels of low concentrations (< 0.01 mg/mL) the binding of Jacalin to ASF is enhanced, indicated by a higher fluorescence signal than the value for lectin binding without glycogel. Jacalin is a tetrameric lectin and thus, it is able to crosslink the glycogel with the glycoprotein immobilized on the surface.[269,274,275] In this way, the overall amount of glycans on the surface increases and it is possible that more lectins bind to the crosslinked nanogels, resulting in a higher fluorescence being measured. For calculating the IC50 values, these data points were neglected.

We also included NiPAm controls without sugar content in our binding study. NiPAm nanogels of small size (G-2) as well as of larger size (G-1) did not inhibit the Jacalin binding (Figure 23e). The same goes for a lactose containing nanogel—no inhibition was observed. Taking these findings together, the synthesized melibiose nanogels contain melibiose units fully functional for lectin binding. The averaged IC50 value of melibiose nanogels that inhibit Jacalin binding almost completely is 0.15 mg/mL. In comparison, melibiose as free sugar shows an

IC50 value of 0.5 mg/mL. In consequence, the glycogels show a multivalent effect that is even higher in consideration of the ratio of sugar monomer during the synthesis of approximately 20 % compared to the overall monomer amount. After determining the sugar content of the glycogels and calculating the apparent IC50 values from mg/mL glycogel into mM sugar amount (Figure 24b), the multivalent effect of all melibiose nanogels is even more emphasized. Due to the small amount of incorporated melibiose during the synthesis, the IC50 values are in average approximately 15-times lower than for melibiose. MG-0 as most potent inhibitor shows even 100-fold higher inhibition than melibiose. Despite not complete inhibition for MG-3, MG-6 and MG-8, those IC50 values are still lower than melibiose showing again the multivalent character of sugar presentation of the glycogels. The incomplete inhibition of MG-8 might be due to possible differences in the glycogel structure. The lower inhibition strength of MG-3 and MG-6 can also be explained by different structures as we synthesized MG-3 with high concentrations of stabilizer, which influences the size and morphology of the nanogels. The lower crosslinking density in MG-6 determines the morphology of nanogels as well.[268] With regard to one type of glycogel, and therefore the same sugar content, the inhibitory potency seems to be strongly dependent on the morphology of the glycogels.

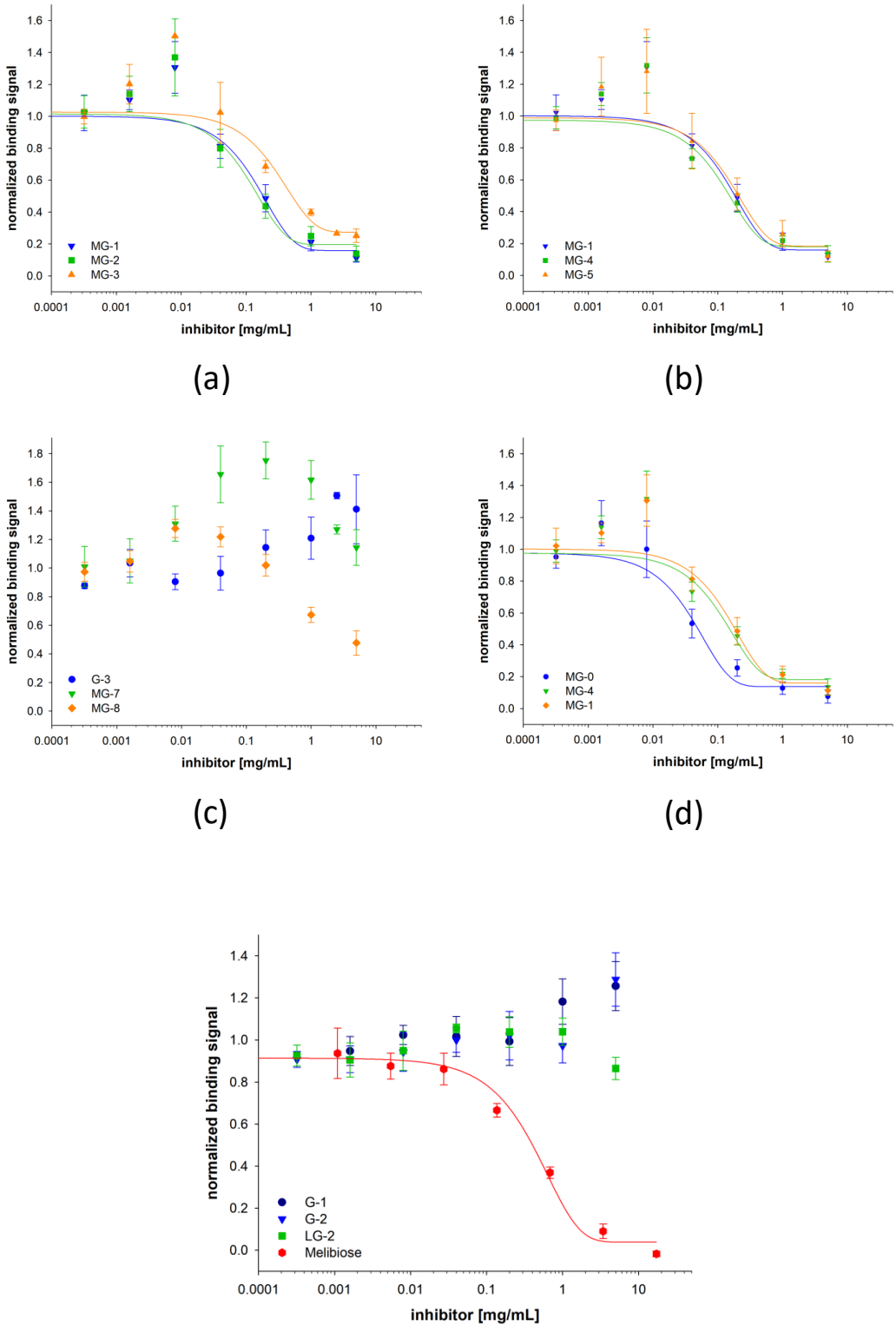

Figure 23. Inhibition of Jacalin binding by glyco-nanogels. Melibiose nanogels were investigated in inhibition studies with Jacalin and compared regarding (a) SDS amount during the synthesis, (b) initiation method of polymerization, (c) type of comonomer and crosslinker, and (d) the size of the gels. In (e), control nanogels without sugar or containing a non-inhibiting sugar show no inhibition. The complete inhibition by the disaccharide melibiose proved the suitability of the assay.

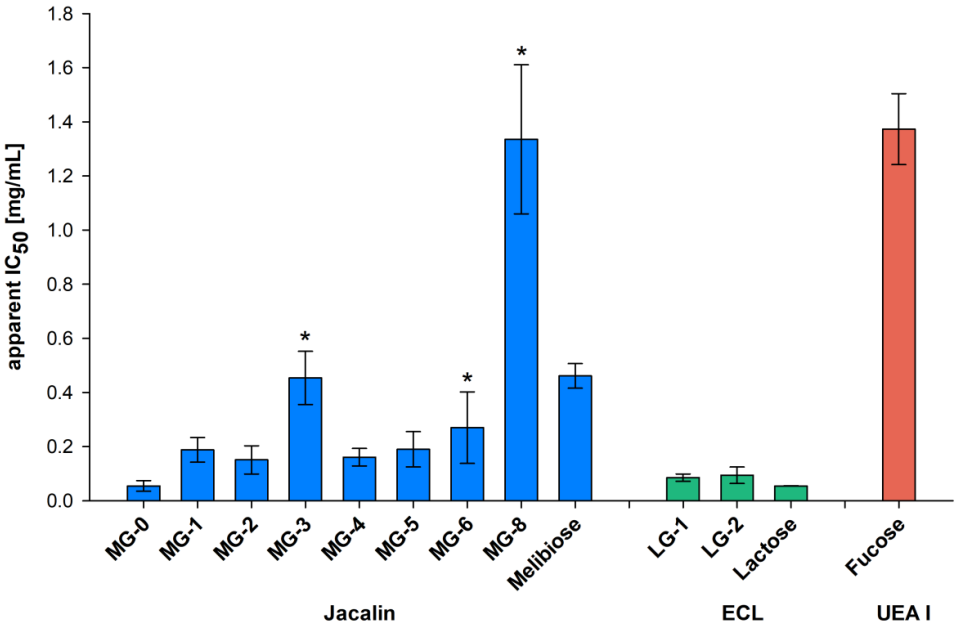

(**a**)

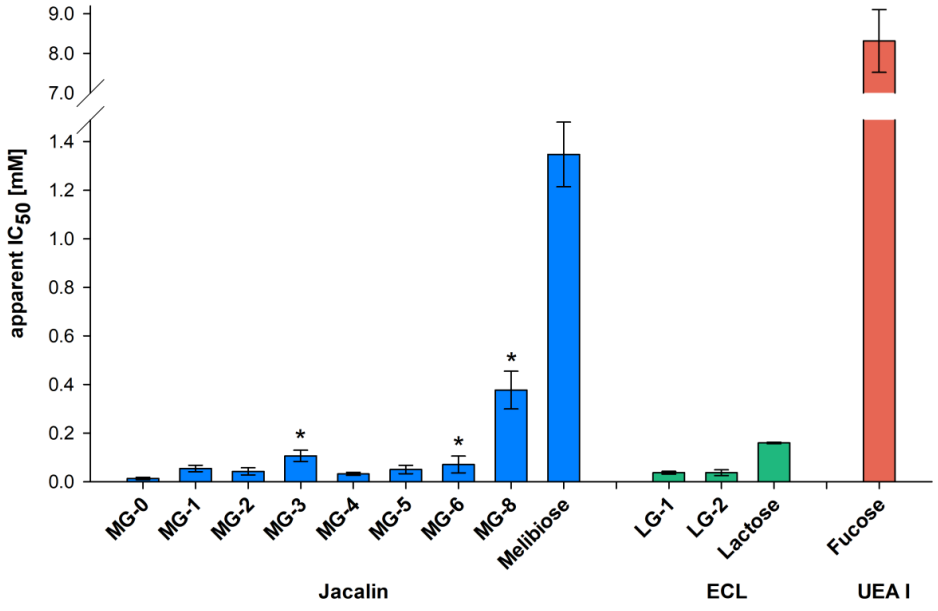

(**b**)

Figure 24. Apparent IC_{50} values of glycogels and free saccharides. The concentration (a) (mg/mL) glycogel and (b) (mM) sugar content that is needed for half maximal inhibition is shown for melibiose nanogels and free melibiose regarding Jacalin binding, lactose nanogels and free lactose regarding ECL binding and fucose regarding UEA I binding. Gels marked with asterisks did not show complete inhibition.

The synthesized lactose nanogels were analyzed in binding assays using ECL, a lactose binding lectin.[270] LG-1 and LG-2 are two lactose-containing NiPAm nanogels of very similar syntheses. Both glycogels show complete inhibition of ECL binding to ASF with identical IC50 values (Figure 24 and Figure 25a). For ECL, no binding enhancement at low glycogel concentrations is visible. Due to the dimeric structure of ECL, crosslinking of the glycogel with the immobilized glycoprotein is less pronounced and not enough to yield an increased fluorescence signal. G-1, a control PNiPAm nanogel without sugar, as well as MG-0, a melibiose containing nanogel, did not inhibit ECL binding proving the binding specificity to lactose. Moreover, free lactose is a potent inhibitor for ECL with IC50 in the same range as the lactose nanogels (Figure 24a). However, due to the limited amount of lactose monomer (approximately 20%) during synthesis, both lactose nanogels contain 0.4 µmol lactose per mg nanogel (Table 7). With IC50 values that are over four-times lower compared to free lactose, when regarding the sugar content (Figure 24b), the lactose nanogel also has a multivalent character and led to good inhibition potency. The multivalent effect of the lactose nanogels, however, is less distinct than that of the melibiose nanogels.

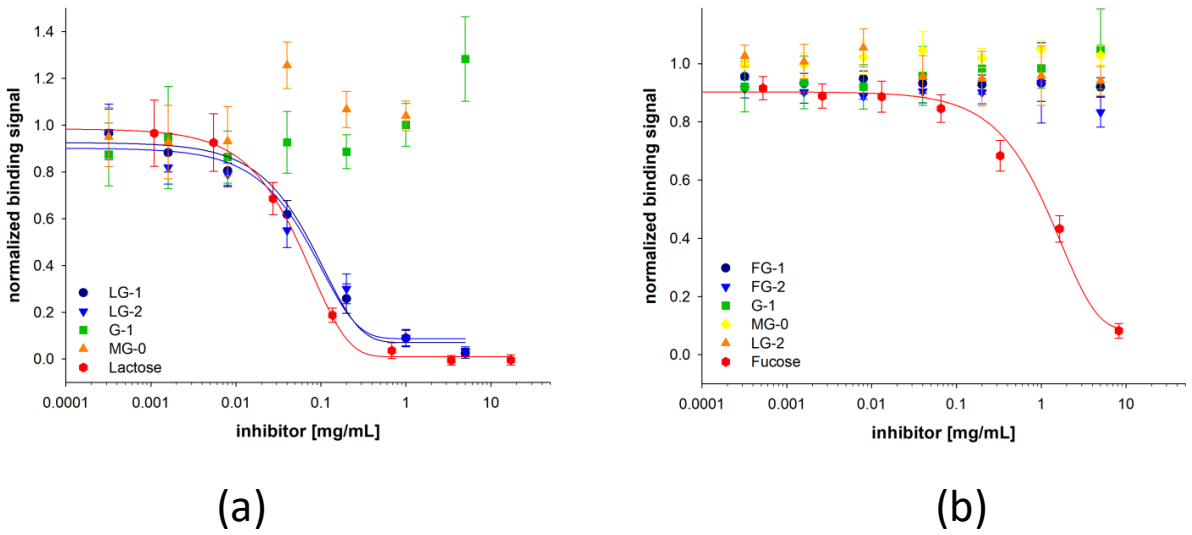

Figure 25. Inhibition of ECL and UEA I binding by glyco-nanogels. (a) ECL binding is inhibited by lactose containing nanogels and by free lactose, but not by the control nanogel without sugar and by melibiose nanogel. (b) UEA I is only inhibited by free fucose; no synthesized glycogel is bound by UEA I.

The third type of glyco-nanogel we synthesized contains fucose. Therefore, the binding assay was performed with UEA I, a fucose binding lectin.[271] Two different fucose nanogels,

FG-1 and FG-2, were tested but no inhibition was observed (Figure 25b). Our synthesis route led predominantly to β-fucose that is rarely found in nature.[276] Thus, it was no surprise that UEA I did not bind to the glycogel. In addition, UEA I is described to be a lectin binding to α-fucose.[271] As seen in Figure 25b, all controls gave the correct results: Nanogel without sugar as well as melibiose and lactose containing nanogels did also not inhibit the UEA I binding, whereas with free fucose selective binding of UEA I to immobilized mucin was proven because it was completely inhibitable. The UEA I binding is the strongest binding to its immobilized glycoprotein among the three tested plant lectins, here. The IC50 value of fucose for UEA I binding is three-times (six-times for mM value) higher than melibiose for Jacalin binding and 25-times (50-times for mM value) higher than lactose for ECL binding (Figure 24).

8.3.4 Influence on Pseudomonas aeruginosa

In a small preliminary study, we investigated the influence of the glycogels on the growth of PA. For this, gels were selected by the before mentioned lectin-assay and PA was incubated for 24 h with MG-0, MG-4, LG-1, FG-1 and G-2. FG-1 was chosen despite the fact no binding was detected in the lectin studies, because reports suggest that LecB is capable of binding β-fucose moieties.[257,265,266] The gel concentration was kept at 2 mg mL^{-1} in the cultivation broth and as additional control, we used unmodified melibiose and fucose (2 mg mL^{-1} each).

In this first study, we focused on the secretion of the fluorescent siderophore pyoverdine, which is an essential virulence factor of PA.[277] Pyoverdine is involved in various processes, including regulation of other virulence factors as well as the enabling the formation of biofilms, which decreases the sensitivity of PA towards antibiotics.[278,279] Figure 26 shows a fluorescence image of the 24-well plates with PA and gels.

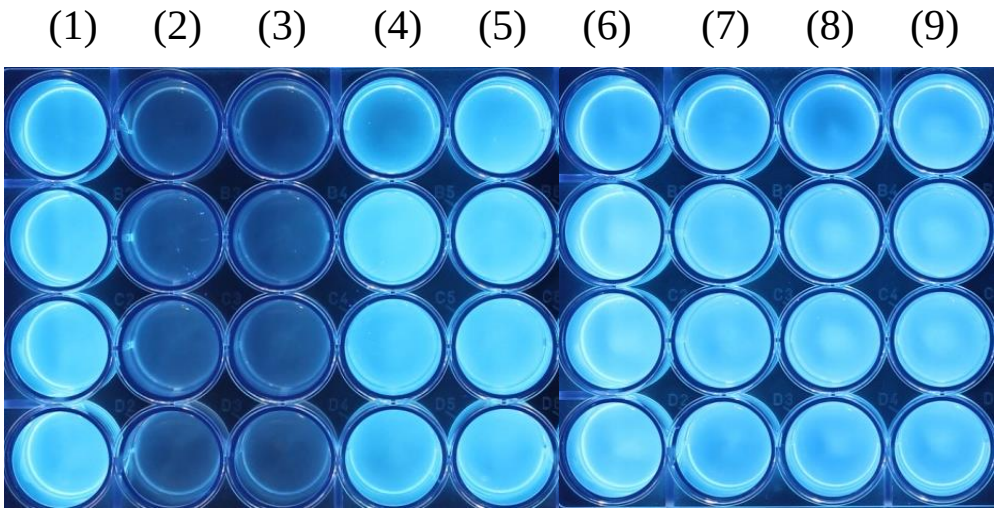

Figure 26. Fluorescence images of *Pseudomonas aeruginosa* (PA) incubated with glycogels. The fluorescence is caused by the secreted fluorescent siderophore pyoverdine. Note the strong decrease in fluorescence signal in the wells containing FG-1. All samples were run as quadruples. Each well in a column is treated identically. (1): MG-0; (2): MG-0 and FG-1; (3): FG-1; (4): LG-1; (5): No gel; (6): MG-4; (7): G-2; (8): Unmodified melibiose and fucose; (9): Same as (5).

Surprisingly, FG-1 decreased the detectable fluorescence based on pyoverdine secretion clearly. All other samples showed no effect in this regard. To the best of our knowledge there is no hint reported so far that fucose-derivatives are somehow influencing the secretion status of pyoverdine in PA. To investigate if there is really a change in pyoverdine secretion or just an antimicrobial activity of FG-1, the PA were subsequently plated on petri dishes and cultivated for 24 h. All samples showed the formation of colonies, which proves that the effect was not due to antimicrobial activity of FG-1 (see Figure 74, Supporting Information). As these are the first results on this interesting topic, we will proceed with setting up biofilm assays with PA and our glycogels as well as a more in-depth investigation on the influence of fucose containing gels on the secretion of pyoverdine.

8.4 Materials and Methods

8.4.1 Materials

All chemicals were purchased from commercial sources. We recrystallized *N*-isopropylacrylamide (NiPAm; 97 %, Sigma Aldrich, Taufkirchen, Germany) and *N*-isopropylmethacrylamide (NiPMAm; 97 %, Sigma Aldrich) from *n*-hexane. Water was double deionized by a Milli-Q purification system (18.2 MΩ cm, Millipore Quantum® TEX, Darmstadt, Germany). The crosslinkers *N*,*N*′-methylenebis(acrylamide) (MBA; 99 %, Sigma

Aldrich) and ethylene glycol dimethacrylate (EGDMA; 98 %, Sigma Aldrich), the initiator 4,4′-azobis(4-cyanovaleric acid) (ABCVA; ≥ 98 %, Sigma Aldrich), dichloromethane (CH_2Cl_2; for synthesis) and chloroform ($CHCl_3$; extra pure) were redistilled before use. D-(+)-Melibiose monohydrate (Mel; ≥ 99 %, Carl Roth, Karlsruhe, Germany), L-(−)-fucose (Fuc; ≥ 99 %, Sigma Aldrich), D-lactose monohydrate (Lac; Carbosynth, Compton, United Kingdom), ammonium carbonate ($(NH_4)_2CO_3$; ≥ 30.5 % NH_3, extra pure, Carl Roth), dimethyl sulfoxide (DMSO; VWR, Darmstadt, Germany), methacryloyl chloride (purum, dist., ≥ 97 %, Sigma Aldrich), sodium carbonate (≥ 99 %, anhydrous, Carl Roth), tetrahydrofuran (THF; p. a., Chemsolute, Renningen, Germany), acetonitrile (≥ 99.8 %, for preparative HPLC, Carl Roth), hydroquinone (99.5 %, Acros Organics, Darmstadt, Germany), diethylether (Et_2O; p. a., Chemsolute), methanol (MeOH; extra pure), silica gel (high-purity grade, pore size 60 Å, Sigma Aldrich), sodium dodecyl sulfate (SDS; ≥ 99.5 %, blotting-grade, Carl Roth) were used as received.

8.4.2 Methods

8.4.2.1 Dynamic Light Scattering (DLS)

We investigated the hydrodynamic diameter by using dynamic light scattering (DLS) (Malvern Zetasizer Nano-ZS, Kassel, Germany). Measurements were performed in disposable polymethylmethacrylate cuvettes at a backscattering angle of 173° five times. We chose temperatures of 20 and 50 °C. For the measurements at 20 °C, we let the samples equilibrate for 5 min, and for the measurements at 50 °C, the samples were allowed to equilibrate for 10 min to ensure complete collapse of the glycogels. We measured the hydrodynamic diameter of PNiPAm nanogel G-1 and melibiose gel MG-4 as a function of the temperature, ranging from 20 to 50 °C.

8.4.2.2 Scanning Electron Microscopy (SEM)

Diluted samples were dropped onto tilted silicon wafers (CrysTec) to let excess liquid drip off. After letting the wafers dry, the samples were sputtered with platinum (4 nm). Images were taken on a GeminiSEM 300 (Fa. Zeiss, Jena, Germany).

8.4.2.3 Atomic Force Microscopy (AFM)

AFM analysis was performed on a Bruker Dimension Icon using NanoScope 9.1 (Karlsruhe, Germany) for measurements and NanoScope Analysis 1.5 for image processing. We measured in ScanAsyst air mode using a ScanAsyst air tip with a spring constant of ~0.4 N/m and a resonant frequency of 70 Hz.

8.4.2.4 NMR and ESI-MS

NMR spectra were recorded on a Bruker Avance 300 MHz Spektrometer (Ettlingen, Germany). Mass spectra were recorded on FlexarTM SQ 300 MS Detector (PerkinElmer, Rodgau, Germany).

8.4.2.5 Thermogravimetric Analysis (TGA)

TGA measurements (TGA 500, TA Instruments, Hüllhorst, Germany) were conducted in nitrogen flow (60 mL/min) with heating rate of 10 K/min up to 200 °C. The water content in the gels was determined to be 5 – 11 wt.%. For analysis and discussion, we used the wet weight of the gels.

8.4.3 Glycomonomers

The glycomonomers were synthesized in a two-step procedure. For the first step, the respective glycoamines were prepared via Kochetkov amination accelerated by microwave irradiation.[185,206] The second step involves the introduction of a polymerizable moiety following a modified procedure of Ghadban *et al.*.[219]

8.4.3.1 Synthesis of Glycosylamines

The saccharide was dissolved in solvent and ammonium carbonate was added. The respective amounts of reactants and solvents used are listed in Table 8. Afterwards the reaction mixture was heated in the microwave reactor (START 1500 rotaPREP, MSL, Leutkirch, Germany) to 40 °C for 90 min under stirring. The mixture was allowed to cool down and the

ammonium carbonate and the solvent were removed by rotary evaporation at 40 °C under reduced pressure. In case of $LacNH_2$, the glycosylamine was precipitated with 40 mL of MeOH after reaction and dried. The crude product was dried in high vacuum and stored at 4 °C. We used the glycosylamines for monomer syntheses without further purification. It has to be noted that residual ammonium carbonate was found in all glycosylamines which could not be removed.[221]

Table 8. Synthesis details of glycosylamines.

Reactant	n [mmol]	m [g]	V [mL]
Lactose monohydrate	8.33	3.3	-
DMSO	-	-	12.0
$(NH_4)_2CO_3$	52.0	5.0	-
Melibiose monohydrate	13.9	5.0	-
H_2O	-	-	100
$(NH_4)_2CO_3$	520	50	-
Fucose	9.14	1.5	-
MeOH	-	-	13.0
$(NH_4)_2CO_3$	78.1	7.5	-

8.4.3.2 Synthesis of Glycosyl Methacrylamides

We dissolved the glycosylamine in a mixture of methanol and Milli-Q water (1:1) and added sodium carbonate. The reaction mixture was cooled in an ice-water bath. Methacryloyl chloride was diluted with THF and dropwise added into the mixture within 10 min under stirring. The reaction was allowed to proceed for further 30 – 90 min in the ice-water bath (Table 9). Then the volatile solvents were removed by rotary evaporation at 30 °C. The products were purified by silica gel column chromatography (LacMAm: acetonitrile/H_2O 9:1; MelMAm: acetonitrile/H_2O 9:1 → 4:1; FucMAm: $CHCl_3$/MeOH 5:1), followed by the extraction with diethyl ether in the case of LacMAm. We stabilized MelMAm with hydroquinone (3 ppm) as it tends to polymerize spontaneously. FucMAm was hydrolyzed in 30 mL with 106 mg sodium carbonate (1 mmol; 250 mM) overnight as the NMR spectra showed additional methacrylate peaks. Afterwards, we purified FucMAm by a second column chromatography ($CHCl_3$/MeOH 5:1). The products were concentrated and then freeze-dried to obtain white solids (LacMAm:

680 mg, total yield: 57 %; MelMAm: 1.12 g, total yield: 18 %; FucMAm: 817 mg, total yield: 26 %).

Table 9. Synthesis details of glycomonomers.

Reactant	n [mmol]	m [g]	V [mL]
$LacNH_2$	3.17	1.0815	-
Sodium carbonate	12.67	1.3434	-
MeOH/H_2O (1:1)	-	-	16.4
Methacryloyl chloride	9.5		0.9141
THF	-	-	6.3373
$MelNH_2$	13.9	5	-
Sodium carbonate	77.8	8.25	-
MeOH/H_2O (1:1)	-	-	150
Methacryloyl chloride	42.6		4.77
THF	-	-	35
$FucNH_2$	12.2	2	-
Sodium carbonate	68.1	7.22	-
MeOH/H_2O (1:1)	-	-	132
Methacryloyl chloride	42.5		4.1
THF	-	-	35

LacMAm. ^{1}H NMR (D_2O, 300 MHz): δ = 5.83 (s, 1 H), 5.53–5.67 (m, 1 H), 5.12 (d, ^3J = 9.2 Hz, 1 H), 4.51 (d, ^3J = 7.7 Hz, 1 H), 3.53–4.01 (m, 12 H), 1.99 (s, 3 H); ^{13}C NMR (DMSO, 75 MHz): δ = 184.23 (C), 140.32 (C), 123.87 (CH_2), 104.46 (CH), 81.09 (CH), 79.40 (CH), 78.02 (CH), 76.94 (CH), 76.70 (CH), 74.09 (CH), 72.91 (CH), 72.52 (CH), 70.13 (CH), 62.62 (CH_2), 61.44 (CH_2), 19.26 (CH_3); ESI-MS, *m*/*z* calcd for $C_{16}H_{28}NO_{11}$: $[M + Na]^+$ 432.38, found: 432.11 $[M + Na]^+$.

MelMAm. ^{1}H NMR (300 MHz, D_2O): δ = 5.81 (s, 1 H), 5.59 (d, ^3J = 1.6 Hz, 1 H), 5.08 (d, ^3J = 8.9 Hz, 1 H), 5.00 (d, ^3J = 3.5 Hz, 1 H), 3.45–4.05 (m, 12 H), 1.98 (s, 3 H); ^{13}C NMR (DMSO, 75 MHz): δ 174.27 (C), 140.28 (C), 123.87 (CH_2), 99.70 (CH), 81.38 (CH), 78.24 (CH), 77.73 (CH), 73.04 (CH), 72.42 (CH), 70.99 (CH), 69.95 (CH_2), 62.67 (CH_2), 19.24 (CH_3); ESI-MS, calcd for $C_{16}H_{27}NO_{11}$: $[M + Na]^+$ 432.38, found: 432.10 $[M + Na]^+$.

FucMAm. ^{1}H NMR (300 MHz, D_2O): δ = 5.78 (1 H, s), 5.56 (1 H, s), 4.98 (1 H, d, ^{3}J = 8.2 Hz), 3.90 (1 H, q, ^{3}J = 6.4 Hz), 3.79–3.94 (1 H, m), 3.61–3.73 (3 H, m), 1.95 (1 H, s), 1.24 (1 H, d, ^{3}J = 6.5 Hz); ^{13}C NMR (DMSO, 75 MHz): δ = 173.69 (C), 140.22 (C), 123.49 (CH_2), 81.21 (CH), 74.99 (CH), 73.98 (CH), 72.80 (CH), 70.32 (CH), 19.19 (CH_3), 17.17 (CH_3); ESI-MS, calcd for $C_{10}H_{17}NO_5$: $[M + Na]^+$ 254.24, found: 254.04 $[M + Na]^+$.

8.4.4 Synthesis of Nanogels via Precipitation Polymerization

8.4.4.1 Synthesis of PNiPAm Nanogel G-1

The reactants, except the initiator, were dissolved in Milli-Q water in a 100 mL-Schlenk flask. We purged the solution with nitrogen and equilibrated at 80 °C in an oil bath for 30 min. Afterwards, the reaction was started by adding the initiator in nitrogen countercurrent. We allowed the turbid mixture to cool down after 4 h of reaction. The nanogels were dialyzed against deionized water for several days and then lyophilized to obtain a white solid.

8.4.4.2 Synthesis of PNiPAm Nanogel G-2 and PNiPMAm Nanogel G-3

We dissolved every reactant in Milli-Q water in a 100 mL-Schlenk flask or 50 mL-Schlenk flask and purged the reaction solution with nitrogen for 30 min (Table 10). The reaction was started by submerging the flask into an 80 °C oil bath. After reaction, we let the slightly turbid mixture cool down and purified the product by dialysis against deionized water for several days, followed by lyophilization. We obtained white solids.

Table 10. Synthesis details of PNiPAm and PNiPMAm nanogels.[a]

Nanogel	$V_{(H2O)}$ [mL]	$c_{(Monomer)}$ [mmol/L]	$n_{(Monomer)}$ [mmol]	$X_{(CL)}$ [mol%]	$c_{(SDS)}$ [mmol/L]	$X_{(ABCVA)}$ [mol%]	t_1 [h]	Yield [%]
G-1	50	100	5	5	0.2	0.25	4.0	-
G-2	50	100	5	10	4.0	2.00	22	86
G-3 [b]	25	100	2.5	5	1.0	2.00	4.5	78

[a]The molfraction X refers to the total monomer amount of substance. Comonomer is NiPMAm if not stated otherwise. Crosslinker is MBA if not stated otherwise. [b] Comonomer is NiPMAm. Crosslinker is EGDMA.

8.4.4.3 Synthesis of Melibiose Glycogels MG-1–MG-8

MelMAm (40.9 mg, 0.1 mmol), comonomer (0.4 mmol; 4 eq.), crosslinker, SDS and initiator were dissolved in 5 mL of Milli-Q water (100 mM total monomer concentration) in a 25 mL-Schlenk flask. The respective amounts of the chemicals used are listed in Table 11. We purged the solution with nitrogen for 30 min, before submerging the flask into an 80 °C oil bath. For some glycogels, we added an additional amount of initiator after approximately 2 h in nitrogen countercurrent (see t_1 in Table 11). The reaction was allowed to proceed for a further amount of time (see t_2 in Table 11). After cooling down the turbid reaction mixture, we purified the glycogel by dialysis against deionized water for several days and lyophilized the product to obtain a white solid. If large, aggregated sediments were observed after reaction, the product was filtered through Kimtech Science® precision wipes (Darmstadt, Germany) before freeze-drying.

Table 11. Synthesis details of melibiose glycogels.[a]

Glycogel	$n_{(Comonomer)}$ [mmol]	$X_{(CL)}$ [mol%]	$c_{(SDS)}$ [mmol/L]	$X_{1(ABCVA)}$ [mol%]	t_1 [h]	$X_{2(ABCVA)}$ [mol%]	t_2 [h]	Yield [d] [%]
MG-1	0.4	10	0.4	1	2.0	2	17	67
MG-2	0.4	10	2.0	1	1.7	2	16	67
MG-3	0.4	10	4.0	1	2.0	2	20	43
MG-4	0.4	10	0.4	3	22	-	-	61
MG-5	0.4	10	0.4	3	22	-	-	66
MG-6	0.4	5	1.0	2	24	-	-	46
MG-7 [b, c]	0.4	5	0.2	2	23	-	-	37
MG-8 [c]	0.4	10	0.4	1	2	2	17	64

[a] The molfraction X refers to the total monomer amount of substance. Comonomer is NiPMAm if not stated otherwise. Crosslinker is MBA if not stated otherwise. [b] Comonomer is NiPMAm. [c] Crosslinker is EGDMA. [d] Yields were determined once.

In case of MG-5, every reactant was dissolved in Milli-Q water with the exception of the initiator. After purging the reaction solution with nitrogen and equilibrating at 80 °C for 30 min, we added the initiator to start the reaction.

8.4.4.4 Synthesis of Melibiose Glycogel MG-0

We first tested the precipitation polymerization with a previously synthesized melibiose monomer that was not stabilized with hydroquinone. We dissolved MelMAm (81.8 mg, 0.2 mmol), NiPAm (90.5 mg, 0.8 mmol; 4 eq.), MBA (15.4 mg, 0.1 mmol; 10 mol%), SDS (1.15 mL of a 10 mg/mL stock solution, 4×10^{-5} mmol; 4 mM) and ABCVA (0.7 mg, 2.5×10^{-3} mmol; 0.25 mol%) in Milli-Q water (9 mL; 100 mM total monomer concentration). We purged the reaction solution with nitrogen for 30 min. Then, we started the reaction by submerging the reaction flask into an 80 °C oil bath. After 2 h, the reaction mixture remained clear. Additional initiator was added, and the mixture turned slightly turbid. We let the reaction proceed for further 4 h before letting it cool down. The glycogel was purified by dialysis against deionized water for several days and then freeze-dried. We obtained 99.7 mg of white solid (53 %).

8.4.4.5 Synthesis of Lactose Glycogel LG

We dissolved LacMAm (40.9 mg, 0.1 mmol), NiPAm (45.3 mg, 0.4 mmol; 4 eq.), MBA (3.9 mg, 2.5×10^{-2} mmol; 5 mol%), SDS (288 µL of a 1 mg/mL stock solution, 1.0×10^{-6} mmol; 0.2 mM) and ABCVA (2.8 mg, 0.01 mmol; 2 mol%) in Milli-Q water (4.712 mL; 100 mM total monomer concentration) in a 25 mL-Schlenk flask. We purged the solution with nitrogen for 30 min. Then the reaction was started by submerging the reaction flask into an 80 °C oil bath. After 20 h of reaction, we let the reaction mixture cool down. We dialyzed the product against deionized water for several days and lyophilized the product to obtain a white solid (72.5 mg, 75 %).

8.4.4.6 Synthesis of Fucose Glycogels FG-1 and FG-2

We dissolved FucMAm (23 1 mg, 0.1 mmol), NiPAm (45.3 mg, 0.4 mmol; 4 eq.), MBA (FG-1: 3.9 mg, 2.5×10^{-2} mmol; 5 mol%; FG-2: 7.7 mg, 5.0×10^{-2} mmol; 10 mol%), SDS (57.67 µL of a 10 mg/mL stock solution, 2.0×10^{-6} mmol; 0.4 mM) and initiator in Milli-Q water (5 mL; 100 mM total monomer concentration) in a 25 mL-Schlenk flask. We purged the solution with nitrogen for 30 min, before submerging the flask into an 80 °C oil bath. The reaction was allowed to proceed for 4 h. After cooling down, we purified the glycogel by

dialysis against deionized water for several days, filtered through Kimtech Science® precision wipes and lyophilized the product to obtain a white solid (FG-1: 41.5 mg, 56 %: FG-2: 25.9 mg, 33 %).

8.4.5 Phenol-Sulfuric Acid Assay for Determination of Total Sugar Content

The phenol-sulfuric acid assay was performed similar to a described method.[280] Two different concentrations of glycogels (1.5 and 0.75 mg/mL for lactose and melibiose nanogels, 4.0 and 2.0 mg/mL for fucose nanogels) were prepared in water. 50 µL of sample was thoroughly mixed with 150 µL sulfuric acid (95 %, Th. Geyer, Renningen, Germany). Subsequently, 30 µL of 5 % phenol (Sigma-Aldrich) was added, followed by mixing. The mixture was incubated at 90 °C for 5 min and let cool down in a water bath for further 5 min. After transferring the solution into a 96-well plate (Carl Roth) the absorption at 490 nm was measured.

For calculating the total sugar amount for each type of saccharide, lactose, melibiose and fucose were used separately for calibration. Control gels without sugar were also measured to prove suitability of the assay.

8.4.6 Lectin Studies

To prove the accessible sugar content of the nanogels, different sugar binding proteins (lectins) were used for binding studies. Fluorescein-labeled lectins were chosen for easy detection: ECL for lactose (β-galactose) binding, Jacalin for melibiose (α-galactose) binding and UEA I for α-fucose binding (all from Vector Laboratories, via BIOZOL Diagnostica Vertrieb GmbH, Eching, Germany).

The lectin binding to the nanogels was proven by an ELISA-type competitive inhibition assay, similar to previously described assays.[193,195] Glycogels that are bound by the lectin inhibit the lectin binding to an immobilized glycoprotein. The standard glycoprotein for ECL and Jacalin is ASF. For UEA, we found good binding to mucin from porcine stomach. The binding of the three lectins to its appropriate ligands was proven in a binding assay varying the lectin concentration.

In microtiter plates (MaxiSorp, Nunc, Wiesbaden, Germany) ASF (100 µL of 5 µg/mL bovine ASF (Sigma-Aldrich)) or mucin (100 µL of 100 µg/mL porcine stomach mucin (Sigma-Aldrich), both in sodium carbonate buffer pH 9.6) was immobilized overnight. After washing with PBS-Tween (0.05 % (v/v) Tween-20) residual binding sites were blocked with 2 % BSA (bovine serum albumin, Carl Roth) in PBS. Wells were washed once with PBS-Tween and twice with lectin buffer (10 mM HEPES, 150 mM NaCl, 0.1 mM $CaCl_2$, pH 7.5). Varying concentrations of inhibitor and 5 or 10 µg/mL of lectin were incubated simultaneously for 1 h. Controls without inhibitor and without lectin were performed to indicate minimal and maximal binding, respectively. Wells were again washed with lectin buffer and residual bound lectin was detected by fluorescence read-out at 488/520 nm. Measured data were analyzed using Sigma Plot (Systat software GmbH, 11.0, Erkrath, Germany).

8.4.7 Cultivation of PA

The nanogels (4 mg) were swollen over night at 37 °C under shaking conditions in 1 mL Nutrient Broth (NB, Carl Roth).

Nutrient broth was inoculated with Pseudomonas aeruginosa and grown under shaking conditions (110 rpm) at 37 °C overnight. The overnight culture was diluted to an OD600 nm of 0.2 with NB and subsequently diluted with the nanogel suspension in a ratio of 1:2 (nanogel 2 mg/mL, PA OD 0.1). 500 µL of this mixture were plated in a 24-well plate (n = 4) (TPP, Techno Plastic Products AG, Trasadingen, Switzerland)) and cultivated under static condition overnight at 37 °C. Then the fluorescence of pyoverdine was detected using UV light (Dark Hood DH-50, BIOSTEP, FELIX 2000, Burkhardtsdorf, Germany).

All samples and the controls (PA in NB) showing fluorescence were diluted to 10^{-4} – 10^{-6} with PBS (Biochrom AG, Berlin, Germany). Samples without fluorescence were diluted to 10^{-2}. Subsequently, 100 µL of each sample was plated on cetrimid agar plates (Carl Roth) and stored overnight (37 °C).

8.5 Conclusions

For the first time, we prepared melibiose, fucose and lactose containing nanogels via precipitation polymerization of NiPAm and glycomonomers. We varied the reactions conditions of the gel production and analyzed the inhibitory potency of the gels in lectin assays. The gels showed sugar dependent inhibition of the lectin binding and a prominent multivalent effect compared to unmodified saccharides. We found that overal the inhibition strength increases with decreasing gel size. Furthermore, the monomer NiPAm and crosslinker MBA are more suitable for these lectin assays than NiPMAm and EGDMA as the latter two themselves influence the binding behavior. The crosslinker amount influences the yield and the lectin binding differently, depending on the glycomonomer. At the same sugar content, the inhibitory potency seems to be strongly dependent on the morphology of the glycogel. Interestingly, the amount of incorporated sugar is not strongly influenced by the reaction parameters but by the type of glycomonomer. This enables a tuning of the synthesis towards yields, optimized size and morphology without decreasing sugar content in the gels. Fucose containing gels showed no inhibition due to the β-anomeric form of the glycomonomer. However, LecB is reported to bind β-fucose residues. Due to the biocompatibility of the materials a potential use of the gels in alternative treatments of Pseudomonas aeruginosa infections could be possible in the future. First trials suggest an influence of fucose gels on the secretion of pyoverdine. Work is in progress to establish biofilm formation assays with PA in the presence of the glycogels as well as a more in-depth investigation of the effect in pyoverdine secretion of β-fucose gels.

8.6 Acknowledgements

We thank Xuepu Wang, Steffi Grunst and Kathrin Geßner from Fraunhofer Institute for Applied Polymer Research for AFM analysis, SEM images and for TGA analysis, respectively.

9 Protection group- free synthesis of α- mannopyranosyl methacrylamide

9.1 Abstract

Regioselective derivatization of carbohydrate structures include tedious (de)protection steps. Lectins, which are important and interesting in the field of biotechnology, specifically bind terminal carbohydrate structures in α-configuration. Herein, we report a synthetic route for the isolation of mannopyranosyl methacrylamide as an α-anomer for subsequent polymerizations. This targeted synthesis enables the isolation of glycopolymers from α-carbohydrate derivatives to gain further insight in areas such as drug delivery, biofunctional materials as well as tissue engineering.

9.2 Introduction

Among many biological processes, glycan-mediated interactions are jointly the key to cellular adhesion, pathogen control, immune response, and many more.[281,282,283,284,285] Many pathogens have altered carbohydrate and glycoprotein expression that can be recognized by lectins through strong multivalent, non-covalent binding to several active binding sites. By mimicking these natural glycostructures with glycopolymers, a higher glycan density can be achieved causing the "cluster glycoside effect".[286,287] The application of these macromolecules extends to biological analysis, especially binding assays with lectins for carbohydrate-protein interaction studies as an effective tool to analyze diverse cell processes.[288,289] Lectins are naturally occurring proteins that participate in various physiological processes, mostly in the field of cell communication and cell recognition by binding to glycan structures.[290] The lectins type 1 fimbriae (FimH) and *Galanthus nivalis* agglutinin (GNA) bind specifically to terminal α-D-mannosyl derivatives, while *Pisum sativum* agglutinin (PSA), *Lens culinaris* agglutinin (LCA) and concanavalin A (ConA) additionally recognise α-D-glucosyl derivatives.[291,292,293,294,295]

The synthesis of required glycomonomers often involves the tedious introduction and removal of protecting groups due to reactive hydroxyl groups.[97,296] To elude these, enzymes as catalysts or two-step synthetic routes via Kochetkov amination or Likhoshertov with subsequent (meth)acrylation have been reported.[105,201] Enzyme-catalyzed synthesis of

glycomonomers using Novozym 435 is feasible to derivatize the C6 position in hexoses.[102,297,298] Nevertheless, in order to generate a carbohydrate-lectin interaction, addressing of the C1 position is necessary.[299] Optimization of the microwave assisted Kochetkov or Likhoshertov amination were presented with several carbohydrate structures.[164] However, stereoselective synthesis of glycomonomers is challenging facing configural instability due to the anomeric effect. Thus, glycosylamines prefer the more stable β-configuration, which results in the isolation of β-glycomonomers. Glycosyl azides can be used to circumvent this issue. By reducing with suitable acylating agents, the formation of free amine can be prevented. This approach using the Staudinger ligation has already been applied to obtain stereoselective glycoconjugates.[300] Depending on whether benzylic or acetylic protecting groups were incorporated, the glycoconjugate resulted as the α- or β- anomer, respectively.

Due to the electron-withdrawing effect of acetates, the acylation step is slowed down, leading to anomerization. The isolation of α-glycoconjugates by Staudinger ligation was also described, though this time without the use of protecting groups.[301]

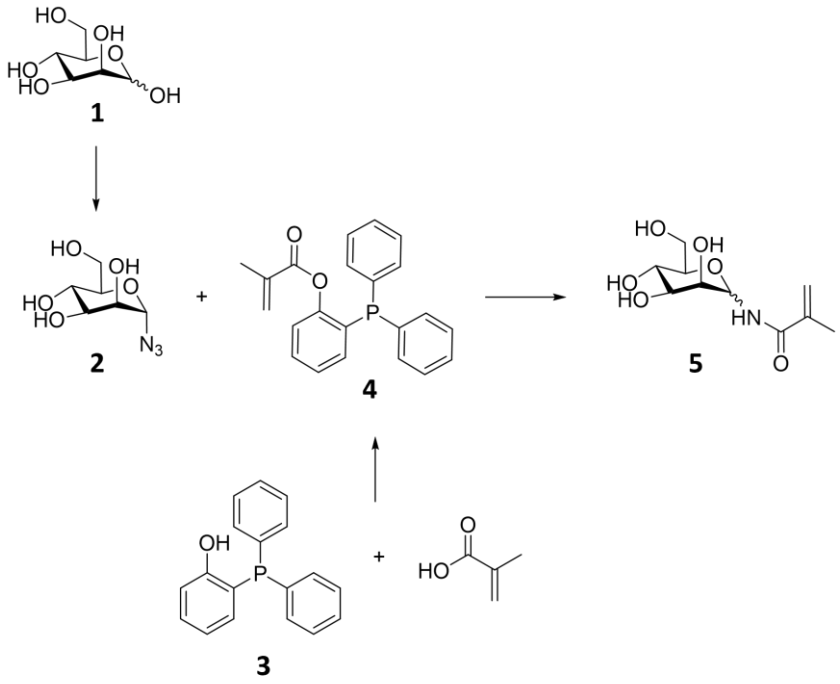

Scheme 13. Reaction scheme of the synthesis of mannopyranosyl methacrylamide.

This work describes a new protecting group free route for the efficient synthesis of mannose-containing monomers in α-configuration for the first time. For this purpose, "traceless" Staudinger ligation was chosen as the central synthesis method (Scheme 13). Its advantage lies in its specificity with respect to the reactive groups as well as the isomerism of

the product. This reaction type required the prior synthesis of a triphenylphosphine derivative bearing a polymerizable functional group and an azide functionalized D-mannose derivative as the reactant. Modifications of several reaction conditions of the ligation step were evaluated to achieve reasonable yields and isomeric purity.

9.3 Results and Discussion

Synthesized α-mannosyl azide was used as the substrate for the Staudinger ligation reaction. The synthesis and characterization are reported in the Supporting Information. α-Mannosyl azide was isolated with complete stereocontrol by reacting D-mannose with 2-chloro-1,3-dimethylimidazolinium chloride (DMC) and NaN_3 under basic reaction conditions, as already described.

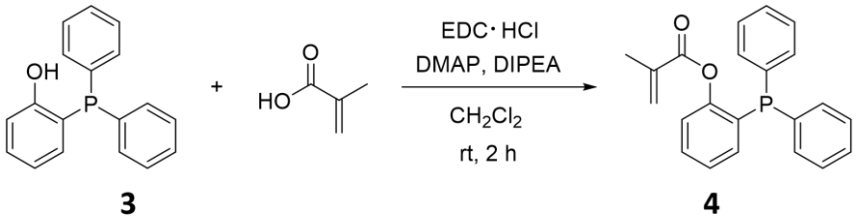

Scheme 14. Synthesis of phosphine derivative with a polymerizable functional group **4**.

Triphenylphosphine derivatives show lower lability towards air compared to other triphosphine derivatives. To introduce a polymerizable functionality, (2-hydroxyphenyl)diphenylphosphine was derivatized with a short methacrylate group to 2-(diphenylphosphonyl)phenyl methacrylate **4** (Scheme 14).

Methacryloyl chloride and methacrylic acid were used to modify the triphenyl phosphine derivative via a S_N2 displacement and esterification reaction mechanism, respectively. It was found that applying methacrylic acid was more suitable for derivatization due to the isolation of higher yields and reproducibility. In addition, the removal of the by-products using the synthesis route with methacryloyl chloride were aggravated. Syntheses using methacryloyl chloride were tested in diethylether and dichloromethane under the formation of triethylamine hydrochloride. The latter reaction solvent resulted in higher final yields as purification was more straightforward due to the higher vapour pressure compared to diethyl ether. Conversion with methacrylic acid was obtained under the activation with EDC•HCl, followed by a Steglich esterification mechanism with DMAP. DMAP reacts with the activated

carboxylic acid, resulting in a formation of a DMAP-acid-compound, which can be attacked by the hydroxyl functionality to form an ester bond. The base DIPEA serves as a proton scavenger and enables the catalytic use of DMAP by accelerating the regeneration of catalytic DMAP, thus improving the reaction rate. ^{1}H NMR spectroscopy analysis verified the isolation of the desired compound after purification using column chromatography. Vinyl protons are shifted to the downfield at 6.0 and 5.5 ppm.

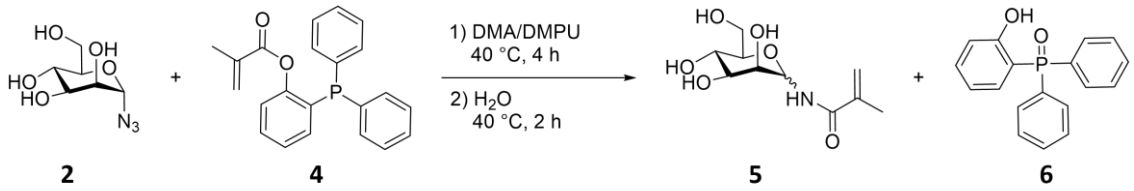

2 **4** **5** **6**

Scheme 15. Synthesis of mannosyl methacrylate **5** via Staudinger ligation.

The driving force of the Staudinger ligation is the formation of the phosphorus-oxygen double bond, which requires reaction conditions with exclusion of water and oxygen. A premature formation of the phosphorus-oxygen bond leads to a deactivation of the phosphine derivative and therefore is unusable for a Staudinger ligation reaction. The Staudinger ligation proceeds in two reaction steps. The first step includes the formation of iminophosphorane as transition state, which is only stable in a non-oxidating and non-hydrolyzing environment. The second step contains the hydrolysis of the formed iminophosphorane by adding water to result in the desired α-mannopyranosyl methacrylamide and the by-product triphenylphosphine oxide (Scheme 13). The optimization experiments were performed with the unpurified crude product 2-(diphenylphosphonyl)phenyl methacrylate **4**. The optimal conditions found were subsequently applied to the synthesis of α-mannopyranosyl methacrylamide **5** with the purified, isolated product **4**.

Table 12. Optimization of the synthesis of mannosyl monomer **5** via Staudinger ligation with unpurified crude 2-(diphenylphosphonyl)phenyl methacrylate **4**.

Entry	T[a] [°C]	t[a] [h]	T[b] [°C]	t[b] [h]	α-yield[c] [%]	α/β ee[d]
1	70	4	70	2	10	1:9
2	40	4	40	16	7	1:3
3	70	4	40	16	2	1:4
4	70	16	70	5	6	2:3
5	70	16	70	16	3	1:3
6	40	4	40	2	17	3:1
7	40	16	40	5	6	33:1

[a]First reaction section: formation of iminophosphorane; [b]Second reaction section: hydrolysis; [c]gravimetric determination after purification; [a]according to HPLC elugram.

^{1}H NMR spectroscopy analyses revealed a mixture of α- and β-mannopyranosyl methacrylamide, which could be separated with reverse-phase HPLC. Low reaction temperature at 40 °C and short reaction times of both reaction sections resulted in a high α- to β-monomer ratio and a reasonable yield of 17 % of the α-mannosyl derivative. Long reaction times of both reaction sections resulted in lower yields due to the instability of the formed iminophosphorane. Reaction temperature seems to play a minor role regarding yield but does affect the isomeric equilibrium shift of the product. Increased temperature led to a faster rearrangement of the iminophosphorane from the α- to the β-isomer and thus to a lower α to β ratio according to HPLC analyses (Table 12). The total yield of reactions at 40 °C are lower with less conversion of the starting material, however, the α- to β-monomer ratio is increased. Nevertheless, since the separation of α- and β-monomer is potentially more difficult than that of α-monomer and reactant, the reaction at 40 °C is preferred. To determine the accurate yield of this Staudinger ligation, the reaction was carried out with pure **4** under the optimized reaction conditions of reaction number 6 identified. At a reaction temperature of 40 °C and a total reaction time of 6 h, a yield of **5** in α-configuration with 70 % was obtained, which could be reproduced.

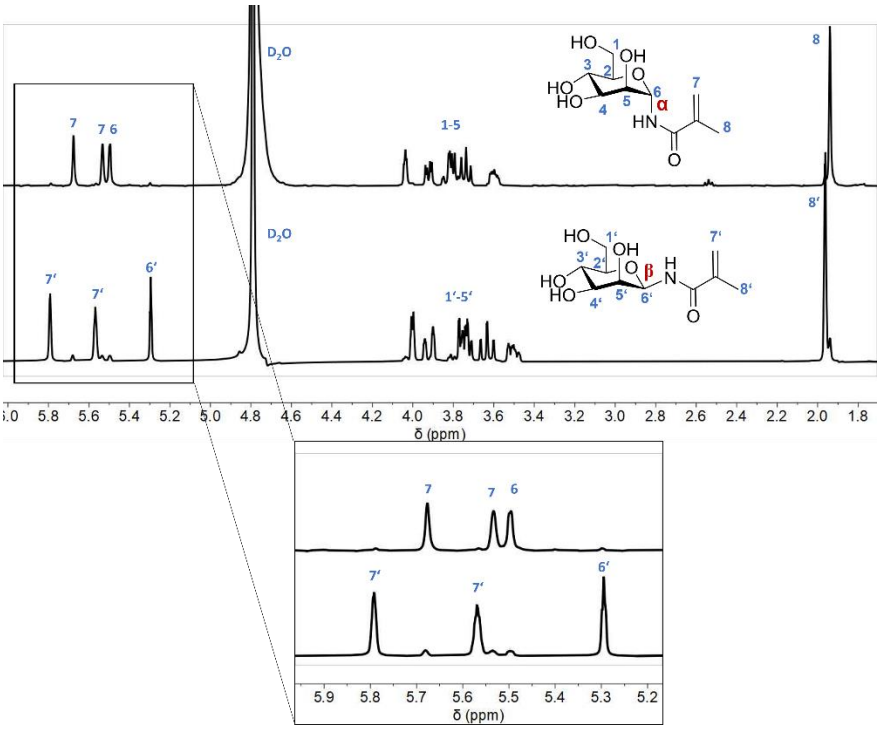

Figure 27. Comparison of ^{1}H NMR spectrum of α- and β- mannosyl methacrylate **5**.

The peaks at 5.7 and 5.5 ppm in the ^{1}H NMR spectrum are attributed to the vinyl protons (Figure 27). The doublet at 5.5 ppm can be assigned to the anomeric proton of the α-isomer, whereas the one of the β-isomer appears at 5.3 ppm. Resonance shift of protons in an equatorial position are shielded due to the spatial proximity to the ring oxygen compared to protons in an axial position.

9.4 Conclusion

The field of glycopolymers increased regarding biological recognition processes to gain insights in carbohydrate-protein interactions. Potential applications of glycopolymers are biofunctional materials, drug delivery or tissue engineering due to the advantage of the present of high glycan densities. The isolation of these glycan-bearing macromolecules requires the synthesis of the desired monomer precursors. Due to high density of reactive functional groups of carbohydrates, the synthesis of glycomonomers requires time-consuming protection or deprotection steps for derivatization. In addition, isolation of glycoderivatives in their α-anomerism is challenging in terms of configural instability. This work descried for the first time the synthesis of a mannose-containing monomer in its α-anomer without (de)protection steps within two synthesis steps. The phosphine derivative required for this procedure was prepared via an EDC•HCl mediated Steglich esterification with methacrylic acid to introduce a

polymerizable functional group. By reaction with α-mannopyranosyl azide, mannopyranosyl methacrylamide was yielded using the Staudinger ligation reaction mechanism as an α and β anomeric mixture. The anomeric ratio depends on the reaction conditions. Varying the synthesis parameters revealed significant shifting of the anomeric equilibrium to the α-glycomonomer with shorter reaction times and lower reaction temperatures of 40 °C. Chromatographic purification succeeded in separating the mixture and thus the α-anomeric glycomonomer was isolated in its pure form. NMR and ESI-MS analyses confirmed the successful isolation of the desired compounds. Proceeding polymerizations with the synthesized glycomonomer are scheduled for potential lectin binding studies.

9.5 Experimental

9.5.1 Materials and instrumentation

9.5.1.1 Chemicals

All reagents and solvents were used without further purification. *N*-(3-Dimethylaminopropyl)-*N*′-ethylcarbodiimide hydrochloride (EDC,> 99 %), *N*, *N*′-dimethylpropyleneurea (DMPU,> 99 %), D-mannose (> 99.5 %), $NaHCO_3$ (> 99 %) and diethyl ether (dry, > 99.5 %) were purchased from Carl Roth (Karlsruhe, Germany). Na2SO4 (> 99 %), HCl (37 %), *n*-hexane (95 %), toluene (> 99.5 %) and dichloromethane (> 99.8 %) were received from Chemsolute (Renningen, Germany), 1,4-dioxane (> 99 %) from Acros Organics (Geel, Belgium). (2-Hydroxyphenyl)diphenylphosphine (97 %), 4-dimethylaminopyridine (DMAP,> 98 %), methacryloyl chloride (97 %), methacrylic acid (99 %), Et_3N (> 99.5 %), DIPEA (99.5 %), dimethyl acetamide (DMA, 99 %) and methanol (> 99.9 %) were obtained from Merck KGaA (Darmstadt, Germany). NaN_3 (99 %) was from Alfa Aesar (Kandel, Germany), 2-chloro-1,3-dimethylimidazolinium chloride (DMC,> 98 %) from TCI (Tokyo, Japan). Ethyl acetate (> 99.8 %) was purchased from VWR (Radnor, US). Deuterated solvents D_2O (99.9 %) was received from Deutero (Kastellaun, Germany), $CDCl_3$ (> 99.8 %) from Merck KGaA (Darmstadt, Germany).

9.5.1.2 Instrumentation

ESI-MS spectra were recorded with a Perkin Elmer Flexar SQ 300 MS Detector. Samples were prepared by solving in an acetonitrile/water (1:1) mixture with additional formic acid (0.1 %) and measured at a temperature of 300 °C with a flow rate of 15 µL/min. Nuclear magnetic resonance (NMR) spectroscopy was performed with a Bruker AVANCE NEO (400 MHz) spectrometer. Deuterated solvents were used as standards. Chemical shifts are given in the δ-scale in ppm relative to solvent peaks. Multiplicities are displayed with the coupling constants in Hertz (Hz). Preparative HPLC was conducted with an Azura from Knauer equipped with an Azura UVD 2.15 UV detector. Samples were prepared by dissolving in water. The eluent was 100 % water with a flow rate of 10 mL/min. α/β ratio was determined by integrating the peaks of α, starting to eluent at around 41 min and β, starting to eluent at around 48 min.

9.5.2 Syntheses procedure

*9.5.2.1 Synthesis of α-mannopyranosyl azide **2***

D-Mannose (0.50 g, 2.78 mmol), DMC (1.41 g, 8.34 mmol), NaN_3 (1.63 g, 25.02 mmol) and Et_3N (3.47 mL, 25.02 mmol) were stirred in a 1:1 solvent mixture of H_2O/ 1,4-dioxane (11 mL) for 1 h at -10 °C. The reaction mixture was purified using column chromatography (dichloromethane/ methanol 5:1) and additionally extracted from diethyl ether (3 x 100 mL). After freeze-drying, the desired compound was yielded in 80 % (0.46 g, 2.22 mmol) as a white solid.

^{1}H NMR (D_2O, 400 MHz, rt): δ [ppm] = 5.5 (d, ^3J = 1.9 Hz, 1H, N_3-C_1-H), 4.0 – 3.6 (m, 6H).

ESI-MS: m/z for $C_6H_{11}N_3O_5$: $[M + Na]^+$ calculated: 228.16, found: 228.14.

*9.5.2.2 Synthesis of 2-(diphenylphosphonyl)phenyl methacrylate **4***

Et_3N (60.3 µL, 0.82 mmol) was added to (2-hydroxyphenyl)diphenylphosphine (0.20 g, 0.72 mmol), dissolved in dry dichloromethane (7.2 mL). Freshly distilled methacryloyl chloride (91.7 µL, 0.82 mmol) was added to the clear reaction solution and was stirred for 1 h at room temperature under N_2 atmosphere. Afterwards, the solvent was removed under vacuum and the reaction mixture was taken up in ethyl acetate, washed with $NaHCO_3$ solution (5 %, 3 x

100 mL) and water (2 x 100 mL). The organic layer was dried over Na_2SO_4, concentrated and dried under high vacuum. The side products were removed by precipitation from cold *n*-hexane, added to the reaction mixture in dichloromethane. After concentrating the filtrate, the desired phosphine derivative was received with a purity of 70 % (82.80 mg, 0.24 mmol) as a white powder.

(2-Hydroxyphenyl)diphenylphosphine (0.20 g, 0.72 mmol) was dissolved in dried dichloromethane (3.6 mL) with methacrylic acid (75.5 µL, 0.86 mmol) and DMAP (8.80 mg, 72.0 µmol). In another flask, EDC (0.19 g, 1.00 mmol) was dissolved in dried dichloromethane (3.6 mL) with DIPEA (95.9 µL, 1.00 mmol). Both solutions were combined under N_2 and stirred for 2 h at room temperature. After diluting with dichloromethane (5 mL), the reaction solution was washed with HCl solution (10 %, 2 x 100 mL) and water (2 x 100 mL). The organic layer was dried over Na_2SO_4, concentrated under vacuum and purified using column chromatography (*n*-hexane/ethyl acetate 9:1). Pure 2-(diphenylphosphonyl)phenyl methacrylate was isolated with a yield of 12 % (29.9 mg, 86.4 µmol) as a white solid.

^{1}H NMR ($CDCl_3$, 400 MHz, rt): δ [ppm] = 7.4 – 7.3 (m, 11H, Ar-H), 7.2 (ddd, ^3J = 8.1 Hz, ^3J = 4.1 Hz, ^4J = 1.0 Hz, 1H, Ar-H), 7.1 (t, ^3J = 7.5 Hz, 1H, Ar-H), 6.8 (ddd, ^3J = 7.6 Hz, ^3J = 4.2 Hz, ^4J = 1.6 Hz, 1H, Ar-H), 6.0 (p, J = 1,0 Hz, 1H, C=CH_2), 5.5 (p, J = 1.3 Hz, 1H, C=CH_2), 1.8 (t, ^4J = 2.5 Hz, 3H, C-CH_3).

ESI-MS: m/z for $C_{12}H_{19}O_2P$: $[M + H]^+$ calculated: 347.4, found: 347.5; $[M + Na]^+$ calculated: 369.4, found: 369.1; $[M + K]^+$ calculated: 385.3, found: 385.1.

*9.5.2.3 Synthesis of α-mannopyranosyl methacrylamide **5***

α-Mannopyranosyl azide (51.3 mg, 0.25 mmol) was dissolved in DMA (1 mL) and added to a solution of 2-(diphenylphosphonyl)phenyl methacrylate (86.6 mg, 0.25 mmol) in DMA (1.94 mL) under N_2 atmosphere. After adding DMPU (60.0 µL), the reaction mixture was stirred at 40 °C overnight. Afterwards, H_2O (120 µL) was added and stirred for additional 2 h at 40 °C, before removing the solvents under vacuum. The concentrated crude mixture was dissolved in H_2O (5 mL) and extracted from dichloromethane (3 x 50 mL). The aqueous layer was concentrated and the desired product was obtained with a yield of 70 % (43.3 mg, 0.18 mmol) after purifying using a preparative reverse-phase HPLC (100 % H_2O).

α: ^{1}H NMR (D_2O, 400 MHz, rt): δ [ppm] = 5.7 (s, 1H, C=CH_2), 5.5 (s, 1H, C=CH_2), 5.5 (d, ^{3}J = 1.7 Hz, 1H, C1-H), 4.0 – 3.6 (m, 6H), 1.9 (s, 3H, C-CH_3).

β: ^{1}H NMR (D_2O, 400 MHz, rt): δ [ppm] = 5.8 (s, 1H, C=CH_2), 5.6 (s, 1H, C=CH_2), 5.3 (s, 1H, C1-H), 4.0 – 3.5 (m, 6H), 2.0 (s, 3H, C-CH_3).

ESI-MS: m/z for $C_{10}H_{17}NO_6$: $[M + Na]^+$ calculated: 270.2, found: 270.2; $[2M + Na]^+$ calculated: 517.5, found: 517.2.

9.6 Acknowledgment

The authors gratefully acknowledge Angela Krtitschka from the University of Potsdam for enabling measurements of NMR spectra.

10 Microwave-assisted synthesis of 5'-*O*-methacryloylcytidine using the immobilized lipase Novozym 435

10.1 Abstract

Nucleobase building blocks demonstrated to be strong candidates when it comes to DNA/RNA-like materials by benefiting from hydrogen bond interactions as physical properties. Modifying at the 5' position is the simplest way to develop nucleobase-based structures by transesterification using the lipase Novozym 435. Herein, we describe the optimization of the lipase-catalyzed synthesis of the monomer 5'-*O*-methacryloylcytidine with the assistance of microwave irradiation. Variable reaction parameters, such as enzyme concentration, molar ratio of the substrate, reaction temperature and reaction time, were investigated to find the optimum reaction condition in terms of obtaining the highest yield.

10.2 Introduction

Nucleobase-bearing compounds are gaining interest in Material Science by mimicking DNA/RNA structures. Strong base-pairing properties of complementary nucleobases adenine with thymine and cytosine with guanine are the fundamental building block for the development of smart programmable materials.[302,303,304,305,306] In particular, thermoresponsitivity can be targeted since hydrogen bond interactions are labile when exposed to heat.[307] The synthesis of nucleobase-based polymers requires challenging isolation of their monomers. Low solubility of nucleobases or reactive functional groups of nucleosides and especially, of integrated ribose require the development of a multi-step synthesis, including protection and deprotection steps.[308,309,310] Applying enzymes as biocatalysts greatly facilitates these syntheses due to their regioselectivity and specificity.[102,311] The tedious protection-deprotection methods for hydroxyl groups can be avoided to reduce the synthesis steps. The opportunity for a one-step functionalization is not the only advantage; it is also beneficial in terms of "green chemistry". Enzymes are highly efficient, even under mild conditions, such as low temperature and low pressure. After proper work-up, they can even be reused in several synthesis cycles.[312]

The industrial application of the enzyme class lipases (EC 3) ranges from the detergent to the pharmaceutical industry.[313,314] Their biological function is focused on the hydrolysis of lipids. This hydrolysis is an equilibrium reaction, and depending on the reaction condition, the reverse reaction, (trans)esterification, may be favored.[107] Due to their high selectivity and specificity towards functional groups, lipases are a good choice for introducing polymerizable groups into nucleosides for further thermoresponsive material designs. Uridine was esterified using the non-commercially available methacrylocylacetone oxime and the lipase Novozym 435, a commercially available isoform B of *Candida antarctica* (Cal B) lipase with a microporous acrylic polymer resin, which comes with a spherical pearl morphology. The yield was 83 % after a reaction time of 52.5 h. Complementary adenine yielded in 44 %.[315] Based on these results, cytidine was functionalized with a polymerizable group. The isolation required a reaction time of 22 h resulted in a yield of 47 %. Synthesis of the complementary guanosine-based monomer using the lipase Novozym 435 was only feasible with time-consuming protection-deprotection steps.[311]

Over the last 30 years, the application of microwave irradiation to chemical reactions has increased significantly. It is used in organic [164,165,316] and organometallic synthesis,[317,318] inorganic solid-state reactions,[123] catalysis and even peptide synthesis,[319,320] polymer chemistry or nanotechnology.[321] Due to the steady heat distribution, the yield in organic syntheses can be increased in a reduced reaction time compared to conventional heating with an oil bath. Combining microwave irradiation with enzyme catalysis is a common method for the synthesis of compounds.[322,323,324] The application of a biocatalyst enables derivatization of carbohydrate moieties without the use of protecting groups, while microwave irradiation significantly increases reaction kinetics, as reflected in reaction time and/ or reaction yield. This synergy of microwave irradiation and enzymatic catalysis for derivatization of carbohydrate structures was revealed. In the past, the enzymatic conversion of methyl α-D-glucosides with dodecanoic acid was studied. Compared to conventional heating, the assistance of microwave irradiation increased the yield from 55 % to 95 % at a reaction temperature of 95 °C.[325] The synthesis of sorbitan methacrylate was also optimized using the combination of the biocatalyst and microwave radiation.[326]

This work focused on the optimization of a lipase-catalyzed synthesis of cytidine-based monomer for further programmable material designs under microwave irradiation (Scheme 16). The use of lipase makes it possible to minimize the synthesis of such elaborately synthesized cytidine monomers to a single synthesis step. The combination with microwave irradiation

accelerates the reaction rate and is, therefore, more efficient due to a reduced reaction time. The lipase Novozym 435 enables functionalization of the 5’-hydroxyl group without protection of the remaining hydroxyl groups. The influence of synthesis parameters was analyzed to determine the optimal reaction conditions. Varying reaction parameters, such as enzyme concentration, substrate, molar ratio, reaction temperature and reaction time, were analyzed to determine optimal reaction conditions.

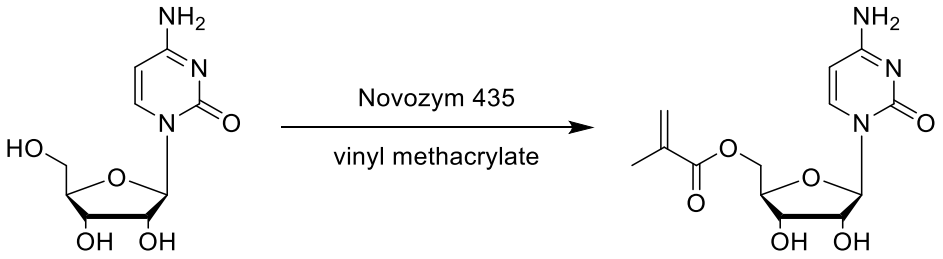

Scheme 16. Enzyme-catalyzed synthesis of 5'-*O*-methacryloylcytidine.

10.3 Materials and Methods

10.3.1 Materials and Instrumentation

10.3.1.1 Chemicals

All reagents and solvents were used without further purification. Cytidine (99 %) was purchased from Carbosynth (Berkshire, UK), 1,4-dioxane (> 99.5 %) from Carl Roth (Karlsruhe, Germany). Novozym 435 (Lipase B from *Candida antarctica*, immobilized on acrylic resin, > 5000 U/g), vinyl methacrylate (98 %), methyl methacrylate (99 %) and 2,6-di-*tert*-butyl-4-methylphenol (BTH, > 99 %) were received from Sigma Aldrich (St. Louis, MO, USA). The solvents for chromatographic purification acetonitrile (> 99.95 %), ethyl acetate (> 99.8 %) and methanol (> 98.5 %) were from VWR (Radnor, PA, USA). Deuterated solvents D_2O (99.9 %) and DMSO-d_6 (99.8 %) were obtained from Deutero (Kastellaun, Germany).

10.3.1.2 Instrumentation

ESI-MS spectra were recorded with a Perkin Elmer Flexar SQ 300 MS Detector. Samples were prepared by solving in an acetonitrile/water (1:1) mixture with additional formic acid (0.1 %) and measured at a temperature of 300 °C with a flow rate of 15 µL min^{-1}. Nuclear magnetic resonance (NMR) spectroscopy was performed with a Bruker AVANCE NEO

(400 MHz) spectrometer. Deuterated solvents were used as standards. Chemical shifts are given in the δ-scale in ppm relative to solvent peaks. Multiplicities are displayed with the coupling constants in Hertz (Hz).

10.3.2 Enzymatic Transesterification

10.3.2.1 Conventional heating

5'-*O*-methacryloylcytidine was prepared conventionally using a modified synthesis.[327] Briefly, cytidine (50.3 mg, 0.207 mmol, 1 eq) was suspended in 1,4-dioxane (2 mL), following the addition of a catalytic amount of BTH, vinyl methacrylate (0.740 mL, 0.616 mmol, 3 eq) and Novozym 435 (0.277 mg, 5.5 wt%). The reaction mixture was stirred overnight under N_2 atmosphere at 60 °C. After reacting over 22 h, the reaction mixture was concentrated and purified using column chromatography (SiO_2, 7:3 EtOAc/MeOH). The desired compound was isolated as a white solid (11.0 mg, 35.2 µmol) with a yield of 16.9 %.

^{1}H NMR (D_2O, 400 MHz, rt): δ (ppm) = 7.67 (d, ^3J = 7.6 Hz, 1H, H-17); 6.14 (s, 1H, CH_2(21)); 5.99 (d, ^3J = 7.5 Hz, 1H, H-16); 5.87 (d, ^3J = 2.6 Hz, 1H, H-8); 5.77 (s, 1H, CH_2(21)); 4.59 (dd, J = 12.6 Hz, ^3J = 2.2 Hz, 1H, CH_2(2)); 4.45 (dd, J = 12.6 Hz, ^3J = 4.1 Hz, 1H, CH_2(2)); 4.28 – 4.38 (m, 3H, H-3, H-6, H-4); 1.94 (s, 3H, CH_3(22)).

^{13}C NMR (D_2O, 400 MHz, rt): δ (ppm) = 168.98 (C=O(4)); 166.06 (C-NH_2(12)); 157.29 (C=O(13)); 141.02 (C-H(10)); 135.44 (C-(3)); 127.29 (CH_2(2)); 96.04 (C-H(11)); 90.77 (C-H(9)); 80.81 (C-H(6)); 74.05 (C-H(8)); 69.11 (C-H(7)); 63.34 (CH_2(5)); 17.45 (CH_3(1)).

10.3.2.2 Microwave Irradiation

The used multimode microwave reactor was a START microchemist 1500 from MLS GmbH. The warmup time was set to 5 min to reach the desired temperature, and the maximum power to 1000 W for the whole synthesis procedure. Actual reaction temperature and reaction time were varied as followed as specified in experiments below.

10.3.2.3 Choice of Substrate

Cytidine (100 mg, 0.414 mmol) was impregnated with Novozym 435 (12.7 wt%) by stirring the lipase with an aqueous solution of cytidine. After freeze-drying, vinyl methacrylate (1.50 mL, 14.5 mmol, 1:35) or methyl methacrylate (1.37 mL, 14.5 mmol, 1:35) was added to the reaction mixture with BHT (150 µg, 0.681 µmol). The reaction mixture was then stirred at 95 °C for 30, 95 and 120 min under microwave irradiation and purified using a preparative HPLC device (reverse phase C_{18} silica, 15 % acetonitrile in H_2O).

10.3.2.4 Effect of Enzyme Concentration

An aqueous solution of cytidine (100 mg, 0.414 mmol) was stirred with Novozym 435 with either 5.5, 12.7 or 22.5 wt%. To impregnate, this cytidine Novozym 435 mixture was stirred at room temperature for 10 min, followed by drying. Afterwards, vinyl methacrylate (1.50 mL, 14.5 mmol, 1:35) and BHT (150 µg, 0.681 µmol) were added to the reaction mixture in a microwave vessel at 95 °C for 30, 60 and 120 min. The desired compound was isolated after purifying using a preparative HPLC device (reverse phase C_{18} silica, 15 % acetonitrile in H_2O).

10.3.2.5 Effect of Reaction Temperature and Reaction Time

To Novozym 435 (12.7 wt%)-impregnated cytidine (100 mg, 0.414 mmol), BHT (150 µg, 0.681 µmol) and vinyl methacrylate (1.50 mL, 14.5 mmol, 1:35) were added. The reaction mixture was radiated with microwaves for 30, 60 and 120 min at reaction temperatures of 45, 60, 95 and 120 °C, respectively. The product was yielded by a preparative HPLC device (reverse phase C_{18} silica, 15 % acetonitrile in H_2O).

10.3.2.6 Effect of Molar Ratio

To investigate the excess of the substrate, two different molar ratios to the starting material were used. Therefore, cytidine (100 mg, 0.414 mmol) was impregnated with Novozym (12.7 wt%) before reacting with BHT (150 µg, 0.681 µmol) and vinyl methacrylate with a molar ratio of either 1:35 or 1:76 to cytidine under microwave irradiation at 95 °C for 30, 60 and

120 min. Purification of the reaction mixture occurred with a preparative HPLC device (reverse phase C_{18} silica, 15 % acetonitrile in H_2O).

10.3.2.7 Recyclability

To examine the recyclability of Novozym 435 after the performed synthesis, the enzyme was filtered and washed with 100 mL of H_2O. After freeze-drying, Novozym 435 was used for recyclability tests. Cytidine (100 mg, 0.414 mmol) was impregnated with recycled Novozym 435 (12.7 wt%). Afterwards, vinyl methacrylate (1.50 mL, 14.5 mmol, 1:35) and BHT (150 µg, 0.681 µmol) were added. The mixture was reacted under microwave irradiation for 30 min at 95 °C, before purifying with a preparative HPLC device (reverse phase C_{18} silica, 15 % acetonitrile in H_2O).

10.4 Results and Discussion

10.4.1 Synthesis approach and Regioselectivity

Cytidine was functionalized with the polymer-bound lipase Novozym 435 and a suitable transesterification substrate to obtain a polymerizable compound via a one-step synthesis for future development of smart programmable materials. As preliminary trials showed an increase in yield after impregnation of cytidine with Novozym 435, this is necessary to maintain a high yield. To increase the reaction rate, microwave radiation was applied. Due to the consistent heating, in which the molecules are set in motion by vibration and rotation, the addition of microwave radiation increases the energy transfer compared to conventional heating. Since the choice of substrate, enzyme concentration, reaction temperature, reaction time and substrate concentration are decisive factors for the yield, the effects of these parameters are described in more detail in the next chapters. The addition of the radical inhibitor BHT in a catalytic amount is intended to prevent premature polymerization under such harsh conditions of heat and/ or microwave irradiation. The conversion rate of an enzymatic (trans)esterification depends on the polarity of the used solvent. The higher log P value, the higher is the yield. Hydrophilic solvents, defined by lower log P values, showed reduced enzyme activity.[328] Polar solvents, such as DMF, may deactivate enzymes. Nevertheless, apolar solvents are not able to dissolve polar substrates. Previous work showed a peak in conversion rate when using hydrophobic solvents like hexane. First, the yield improved with increased hexane concentration, but depicted a

turning point after higher hexane amounts.[329] Evaluation of microwave-assisted lipase-catalyzed reactions in different solvents indicated that the highest conversion yield was achieved when avoiding typical organic solvents. The advantage of using a solvent-free system or using the substrate as the solvent is that the polarity of the substrate is not affected. Therefore, the synthesis with the substrate as solvent was strived for in this work. The yield was determined gravimetrically after chromatographic purification, either in a solvent mixture of ethyl acetate and methanol for column chromatography or a mixture of acetonitrile and water for preparative HPLC. According to the literature described, similar molecular derivatives were isolated with the solvents mentioned and, therefore, after some TLC analyses, they were also used for our purpose. After screening various reaction parameters, a yield of 36.2 % was obtained after a reaction time of 30 min at 95 °C with a vinyl methacrylate molar ratio of 1:35 and an enzyme concentration of 12.7 wt%.

To ensure isolation of the correct product, 5'-*O*-methacryloylcytidine was synthesized by conventional heating, according to the literature. Compared to the reaction experiments with microwave irradiation, a molar ratio of the substrate vinyl methacrylate of only 1:3 was used and additionally 1,4-dioxane as solvent. After a reaction time of 22 h at 60 °C and purification by column chromatography, the desired product was isolated with a yield of 16.9 %.

The advantage of the regioselectivity of enzymes is especially useful in sugar chemistry, which eliminates the need for protection and deprotection steps.[102,325,330] Due to less steric hindrance, primary hydroxyl groups are favored for the interaction compared to remaining hydroxyl groups. In our case, the C5 position is targeted. As such, 2D NMR spectroscopy analysis in DMSO of the isolated compound revealed the cytidine derivatization of the 5’-OH functional group, indicating an absolute regioselectivity (see Supplementary Materials).

10.4.2 Choice of Substrate

The choice of a suitable substrate must not be neglected, as the type of acyl donors influences the reaction. We selected vinyl methacrylate for the synthesis of cytidine-based monomer by transesterification based on the following. Since enzymatic transesterification is a reversible reaction, the acyl donor selected should be chosen wisely to shift the equilibrium on the desired reaction side. Compared to alkyl esters, the use of vinyl esters provides better leaving groups, since resulting vinyl alkoxides can stabilize the negative charge more easily

than resulting alkyl alkoxide leaving groups.[331] In addition, unlike alkyl esters, transesterification with vinyl esters is irreversible because the resulting leaving group rapidly tautomerizes to a non-nucleophilic carbonyl species. In this case, the leaving group is vinyl alcohol, which is a weak nucleophile and, thus, less involved in reverse reactions. Rapid tautomerization of vinyl alcohol to acetaldehyde leads to irreversibility of transesterification. This leads to increased reaction rates compared to alkyl esters and, thus, also to acid equivalents, such as methacrylic acid, confirmed in previous studies.[326,332] In our case, the first experiments with methyl methacrylate also showed decreased reaction yields compared to vinyl methacrylate. Due to these, vinyl methacrylate was used for further investigations. The highest yield could be observed with a reaction time of 30 min but decreases in the case of longer reaction times. This decrease is unusual compared to reported literature, wherein the yield reaches a plateau. To check whether this occurrence is due the substrate, microwave-assisted reactions were performed additionally with methyl methacrylate. Here, the same trend can be observed: the yield decreases in terms of long reaction times of 2 h, except that the highest achieved yield is shifted to 1 h compared to the reaction with vinyl methacrylate at 30 min (Figure 28).

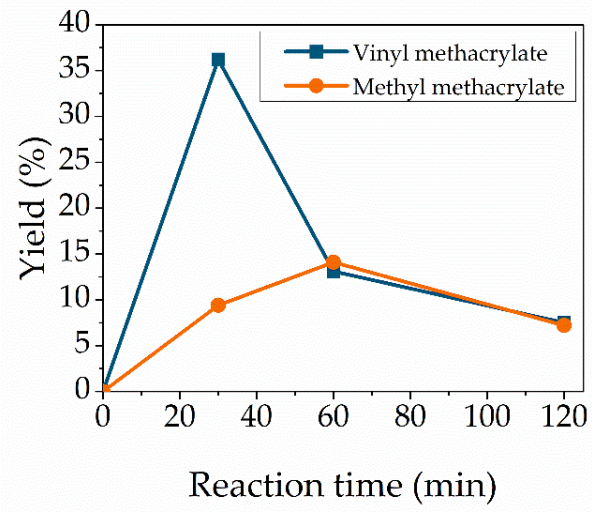

Figure 28. Effect of the choice of the substrate. Reaction conditions: cytidine (100 mg, 0.414 mmol), Novozym 435 (12.7 wt%), 95 °C, 1:35 vinyl methacrylate (blue) or methyl methacrylate (orange). Lines are included as a guide to the eye.

10.4.3 Enzyme Concentration

As the amount of lipase plays a role in economical factor, the ratio of Novozym 435 to the starting material cytidine was evaluated. To investigate the enzyme effect, three different quantities were evaluated: 5.5, 12.7 and 22.5 wt% at a temperature of 95 °C (Figure 29). As expected, the conversion increases when using 12.7 wt% of lipase compared to 5.5 wt%. Using a higher concentration of 22.5 wt% decreases the yield due to enzyme aggregation formation.[312] The enzyme beads at the inside of these nuggets can, therefore, not react with the substrate due to the reduction of available active sites.[333] There is an increase in the yield until the reaction time of 30 min for every enzyme concentration. Therefore, an enzyme loading of 12.7 wt% was considered as optimum.

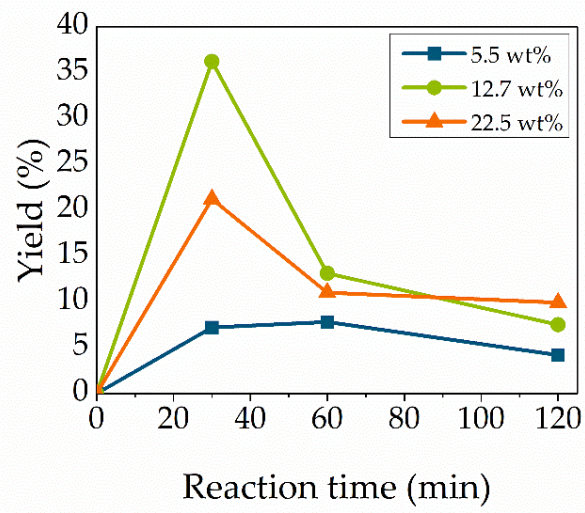

Figure 29. Effect of enzyme concentration. Reaction conditions: cytidine (100 mg, 0.414 mmol), 1:35 molar ratio vinyl methacrylate, 95 °C and Novozym 435 5.5 wt% (blue), 12.7 wt% (green) or 22.5 wt% (orange). Lines are included as a guide to the eye.

10.4.4 Effect of Reaction Temperature

Temperature is one of the most crucial parameters in enzymatic catalyzed reactions. Reaction temperatures were varied between 45 °C to 120 °C to synthesize cytidine-based monomer (Figure 30). High temperatures were chosen, as Novozym 435 is tolerant towards high temperature and is still active at temperatures higher than 90 °C.[325] The used substrate vinyl methacrylate exhibits a boiling temperature of 112 °C. Applying microwave irradiation enables us to heat chemicals above their usual boiling temperature due to increased pressure inside the reaction vessel and to the energy input.[334] The optimal temperature of Novozym is

declared between 40 °C and 65 °C. However, the yield increased with the rise in the temperature to a maximum yield of 36.2 % at 95 °C, but lowers with a further rise to 120 °C. The color of the reaction mixture changed from clear to yellow at a temperature of 120 °C. The yield reduction at increased temperature is related to enzyme deactivation at high temperatures. The same trend was observed with lower enzyme and substrate concentrations. In addition, increasing the temperature leads to an increased reaction rate, resulting in a faster formation of by-products. The optimal reaction temperature with the highest conversion was at 95 °C.

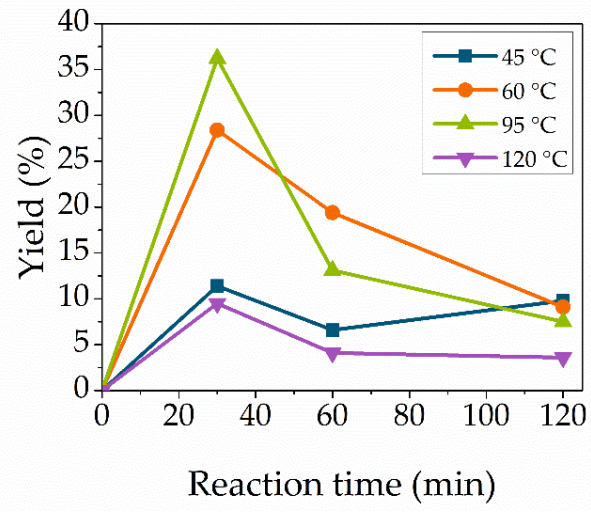

Figure 30. Effect of reaction temperature. Reaction conditions: cytidine (100 mg, 0.414 mmol), Novozym 435 (12.7 wt%), 1:35 molar ratio vinyl methacrylate at temperatures of 45 °C (blue), 60 °C (orange), 95 °C (green) or 120 °C (purple). Lines are included as a guide to the eye.

10.4.5 Effect of Reaction Time

The effect of different reaction times was investigated. The reaction times were 10, 20, 30, 45, 60, 120 and 300 min (Figure 31). Reactions with reaction temperature of 45, 60 and 95 °C showed all a yield maximum at 30 min. Shorter and longer reaction times resulted in lower yields. This observation might be explained by the equilibrium of this lipase-catalyzed transesterification as methacrylic acid could be detected in ^{1}H NMR spectroscopy analysis. Longer reaction times lead to more undefined by-products according to TLC, HPLC and NMR spectroscopy analysis. Comparing these observations with previously described lipase-catalyzed (trans)esterification resulted in an opposite behavior.[325,326,298] While the yields in the literature reached a plateau at long reaction time, the yields decreased after a yield maximum. Initial attempts to explain this discrepancy were based on the formation of acetaldehyde, which

results from tautomerization of the resulting vinyl alcohol when vinyl methacrylate is used as the substrate. In the presence of acetaldehyde, deactivation of the enzyme might occur.[335] Since, here, it is a closed reaction system, acetaldehyde cannot evaporate from the microwave reaction vessel, despite the low boiling temperature. To confirm this assumption, several experiments were repeated with a dissimilar substrate. Utilization of methyl methacrylate instead of vinyl methacrylate in the enzyme-catalyzed synthesis, likewise, displayed a decrease in yield with increased reaction times. Based on this result, the determining factor might be the combination of the starting material cytidine with Novozym 435 under microwave irradiation. In addition, cytidine bears a nucleophilic amino group, which can interfere the reaction. Based on this result, the presence of acetaldehyde of previous experiments plays a more minor role than assumed. Rather, the discrepancy in the results compared with those in the literature is related to the combination of Novozym 435 with the starting material cytidine upon microwave irradiation. Thus, cytidine bears a nucleophilic amine group, which can interfere with the outcome of the reaction.

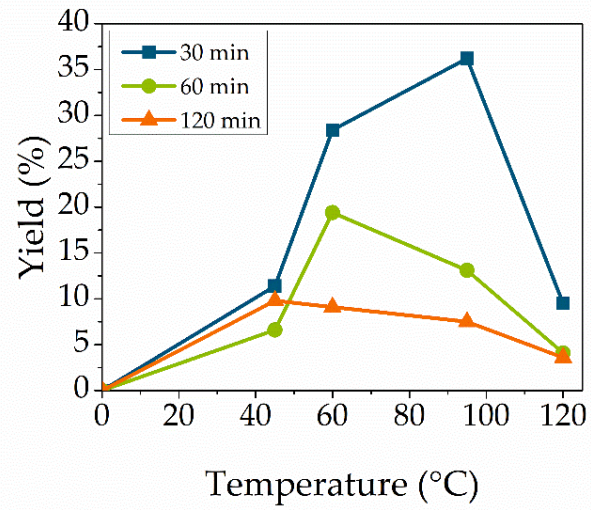

Figure 31. Effect of reaction time. Reaction conditions: cytidine (100 mg, 0.414 mmol), Novozym 435 (12.7 wt%), 1:35 molar ratio vinyl methacrylate at reaction times of 30 min (blue), 60 min (green) or 120 min (orange). Lines are included as a guide to the eye.

10.4.6 Effect of Molar Ratio

High molar ratios of the substrate were necessary as a certain volume is necessary for the microwave sensor and to prevent reverse reaction of the transesterification equilibrium. To evaluate the influence of the amount of the substrate vinyl methacrylate, the molar ratio to cytidine was changed from 1:35 to 1:76 (Figure 32). This obviously high excess of vinyl methacrylate showed first a yield decreases at a reaction time of 30 min compared to 1:35 but increases after a reaction time of 1 h and 2 h. After reaching the yield maximum, the yield decreases as well. This decrease in yield indicates enzyme inhibition when using high molar ratios of substrates. The active sites of the enzymes are inhibited due to the interaction between lipase and substrate, which leads to the formation of enzyme-substrate complexes.[336] Using a high excess of vinyl methacrylate can promote the formation of methacrylic acid, leading to a yield decrease.

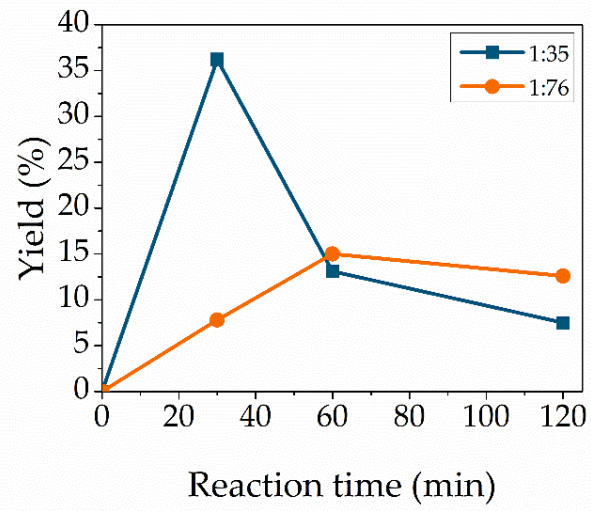

Figure 32. Effect of molar ratio. Reaction conditions: cytidine (100 mg, 0.414 mmol), Novozym 435 (12.7 wt%), 95 °C, vinyl methacrylate with a molar ratio of 1:35 (blue) or 1:76 (orange). Lines are included as a guide to the eye.

10.4.7 Recyclability

The advantage of using immobilized enzymes for reactions is the reusability. Due to the strong support to polymer, Novozym 435 can be easily filtrated from the reaction mixture. After washing and drying, the immobilized lipase is ready to be reprocessed. The reuse cycle is limited, as stirring and handling can cause physical damages. To verify the recyclability, the reaction with recycled Novozm 435 was compared with previously unused enzyme. Using the

same reaction conditions of 95 °C and 2 h, the yield decreased from 7.5 % to 1.7 %. These results lead to the statement that a reuse of Novozym 435 for the enzyme-catalyzed, microwave-assisted synthesis of 5’-*O*-methacryloylcytidine is possible; an optimized purification method is necessary.

10.5 Conclusions

The enzymatic microwave-assisted synthesis of 5’-*O*-methacryloylcytidine was optimized by using variable reaction conditions. Therefore, the impact of changing the enzyme and substrate concentration, reaction temperature and reaction time was observed. The optimum yield of 36 % was obtained with a reaction temperature of 95 °C and time of 30 min, with a 12.7 wt% enzyme concentration and a 1:35 molar ratio for the substrate vinyl methacrylate. Vinyl methacrylate proved to be the preferable substrate compared to methyl methacrylate due to the poorer leaving group methanol. Higher enzyme concentration led to decreased yields, as the active sites are blocked due to aggregate formation. Increasing the reaction temperature and reaction time lowered the conversion due to enzyme deactivation and formation of undefined by-products. Using a higher molar ratio of 1:76 of vinyl methacrylate resulted in an inhibition of the active sites of the enzymes by forming strong enzyme-substrate complexes. With an optimized purification method, the used Novozym 435 can be reused and is, therefore, one step closer to green chemistry.

10.6 Acknowledgment

The authors gratefully acknowledge Angela Krtitschka from the University of Potsdam for enabling measurements of NMR spectra.

11 Synthesis and self-assembly of cytidine- and guanosine-based copolymers

11.1 Abstract

The base pairing property and the “melting” behavior of oligonucleotides can take advantage to develop new smart thermoresponsive and programmable materials. Complementary cytidine- (C) and guanosine- (G) based monomers were blockcopolymerized using RAFT polymerization technique with poly-(*N*-(2-hydroxypropyl) methacrylamide) (pHPMA) as the hydrophilic macro chain transfer agent (macroCTA). C-C, G-G and C-G hydrogen bond interactions of blockcopolymers with respectively C and G moieties have been investigated using SEM, DLS and UV-Vis. Mixing and heating both complementary copolymers resulted in reforming new aggregates. Due to the ribose moiety of the isolated nucleoside-bearing blockcopolymers, the polarity is increased for better solubility. Self-assembly investigations of these bioinspired compounds are the crucial basis for the development of potential future drug delivery systems.

11.2 Introduction

The integration of hydrogen bond interactions in polymeric materials results in supramolecular programmable, stimuli responsive architectures with captivating optoelectronic,[302,337] mechanical,[303,305] self-assembled[306,341,338] and thermal properties,[304,338] which is inspired by nature. These noncovalent interactions are crucial in biological systems, for example for stability reasons of secondary, tertiary and quaternary structures of proteins or for the molecular self-assembly of nucleic acids based on the complementary base pairing property. Regarding to Watson-Crick base pairing, the nucleobases adenine (A) and thymine (T) (or uracil in RNA) as well as guanine (G) and cytosine (C) interact. While the interaction of A and T involves 2 hydrogen bonds, G and C interact by 3 hydrogen bonds, which results in a stronger interaction of G-C compared to A-T.[339,340] The versatile properties of nucleic acids like DNA or RNA have motivated the synthesis of nucleobase-bearing compounds.[306,340,341] DNA/RNA-like polymers result in controlled self-assembled structures with attractive properties like a thermoresponsive, DNA-like melting behaviour.[307,342]

Various nucleobase-containing polymers were prepared by different polymerization methods.[306,341,343] For "melting" behaviour investigations, A- and T-functionalized copolymers were prepared using free radical polymerization technique.[307] Silyl-protected uridine- and adenosine based (PEG-functionalized) copolymers were prepared using atom transfer radical polymerization (ATRP).[327,344,345] In addition, nucleobase monomer derivatives were used for a templated copper-mediated living radical polymerization on solid support, which was mediated by complementary nucleoside interactions.[327,344] However, the ability to coordinate with metal ions might affect ATRP polymerization kinetics of nucleobases. Cu(I), which is involved in ATRP, coordinates purine and pyrimidine derivatives.[346] Reversible addition-fragmentation chain transfer (RAFT) mediated polymerization might be a preferable method to isolate nucleobase-containing polymers.[341,347] RAFT polymerization enables the synthesis of synthetic polymers with a defined molecular weight, low molar mass dispersity (PDI) and an opportunity for chain growth. It allows to polymerize a broad spectrum of monomers with high conversions.[201,348,353] In addition, this technique has a high tolerance regarding implementation and is inexpensive compared to competitive methods. In terms of a RAFT-mediated synthesis of nucleobase containing polymers, the choice of the polymerization solvent is significant as it influences the morphology of the polymers.[349,350] While syntheses of A- and T-containing polymer architectures have already been described successfully, the synthesis of G-based molecules remains more challenging due to the lower solubility.[340]

To increase the solubility of nucleobase functionalized derivatives, an extension with water soluble polymer chains is possible. Polyethylene glycol (PEG) is the gold standard when it comes to drug delivery systems. Even though PEG has many advantages like low toxicity, biocompatibility and hydrophilicity, it has its limits when it comes to biodegradability or immunogenicity.[351,352] The use of poly-(*N*-(2-hydroxypropyl) methacrylamide) (pHPMA) as an alternative to PEG has grown interest in recent years.[353] pHPMA is a linear, biocompatible and non-immunogenic polymer, which accomplished clinical trials in the past. The predominant application of pHPMA includes the use as potential anticancer therapeutics.[354]

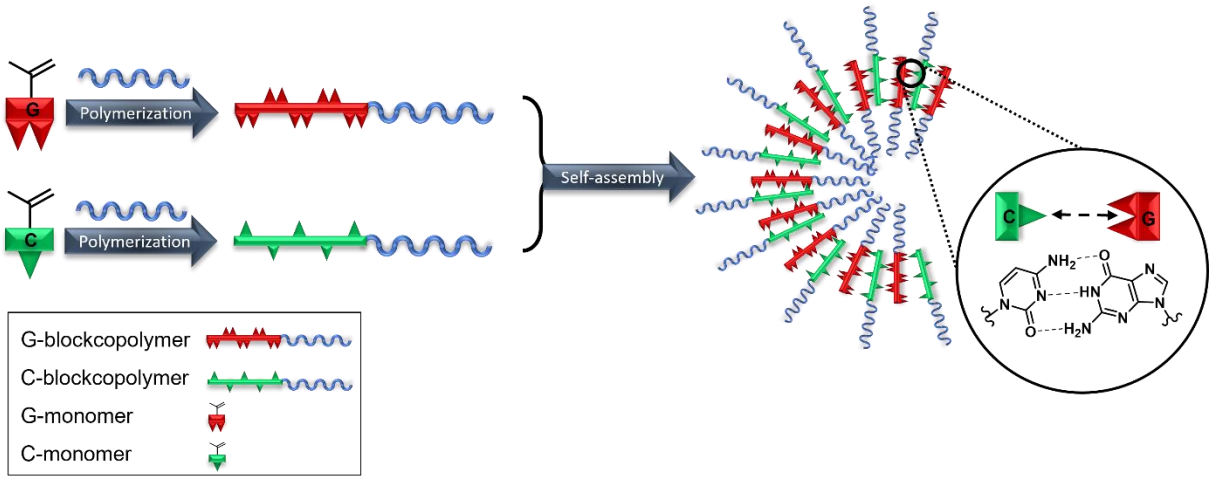

Scheme 17. Polymerization and self-assembly of complementary nucleoside (C and G) blockcopolymers.

In this work, we describe the synthesis and characterization of a new class of ribonucleoside-bearing block copolymers. Therefore, methacrylamide-based monomers with cytidine and guanosine moieties (Figure 33) were synthesized by a two-step synthesis. RAFT-mediated polymerization was applied to isolate blockcopolymers using pHPMA as the macro chain transfer agent (macroCTA) to increase the hydrophilicity and therefore the solubility. The nucleoside-based blockcopolymers were further investigated in their base-pairing interactions and self-assembly behavior (Scheme 17) by SEM, DLS and UV-Vis.

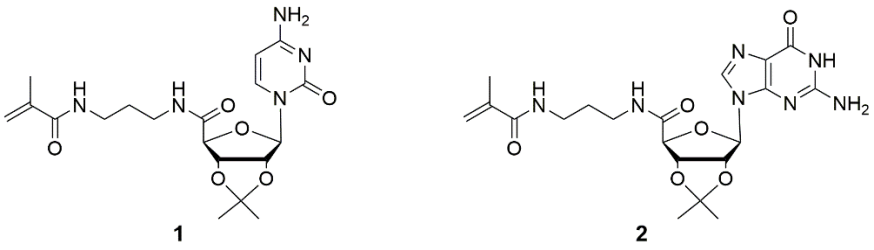

Figure 33. Chemical structures of ribonucleoside methacrylamides, including cytidine (**1**) and guanosine (**2**) derivatives.

11.3 Results and Discussion

11.3.1 Monomer Synthesis

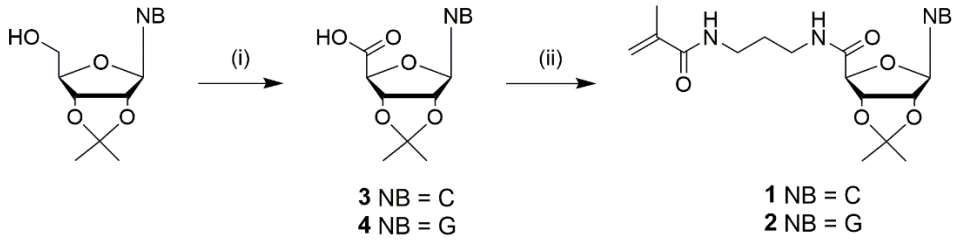

Scheme 18. Synthesis of nucleobase (NB) monomer derivatives: (i) TEMPO, BAIB, CH_3CN/H_2O, rt, overnight (**3**: 44 %, **4**: 98 %); (ii) APMA*HCl, CDMT, NMM, MeOH, rt, overnight (**1**: 44%, **2**: 52 %).

The nucleosides were used as the protected 2',3'-acetonide forms to address the 5'-position. Due to stability reasons, methacrylamide functionalized ribonucleosides were preferred compared to methacrylate derivatives, which can be synthesized enzymatically.[327,344] The synthesis of the cytidine- (**1**) and guanosine-based monomers (**2**) were prepared via a two-step procedure, including the oxidation of the primary hydroxyl group, followed by an amide coupling with *N*-(3-aminopropyl)-methacrylamide (Scheme 18). Despite the higher nucleophilicity of the exocyclic $-NH_2$, a protection step of this functionality was not required, unlike the enzymatic esterification route.[327]

The oxidation of commercially available 2',3'-isopropylidene cytidine and guanosine to the carboxylic derivatives has been described previously.[355] Shortly, the acetal protected ribonucleosides were oxidized with TEMPO and BAIB in the presence of $NaHCO_3$. After filtration of the precipitate, oxidized cytidine (**3**) was afforded in a yield of 44 %, while the yield of oxidized guanosine (**4**) was quantitative as a white powder. **1** and **2** were obtained after the amide coupling of the **3** and **4** with *N*-(3-aminopropyl)-methacrylamide hydrochloride using 2-chloro-4,6-dimethoxy-1,3,5-triazine (CDMT) and *N*-methylmorpholine (NMM) with a yield of 44 % and 52 % respectively. The chemical structure was confirmed by NMR spectroscopy and ESI-MS analyses. Attempts using DCC, EDC and HATU as coupling agents resulted in lower yields. Coupling of 2-aminoethyl methacrylate hydrochloride instead of *N*-(3-aminopropyl)-methacrylamide hydrochloride with the stated coupling reagents resulted in an isolation of the methacrylate pendant with undefined byproducts resulting in a significantly lower yield. **2** exhibit a lower solubility compared to **1**, but both ribonucleoside methacrylamide-based monomers showed appropriate solubility in non-polar solvents like chloroform and diethyl ether as well in polar solvents like dichloromethane, acetone and

dimethylformamide as aprotic solvents and water, methanol and ethanol as protic solvents. This solubility property can be explained by both the formation of hydrogen bond interactions and the hydrophobic parts in one molecule simultaneously. Due to the high solubility of both monomer molecules, the nucleoside monomers were refrained from further deprotection for polymerizations.

As the hydrophilic part of the desired blockcopolymer, poly(*N*-(2-hydroxypropyl)methacrylamide) (pHPMA) was chosen due to its biocompatibility. The synthesis of *N*-(2-hydroxypropyl)methacrylamide (HPMA) was described before.[356] The HPMA structure was confirmed by ^{1}H NMR spectroscopy analysis after isolation following the published protocol.

11.3.2 Polymerization

RAFT-mediated polymerization ranks among the crucial and well-known polymerization techniques, which involves a radical initiator and the chain transfer agent (CTA). As the selected CTA influences the polymerization efficiency, the choice needs to be done carefully. CTA's consist of a stabilizing Z and a leaving R group.[357]

Table 13. Analytical data of piCPMA **5** and piGPMA **6**.

Monomer	Solvent	Conversion	Polymer	$M_{n,\ theory,\ NMR}$	$M_{n,\ SEC}$[a]	PDI
1	DMF/H_2O 8:2	40 %	**5**	4.5 kDa	2.1 kDa	1.3
1	1,4-dioxane/H_2O 9:1	34 %	**5**	3.9 kDa	4.1 kDa	1.3
2	DMF/H_2O 8:2	70 %	**6**	8.4 kDa	11.4 kDa	1.3
2	1,4-dioxane/H_2O 9:1	94 %	**6**	11.4 kDa	10.2 kDa	1.3

[a]DMF, PMMA standard

The dithioester-based CTA 4-cyano-4-(phenylcarbonothioylthio)pentanoic acid (CPADB) was selected, as it is described for polymerization of methacrylamide-based monomers. After polymerization using RAFT technique, a macroCTA with the derived CTA end groups was achieved. This macroCTA can form block copolymers by reacting further with other monomers. Dithiobenzoate (Z-group) as the end-group was confirmed by ^{1}H NMR and UV-Vis analysis.

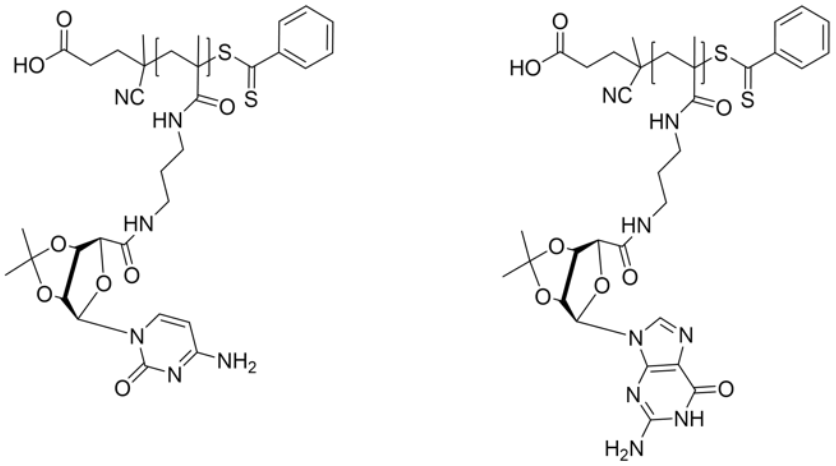

5 **6**

Figure 34. Chemical structures of ribonucleoside-based homopolymers piCPMA **5** and piGPMA **6**.

1 and **2** were homopolymerized using RAFT polymerization with ACVA as the thermal initiator at 75 °C (Figure 34). Polymerizations of nucleoside-based monomers were conducted with a $[M_0]:[CTA_0]:[I_0]$ ratio of 75:3:1. Solvent mixtures observations of 8:2 DMF/H_2O and 9:1 1,4-dioxane/H_2O showed different effects depending on the nucleoside type. The choice of solvent mixtures was respectively related to previously described (co-)polymerizations of nucleobase analogues and pHPMA.[327,349,350,358,359,360,361] Using a 9:1 1,4-dioxane/H_2O mixture gave a high conversion (94 %) of the G-based polymer (piGPMA), while the conversion of cytidine-based polymer (piCPMA) was lowered to 34 % with the same solvent mixture. On the other hand, the conversion of piCPMA was increased to 40 % and of the piGPMA was decreased to only 70 % in 8:2 DMF/H_2O. Polymerizations of nucleoside homopolymers and their monomer conversions were determined by comparing the integrals of the typical C-4 protons of piCPMA (δ 4.43 ppm) and piGPMA (δ 4.50 ppm) with the integrals of the monomer vinyl peaks of iCPMA (δ 5.64 ppm and 5.30 ppm) and iGPMA (δ 6.39 ppm and 5.61 ppm). The theoretical molecular weights ($M_{n,\ theory,\ NMR}$) were calculated following eq. 3 (see Supporting Information) based on the resulted conversion and are summarized in Table 13.

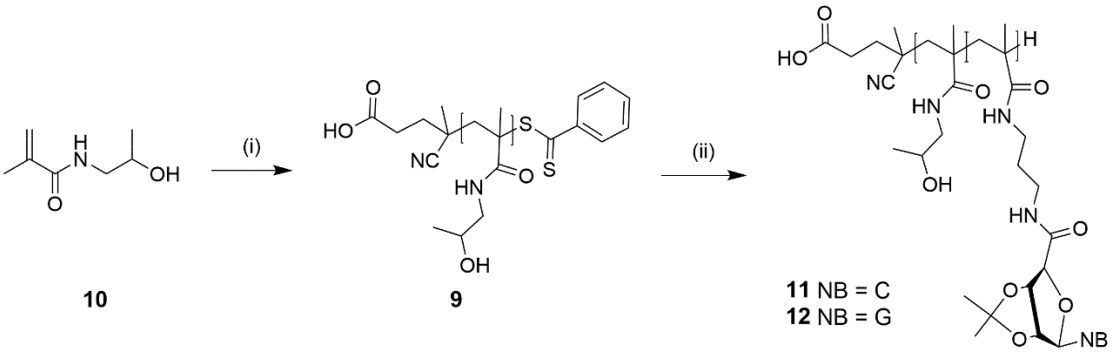

Scheme 19. Synthesis of pHPMA **9** and nucleoside-based blockcopolymers pHPMA-*b*-piCPMA **11** and pHPMA-*b*-piGPMA **12**: (i) ACVA, acetate buffer (pH 5)/ EtOH, 70 °C, 24 h; (ii) ACVA, DMF/H_2O or 1,4-dioxane/H_2O, 75 °C, 24 h.

The presence of the nucleobases might be responsible for the long polymerization time, as the basic aromatic rings (purine and pyrimidine) can act as radical scavengers. The acetonide protecting groups of homopolymers of both ribonucleosides were removed under acidic conditions with trifluoroacetic acid to improve the hydrophilicity due to demanding solubility properties. The deprotection steps were observed by ^{1}H NMR spectroscopy. The reduction of the two shielded singlets of piCPMA (δ 1.47 ppm and 1.29 ppm) and piGPMA (δ 1.49 ppm and 1.31 ppm) indicated a successful removal of the acetonide functional groups. Even after increasing the hydrophilicity by deprotection, the homopolymers **7** and **8** still exhibited low solubility, so the synthesis of the hydrophilic pHPMA **9** as the macromolecular chain transfer agent (macroCTA) for further copolymerization with nucleoside monomers was decided (Scheme 19).

HPMA macroinitiator was prepared using a modified procedure via RAFT-mediated polymerization.[357] The monomer concentration was kept low, as the propagation kinetic constant (K_P) of hydrophilic monomers influences positively the transition state of propagation step and can be increased by using water as polymerization solvent and using a decreased monomer concentration.[362] The structure of pHPMA was confirmed by ^{1}H NMR spectroscopy. Monomer conversion was at 75 %, resulting in a theoretical M_n of 7.8 kDa. DP was determined by comparing the integrals of the phenylic peaks (δ 7.93 and 7.81 ppm) of the end-group with the peaks of the pHPMA backbone (δ 4.69 ppm). In addition, UV-Vis analysis confirmed the attachment of the dithiobenzoyl end group and showed a similar DP like ^{1}H NMR spectroscopy DP determination. Theoretical and actually determined M_n do not go together, which means that the RAFT agent did not get completely consumed.

Table 14. Analytical data of pHPMA-*b*-piCPMA **11** and pHPMA-*b*-piGPMA **12**.

Monomer	Solvent	Conversion	Polymer	$M_{n,\ theory,\ NMR}$	$M_{n,\ NMR}$	$M_{n,\ SEC}$[a]	PDI
1	DMF/H_2O	68 %	**11**	83.0 kDa	91.4 kDa	11.7 kDa	1.1
2	1,4-dioxane/H_2O	78 %	**12**	94.0 kDa	163.2 kDa	24.7 kDa	2.5

[a]DMF, PMMA standard

Block copolymers of nucleosides (pHPMA-*b*-piCPMA **11** and pHPMA-*b*-piGPMA **12**) were prepared using the RAFT-mediated polymerization technique. As the resulting blockcopolymers were analyzed via UV-Vis spectroscopy to evaluate the hydrogen-bonding interactions of the nucleobases, blockcopolymers were synthesized with a low "livingness" rate. "Livingness" is a feature, which allows the chain extension. It implies, how many "living" chains remain intact for further blockcopolymerizations. A low "livingness" results in high quantities with dead ends led to nucleobase-based polymers without the phenylic Z-group, which may interfere in further UV-Vis spectroscopy analysis. The calculated "livingness" rates were kept low and are 36.0 % of **11**, whereas of **12** is at 15.6 %.

Polymerization of both nucleosides were performed in the solvent system, which worked the best for the homopolymers, respectively: **1** in 8:2 DMF/H_2O, **2** in 9:1 1,4-dioxane/H_2O. Purine-based **2** monomer lead to higher conversion and therefore higher molecular weight in our case, unlike A-based monomers, which were polymerized via ATRP with possibly complexation of Cu(I) affording lower conversion compared to the pyrimidine counterpart.[344] The monomer conversion was specified using eq. 1 by comparing the integrals of the monomer peak (**1**: δ 5.30 ppm; **2**: δ 5.61 ppm) with the nucleoside-based polymer peak (*b*-piCPMA δ 4.37 ppm or *b*-piGPMA δ 6.14 ppm). The monomer conversion of **11** was 68 %, while **12** was at 78 %, summarized in Table 14. The lower PDI of polymer **11** compared to macroCTA **10** is due to the different purification methods. While **10** was purified by dialysis against H_2O, **11** was purified by repeated precipitation, which may lead to fractional precipitation. Due to the poor similarity of the standard used with the polymers and the difficult solubility of them, the values of the SEC analysis are to be regarded as inaccurate and therefore not really reliable. They only give an indication of the comparison of the polymers with each other.

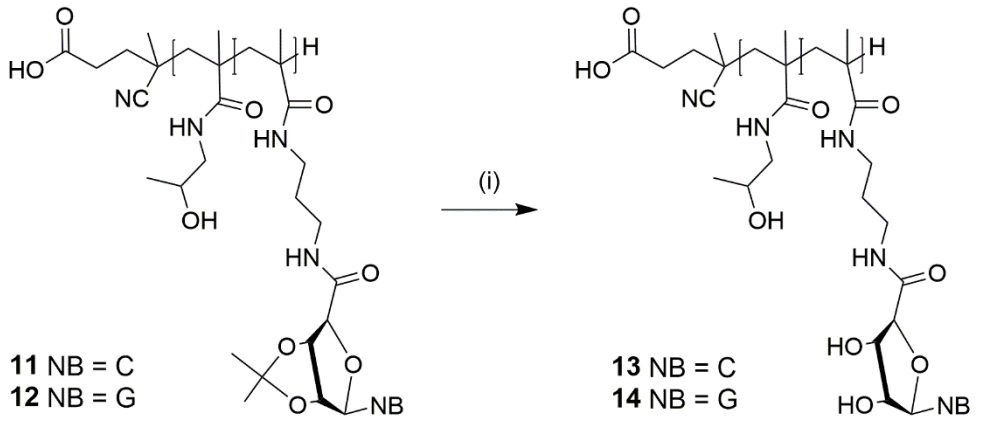

Scheme 20. Acidic deprotection of the acetonide functional group of pHPMA-*b*-piCPMA **11** and pHPMA-*b*-piGPMA **12**: (i) TFA, H_2O, rt, 2 h (**11**: 53 %, **12**: 81 %).

Both nucleoside-based blockcopolymers **11** and **12** revealed low solubilities due to the integrated nucleobases. The blockcopolymers were removed by an acidic deprotection of the acetal functionalities with trifluoroacetic acid (Scheme 20). The successful deprotection was confirmed by the disappearance of the two singlets in the upfield resulting from the acetal protecting groups of **11** (δ 1.46 ppm and 1.28 ppm) and **12** (δ 1.48 and 1.33 ppm) in ^{1}H NMR spectroscopy analysis. Agitating for in total 2 h yielded **13** and **14**.

11.3.3 Self-assembly analysis

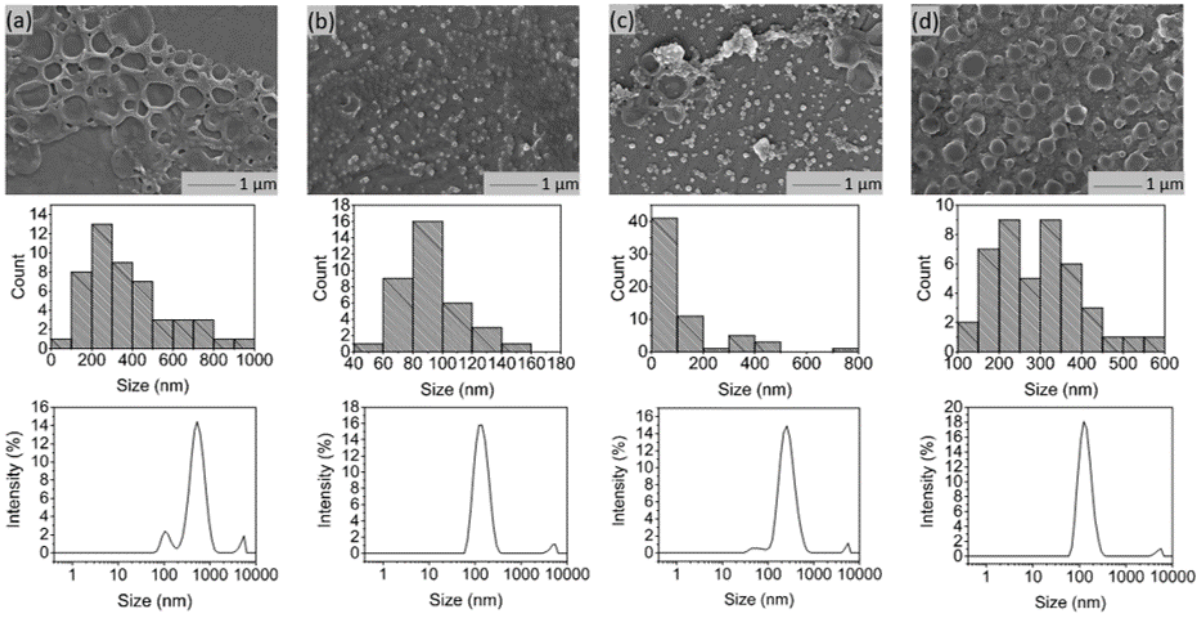

Figure 35. SEM-image, size distribution and hydrodynamic size distribution by DLS of (a) pHPMA-*b*-pCPMA **13**, (b) pHPMA-*b*-pGPMA **14**, (c) mixture of **13** and **14** before heating and (d) mixture of **13** and **14** after heating.

Due to lower solubilities caused by 3 strong hydrogen binding sites, self-assembly studies of G- and C-based blockcopolymers were less reported compared to A- and T-containing polymers.[345,344,347,349,350] To investigate aggregate formation due to hydrogen bonding interactions between the purine and pyrimidine functionalities, SEM and DLS analysis were carried out (Figure 35). Regarding to SEM images, A- and T-containing polymers showed popcorn-like structures in $CHCl_3$ and 1,4-dioxane,[350] whereas our synthesized pHPMA-*b*-pCPMA **13** polymers form large network structures in aqueous solution. Since a gentle precipitation was already observed in the aqueous solution, the formation of the network structures seen in the SEM image due to cohesion during the drying process is unlikely. These structures result from stronger C-C interactions with a broad size distribution and an average size of 280 nm. This broad size distribution was also detected with DLS with a polydispersity index (PDI) of 0.421. The average hydrodynamic diameter of **13** is around 507 nm. However, SEM images of pHPMA-*b*-pGPMA **14** revealed small particles due to G-G interactions with an average size of 86 nm. The size distribution was smaller according to DLS with an average hydrodynamic diameter of around 144 nm (PDI = 0.213). Mixing both complementary blockcopolymers results in particle with an average hydrodynamic diameter of around 165 nm and a PDI of 0.3. Heating up to 100 °C for 30 min and cooling down of this mixture led to a

narrower size distribution and a smaller average size of 266 nm and a hydrodynamic diameter of 136 nm. This observation might be explained by breaking the strong C-C and G-G hydrogen bond in increased temperatures and re-assembling of C-G interactions when cooling down to room temperature (rt). Sonication of **13**, **14** and the mixture of both lead to no morphology change indicating a strong stability like previously reported nucleobase-containing polymers.[350]

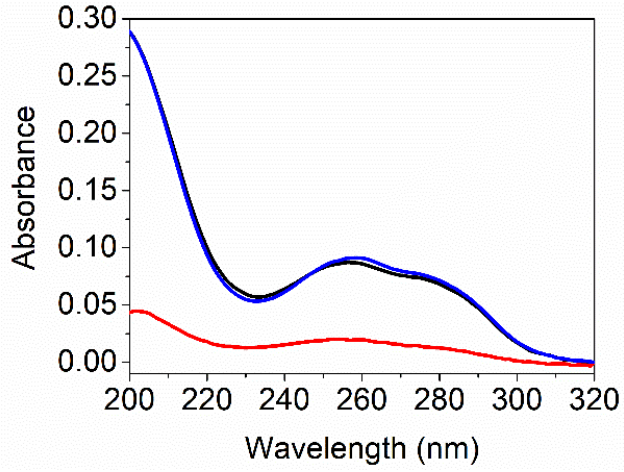

Figure 36. UV-Vis spectrum of the average of individual **13** and **14** (blue), mixture of **13** and **14** before heating (black) and mixture of **13** and **14** after heating (red).

Nucleobases show strong UV absorption due to hydrogen bond and π- π interactions.[363] Base-pairing interactions of nucleobase derivatives result in changes in the UV-Vis spectroscopy. To investigate hydrogen bonding interactions of the complementary nucleoside-containing polymers **13** and **14**, spectrophotometric measurements were conducted (Figure 36). The UV absorption spectra of the individual polymers were compared with the spectrum of the mixture after heating. The average values of the individual polymers pHPMA-*b*-pCPMA **13** and pHPMA-*b*-pGPMA **14** matches with the absorption values of the mixture of both polymers using same concentrations due to hydrogen bond pre-assembly of the single polymers. After heating the polymer mixture for 30 min at 100 °C, hypochromicity was observed like expected from literature.[307] This decrease of absorbance resulted from re-assembly of the complementary C-G interactions after heating and cooling down. Hypochromicity at a wavelength of 260 nm might be an indication for dsDNA-like structures, which show lower absorbance compared to ssDNA. Absorption maxima of both polymers individually at 274 nm for **13** and at 258 nm for **14** were comparable with other previously described amphiphilic blockcopolymers containing T- and A-structures.[345,344]

11.4 Conclusion

Two complementary nucleoside-based monomers were isolated by a two-step synthesis starting with the oxidation of the primary hydroxyl group which was followed by an amide coupling affording a methacrylamide-based nucleoside monomer. Nucleoside-bearing monomers were homopolymerized using the RAFT polymerization technique. The monomer conversion was depended on the polymerization solvent system. C-based polymer showed a higher monomer conversion using a solvent mixture of DMF/H_2O, whereas G-based polymer yielded higher using 1,4-dioxane/H_2O. Chain extension with HPMA of both homopolymers were due to high insolubility hampered, even after removal of the protection groups. Therefore, pHPMA was synthesized as the macroCTA for further polymerizations of both nucleoside-based monomers. Using the RAFT techniques in the solvent system, which works the best for homopolymerization of the nucleosides, two complementary blockcopolymers were isolated with a low solubility. After acidic deprotection, the C-G hydrogen bond interaction between these two blockcopolymers was studied by SEM, DLS and UV-Vis. These analyses revealed strong C-C and G-G interactions within one nucleoside-based polymer type. C-based blockcopolymers aggregate to a network with a broad size distribution, whereas G-based blockcopolymers assemble to smaller particles with a narrower size distribution. Heating the polymer mixtures resulted in breaking these base pairing of the same nucleobase type to form new aggregates by forming C-G interactions after cooling down. Further investigation of complementary blockcopolymers in different sizes and their analysis can lead to a programmable, thermoresponsive material for a targeted drug delivery.

11.5 Experimental

11.5.1 Materials

All reagents and solvents were used without further purification. Na_2CO_3 (> 99.5 %), $NaHCO_3$ (> 99 %), acetic acid (100 %), *N*-methylmorpholine (NMM, > 99%) and 1,4-dioxane (> 99.8 %) were purchased from Carl Roth (Karlsruhe, Germany). Na_2SO_4 (> 99 %), NaCl (> 99 %), dichloromethane (> 99.8 %), acetone (> 99 %) and ethanol (EtOH, > 99.5 %) were received from Chemsolute (Renningen, Germany), sodium acetate (> 99 %) and trifluoroacetic acid (TFA, 99 %) from Acros Organics (Geel, Belgium). Et_3N (> 99.5 %), methacryloyl chloride (97 %), 2,2,6,6-tetramethyl-1-piperidinyloxy free radical (TEMPO, 98 %), 2-chloro-4,6-

dimethoxy-1,3,5-triazine (CDMT, 97 %), 4-cyano-4-(phenylcarbonothioylthio)-pentanoic acid (CPADB), 4,4′-azobis(4-cyanovaleric acid) (ACVA, > 98%) and DMF (> 99 %) were obtained from Merck KGaA (Darmstadt, Germany). 1-Aminopropan-2-ol (94 %) was from Alfa Aesar (Kandel, Germany), 2',3'-*O*-isopropylidene cytidine and 2',3'-*O*-isopropylidene guanosine from Biosynth (Berkshire, UK). Bis(acetoxy)iodobenzene (BAIB, 97 %) and *N*-(3-aminopropyl)-methacrylamide hydrochloride (APMA, 97 %) were purchased from BLD pharm (Shanghai, China), Acetonitrile (> 99.9 %) and THF from VWR (Radnor, US). Deuterated solvents D_2O (99.9 %) and DMSO-d_6 (99.8 %) were received from Deutero (Kastellaun, Germany).

11.5.2 Characterization techniques

ESI-MS spectra were recorded with a Perkin Elmer Flexar SQ 300 MS Detector. Nuclear magnetic resonance (NMR) spectroscopy was performed with a Bruker AVANCE NEO (400 MHz) spectrometer. Deuterated solvents were used as standards. Chemical shifts are given in the δ-scale in ppm relative to solvent peaks. Multiplicities are displayed with the coupling constants in Hertz (Hz).

Size exclusion chromatography (SEC) was performed in HPLC grade DMF containing 0.1% LiBr with a flow rate at 1 mL/min and calibrated with polystyrene (PS) or poly(methyl methacrylate) (PMMA). $M_{n,UV\text{-}Vis}$ was determined using a Specord 210 spectrophotometer.

Individual polymeric samples (pHPMA-*b*-pCPMA 13 and pHPMA-*b*-pGPMA **14**) for UV-Vis, dynamic light scattering (DLS) and SEM investigations were prepared by the solvent switch method separately. Blockcopolymers **13** and **14** were dissolved in DMSO with a concentration of 8 mg/mL. After stirring for 10 min, 7 mL of water was added using a syringe pump with a rate of 1 mL/h. The solutions were dialyzed against water for 3 days to remove DMSO. Samples have a final concentration of around 1 mg/mL. Diluted polymer solutions with a final concentration of 10 µg/mL were placed in a 10 mm quartz cuvette for UV-Vis and DLS investigations. DLS analysis were conducted with a Malvern Zetasizer Nano ZS.

11.5.3 Synthesis of *N*-(2-hydroxypropyl)methacrylamide (HPMA) **10**

1-Aminopropan-2-ol (8.35 mL, 107 mmol) and Na_2CO_3 (12.6 g, 119 mmol) were added to cold dichloromethane (28 mL). The reaction solution was cooled to -10 °C and freshly

distilled methacryloyl chloride (10.6 mL, 110 mmol), diluted in dichloromethane (11 mL) was added dropwise within 35 min. After complete addition, the reaction solution was stirred for additional 20 min at 5 °C and then allowed to warm up to rt. The white precipitate was filtered and washed with dichloromethane (3 x 100 mL). The resulting filtrate was dried over anhydrous Na_2SO_4, filtered, washed with dichloromethane (3 x 100 mL) and concentrated under vacuo. The concentrate was left in the fridge to crystallize. The resulting crystals were filtrated and washed with cold dichloromethane. After recrystallization in acetone, **10** was isolated as white crystals (9.96 g, 69.6 mmol, 65 %); δ_H (D_2O, 400 MHz): 5.72 (1H, t, ^4J = 0.8 Hz, H2'), 5.47 (1H, qin, ^4J = 1.6 Hz, H2''), 3.96 (1H, ddt, ^3J = 4.8 Hz, ^3J = 13.2 Hz, ^3J = 6.4 Hz, H4), 3.33 (1H, dd, J = 4.8 Hz, ^3J = 13.8 Hz, H3'), 3.25 (1H, dd, J = 6.8 Hz, ^3J = 13.8 Hz, H3''), 1.95 (3H, s, H1), 1.18 (3H, d, ^3J = 6.4 Hz, H5) ppm.

11.5.4 Synthesis of 2',3'-*O*-isopropylidene-5'-carboxynucleosides (iC-COOH **3** and iG-COOH **4**)

A solution of 2,2,6,6-tetramethyl-1-piperidinyloxy free radical (TEMPO) (0.331 g, 2.12 mmol) in acetonitrile (10.1 mL) was added to a reaction solution of 2',3'-*O*-isopropylidene nucleoside (10.6 mmol), $NaHCO_3$ (1.78 g, 21.2 mmol) and bis(acetoxy)iodobenzene (BAIB) (6.80 g, 21.2 mmol) in H_2O (10.1 mL). The reaction solution was stirred for 1 h at 0 °C and then overnight at rt. The precipitate was filtered, washed with acetone (3 x 50 mL) and diethyl ether (3 x 50 mL) and dried in vacuo to afford oxidized nucleosides.

iC-COOH **3**: white powder, yield: 44 %, δ_H (D_2O, 400 MHz): 8.99 (1H, d, ^3J = 7.6 Hz, H5), 6.12 (1H, d, ^3J = 7.6 Hz, H6), 5.86 (1H, s, H2), 5.27 (1H, dd, ^3J = 2 Hz, ^3J = 6 Hz, H3), 5.23 (1H, d, ^3J = 6.4 Hz, H2), 4.66 (1H, d, ^3J = 2 Hz, H7), 1.59 (3H, s, H1'), 1.43 (3H, s, H1'') ppm.

iG-COOH **4**: white powder, yield: 98 %, δ_H (D_2O, 400 MHz): 7.85 (1H, s, H5), 6.15 (1H, s, H4), 5.58 (1H, d, ^3J = 5.6 Hz, H2), 5.47 (1H, d, ^3J = 5.6 Hz, H3), 4.63 (1H, s, H6), 1.62 (3H, s, H1'), 1.47 (3H, s, H1'') ppm.

11.5.5 Synthesis of 2',3'-*O*-isopropylidene-5'-propylmethacrylamide nucleosides (iCPMA **1** and iGPMA **2**)

2',3'-*O*-Isopropylidene-5'-carboxynucleoside **3** or **4** (7.27 mmol) was reacted with *N*-(3-aminopropyl)-methacrylamide hydrochloride (APMA) (1.43 g, 8.02 mmol), 2-chloro-4,6-dimethoxy-1,3,5-triazine (CDMT) (1.40 g, 7.98 mmol) and *N*-methylmorpholine (NMM) (1.76 mL, 16.0 mmol) in methanol (65 mL) overnight at rt. The crude product was purified by a preparative HPLC device (reverse phase C_{18} silica, gradient of 10% to 20% acetonitrile in H_2O) to afford nucleoside monomers.

iCPMA **1**: white powder, yield: 38 %, δ_H (D_2O, 400 MHz): 7.63 (1H, d, ^3J = 7.6 Hz, H5), 5.96 (1H, d, ^3J = 7.2 Hz, H4), 5.73 (1H, s, H6), 5.68 (1H, s, H11'), 5.44 (1H, s, H11''), 5.40-5.38 (2H, m, H2, H3), 4.68 (1H, d, ^3J = 0.8, H7), 3.29 - 3.07 (4H, m, H8, H10), 1.92 (3H, s, H12), 1.78 - 1.61 (2H, m, H9), 1.58 (3H, s, H1'), 1.43 (3H, s, H1'') ppm; δ_H (DMSO-d_6, 400 MHz): 7.87 (1H, t, ^3J = 6 Hz, H5), 7.75 - 7.73 (2H, m, H9, H13), 7.27 (2H, s, H7), 5.75 (1H, d, ^3J = 1.2 Hz, H4), 5.69 (1H, d, ^3J = 7.2 Hz, H6), 5.64 (1H, s, H14'), 5.30 (1H, t, J = 1.6 Hz, H14''), 5.08 (1H, dd, ^3J = 2.8 Hz, ^3J = 6.4 Hz, H3), 5.02 (1 H, dd, ^3J = 1.2 Hz, ^3J = 6.2 Hz, H2), 4.35 (1H, d, ^3J = 2.8 Hz, H8), 3.17 - 2.88 (4H, m, H10, H12), 1.85 (3H, s, H15), 1.50 (2H, quin, ^3J = 6.8 Hz, H11), 1.47 (3H, s, H1'), 1.29 (3H, s, H1'') ppm; δ_C (D_2O + DMSO-d_6, 100 MHz): 173.58, 158.39, 148.01, 140.75, 122.47, 115.33, 115.31, 99.88, 97.24, 90.11, 85.80, 85.55, 38.39, 37.84, 29.52, 27.23, 25.64, 19.32 ppm; ESI-MS: m/z for $C_{19}H_{27}N_5O_6$: $[M + H]^+$ calculated: 422.46, found: 422.25; $[M + Na]^+$ calculated: 444.44, found: 444.24.

iGPMA **2**: white powder, yield: 52 %, δ_H (D_2O, 400 MHz): 7.89 (1H, s, H5), 6.30 (1H, s, H4), 5.74 (1H, d, ^3J = 6.0 Hz, H3), 5.64 (1H, d, J = 0.8 Hz, H10'), 5.53 (1H, d, ^3J = 6.0 Hz, H10''), 5.42 (1H, d, J = 0.7 Hz, H2''), 3.05 - 2.83 (4H, m, H7, H9), 1.90 (3H, s, H11), 1.62 (3H, s, H1'), 1.47 (3H, s, H1''), 1.36 (1H, dp, J = 6.9 Hz, ^3J = 13.9 Hz, H8'), 1.21 (1H, dp, J = 7.1 Hz, ^3J = 14.2 Hz, 8'') ppm; δ_H (DMSO-d_6, 400 MHz): 10.57 (1H, bs, H6), 7.82 (1H, s, H5), 7.78 (1H, t, ^3J = 6 Hz, H13), 7.54 (1H, t, ^3J = 6 Hz, H9), 6.41 (2H, s, H7), 6.14 (1H, d, ^3J = 1.6 Hz, H4), 5.61 (1H, s, H14'), 5.43 (1H, dd, ^3J = 2.4 Hz, 3J = 6 Hz, H3), 5.29 (1H, t, J = 1.2 Hz, H14''), 5.25 (1H, dd, ^3J = 1.2 Hz, ^3J = 6.2 Hz, H2), 4.50 (1H, d, ^3J = 2.4 Hz, H8), 2.99 - 2.78 (4H, m, H10, H12), 1.83 (3H, s, H15), 1.51 (3H, s, H1'), 1.33 (2H, do, J = 6.8 Hz, ^3J = 31.4 Hz, H11), 1.33 (3H, s, H1'') ppm; δ_C (D_2O + DMSO-d_6, 100 MHz): 172.27, 171.99, 160.05,

154.54, 151.80, 140.00, 139.73, 121.70, 117.03, 114.78, 90.99, 88.32, 84.44, 84.30, 37.19, 36.98, 28.56, 26.35, 24.89, 18.47 ppm; ESI-MS: m/z for $C_{20}H_{27}N_7O_6$: $[M + H]^+$ calculated: 462.49, found: 462.27; $[M + Na]^+$ calculated: 484.47, found: 484.25.

11.5.5 Homopolymerization of nucleoside-based monomers (piCPMA **5** and piGPMA **6**)

Cytidine-based monomer **1** (63.0 mg, 150 μmol), CPADB (1.70 mg, 6.00 μmol) and ACVA (0.560 mg, 2.00 μmol; CTA/I molar ratio = 3) were dissolved in a solvent mixture of 8:2 DMF/H_2O or 9:1 1,4-dioxane/ H_2O (437 μL) and purged with N_2 for 30 min. The reaction mixture was then placed in a preheated oil bath at 75 °C and reacted for 24 h. The reaction was quenched by exposing to air and cooling to rt. The polymer was isolated purified by repetitive precipitation from cold acetone and dried on high vacuum.

The same procedure was applied to isolate the guanosine-based homopolymers using **2** as the starting material.

piCPMA **5**: pinkish powder, monomer conversion: 40 % ($piCPMA_{DMF}$) and 34 % ($piCPMA_{1,4\text{-dioxane}}$); M_n = 2.1 kDa ($piCPMA_{DMF}$) and 4.1 kDa ($piCPMA_{1,4\text{-dioxane}}$), PDI = 1.3 (SEC-DMF, PS standard); δ_H (DMSO-d_6, 400 MHz): 7.92 - 7.82 (H5, H9, H13), 5.98 (H7), 5.82 (H4), 5.11 (H6, H8), 4.43 (H2), 3.32 - 2.99 (H10, H12), 1.47 (H1'), 1.29 (H1''), 0.94 - 0.80 (H11) ppm.

piGPMA **6**: pinkish powder, monomer conversion: 70 % ($piGPMA_{DMF}$) and 94 % ($piGPMA_{1,4\text{-dioxane}}$); M_n = 8.4 kDa ($piGPMA_{DMF}$) and 11.4 kDa ($piGPMA_{1,4\text{-dioxane}}$), PDI = 1.3 (SEC-DMF, PS standard); δ_H (DMSO-d_6, 400 MHz): 10.79 (H6), 7.85 (H5), 7.62 (H9, H13, H16)), 6.49 (H7), 6.15 (H4), 5.42 (H3), 5.27 (H2), 4.50 (H8), 2.88 (H10, H12), 1.49 (H1'), 1.31 (H1''), 1.23 (H14), 0.96 - 0.68 (H11) ppm.

11.5.6 Deprotection of nucleoside-based homopolymers (pCPMA **7** and pGPMA **8**)

Cytidine- and guanosine-based homopolymers **5** and **6** were deprotected under acidic conditions, respectively. 5 and 6 (23.4 mg) were stirred for 2 h at rt in H_2O (93.6 μL) and trifluoroacetic acid (TFA) (608 μL), followed by reprecipitation into cold THF/Et_3N (9:1).

Precipitated polymers were centrifuged, washed with THF (3 x), acetone (3 x) and dichloromethane (3 x). Deprotected nucleoside homopolymers were isolated after drying on high vacuum as pale red powders (23.0 mg).

pCPMA **7**: yield: 50 %; δ_H (DMSO-d_6, 400 MHz): 10.91 (H6), 8.32 (H5), 8.17 (H9, H13), 7.54 - 7.32 (H16), 6.62 (H7), 5.84 (H4), 4.53 (H2), 4.32 (H3), 4.21 (H8), 3.88 (H1), 2.94 (H10, H12), 1.50 (H14), 0.96 - 0.66 (H11) ppm.

pGPMA **8**: yield: 62 %; δ_H (DMSO-d_6, 400 MHz): 8.51 (H5, H6), 8.31 (H9, H13), 7.44 (H16), 6.10 (H7), 5.79 (H4), 4.32 (H2), 4.22 (H3), 4.04 (H8), 3.50 (H1), 2.96 (H10, H12), 1.54 (H14), 0.97 - 0.80 (H11) ppm.

11.5.7 Polymerization of HPMA (pHPMA **9**)

A mixture of HPMA 10 (1.10 g, 7.69 mmol), CPADB (31.0 mg, 110 µmol; target DP = 70), ACVA (10.3 mg, 136.5 µmol; CTA/I molar ratio = 3), ethanol (3 mL) and acetate buffer (7 mL; pH 5) was purged with N_2 for 30 min before placing in a preheated oil bath at 70 °C. After 24 h, the reaction was stopped by exposing to air and cooling to rt. Resulting **9** was purified by dialysis against water for 5 days, followed by freeze-drying as a pinkish powder (monomer conversion: 75 %, yield: 70 %); M_n = 38.7 kDa (by ^{1}H NMR); M_n = 42.8 kDa (by UV-Vis); M_n = 9.1 kDa, PDI = 1.66 (SEC-DMF, PMMA standard); δ_H (DMSO-d_6, 400 MHz): 7.17 (1H, bs, H5), 4.69 (1H, s, H3), 3.67 (1H, s, H1), 2.90 (2H, s, H4), 1.57 (1H, m, H7), 1.02 (3H, s, H6), 0.89 (3H, d, ^3J = 64.4 Hz, H2) ppm.

11.5.8 Blockcopolymerization of pHPMA-*b*-piCPMA **11**

A mixture of iCPMA **1** (101 mg, 0.240 mmol), pHPMA **9** (40 kDa) (68.5 mg, target DP = 150) and ACVA (0.815 mg, 2.90 µmol, CTA/I molar ratio = 0.55) in 8:2 DMF/ H_2O (899 µL) was flushed with N_2 for 30 min before placing in a preheated oil bath at 75 °C. The reaction mixture was reacted for 24 h and purified by repetitive precipitation from cold acetone, followed by drying under high vacuum. The desired product was yielded as a white powder (monomer conversion: 77 %, yield: 76 %); δ_H (DMSO-d_6, 400 MHz): 7.74 (H5, H9, H13), 7.18

(H18), 5.75 (H4, H7), 5.10 - 5.05 (H6, H8), 4.69 (H20), 4.37 (H2), 3.68 (H22), 2.91 (H10, H12, H19), 1.57 (H15, H17), 1.46 (H1'), 1.28 (H1''), 1.02 (H16), 0.81 (H11, H21) ppm.

11.5.9 Block-copolymerization of pHPMA-*b*-piGPMA **12**

iGPMA **2** (62.0 mg, 0.134 mmol), pHPMA **9** (40 kDa) (11.5 mg, target DP = 150) and ACVA (0.415 mg, 1.50 µmol, CTA/I molar ratio = 0.134) were dissolved in 9:1 1,4-dioxane/H_2O (938 µL) and flushed with N_2 for 30 min. The reaction mixture was placed in a preheated oil bath at 75 °C and reacted for 24 h. The desired compound was isolated after dialysis against water for 3 days and drying as a white powder (monomer conversion: 77 %, yield: 68 %); δ_H (DMSO-d_6, 400 MHz): 10.77 (H6), 7.85 (H5), 7.18 (H9, H13, H16), 7.18 (H18), 6.53 (H7), 6.15 (H4), 5.43 (H3), 5.27 (H2), 4.69 (H20), 4.50 (H8), 3.68 (H22), 2.91 (H10, H12, H19), 1.42 (H1'), 1.32 (H1''), 1.19 (H14), 1.02 (H16), 0.82 (H11, H21) ppm.

11.5.10 Deprotection of pHPMA-*b*-nucleosides (pHPMA-*b*-pCPMA **13** and pHPMA-*b*-pGPMA **14**)

pHPMA-*b*-nucleosides **11** and **12** (20 mg) were deprotected under acidic conditions by agitating with TFA (520 µL) and H_2O (80 µL) for 2 h. The reaction mixtures were dialyzed against water for 3 days and dried by freeze-drying.

pHPMA-b-pCPMA **13**: yield: 53 %; M_n = 91.4 kDa (by ^{1}H NMR), M_n = 11.7 kDa, PDI = 1.10 (SEC-DMF, PMMA standard); δ_H (DMSO-d_6, 400 MHz): 9.12 (H6), 8.73 - 8.44 (H5, H9, H13), 7.15 (H18), 6.15 (H7), 5.81 (H4), 4.48 - 4.03 (H1, H2, H3, H8, H20), 3.68 (H22), 2.99 (H10, H12, H19), 1.57 (H15, H17), 1.26 (H14), 1.01 (H16), 0.62 (H11, H21) ppm.

pHPMA-b-pGPMA **14**: yield: 81 %; M_n = 163.2 kDa (by ^{1}H NMR), M_n = 24.7 kDa, PDI = 2.50 (SEC-DMF, PMMA standard); δ_H (DMSO-d_6, 400 MHz): 10.81 (H6), 8.13 (H5, H9, H13), 7.18 (H18), 5.84 (H4), 5.61 (H7), 4.70 (H20), 4.38 (H1), 4.28 - 4.18 (H3, H8), 3.68 (H22), 2.90 (H10, H12, H19), 1.57 (H15, H17), 1.23 (H14), 1.02 (H16), 0.81 (H11, H21) ppm.

11.6 Acknowledgements

The authors gratefully acknowledge Angela Krtitschka from the University of Potsdam for enabling measurements of NMR spectra and Dr. Matthias Hartlieb from the University of Potsdam for scientific advice. In addition, the authors thank Dr. Andreas Bohn and Minh Thu Tran from Fraunhofer IAP for taking SEM pictures. Thanks also go to Dr. Erik Wischerhoff from Fraunhofer IAP for GPC measurements.

12 Discussion

The ubiquity of carbohydrate structures makes them one of the most fundamental classes of biomolecules in our lives. Therefore, the rise of literatures on glyco-based materials is not unexpected. Glycopolymers are a preferred selection due to their diverse applications, such as drug delivery systems, pathogen inhibition and lectin binding. This thesis focusses on the synthesis of carbohydrate-bearing monomers and polymers, including the required precursors depending on the desired application. The application as a thermoresponsive glycomaterial is explained in more detail here.

12.1 Synthesis of glycomonomers and precursors

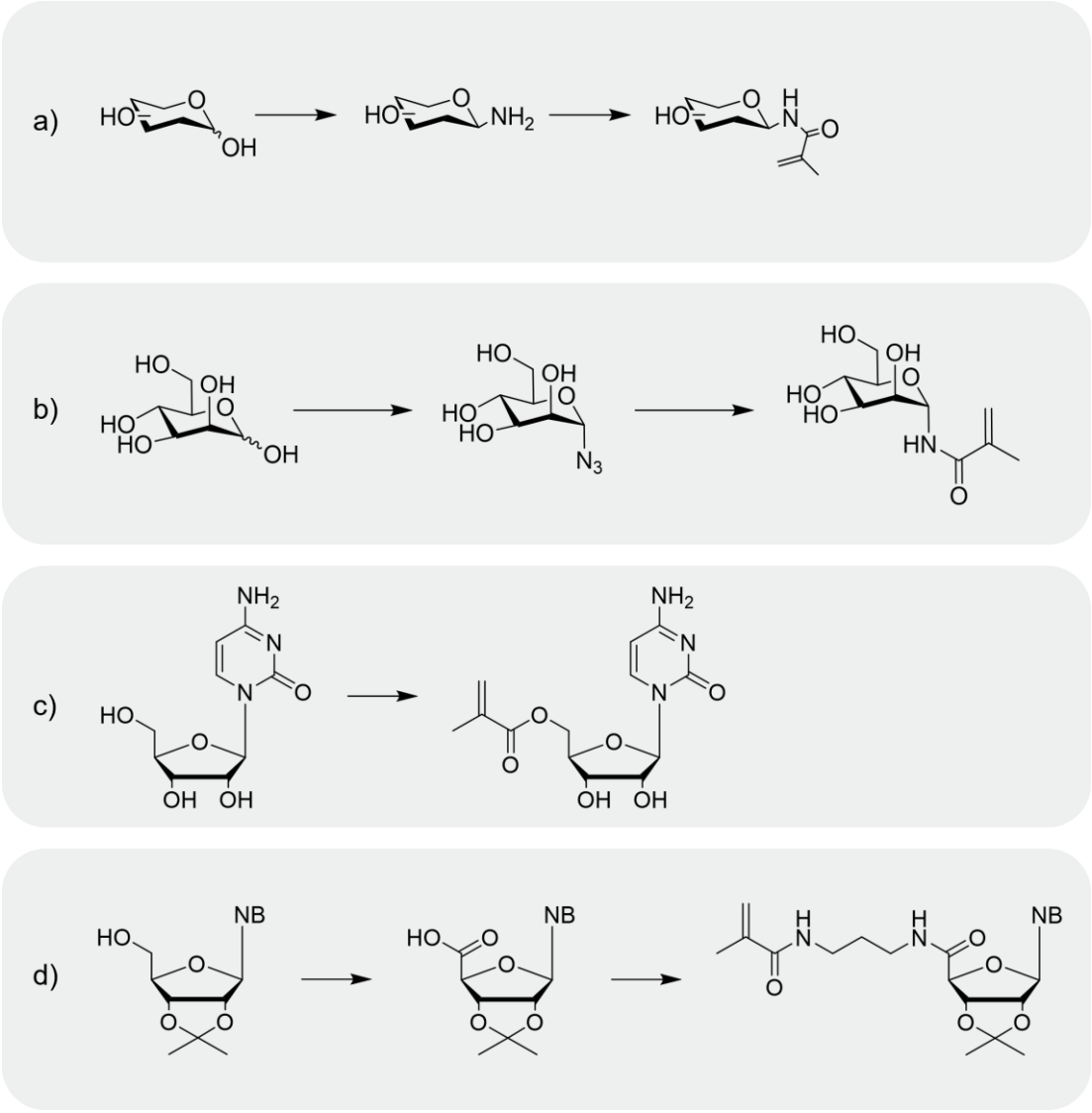

Scheme 21. Synthesis of glyco-bearing monomers in this thesis via a) methacrylation after Kochetkov/ Likhorshetov amination; b) Staudinger ligation; c) enzyme-catalyzed transesterification and d) amide coupling after oxidation.

To integrate a polymerizable group, the desired sugar-containing molecule must first be suitably derivatized. In doing so, reference was made to the enormous pool of organic reaction syntheses and amidation, esterification and Staudinger ligation were selected for this purpose (Scheme 21).

The syntheses of the precursors for these reactions concentrated on simplicity and were carried out either with or without the use of protective groups. In this work, a polymerizable group was incorporated regiospecifically at the anomeric C1 position of hexoses or at the C5 position of a ribose-containing compound, depending on the desired application. In the preparation targeting the C1 position, the focus was on a protection group-free approach in order to keep the total number of synthesis steps low.

The synthesis reaction of amidation is a well-established method to attach a polymerizable group to a carbohydrate. Amidation is a nucleophilic acyl substitution reaction, which demands a nucleophile and an electrophile. Using commercially available glycosamines as nucleophiles like glucos- or galactosamines, (meth)acrylates can be introduced under basic reaction conditions in only one reaction step.[364,365] Depending on the application, this is a suitable and simple method for the preparation of glycomonomers functionalized at the C2 position. However, to ensure lectin activity, modification of carbohydrate structures should focus on the C1 hydroxyl group.[102,366] The equilibrium between α- and β-saccharide proceeds via the aldose in the open chain form. The enclosed aldehyde group thus provides an electrophilic character for reductive amination to derivatize the anomeric carbon atom. The use of $NaCNBH_3$ allows the isolation of glycomonomers under pH conditions of 6 – 7 without the use of protection chemistry.[367,368,369] However, the resulting product is open-chained and therefore not suitable for studies of lectin activity, as recognition only occurs in the presence of the carbohydrate in its intact cyclic configuration. To circumvent this, at least disaccharides can be used so that a minimum of one sugar ring remains for biological recognition.[112,370,371] Unfortunately, reductive amination is not implementation-friendly due to the use of the cyanide compound required. In addition, boron complexes are formed when $NaCNBH_3$ is used. This strong affinity of boron atoms to hydroxyl groups are difficult to break and therefore removal from the final product is challenging.[372] A combination of the two described procedures for the synthesis of glycomonomers through an amide bond therefore seems to be a valid approach for lectin recognition and pathogen inhibition desired in the future: an amidation reaction at the anomeric site.

Before the polymerizable group can be introduced via amidation, the appropriate nucleophilic glycosylamine must be generated for this purpose. According to literature, C1 functionalized glycosylamines can be produced via three reaction steps, without listing the introduction and removal of protection groups. These include bromination of the protected carbohydrate via HBr in an acidic environment, followed by azidation using NaN_3 and subsequent reduction to the amine using Pd/C and H_2.[373,374]

The use of the synthesis developed by Kochetkov makes it possible to reduce the synthesis steps for the isolation of glycosylamines to a minimum of one step. This not only saves time, but also reaction reagents and therefore costs. Furthermore, the introduction of protective groups is not necessary, so that additional two reaction steps can be skipped. Kochetkov amination requires the use of a 50-fold excess of ammonium carbonate. Glycosylamines, however, tend to hydrolyze at a wide pH range from 1.5 to 9 and form into diglycosylamines in concentrated solutions.[375] These drawbacks can be circumvented, on the other hand, by using ammonium carbamate instead of bicarbonate according to the further developed reaction of Likhoshertov.[202,203,204,205] As the proposed method of Likhoshertov include the formation of the carbamic acid salt of glycosylamine, hydrolysis and glycosylamine-dimer formation can be prevented. The desired free glycosylamine can be easily generated afterwards by treating with a base or under high vacuum conditions. The amination reaction proceeded via a condensation mechanism according to Kochetkov or Likhoshertov and leads predominantly to the isolation of glycosylamines in β-configuration.

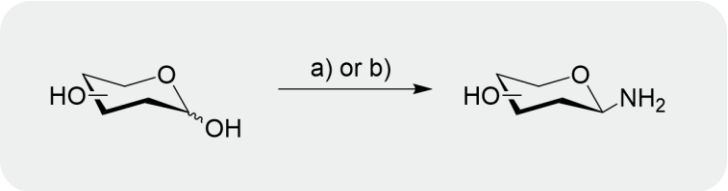

Scheme 22. Synthesis of glycosylamines via the method of Kochetkov/ Likhoshertov with following reaction conditions: a) 50-fold ammonium salt, rt, 5 d or b) 5-fold ammonium salt, ΔT, 90 min, MW.

Assisting with microwave irradiation enhances the quality of amination reaction significantly. Compared to the conventional reaction using an oil bath, the use of microwave irradiation is able to reduce the reaction time of the Kochetkov amination from 5 d to 90 min (Scheme 22).[376] In addition, the quantity of ammonium carbonate could be significantly reduced in this way, which leads to a simplification of isolation, as less ammonium carbonate needs to be removed. GalNAc, Lac, GlcA and Fuc were derivatized this way to provide the necessary nucleophile for amidation.

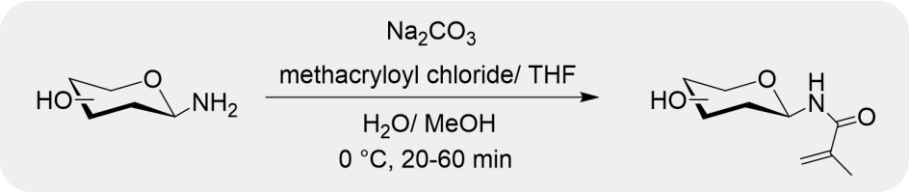

Scheme 23. Synthesis of glycomonomers via methacrylation of glycosylamines.

After successful amination via the procedure of Kochetkov or Likhoshertov, an insertion of a polymerizable group via amidation under basic conditions is feasible. This amidation is based on the described derivatization of commercially available glycosamines. In this thesis, fucosylamine, lactosylamine and melibiosylamine were derivatized in this manner to a polymerizable glycomonomer, respectively. Functional methacrylic group was introduced in the anomeric C1 position to retain lectin recognition (Scheme 23). Since the configuration is determined by the preceding amination reaction, a β-configuration is also present in this case. The isolation of glycomonomers via Kochetkov or Likhoshertov amination is therefore only achievable in their β-configuration. Derivatization to the monomer at the C1 position can also be achieved by using glycosidase referring to literature.[102,103] This has the disadvantage that the reaction time is significantly higher at 24 h. Moreover, only ester bonds and no amide bonds can be formed in these enzymatic-catalyzed synthesis routes. Another drawback is that only specific glycosidases for specific sugars can be used. For example, glucosidases can only convert Glc and galactosidases can only convert Gal. Other enzymes, such as proteases or lipases, catalyze the derivatization of the primary hydroxyl group at the C5 or C6 position, but not the desired anomeric C1 position. [102,105] Alternatively, transition metal mediated syntheses, such as Ag(I), Cu(I) or Au(III) ions, were described to introduce a polymerizable element into the C1 position.[83,92,93] Nevertheless, these synthesis approaches require the introduction of protecting groups, which increases the number of synthesis steps by two. In addition, these metals must be thoroughly removed from the final product when used in a biomedical application, as they may be toxic.

However, since some lectins can only recognize saccharide structures in their α-configuration, this amidation method is not always suitable for the isolation of glycomonomers via the amination procedure described above. For example, ConA, one of the best-studied lectins for investigating receptor interactions of glycopolymers, binds only D-mannosyl and D-glucosyl residues in their α-configuration.[294,295] Syntheses of Man-containing compounds in their α-configuration is more simplified by the axial position of the alcohol group in C2 position in contrast to Glc-containing compounds. The synthesis of a glycomonomer in α-configuration

proceeds through the formation of an *O*-glycosidic bond. For this purpose, according to the literature, acetyl-protected Man was equipped with an azide as end group functionality by means of BF_3•OEt_2 directly or via a bromination step. This azide functionality was thereafter reduced with H_2 and a metal catalyst to the free amine form, which was then reacted with acryloyl chloride via the amidation mechanism to isolate the glycomonomer.[377,378] Instead of the reduction to the free amine, the azide functionality can also be used directly as a click reagent as described in literature. In combination with a polymerizable alkyne counterpart, the use of click chemistry can shorten the isolation of α-Man-containing monomer by one step compared to amidation.[379,380] The use of click chemistry requires either high reaction temperatures or the use of Cu-catalysts. However, carbohydrates are known to oxidize at high temperatures and incomplete removal of metal catalysts is fatal for biomedical applications; click chemistry is not always the preferred choice.

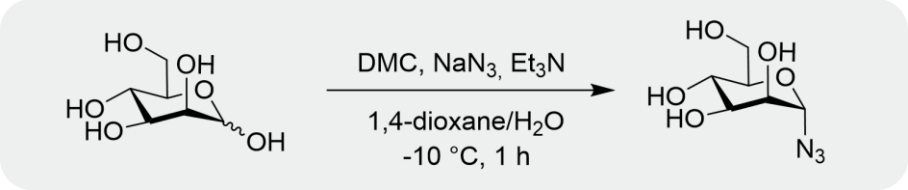

Scheme 24. Synthesis of α-mannosyl azide without the introduction of protecting groups.

Staudinger ligation offers an appealing alternative. In this work, for the first time, the synthesis of Man-containing monomer in its α-configuration is carried out with a reduced number of synthesis steps compared to the previously described synthesis routes. Since the introduction and removal of protective groups is not a necessity, the synthesis pathway now presented is narrowed down to two reactions starting form D-Man. Adapted from the literature, α-mannosyl methacrylamide was isolated via the mechanism of Staudinger ligation.[300,301] A characteristic of Staudinger ligation is its impact on stereochemistry. It can be subdivided into two stages: the formation of the iminophosphorane by an intramolecular rearrangement and the formation of an amide bond by cleavage of triphenylphosphinooxide by hydrolysis. Depending on the derivatization and reaction conditions, the stereoisomerism of the azide used can be maintained or inverted. For the maintenance of stereoisomerism, the kinetics of the second reaction step, is relevant. The hydrolysis of the formed iminophosphorane should be as rapid as practicable, as the glycoiminiophosphorane is in an anomeric equilibrium, which might lead to an inversion of the stereocenter. To apply this ligation, an azide on the one hand and a triphenylphosphine derivative on the other hand is required. The synthesis of α-mannosyl azide by TMS-activation has been described in the past, which requires prior equipment with

protecting groups.[381,382] When using chloroamidinium salt like 2-chloro-1,3-dimethylimidazolinium chloride (DMC) as coupling reagent, D-Man can be azidified under basic reaction conditions directly without protection groups (Scheme 24).

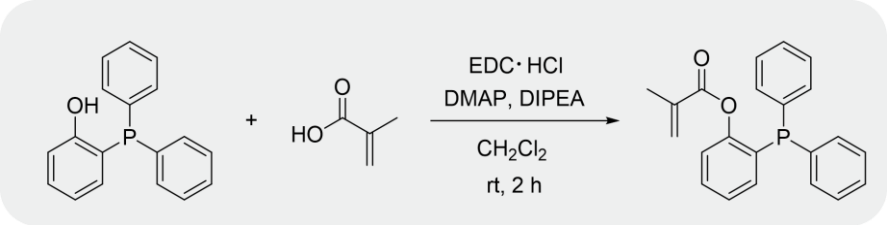

Scheme 25. Synthesis of methacrylic triphenylphosphine derivative via Steglich esterification.

Furthermore, (2-hydroxyphenyl)diphenylphosphine was provided with a polymerizable group by 1-ethyl-3-(3-dimethylaminopropyl)carbodiimide (EDC) activation of methacrylic acid and subsequent Steglich esterification in the presence of 4-dimethylaminopyridine (DMAP) with a modified procedure described (Scheme 25).[301,383,384] In the literature, a yield of 50 - 90 % of several triphenylphosphine derivatives is described. The obtained yield of 2-(diphenylphosphonyl)phenyl methacrylate is low at 12 %, so that further optimization experiments are necessary. Attempts using methacryloyl chloride were discontinued due to the formation of byproducts and therefore due to the aggravated purification.

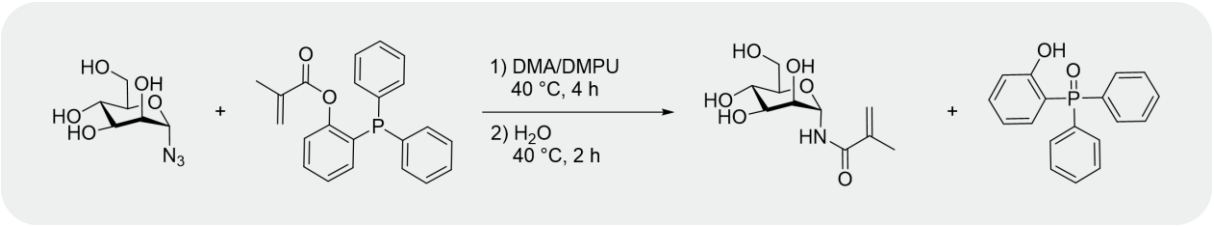

Scheme 26. Synthesis of mannosyl methacrylamide via Staudinger ligation.

By forming a triphenylphosphine oxide derivative, the α-mannosyl azide reacted with the methacrylic triphenylphosphine derivative to isolate the desired Man-containing methacrylamide in its α-configuration. Depending on the reaction conditions, the product ratio of α- and β-anomers differs. By keeping the reaction temperature low at 40 °C and a minimum total reaction time of 6 h, the anomeric equilibrium can be shifted to the α-mannosyl methacrylamide with a yield of 70 % (Scheme 26). Higher reaction temperatures at 70 °C resulted in an enantiomeric excess towards β-configuration. The yield is consistent with the described synthesis which was modified by the use of a different triphenyl phosphate derivative.[301]

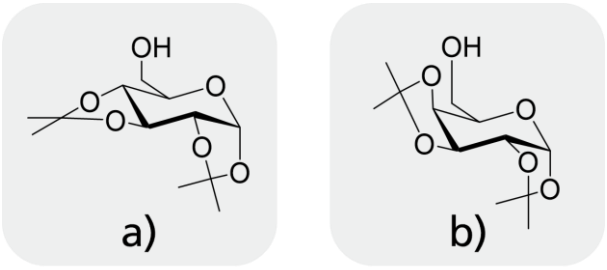

Figure 37. Examples of acetonide-protected saccharides, a) 1,2:3,4-di-*O*-isopropylidene-α-D-glucopyranose and b) 1,2:3,4-di-*O*-isopropylidene-α-D-galactopyranose.

If subsequent lectin recognition is not required or the C1 position is already blocked (e.g. with nucleobase), the primary alcohol group (C5 for furanoses, C6 for pyranoses) can be targeted, as it has a higher basicity and thus a higher nucleophilicity compared to the other remaining secondary hydroxyl groups. This primary alcohol can hence serve as a nucleophile in (trans)esterification reactions to introduce functional groups. In practice, however, the targeted functionalization of the primary hydroxyl group is still challenging, so that protecting groups are still required. Acetonide protecting groups enable the protection of hydroxyl groups that are spatially close to each other in the chair conformation. To keep the C6 (for pyranoses) or C5 (for furanoses) position unprotected, only selected sugars can be functionalized with this method (Figure 37).

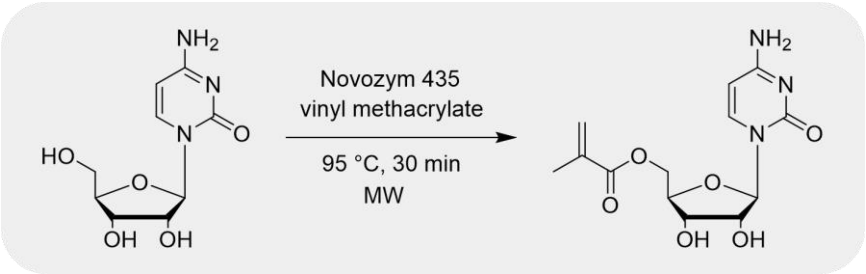

Scheme 27. Enzyme-catalyzed synthesis of 5'-*O*-methacryloylcytidine with MW irradiation.

For the protecting group free synthesis, the use of enzymes, more specifically lipases, can be considered in more detail. In their immobilized form, they can modify the primary hydroxyl group of the sugar (C5 for furanoses, C6 for pyranoses) without using protecting groups. Applying enzyme catalysts shortens syntheses of glyco-derivatives due to regioselectivity and specificity significantly; plus, they are a popular tool in glyco-chemistry to introduce functional groups into carbohydrates. These biocatalysts have been widely used in the past for (trans)esterification of compounds related to green chemistry due to their high efficiency under mild reaction conditions, non-toxicity and reusability.[312] In particular

Novozym 435, an immobilized commercially available Cal B lipase, is not only used for research purposes but has already been able to establish itself in industry.[313] In conjunction with the synthesis of glycomonomers, Glc-derived monomers were isolated with Novozym 435 in accordance with the literature.[102] Optimization trials demonstrated that the use of the solvent *t*-BuOH at 45 °C for the synthesis of methacylic β-methyl glucoside gave the highest conversion.[298] In combination with microwave irradiation, even the reaction time for the isolation of methyl glucoside derivatives can be shortened from 13 to 3 h significantly.[325] Furanoses, such as several nucleoside derivatives, were likewise derivatized with biocatalysts.[311] Polymerizable cytidine was functionalized with Novozym 435 and presynthesized methylcryloylacetone oxime as substrate with a reaction time of 22 h and the addition of the solvent 1,4-dioxane with a yield of 47 %.[108] The synthesis of 5'-*O*-methacryloylcytidines was optimized in this thesis by varying reaction parameters. The optimum yield of 36 % was achieved at a reaction temperature of 95 °C and a reaction time of 30 min with an enzyme concentration of 12.7 wt.% and a molar ratio of the substrate vinyl methacrylate of 1:35. The yield is lower than described in the literature, but the reaction time could be shortened considerably and the use of the solvent 1,4-dioxane could be avoided (Scheme 27). Increasing the reaction time resulted in lower yields, indicating a discrepancy with the literature in which other molecules were derivatized with Novozym 435 and reached a plateau with longer reaction times.[266,298,326] The initial suspicion that the choice of substrate was due to the formation of the enzyme-deactivating acetaldehyde was refuted by the use of other substrates.[121] This suggests that the cytidine with the nucleophilic amine group in combination with the microwave irradiation and the polymer-bound lipase is the causative element. Commercially available methacrylate derivatives were consciously chosen as substrates in order to avoid an additional synthesis step. The comparison of methyl methacrylate and vinyl methacrylate showed that a higher yield could be achieved with the latter in this transesterification reaction.

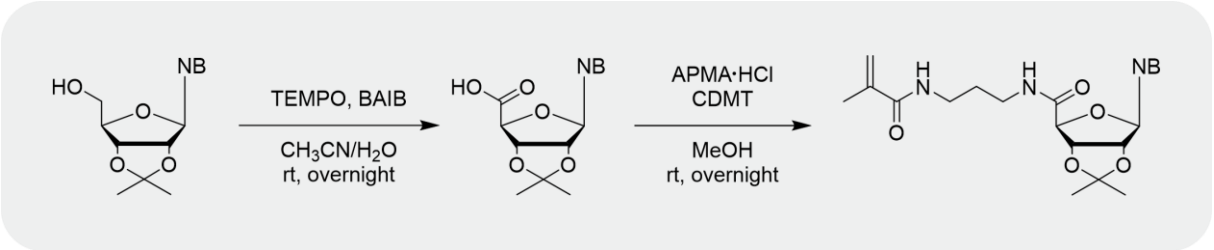

Scheme 28. Synthesis of nucleoside-based monomer via oxidation and subsequent amide coupling.

However, ester bonds tend to hydrolyze in harsh environments, so the formation of an amide bond is preferable. Towards this aim, the secondary hydroxyl groups were protected with an acetal protecting group in order to oxidize the free alcohol at the C5 position to the carboxylic acid with the help of the heterocyclic compound (2,2,6,6-tetramethylpiperidin-1-yl)oxyl (TEMPO). In the presence of the triazine derivative 2-chloro-4,6-dimethoxy-1,3,5-triazine (CDMT), the carboxylic acid provides its activated form for amide coupling. Further coupling approaches with carbodiimides, such as EDC or *N*,*N*'-dicyclohexylcarbodiimide (DCC), and via the uranium salt 1-[bis(dimethylamino)methylene]-1H-1,2,3-triazolo[4,5-b]pyridinium 3-oxide hexafluorophosphate (HATU) resulted in lower yields. The usage of the hydrochloric salt of *N*-(3-aminopropyl)methacrylamide (APMA) led to the introduction of a polymerizable group (Scheme 28). Unlike the enzyme-catalyzed synthetic pathway, this method also enables the synthesis of guanosine-containing monomers. Cytidine- and guanosine-based methacrylamides could thus be isolated in this pure form for the first time with a yield of 44 % and 52 %, respectively. Since nucleobase functionality is of greater significance in this case, nucleobase-containing monomers without the ribose unit were isolated as an alternative by other research groups.[306,349,350,345,341] Due to the formation of strong hydrogen bonds, nucleobases and their derivates are known for their poor solubility.[340] In contrast, the ribonucleoside-based monomers described in this thesis are soluble in both aqueous and organic solvents, which simplifies subsequent polymerization.

12.2 Synthesis of glycopolymers

Numerous polymerization techniques for the isolation of carbohydrate-containing polymers have already been described in the past. FRP has often been chosen for isolating glycopolymers because it offers advantages, such as low cost and scalability. However, this polymerization technique leads to an uncontrolled high distribution of the molecular weight, thus a CLRP method is preferable. The most common controlled polymerization techniques for isolating glycopolymers are the ATRP and RAFT techniques. ATRP is appreciated for its low reaction temperatures and requires a transition metal catalyst. The most common catalysts for this are based on copper, and the resulting macromolecules must be thoroughly purified due to the toxicity of copper ions when used as biomedical material.[385,386] RAFT, on the other hand, does not require transition metals and still offers the advantages of ATRP polymerization in terms of straightforward implementation. Numerous sugar-containing polymers, e.g. Glc-, Gal-

and Man-containing macromolecules, have been isolated by RAFT polymerization. [96,109,151,299,387,388,389]

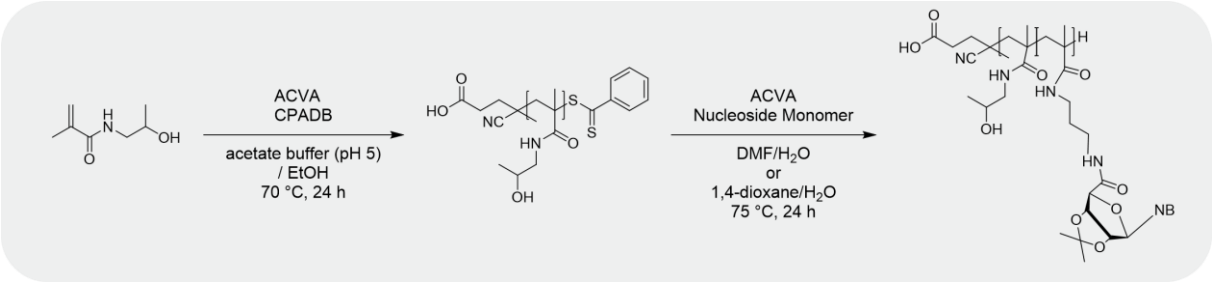

Scheme 29. Synthesis of pHPMA and nucleoside-based block copolymers via RAFT polymerization.

According to literature, thymine- and adenine-based monomers were polymerised with a PEG initiator via ATRP.[345] Uridines and adenosine-based monomers, which include ribose in the chemical structure, were only able to be polymerized via the mechanism of ATRP after the introduction of a silyl protecting group.[315] Depending on the ATRP ligand used, narrow polydispersities between 1.12 and 1.35 were obtained. Extending this, cytidine- and guanosine-containing macromolecules were prepared by radical polymerization on a solid support with satisfactory control over polydispersity.[327] Although nucleobase-containing monomers were mainly polymerized using the ATRP technique, the RAFT technique was deliberately chosen in this thesis to obtain ribonucleoside-containing polymers. Indeed, in the presence of nucleobases, they are coordinated to copper ions, which makes their removal even more difficult. Cytidine- and guanosine-based homopolymers were isolated using a dithioester-based CTA with polydispersities of 1.3, whereby guanosine-containing monomers showed higher conversions compared to the cytidine equivalent. Similar to other nucleobase-containing polymers described, these synthesized ribonucleoside polymers also exhibit low solubility.[315,327,345] Thus, to introduce a hydrophilic HPMA moiety, the HPMA homopolymer had to be synthesized first before copolymerization with the nucleoside monomers could take place (Scheme 29). It was observed that the purine-based guanosine monomer always had a higher conversion than the cytidine equivalent according to NMR spectroscopy. However, the literature reported that the pyrimidine-based thymine monomer leads to higher conversion in ATRP polymerization.[315,327,345] Lastly, the acetal protecting groups of the synthesized ribonucleoside-based block copolymers in this thesis were removed under acidic conditions.

12.3 Thermoresponsive carbohydrate-containing polymer

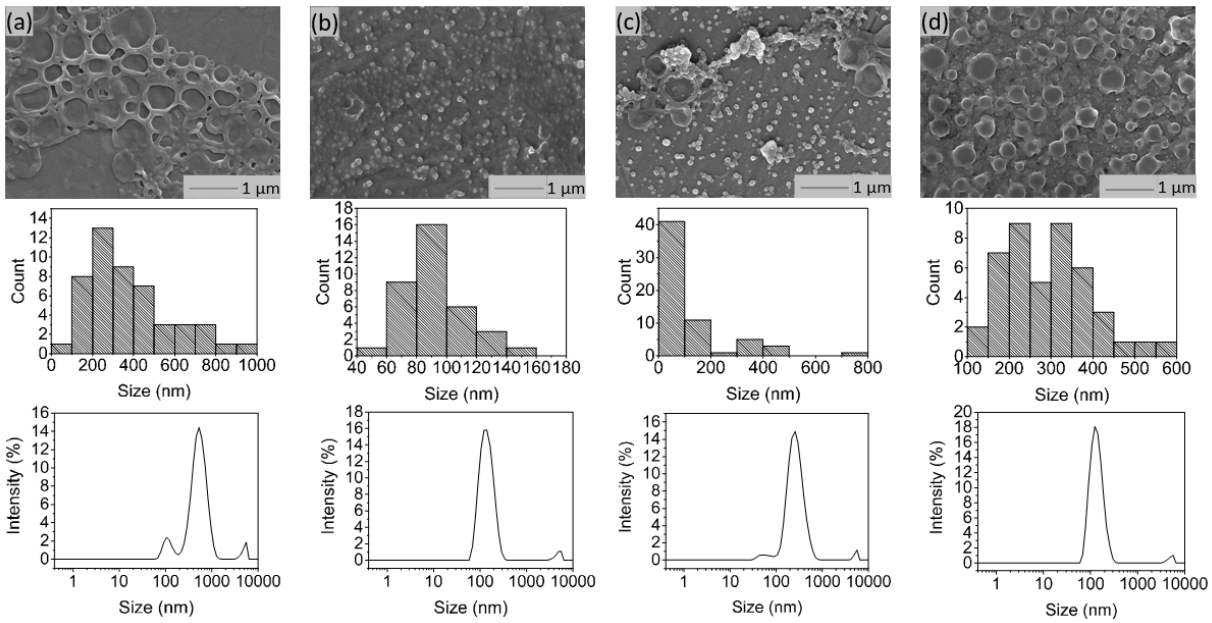

Figure 38. SEM-images, size distributions and hydrodynamic size distributions by DLS of (a) pHPMA-*b*-pCPMA, (b) pHPMA-*b*-pGPMA, (c) mixture of both before heating and (d) mixture of both after heating.

Intelligent materials are based on the reaction to a stimulus. Temperature is particularly promising as a stimulus, as it plays an essential role in nature and can also be reversibly adjusted externally. Thermoresponsive macromolecules have either an LCST or an upper critical solution temperature (UCST) in the aqueous medium suitable for drug delivery. UCST polymers are rare, especially in aqueous media, compared to LCST systems, as they react more sensitively to external influences, such as concentration, pH or ionic strength. Two essential conditions are required for UCST behaviour: 1) the interactions between the polymers must be stronger than the interaction with water, so that the polymer complexes can only be dissolved by thermal activation in water, and 2) the polymers must exhibit a certain degree hydrophpobicity, otherwise they would dissolve due to a gain in configuration entropy. Polymers with formed hydrogen bonds are typical for polymers with UCST dissolution behaviour. Typical representatives are poly(ethylene oxide) (PEO), poly(hydroxyethyl methacrylate) (PHEMA) or poly(vinyl methyl ether) (PVME), which however also have LCST character.[390,391] These polymer systems, though, have a UCST value outside 0 – 100 °C, which makes them unsuitable for most applications. Polymers with a UCST in this range are for example poly(acrylamide-co-acrylonitrile), poly(methacrylamide) or poly(allylamine-co-allylurea) derivatives.[392,393] By introducing hydrophobic monomers or increasing the molecular weight of the homopolymer, the UCST can also be increased. A UCST target of up

to 1 °C difference can be achieved by copying from nature using DNA or RNA-like structures. DNA or RNA strands are kept in place by strong interactions, the hydrogen bonds. These bonds can be disrupted by elevated temperatures, which depends on the type and number of nucleobases. This characteristic so-called melting behavior enables us to develop new programmable materials which respond to temperature changes.[307,341] Due to the presence of nucleobases in the previously described synthetically produced carbohydrate-containing block copolymers, their self-assembly behavior was investigated. First, the nucleoside block copolymers were considered individually before they were combined and heated. As a result of the C-C and G-G interactions, the C-containing polymers form large network structures and the G-containing polymers smaller particles according to SEM images, in contrast to the A- and T-containing polymers described in the literature, which have popcorn-like structures.[350] Combining the complementary block copolymers and subsequent heating followed by cooling resulted in a smaller size distribution, which can be attributed to a break-up of the respective C-C and G-G interactions and reassembly by C-G interactions (Figure 38). This observation was supported by UV-Vis experiments. The absorption maxima of the individual C- and G-containing polymers are comparable to the maxima of the A- and T-containing polymers described in the literature.[108,345] Hypochromicity was also noticed in comparative experiments with the polymer mixtures before and after heating.

To sum up, several carbohydrate-based monomers were synthesized. Either the anomeric C1 position or the primary hydroxyl group in the C5 position was targeted. Derivatization at C1 required prior amination by microwave irradiation according to the procedure of Kochetkov or Likhorshetov. After successful amination, a glycomonomer was isolated by methacrylation. Nucleoside-containing monomers were also synthesized by enzyme-catalyzed, microwave-assisted synthesis or oxidation followed by amidation. The latter synthesis approach required the introduction of protecting groups compared to the other methods. These cytidine and guanosine based monomers were then polymerized using the RAFT method. Their self-assembly behavior was investigated and it was found that networks form due to hydrogen bonds, which can be broken when heat is applied.

13 Conclusion and Outlook

This dissertation describes the synthesis of glycosides, including carbohydrate-containing monomers and polymers. These form the foundation for the development of potential biofunctional and biomedical materials. Applications range from fundamental research to the study of biological processes and drug delivery systems. The focus of the syntheses was on carrying out as few reaction steps as possible in order to achieve high efficiency.

First, the optimization of the syntheses of glycosylamines was described. The desired saccharide is derivatized at the C1 position with the help of an ammonium salt via the method of Kochetkov or Likhorshetov. The combination with microwave irradiation was taken into consideration, as literature reports a shortening of the reaction time and a lower required concentration of the ammonium salt. In order to approach the optimal yield, the parameters reaction time, reaction duration and type and concentration of the ammonium salt were varied. It became apparent that the optimal reaction conditions of one carbohydrate cannot be transferred to another similar carbohydrate. Kochetkov's method at a reaction temperature of 60 °C in MeOH is best for the derivatization of Gal and Lac, while Fuc at 60 °C and GlcA at 45 °C give the best results with Likhorshetov's method. Thus, optimizations are necessary for each individual sugar in order to achieve the highest possible yield.

Glycosylamines form the precursor for glycomonomers, which obtain a polymerizable group through methacrylation. This monomer synthesis strategy was demonstrated here using the synthesis of fucosyl methacrylamide with a total yield of 56 %. This described synthesis, which consisted of microwave-assisted derivatization followed by methacrylation, offers the advantage that the introduction of protecting groups is not required. By avoiding protection groups, the glycomonomer synthesis is shortened by two reaction steps. The column chromatographic purification of the synthesized glycomonomers was still challenging due to their high polarity, so that more suitable methods, such as recrystallization or precipitation experiments, should be conducted and optimized here.

However, this described reaction pathway only resulted in the isolation of glycomonomers in β-configuration, which may not be suitable depending on the application. For example, ConA, FimH and GNA lectins bind terminal carbohydrate structures only to α-Man structures, among others. The synthesis of α-mannosyl methacrylamide could be

accomplished by the mechanism of Staudinger ligation with a yield of 70 %. The synthesis strategy via Staudinger ligation is likewise carried out without the introduction of protecting groups. This required a prior derivatization of the Man to the azide in order to react with the previously synthesized triphenylphosphine derivative with a polymerizable group. Since these are only preliminary attempts, the low yield of 12 % of 2-(diphenylphosphonyl)phenyl methacrylate can be increased by optimization trials.

Instead of the modification at position C1, other positions can also be derivatized if the potential application permits this. Functionalization of the primary hydroxyl group of the saccharide can be realized by using immobilized lipases, such as Novozym 435. This enzyme-catalyzed synthesis allows the introduction of a polymerizable group also without the use of protective groups. In combination with microwave irradiation, the synthesis of 5'-*O*-methacryloylcytidines with Novozym 435 as potential precursors for smart materials was optimized in terms of reaction time, reaction temperature, substrate type and concentration. Using a reaction temperature of 95 °C, reaction time of 30 min, a 12.7 wt% enzyme concentration and a 1:35 molar ratio of substrate vinyl methacrylate resulted in best results of 36 %. Increasing the reaction time resulted in lower yields, which could be due to the nucleophilic amine of the cytosine ring. Further optimization experiments should be performed to significantly increase the yield. For example, the effects of additional polymerizable substrates or the use of solvents can be investigated.

Instead of an ester bond between saccharide and polymerizable group, an amide bond was chosen for the isolation of the nucleoside-based cytidine and guanosine monomers due to their higher stability towards hydrolysis. This was only possible in the presence of protecting groups. The isolation was carried out by oxidation, followed by amide coupling with the triazine coupling reagent CDMT with a yield of 38 % for cytidine-based and 52 % for guanosin-containing monomer. The corresponding monomers were soluble in both aqueous and organic solvents, which greatly facilitated the handling. They were homopolymerized via the RAFT method, whereby a subsequent block copolymerization was hampered due to a low solubility. For this reason, the monomers were polymerized once the pHPMA macroCTA had been obtained. Studies on self-assembly of the synthesized unprotected nucleoside-based block copolymers revealed that the strong hydrogen bonds can be broken by heat and that the nucleoside-containing block copolymers rearrange themselves after cooling to room temperature according to UV-Vis, DLS and SEM analyses. In order to adjust the melting

temperature more precisely, block copolymers with different molecular weights and thus with different contents of nucleoside-containing monomers should be synthesized and investigated.

In summary, this work focuses on the synthesis of saccharide-based monomers and polymers. However, it became evident that the handling of glycosides is challenging due to the large number of hydroxyl groups. In principle, the respective yields can be improved by targeted optimization experiments, which should be carried out in the future. As a possible application, a thermoresponsive material was presented as a potential drug delivery system.

14 Zusammenfassung und Ausblick

Diese Abschlussarbeit beschreibt die Synthese von Glykosiden, einschließlich kohlenhydrathaltiger Monomeren und Polymeren. Diese bilden die Grundlage für die Entwicklung potenzieller biofunktioneller und biomedizinischer Materialien. Die Anwendungen reichen von der Grundlagenforschung über die Untersuchung biologischer Prozesse bis hin zu Drug Delivery Systemen. Der Schwerpunkt der Synthesen lag darauf, so wenige Reaktionsschritte wie möglich durchzuführen, um eine hohe Effizienz zu erreichen.

Zunächst wurde die Optimierung der Synthesen von Glykosylaminen beschrieben. Hierbei wird das gewünschte Saccharid an der C1-Position mit Hilfe eines Ammoniumsalzes über die Methoden von Kochetkov oder Likhorshetov derivatisiert. Die Kombination mit Mikrowellenbestrahlung wurde in Betracht gezogen, da in der Literatur von einer Verkürzung der Reaktionszeit und einer geringeren erforderlichen Konzentration des Ammoniumsalzes berichtet wird. Um sich der optimalen Ausbeute zu nähern, wurden die Parameter Reaktionszeit, Reaktionsdauer sowie Art und Konzentration des Ammoniumsalzes variiert. Dabei wurde deutlich, dass die optimalen Reaktionsbedingungen eines Kohlenhydrats nicht auf ein anderes ähnliches Kohlenhydrat übertragen werden können. Die Methode von Kochetkov bei einer Reaktionstemperatur von 60 °C in MeOH eignet sich am besten für die Derivatisierung von Gal und Lac, während Fuc bei 60 °C und GlcA bei 45 °C die besten Ergebnisse mit der Methode von Likhorshetov erzielen. Somit sind Optimierungen für jeden einzelnen Zucker notwendig, um die höchstmögliche Ausbeute zu erzielen.

Glykosylamine bilden die Vorstufe für Glykomonomere, die durch Methacrylierung eine polymerisierbare Gruppe erhalten. Diese Monomer-Synthesestrategie wurde hier anhand

der Synthese von Fucosylmethacrylamid mit einer Gesamtausbeute von 56 % veranschaulicht. Diese beschriebene Synthese, die aus einer mikrowellenunterstützten Derivatisierung und anschließender Methacrylierung bestand, bietet den Vorteil, dass die Einführung von Schutzgruppen nicht notwendig ist. Durch den Wegfall der Schutzgruppen wird die Glykomonomer-Synthese um zwei Reaktionsschritte verkürzt. Die säulenchromatographische Aufreinigung der synthetisierten Glykomonomere gestaltete sich aufgrund ihrer hohen Polarität noch schwierig, so dass hier geeignetere Methoden wie Umkristallisations- oder Fällungsversuche durchgeführt und optimiert werden sollten.

Dieser beschriebene Reaktionsweg führte jedoch nur zur Isolierung von Glykomonomeren in β-Konfiguration, die je nach Anwendung unter Umständen nicht geeignet sind. Beispielsweise binden ConA-, FimH und GNA-Lektine Glycoside nur unter anderem α-Man-Strukturen. Die Synthese von α-Mannosylmethacrylamid konnte durch den Mechanismus der Staudinger-Ligation mit einer Ausbeute von 70 % erreicht werden. Die Synthesestrategie über Staudinger-Ligation wird ebenfalls ohne die Einführung von Schutzgruppen durchgeführt. Hierfür war eine vorherige Derivatisierung der Man zum Azid notwendig, um mit dem zuvor synthetisierten Triphenylphosphinderivat mit einer polymerisierbaren Gruppe zu reagieren. Da es sich hierbei nur um Vorversuche handelt, kann die geringe Ausbeute von 12 % vom 2-(Diphenylphosphonyl)phenylmethacrylat durch Optimierungsversuche erhöht werden.

Anstelle der Änderung an der Position C1 können auch andere Positionen derivatisiert werden, wenn die potenzielle Anwendung dies zulässt. Die Funktionalisierung der primären Hydroxylgruppe des Saccharids kann durch die Verwendung immobilisierter Lipasen wie Novozym 435 erreicht werden. Diese enzymkatalysierte Synthese ermöglicht die Einführung einer polymerisierbaren Gruppe auch ohne den Einsatz von Schutzgruppen. In Kombination mit Mikrowellenbestrahlung wurde die Synthese von 5'-*O*-Methacryloylcytidinen mit Novozym 435 als potenzielle Vorstufen für intelligente Materialien in Bezug auf Reaktionszeit, Reaktionstemperatur, Substrattyp und Konzentration optimiert. ei einer Reaktionstemperatur von 95 °C, einer Reaktionszeit von 30 Minuten, einer Enzymkonzentration von 12,7 wt% und einem molaren Verhältnis des Substrats Vinylmethacrylat von 1:35 wurden beste Ergebnisse von 36 % erzielt. Eine Verlängerung der Reaktionszeit führte zu geringeren Ausbeuten, was auf das nukleophile Amin des Cytosinrings zurückzuführen sein könnte. Weitere Optimierungsversuche sollten durchgeführt werden, um die Ausbeute deutlich zu erhöhen. So können beispielsweise die Auswirkungen zusätzlicher polymerisierbarer Substrate oder die Verwendung von Lösungsmitteln untersucht werden.

Anstelle einer Esterbindung zwischen Saccharid und polymerisierbarer Gruppe wurde für die Isolierung der Cytidin- und Guanosinmonomere auf Nukleosidbasis aufgrund ihrer höheren Stabilität eine Amidbindung gewählt. Dies war nur in Gegenwart von Schutzgruppen möglich. Die Isolierung erfolgte durch Oxidation, gefolgt von einer Amidkupplung mit dem Triazin-Kupplungsreagenz CDMT mit einer Ausbeute von 38 % für Cytidin-basierte und 52 % für Guanosin-haltige Monomere. Die entsprechenden Monomere waren sowohl in wässrigen als auch in organischen Lösungsmitteln löslich, was die Handhabung erheblich erleichterte. Sie wurden über die RAFT-Methode homopolymerisiert, wobei eine anschließende Blockcopolymerisation aufgrund von Löslichkeitsproblemen erschwert wurde. Aus diesem Grund wurden die Monomere erst nach Erhalt des pHPMA Makro-CTAs polymerisiert. Untersuchungen zur Selbstassemblierung der synthetisierten ungeschützten nukleosid-basierten Blockcopolymere zeigten, dass die starken Wasserstoffbrückenbindungen durch höhere Temperaturen aufgebrochen werden können und sich die nukleosidhaltigen Blockcopolymere nach dem Abkühlen auf Raumtemperatur neu anordnen wie UV-Vis-, DLS- und REM-Analysen zeigten. Um die Schmelztemperatur genauer einzustellen, sollten Blockcopolymere mit unterschiedlichen Molekulargewichten synthetisiert und damit mit unterschiedlichen Anteilen an nukleosidhaltigen Monomeren untersucht werden.

Zusammenfassend lässt sich sagen, dass sich diese Arbeit auf die Synthese von Monomeren und Polymeren auf Saccharidbasis konzentriert. Es stellte sich heraus, dass die Handhabung von Glykosiden aufgrund der vielen Hydroxylgruppen eine Herausforderung darstellt. Grundsätzlich können die jeweiligen Ausbeuten durch gezielte Optimierungsversuche verbessert werden, die in Zukunft durchgeführt werden sollten. Als mögliche Anwendung wurde ein thermoresponsives Material als potenzielles Drug Delivery System vorgestellt.

15 Bibliography

[1] L. Pellerin, *Diabetes Metab.* **2010**, *36*, S59-S63.

[2] S. D. Anton, C. K. Martin, H. Han, S. Coulon, W. T. Cefalu, P. Geiselman, D. A. Williamson, *Appetite* **2010**, *55*, 37.

[3] K. Kavkler, A. Demšar, *Spectrochim. Acta A Mol. Biomol. Spectrosc.* **2011**, *78*, 740.

[4] M. Flury, R. Narayan, *Curr. Opin. Green Sustain.* **2021**, *30*, 100490.

[5] J. Barros-Rios, A. Romaní, G. Garrote, B. Ordas, *GCB Bioenergy* **2015**, *7*, 153.

[6] X. Tong, Y. Ma, Y. Li, *Appl. Catal. A: Gen.* **2010**, *385*, 1.

[7] B. Dou, H. Zhang, Y. Song, L. Zhao, B. Jiang, M. He, C. Ruan, H. Chen, Y. Xu, *Sustainable Energy Fuels* **2019**, *3*, 314.

[8] M.-A. Perea-Moreno, E. Samerón-Manzano, A.-J. Perea-Moreno, *Sustainability* **2019**, *11*, 863.

[9] P. Vasudevanm, S. Sharma, A. Kumar, *J. Sci. Ind. Res.* **2005**, *64*, 822.

[10] M. V. Rodionova, R. S. Poudyal, I. Tiwari, R. A. Voloshin, S. K. Zharmukhamedov, H. G. Nam, B. K. Zayadan, B. D. Bruce, H. Hou, S. I. Allakhverdiev, *Int. J. Hydrog. Energy* **2017**, *42*, 8450.

[11] V. M. Chernyshev, O. A. Kravchenko, V. P. Ananikov, *Russ. Chem. Rev.* **2017**, *86*, 357.

[12] J. Preiss, T. Romeo in *Progress in Nucleic Acid Research and Molecular Biology*, S. 299–329.

[13] O. Abo Alrob, G. D. Lopaschuk, *Biochem. Soc. Trans.* **2014**, *42*, 1043.

[14] B. C. Moulton, K. L. Barker, *Endocrinology* **1971**, *89*, 1131-1136.

[15] D. Benton, P. Y. Parker, R. T. Donohoe, *J. Biosoc. Sci.* **1996**, *28*, 463.

[16] E. M. Widdowson, R. A. McCance, *Biochem. J.* **1935**, *29*, 151.

[17] N. S. Scrimshaw, E. B. Murray, *Am. J. Clin. Nutr.* **1988**, *48*, 1142.

[18] C. H. Haigler, L. Betancur, M. R. Stiff, J. R. Tuttle, *Front. Plant Sci.* **2012**, *3*, 104.

[19] A. Schimmelmann, M. J. DeNiro, M. Poulicek, M.-F. Voss-Foucart, G. Goffinet, C. Jeuniaux, *J. Archaeol. Sci.* **1986**, 553.

[20] V. Gopinath, S. Saravanan, A. R. Al-Maleki, M. Ramesh, J. Vadivelu, *Biomed. Pharmacother.* **2018**, *107*, 96.

[21] P. Prasher, M. Sharma, M. Mehta, S. Satija, A. A. Aljabali, M. M. Tambuwala, K. Anand, N. Sharma, H. Dureja, N. K. Jha et al., *Colloids Interface Sci. Commun.* **2021**, *42*, 100418.

[22] M. A. V. T. Garcia, C. F. Garcia, A. A. G. Faraco, *Starch - Stärke* **2020**, *72*, 1900270.

[23] V. D. Vilivalam, L. Illum, K. Iqbal, *Pharm. Sci. Technol. Today* **2000**, *3*, 64.

[24] P. S. Damus, M. Hicks, R. D. Rosenberg, *Nature* **1973**, 355.

[25] B. Kranjčec, D. Papeš, S. Altarac, *World J. Urol.* **2014**, *32*, 79.

[26] M. Gold, *J. Cosmet. Dermatol.* **2009**, 301.

[27] M. D. Shoulders, R. T. Raines, *Annu. Rev. Biochem.* **2009**, *78*, 929.

[28] S. Reitsma, D. W. Slaaf, H. Vink, M. A. M. J. van Zandvoort, M. G. A. oude Egbrink, *Pflugers Arch.* **2007**, *454*, 345.

[29] M. B. Reed, P. Domenech, C. Manca, H. Su, A. K. Barczak, B. N. Kreiswirth, G. Kaplan, C. E. Barry, *Nature* **2004**, *431*, 84.

[30] R. L. Schnaar, *Arch. Biochem. Biophys.* **2004**, *426*, 163.

[31] T. Matsui, K. Titani, T. Mizuochi, *J. Biol. Chem.* **1992**, *267*, 8723.

[32] X. Chen, M. A. F. V. Gonçalves, *iScience* **2018**, *6*, 247.

[33] M. Babor, V. Sobolev, M. Edelman, *J. Mol. Biol.* **2002**, *323*, 523.

[34] M. N. Piero, *AJBPS* **2015**, *4*, 1.

[35] S. Grünewald, G. Matthijs, J. Jaeken, *Pediatr. Res.* **2002**, *52*, 618.

[36] C. S. Hudson, *J. Chem. Educ.* **1941**, 353.

[37] M. C. Galan, D. Benito-Alifonso, G. M. Watt, *Org. Biomol. Chem.* **2011**, *9*, 3598.

[38] H. Khan, H. R. Mirzaei, A. Amiri, E. Kupeli Akkol, S. M. Ashhad Halimi, H. Mirzaei, *Semin. Cancer Biol.* **2021**, *69*, 24.

[39] D. Kennes, H. N. Abubackar, M. Diaz, M. C. Veiga, C. Kennes, *J. Chem. Technol. Biotechnol.* **2016**, *91*, 304.

[40] M. Marradi, M. Martín-Lomas, S. PenadÉs in *Advances in Carbohydrate Chemistry and Biochemistry*, S. 211–290.

[41] C.-K. Kang, Y.-S. Lee, *J. Ind. Eng. Chem.* **2012**, *18*, 1670.

[42] R. L. Schnaar, *J. Leukoc. Biol.* **2016**, *99*, 825.

[43] A. J. Thompson, R. P. de Vries, J. C. Paulson, *Curr. Opin. Virol.* **2019**, *34*, 117.

[44] J. H. Prestegard, J. Liu, G. Widmalm, *Essentials of Glycobiology*. *Oligosaccharides and Polysaccharides*, 3. Aufl., Cold Spring Harbor (NY), **2015**.

[45] A. V. Demchenko (Hrsg.) *Handbook of chemical glycosylation*. *Advances in stereoselectivity and therapeutic relevance*, Wiley-VCH, Weinheim, **2008**.

[46] J. Hoffman, B. Lindberg, S. Svensson, *Acta Chem. Scand.* **1972**, 661.

[47] I. Tvaroŝka, T. Bleha in *Advances in Carbohydrate Chemistry and Biochemistry*, Elsevier, **1989**, S. 45–123.

[48] G. Gupta, A. Surolia in *Biochemical Roles of Eukaryotic Cell Surface Macromolecules* (Hrsg.: P. R. Sudhakaran, A. Surolia), Springer New York, New York, NY, **2012**, S. 1–13.

[49] R. P. D. Bank, "RCSB PDB - 3CNA: STRUCTURE OF CONCANAVALIN A AT 2.4 ANGSTROMS RESOLUTION", zu finden unter https://www.rcsb.org/structure/3CNA, **2022**.

[50] M. Ambrosi, N. R. Cameron, B. G. Davis, *Org. Biomol. Chem.* **2005**, *3*, 1593.

[51] K. T. Pilobello, L. K. Mahal, *Curr. Opin. Chem. Biol.* **2007**, *11*, 300.

[52] J. J. Lundquist, E. J. Toone, *Chem. Rev.* **2002**, *102*, 555.

[53] C. Fasting, C. A. Schalley, M. Weber, O. Seitz, S. Hecht, B. Koksch, J. Dernedde, C. Graf, E.-W. Knapp, R. Haag, *Angewandte Chemie (International ed. in English)* **2012**, *51*, 10472.

[54] C. Müller, G. Despras, T. K. Lindhorst, *Chem. Soc. Rev.* **2016**, *45*, 3275.

[55] Erwin R. Ruckel/Conrad Schuerch, *J. Am. Chem. Soc.* **1966**, *88*, 2605.

[56] R. Xiao, M. W. Grinstaff, *Prog. Polym. Sci.* **2017**, *74*, 78.

[57] P. H. Seeberger, W. C. Haase, *Chem. Rev.* **2000**, *100*, 4349.

[58] I. Pramudya, H. Chung, *Biomater. Sci.* **2019**, *7*, 4848.

[59] S. R. S. Ting, G. Chen, M. H. Stenzel, *Polym. Chem.* **2010**, *1*, 1392.

[60] Q. Zhang, D. M. Haddleton in *Advances in Polymer Science* (Hrsg.: V. Percec), Springer International Publishing, Cham, **2013**, S. 39–59.

[61] T. Tanaka, *Trends Glycosci. Glyc.* **2016**, *28*, E101-E108.

[62] H. Seto, S. Kamba, T. Kondo, M. Hasegawa, S. Nashima, Y. Ehara, Y. Ogawa, Y. Hoshino, Y. Miura, *ACS Appl. Mater. Interfaces* **2014**, *6*, 13234.

[63] D. Li, J. Chen, M. Hong, Y. Wang, D. M. Haddleton, G.-Z. Li, Q. Zhang, *Biomacromolecules* **2021**, *22*, 2224.

[64] Y. Miura, *J. Polym. Sci. A Polym. Chem.* **2007**, *45*, 5031.

[65] S. Saxena, B. Kandasubramanian, *Int. J. Polym. Mater.* **2022**, *71*, 756.

[66] T. Oh, M. Nagao, Y. Hoshino, Y. Miura, *Langmuir* **2018**, *34*, 8591.

[67] Y. Kimoto, Y. Terada, Y. Hoshino, Y. Miura, *ACS Omega* **2019**, *4*, 20690.

[68] J. Geng, G. Mantovani, L. Tao, J. Nicolas, G. Chen, R. Wallis, D. A. Mitchell, B. R. G. Johnson, S. D. Evans, D. M. Haddleton, *J. Am. Chem. Soc.* **2007**, *129*, 15156.

[69] V. Ladmiral, G. Mantovani, G. J. Clarkson, S. Cauet, J. L. Irwin, D. M. Haddleton, *J. Am. Chem. Soc.* **2006**, *128*, 4823.

[70] L. E. Strong, L. L. Kiessling, *J. Am. Chem. Soc.* **1999**, *121*, 6193.

[71] R. Auzély-Velty, M. Cristea, M. Rinaudo, *Biomacromolecules* **2002**, *3*, 998.

[72] M. Sánchez-Chaves, C. Ruiz, M. L. Cerrada, M. Fernández-García, *Polymer* **2008**, *49*, 2801.

[73] A. Muñoz-Bonilla, O. León, V. Bordegé, M. Sánchez-Chaves, M. Fernández-García, *J. Polym. Sci. A Polym. Chem.* **2013**, *51*, 1337.

[74] J. Chen, X. Gao, K. Hu, Z. Pang, J. Cai, J. Li, H. Wu, X. Jiang, *Biochem. Biophys. Res. Commun.* **2008**, *375*, 378.

[75] D. Appelhans, H. Komber, M. A. Quadir, S. Richter, S. Schwarz, J. van der Vlist, A. Aigner, M. Müller, K. Loos, J. Seidel et al., *Biomacromolecules* **2009**, *10*, 1114.

[76] S. Loykulnant, A. Hirao, *Macromolecules* **2000**, *33*, 4757.

[77] A. L. Chibac, T. Buruiana, V. Melinte, I. Mangalagiu, E. C. Buruiana, *RSC Adv.* **2015**, *5*, 90922.

[78] F. Suriano, R. Pratt, J. P. K. Tan, N. Wiradharma, A. Nelson, Y.-Y. Yang, P. Dubois, J. L. Hedrick, *Biomaterials* **2010**, *31*, 2637.

[79] N. Xu, R. Wang, F.-S. Du, Z.-C. Li, *J. Polym. Sci. A Polym. Chem.* **2009**, *47*, 3583.

[80] J. Cervin, A. Boucher, G. Youn, P. Björklund, V. Wallenius, L. Mottram, N. S. Sampson, U. Yrlid, *ACS Infect. Dis.* **2020**.

[81] L. G. Weaver, Y. Singh, P. L. Burn, J. T. Blanchfield, *RSC Adv.* **2016**, *6*, 31256.

[82] A. Adharis, D. Vesper, N. Koning, K. Loos, *Green Chem.* **2018**, *20*, 476.

[83] C. Weber, I. M. Sokolov, L. Schimansky-Geier, *Phys. Rev. E* **2012**, *85*.

[84] H. Namazi, F. Salimi, *Iran Polym. J.* **2011**, *20*, 77.

[85] M. Obata, R. Otobuchi, T. Kuroyanagi, M. Takahashi, S. Hirohara, *J. Polym. Sci. Part A: Polym. Chem.* **2017**, *55*, 395.

[86] R. Narain, S. P. Armes, *Chem. Commun.* **2002**, 2776.

[87] H. Park, R. R. Rosencrantz, L. Elling, A. Böker, *Macromol. Rapid Commun.* **2015**, *36*, 45.

[88] S. Chernyy, B. E. B. Jensen, K. Shimizu, M. Ceccato, S. U. Pedersen, A. N. Zelikin, K. Daasbjerg, J. Iruthayaraj, *J. Colloid Interface Sci.* **2013**, *404*, 207.

[89] Q. Liu, S. Jiang, B. Liu, Y. Yu, Z.-A. Zhao, C. Wang, Z. Liu, G. Chen, H. Chen, *ACS Macro Lett.* **2019**, *8*, 337.

[90] P. S. Omurtag Ozgen, S. Atasoy, B. Zengin Kurt, Z. Durmus, G. Yigit, A. Dag, *J. Mater. Chem. B* **2020**, *8*, 3123.

[91] G. Sureshkumar, S. Hotha, *Tetrahedron Lett.* **2007**, *48*, 6564.

[92] B. Graham, A. E. R. Fayter, J. E. Houston, R. C. Evans, M. I. Gibson, *J. Am. Chem. Soc.* **2018**, *140*, 5682.

[93] S. Slavin, J. Burns, D. M. Haddleton, C. R. Becer, *Eur. Polym. J.* **2011**, *47*, 435.

[94] T. Tanaka, H. Ishitani, Y. Miura, K. Oishi, T. Takahashi, T. Suzuki, S. Shoda, Y. Kimura, *ACS Macro Lett.* **2014**, *3*, 1074.

[95] A. L. Parry, N. A. Clemson, J. Ellis, S. S. R. Bernhard, B. G. Davis, N. R. Cameron, *J. Am. Chem. Soc.* **2013**, *135*, 9362.

[96] S. N. R. Kutcherlapati, R. Koyilapu, U. M. R. Boddu, D. Datta, R. S. Perali, M. J. Swamy, T. Jana, *Macromolecules* **2017**, *50*, 7309.

[97] Z. Ma, X. X. Zhu, *Mol. Pharm.* **2018**, *15*, 2348.

[98] P. Besenius, S. Slavin, F. Vilela, D. C. Sherrington, *React. Funct. Polym.* **2008**, *68*, 1524.

[99] Z. Wang, T. Luo, R. Sheng, H. Li, J. Sun, A. Cao, *Biomacromolecules* **2016**, *17*, 98.

[100] L. M. Stefan, A.-M. Pană, M.-C. Pascariu, E. Sisu, G. Bandur, L.-M. Rusnac, *Turk. J. Chem.* **2011**, 757.

[101] A. Adharis, K. Loos, *Method Enzymol.* **2019**, *627*, 215.

[102] A. P. P. Kröger, M. I. Komil, N. M. Hamelmann, A. Juan, M. H. Stenzel, J. M. J. Paulusse, *ACS Macro Lett.* **2019**, *8*, 95.

[103] M. Hoffmann, E. Gau, S. Braun, A. Pich, L. Elling, *Biomacromolecules* **2020**, *21*, 974.

[104] W. M. J. Kloosterman, D. Jovanovic, S. G. M. Brouwer, K. Loos, *Green Chem.* **2014**, *16*, 203.

[105] F.-W. Shen, K.-C. Zhou, H. Cai, Y.-N. Zhang, Y.-L. Zheng, J. Quan, *Colloid. Surf. B* **2019**, *173*, 504.

[106] M. R. Borges, R. Balaban, *Macromol. Symp.* **2007**, *258*, 25.

[107] P.-Y. Stergiou, A. Foukis, M. Filippou, M. Koukouritaki, M. Parapouli, L. G. Theodorou, E. Hatziloukas, A. Afendra, A. Pandey, E. M. Papamichael, *Biotechnol. Adv.* **2013**, *31*, 1846.

[108] M. Garcia, K. Kempe, D. M. Haddleton, A. Khan, A. Marsh, *J. Org. Chem.* **2015**, *6*, 1944.

[109] J. Li, Y. Zhang, C. Cai, X. Rong, M. Shao, J. Li, C. Yang, G. Yu, *Biomater. Sci.* **2020**, *8*, 189.

[110] V. A. Korzhikov, S. Diederichs, O. V. Nazarova, E. G. Vlakh, C. Kasper, E. F. Panarin, T. B. Tennikova, *J. Appl. Polym. Sci.* **2008**, *108*, 2386.

[111] R. Narain, S. P. Armes, *Biomacromolecules* **2003**, *4*, 1746.

[112] Z. Deng, S. Li, X. Jiang, R. Narain, *Macromolecules* **2009**, *42*, 6393.

[113] Z. Deng, M. Ahmed, R. Narain, *J. Polym. Sci. Part A: Polym. Chem.* **2009**, *47*, 614.

[114] A. Jans, R. R. Rosencrantz, A. D. Mandić, N. Anwar, S. Boesveld, C. Trautwein, M. Moeller, G. Sellge, L. Elling, A. J. C. Kuehne, *Biomacromolecules* **2017**, *18*, 1460.

[115] A. Tsuchida, K. Kobayashi, N. Matsubara, T. Muramatsu, T. Suzuki, Y. Suzuki, *Glycoconj. J.* **1998**, 1047.

[116] L. Soria-Martinez, S. Bauer, M. Giesler, S. Schelhaas, J. Materlik, K. Janus, P. Pierzyna, M. Becker, N. L. Snyder, L. Hartmann et al., *J. Am. Chem. Soc.* **2020**, *142*, 5252.

[117] T. J. Paul, A. K. Strzelczyk, M. I. Feldhof, S. Schmidt, *Biomacromolecules* **2020**, *21*, 2913.

[118] K. Bhattacharya, S. L. Banerjee, S. Das, S. Samanta, M. Mandal, N. K. Singha, *ACS Appl. Bio Mater.* **2019**, *2*, 2587.

[119] L. Zhang, J. Bernard, T. P. Davis, C. Barner-Kowollik, M. H. Stenzel, *Macromol. Rapid Commun.* **2008**, *29*, 123.

[120] M.-R. Xu, M. Shi, D. H. Bremner, K. Sun, H.-L. Nie, J. Quan, L.-M. Zhu, *Colloid. Surf. B* **2015**, *135*, 209.

[121] G. D. Yadav, P. A. Thorat, *J. Mol. Cat. B: Enzymatic* **2012**, *83*, 16.

[122] C. R. Strauss, R. W. Trainor, *Aust. J. Chem.* **1995**, *48*, 1665.

[123] H. J. Kitchen, S. R. Vallance, J. L. Kennedy, N. Tapia-Ruiz, L. Carassiti, A. Harrison, A. G. Whittaker, T. D. Drysdale, S. W. Kingman, D. H. Gregory, *Chem. Rev.* **2014**, *114*, 1170.

[124] P. Lidström, J. Tierney, B. Wathey, J. Westman, *Tetrahedron* **2001**, *57*, 9225.

[125] H. Katsuki, *J. Porous Mater.* **2001**, *8*, 5.

[126] C. O. Kappe, *Microwaves in organic and medicinal chemistry*, 2. Aufl., Wiley-VCH, Weinheim, **2012**.

[127] C. O. Kappe, *Angew. Chem. Int. Ed. Engl.* **2004**, *43*, 6250.

[128] C. O. Kappe, D. Dallinger, *Mol. Divers.* **2009**, *13*, 71.

[129] C. O. Kappe, D. Dallinger, *Nat. Rev. Drug Discov.* **2006**, *5*, 51.

[130] A. de La Hoz, A. Díaz-Ortiz, A. Moreno, *Chem. Soc. Rev.* **2005**, *34*, 164.

[131] Á. Díaz-Ortiz, P. Prieto, A. de La Hoz, *Chem. Rec.* **2019**, *19*, 85.

[132] A. Mishra, T. Vats, J. H. Clark, *Microwave-assisted polymerization*, Royal Society of Chemistry, Cambridge, **2016**.

[133] P. Priecel, J. A. Lopez-Sanchez, *ACS Sustainable Chem. Eng.* **2019**, *7*, 3.

[134] J. McMurry, *Organic chemistry. With biological applications*, 2. Aufl., Brooks/Cole Cengage Learning, Belmont, Calif., **2011**.

[135] L. M. Harwood, C. J. Moody, *Experimental organic chemistry. Principles and practice*, Blacwell Scientific Publications, Oxford, **1992**.

[136] M. Wilchek, I. Chaiken, *Methods Mol. Biol.* **2000**, *147*, 1.

[137] C. F. Poole, M.-L. Riekkola, P. R. Haddad, S. Fanali (Hrsg.) *Liquid chromatography. Volume 1: Fundamentals and instrumentation*, Elsevier, Amsterdam, Netherlands, **2017**.

[138] S. Borman, *Anal. Chem.* **1987**, *59*, 99A-99A.

[139] G. Eppert, G. J. Eppert (Hrsg.) *Einführung in die schnelle Flüssigchromatographie*, Vieweg, Braunschweig, **1988**.

[140] M. R. Siddiqui, Z. A. AlOthman, N. Rahman, *Arab. J. Chem.* **2017**, *10*, S1409-S1421.

[141] KNAUER Wissenschaftliche Geräte GmbH, "HPLC Principles and parameters", zu finden unter https://www.knauer.net/en/Systems-Solutions/Analytical-HPLC-UHPLC/HPLC-Basics---principles-and-parameters, **2022**.

[142] S. Aryal, *Sagar Aryal* **2022**.

[143] E. Rajakylä, *J. Chromatogr.* **1986**, 1.

[144] X. Yan in *Carbohydrate Analysis by Modern Liquid Phase Separation Techniques* (Hrsg.: Z. El Rassi), Elsevier Science & Technology, San Diego, **2021**, S. 631–644.

[145] Z. El Rassi (Hrsg.) *Carbohydrate Analysis by Modern Liquid Phase Separation Techniques*, Elsevier Science & Technology, San Diego, **2021**.

[146] P. K. Deb, S. F. Kokaz, S. N. Abed, A. Paradkar, R. K. Tekade in *Advances in Pharmaceutical Product Development and Research Ser* (Hrsg.: R. K. Tekade), Elsevier Science & Technology, San Diego, **2018**, S. 203–267.

[147] K. NAGY, K. VÉKEY in *Medical Applications of Mass Spectrometry* (Hrsg.: K. Vekey, A. Telekes, A. Vertes), Elsevier Science, Burlington, **2011**, S. 61–92.

[148] M. K. Singh, A. Singh in *The Textile Institute Book Ser* (Hrsg.: M. K. Singh), Elsevier Science & Technology, San Diego, **2022**, S. 321–339.

[149] P. T. Callaghan, *Principles of nuclear magnetic resonance microscopy*, 1. Aufl., Clarendon Press, Oxford, **2007**.

[150] "NMR Spectroscopy - Theory", zu finden unter https://teaching.shu.ac.uk/hwb/chemistry/tutorials/molspec/nmr1.htm, **2022**.

[151] R. K. Mishra, J. Cherusseri, A. Bishnoi, S. Thomas in *Micro and nano technologies, volume 2* (Hrsg.: S. Thomas, R. Thomas, A. K. Zachariah, R. K. Mishra), Elsevier, Amsterdam, Kidlington, Oxford, Cambridge, MA, **2017**, S. 369–415.

[152] H. Günther, *NMR Spectroscopy*. *Basic Principles, Concepts, and Applications in Chemistry*, 3. Aufl., Wiley-VCH, Weinheim, **2013**.

[153] *Nuclear magnetic resonance spectroscopy*, MDPI, Basel, Beijing, Wuhan, Barcelona, Belgrade, **2018**.

[154] R. B. Cole (Hrsg.) *A Wiley Interscience publication*, Wiley, New York, NY, **1997**.

[155] R. B. Cole (Hrsg.) *Electrospray and MALDI mass spectrometry*. *Fundamentals, instrumentation, practicalities, and biological applications*, Wiley, Hoboken, N.J, **2010**.

[156] M. S. Lee (Hrsg.) *Mass spectrometry handbook*, J. Wiley & Sons, Hoboken, N.J, **2012**.

[157] J. H. Gross, *Mass Spectrometry*. *A Textbook*, 3. Aufl., Springer, Cham, **2017**.

[158] H.-H. Perkampus, *UV-VIS Spectroscopy and Its Applications*, Springer Berlin / Heidelberg, Berlin, Heidelberg, **1992**.

[159] M. S. H. Akash, K. Rehman in *Springer eBook Collection* (Hrsg.: M. S. H. Akash, K. Rehman), Springer Singapore; Imprint Springer, Singapore, **2020**, S. 29–56.

[160] A. S. Franca, L. M. L. Nollet (Hrsg.) *Food analysis & properties*, CRC Press Taylor & Francis Group, Boca Raton, FL, **2017**.

[161] J. Stetefeld, S. A. McKenna, T. R. Patel, *Biophys. Rev.* **2016**, *8*, 409.

[162] R. Borsali, R. Pecora, *Soft matter characterization*, Springer, New York, NY, **2008**.

[163] W. I. Goldburg, *Am. J. Phys.* **1999**, *67*, 1152.

[164] J. S. J. Tang, K. Schade, L. Tepper, S. Chea, G. Ziegler, R. R. Rosencrantz, *Molecules* **2020**, *25*, 5121.

[165] J. S. J. Tang, S. Rosencrantz, L. Tepper, S. Chea, S. Klöpzig, A. Krüger-Genge, J. Storsberg, R. R. Rosencrantz, *Molecules* **2019**, *24*, 1865.

[166] S. Chea, K. T. Nguyen, R. R. Rosencrantz, *Molecules* **2022**, *27*.

[167] C. Reily, T. J. Stewart, M. B. Renfrow, J. Novak, *Nat. Rev. Nephrol.* **2019**, *15*, 346.

[168] S. Chea, K. Schade, S. Reinicke, R. Bleul, R. R. Rosencrantz, *Polym. Chem.* **2022**, *13*, 5058.

[169] L. Krasnova, C.-H. Wong, *Annu. Rev. Biochem.* **2016**, *85*, 599.

[170] H.-J. Gabius, *The Sugar Code*, 2. Aufl., John Wiley & Sons, Hoboken, **2011**.

[171] A. Varki, J. B. Lowe (Hrsg.) *Essentials of glycobiology*, Cold Spring Harbor Laboratory Press, Cold Spring Harbor, N.Y., **2009**.

[172] A. Varki, R. D. Cummings, J. D. Esko, P. Stanley, G. W. Hart, M. Aebi, Darvill, AG, T. Kinoshita, N. H. Packer, J. H. Prestegard et al. **2015**.

[173] W. van Breedam, S. Pöhlmann, H. W. Favoreel, R. J. de Groot, H. J. Nauwynck, *FEMS Microbiol. Rev.* **2014**, *38*, 598.

[174] F. S. Ielasi, M. Alioscha-Perez, D. Donohue, S. Claes, H. Sahli, D. Schols, R. G. Willaert, *mBio* **2016**, *7*.

[175] N. D. S. Rambaruth, M. V. Dwek, *Acta Histochemica* **2011**, *113*, 591.

[176] L. Möckl, *Front. Cell Dev. Biol.* **2020**, *8*, 253.

[177] A. Puri, S. Neelamegham, *Ann. Biomed. Eng.* **2012**, *40*, 816.

[178] P. Bojarová, R. R. Rosencrantz, L. Elling, V. Křen, *Chem. Soc. Rev.* **2013**, *42*, 4774.

[179] S. Wagner, D. Hauck, M. Hoffmann, R. Sommer, I. Joachim, R. Müller, A. Imberty, A. Varrot, A. Titz, *Angew. Chem. Int. Ed.* **2017**, *56*, 16559.

[180] A. H. Ebrahim, Z. Alalawi, L. Mirandola, R. Rakhshanda, S. Dahlbeck, D. Nguyen, M. Jenkins, F. Grizzi, E. Cobos, J. A. Figueroa et al., *Ann. Transl. Med.* **2014**, *2*, 88.

[181] S. Ng, E. Lin, P. I. Kitov, K. F. Tjhung, O. O. Gerlits, L. Deng, B. Kasper, A. Sood, B. M. Paschal, P. Zhang et al., *J. Am. Chem. Soc.* **2015**, *137*, 5248.

[182] Y. Luo, Y. Gu, R. Feng, J. Brash, A. M. Eissa, D. M. Haddleton, G. Chen, H. Chen, *Chem. Sci.* **2019**, *10*, 5251.

[183] C. von der Ehe, T. Buś, C. Weber, S. Stumpf, P. Bellstedt, M. Hartlieb, U. S. Schubert, M. Gottschaldt, *ACS Macro Lett.* **2016**, *5*, 326.

[184] M. Filipová, P. Bojarová, M. Rodrigues Tavares, L. Bumba, L. Elling, P. Chytil, K. Gunár, V. Křen, T. Etrych, O. Janoušková, *Biomacromolecules* **2020**, *21*, 3122.

[185] M. A. Brun, M. D. Disney, P. H. Seeberger, *ChemBioChem* **2006**, *7*, 421.

[186] T. M. Puvirajesinghe, J. E. Turnbull, *Microarrays* **2016**, *5*, 3.

[187] C. Pacholski, S. Rosencrantz, R. R. Rosencrantz, R. F. Balderas-Valadez, *Anal. Bioanal. Chem.* **2020**, *412*, 3433.

[188] C. Schulte-Osseili, M. Kleinert, N. Keil, R. R. Rosencrantz, *Biosensors* **2019**, *9*, 24.

[189] A. Barras, F. A. Martin, O. Bande, J.-S. Baumann, J.-M. Ghigo, R. Boukherroub, C. Beloin, A. Siriwardena, S. Szunerits, *Nanoscale* **2013**, *5*, 2307.

[190] V. Poonthiyil, P. T. Nagesh, M. Husain, V. B. Golovko, A. J. Fairbanks, *ChemistryOpen* **2015**, *4*, 708.

[191] K. G. Witten, C. Rech, T. Eckert, S. Charrak, W. Richtering, L. Elling, U. Simon, *Small* **2011**, *7*, 1954.

[192] S. Böcker, D. Laaf, L. Elling, *Biomolecules* **2015**, *5*, 1671.

[193] S. Böcker, L. Elling, *Bioengineering* **2017**, *4*, 31.

[194] S. Bhatia, M. Dimde, R. Haag, *Med. Chem. Commun.* **2014**, *5*, 862.

[195] P. Kiran, S. Kumari, J. Dernedde, R. Haag, S. Bhatia, *New J. Chem.* **2019**, *43*, 16012.

[196] R. T. Lee, Y. C. Lee, *Glycoconj. J.* **2000**, *17*, 543.

[197] V. Ginsburg (Hrsg.) *Methods in enzymology, Vol. 138,* Academic Press, Orlando, Fla., **1987**.

[198] A. Adharis, K. Loos, *Macromol. Chem. Phys.* **2019**, *220*, 1900219.

[199] Y. A. Kwase, M. Cochran, M. Nitz in *Modern Synthetic Methods in Carbohydrate Chemistry*, John Wiley & Sons, Ltd, **2013**, S. 67–96.

[200] S. Vidal (Hrsg.) *Protecting groups. Strategies and applications in carbohydrate chemistry*, Wiley-VCH Verlag GmbH & Co. KGaA, Weinheim, Germany, **2019**.

[201] S. Rosencrantz, J. S. J. Tang, C. Schulte-Osseili, A. Böker, R. R. Rosencrantz, *Macromol. Chem. Phys.* **2019**, *220*, 1900293.

[202] L. M. Likhosherstov, O. S. Novikova, V. A. Derevitskaja, N. K. Kochetkov, *Carbohydr. Res.* **1986**, *146*, C1-C5.

[203] L. M. Likhosherstov, O. S. Novikova, V. N. Shibaev, *Dokl. Chem.* **2002**, *383*, 89.

[204] L. M. Likhosherstov, *Dokl. Chem.* **2003**, *389*, 73.

[205] L. M. Likhosherstov, O. S. Novikova, A. O. Zheltova, V. N. Shibaev, *Russ. Chem. Bull.* **2004**, *53*, 709.

[206] M. Bejugam, S. L. Flitsch, *Org. Lett.* **2004**, *6*, 4001.

[207] B. Dejaegher, Y. V. Heyden, *J. Pharm. Biomed.* **2011**, *56*, 141.

[208] D. C. Montgomery, *Design and analysis of experiments*, 6. Aufl., Wiley, New York, **2005**.

[209] F. Yates, *The design and analysis of factorial experiments*, Imperial Bureau of Soil Science, Harpenden, **1937**.

[210] H. Tye, *Drug Discov. Today* **2004**, *9*, 485.

[211] D. W. Lendrem, B. C. Lendrem, D. Woods, R. Rowland-Jones, M. Burke, M. Chatfield, J. D. Isaacs, M. R. Owen, *Drug Discov. Today* **2015**, *20*, 1365.

[212] R. Leardi, *Anal. Chim. Acta* **2009**, *652*, 161.

[213] G. D. Bowden, B. J. Pichler, A. Maurer, *Sci. Rep.* **2019**, *9*, 11370.

[214] P. M. Murray, F. Bellany, L. Benhamou, D.-K. Bučar, A. B. Tabor, T. D. Sheppard, *Org. Biomol. Chem.* **2016**, *14*, 2373.

[215] H. Tye, M. Whittaker, *Org. Biomol. Chem.* **2004**, *2*, 813.

[216] Z. Liu, Y. Zhu, P. Gao, Z. Zhang, *Int. J. Appl. Ceram. Technol.* **2020**, *17*, 1231.

[217] S. Hemmati, D. P. Barkey, *ECS J. Solid State Sci. Technol.* **2017**, *6*, P132-P137.

[218] M. R. Karim, M. Ferrandon, S. Medina, E. Sture, N. Kariuki, D. J. Myers, E. F. Holby, P. Zelenay, T. Ahmed, *ACS Appl. Energy Mater.* **2020**, *3*, 9083.

[219] A. Ghadban, L. Albertin, R. W. Moussavou Mounguengui, A. Peruchon, A. Heyraud, *Carbohydr. Res.* **2011**, *346*, 2384.

[220] S. A. Chambers, S. D. Townsend, *Carbohydr. Res.* **2020**, *488*, 107895.

[221] D. Vetter, M. A. Gallop, *Bioconjugate Chem.* **1995**, *6*, 316.

[222] A. Ghadban, L. Albertin, E. Condamine, R. W. M. Mounguengui, A. Heyraud, *Can. J. Chem.* **2011**, *89*, 987.

[223] C. P. R. Hackenberger, M. K. O'Reilly, B. Imperiali, *J. Org. Chem.* **2005**, *70*, 3574.

[224] X. Liu, G. Zhang, K. Chan, J. Li, *Chem. Commun.* **2010**, *46*, 7424.

[225] J. Poole, C. J. Day, M. von Itzstein, J. C. Paton, M. P. Jennings, *Nat. Rev. Microbiol.* **2018**, *16*, 440.

[226] K. Moonens, H. Remaut, *Curr. Opin. Struct.* **2017**, *44*, 48.

[227] A. A. Kulkarni, C. Fuller, H. Korman, A. A. Weiss, S. S. Iyer, *Bioconjugate Chem.* **2010**, *21*, 1486.

[228] L. E. Hartley-Tassell, M. M. Awad, K. L. Seib, M. Scarselli, S. Savino, J. Tiralongo, D. Lyras, C. J. Day, M. P. Jennings, *Infect. Immun.* **2019**, *87*.

[229] T. Dingle, S. Wee, G. L. Mulvey, A. Greco, E. N. Kitova, J. Sun, S. Lin, J. S. Klassen, M. M. Palcic, K. K. S. Ng et al., *Glycobiology* **2008**, *18*, 698.

[230] W. B. Turnbull, B. L. Precious, S. W. Homans, *J. Am. Chem. Soc.* **2004**, *126*, 1047.

[231] B. Ernst, J. L. Magnani, *Nat. Rev. Drug Discov.* **2009**, *8*, 661.

[232] Q. Zhang, L. Su, J. Collins, G. Chen, R. Wallis, D. A. Mitchell, D. M. Haddleton, C. R. Becer, *J. Am. Chem. Soc.* **2014**, *136*, 4325.

[233] S. G. Spain, N. R. Cameron, *Polym. Chem.* **2011**, *2*, 60.

[234] Y. C. Lee, G. S. Johnson, B. White, J. Scocca, *Anal. Biochem.* **1971**, *43*, 640.

[235] Y. C. Lee, R. T. Lee, *Acc. Chem. Res.* **1995**, *28*, 321.

[236] C. R. Becer, *Macromol. Rapid Commun.* **2012**, *33*, 742.

[237] H. Schlaad (Hrsg.) *SpringerLink Bücher*, *Vol. 253*, Springer, Berlin, Heidelberg, **2013**.

[238] C. von der Ehe, C. Weber, M. Gottschaldt, U. S. Schubert, *Prog. Polym. Sci.* **2016**, *57*, 64.

[239] R. R. Rosencrantz, V. H. Nguyen, H. Park, C. Schulte, A. Böker, U. Schnakenberg, L. Elling, *Anal. Bioanal. Chem.* **2016**, *408*, 5633.

[240] J. Lazar, R. R. Rosencrantz, L. Elling, U. Schnakenberg, *Anal. Chem.* **2016**, *88*, 9590.

[241] J. Lazar, H. Park, R. R. Rosencrantz, A. Böker, L. Elling, U. Schnakenberg, *Macromol. Rapid Commun.* **2015**, *36*, 1472.

[242] X. Yan, A. Sivignon, N. Yamakawa, A. Crepet, C. Travelet, R. Borsali, T. Dumych, Z. Li, R. Bilyy, D. Deniaud et al., *Biomacromolecules* **2015**, *16*, 1827.

[243] E. Arias, M. T. Méndez, E. Arias, I. Moggio, A. Ledezma, J. Romero, G. Margheri, E. Giorgetti, *Sensors* **2017**, *17*, 1025.

[244] F. Jacobi, A. La Camaleño de Calle, S. Boden, A. Grafmüller, L. Hartmann, S. Schmidt, *Biomacromolecules* **2018**, *19*, 3479.

[245] A. Jans, R. R. Rosencrantz, A. D. Mandić, N. Anwar, S. Boesveld, C. Trautwein, M. Moeller, G. Sellge, L. Elling, A. J. C. Kuehne, *Biomacromolecules* **2017**, *18*, 1460.

[246] B. R. Saunders, N. Laajam, E. Daly, S. Teow, X. Hu, R. Stepto, *Adv. Colloid Interface Sci.* **2009**, *147-148*, 251.

[247] F. A. Plamper, W. Richtering, *Acc. Chem. Res.* **2017**, *50*, 131.

[248] Y. Guan, Y. Zhang, *Soft Matter* **2011**, *7*, 6375.

[249] R. Pelton, *J. Colloid Interface Sci.* **2010**, *348*, 673.

[250] L. H. Lima, Y. Morales, T. Cabral, *J. Ophthalmol.* **2016**, *2016*, 5356371.

[251] M. A. Cooperstein, H. E. Canavan, *Biointerphases* **2013**, *8*, 19.

[252] M. A. Cooperstein, P. A. H. Nguyen, H. E. Canavan, *Biointerphases* **2017**, *12*, 02C401.

[253] V. Aloush, S. Navon-Venezia, Y. Seigman-Igra, S. Cabili, Y. Carmeli, *Antimicrob. Agents Chemother.* **2006**, *50*, 43.

[254] A. Imberty, M. Wimmerová, E. P. Mitchell, N. Gilboa-Garber, *Microbes and Infection* **2004**, *6*, 221.

[255] C. Chemani, A. Imberty, S. de Bentzmann, M. Pierre, M. Wimmerová, B. P. Guery, K. Faure, *Infect. Immun.* **2009**, *77*, 2065.

[256] S. Weichert, S. Jennewein, E. Hüfner, C. Weiss, J. Borkowski, J. Putze, H. Schroten, *Nutr. Res.* **2013**, *33*, 831.

[257] Grishin A.V., Krivozubov M.S., Karyagina A.S., Gintsburg A.L., G. A.V., K. M.S., K. A.S., G. A.L., *Acta Naturae (англоязычная версия)* **2015**, *7*, 29.

[258] R. Sommer, S. Wagner, K. Rox, A. Varrot, D. Hauck, E.-C. Wamhoff, J. Schreiber, T. Ryckmans, T. Brunner, C. Rademacher et al., *J. Am. Chem. Soc.* **2018**, *140*, 2537.

[259] A. Angeli, M. Li, L. Dupin, G. Vergoten, M. Noël, M. Madaoui, S. Wang, A. Meyer, T. Géhin, S. Vidal et al., *ChemBioChem* **2017**, *18*, 1036.

[260] N. Berthet, B. Thomas, I. Bossu, E. Dufour, E. Gillon, J. Garcia, N. Spinelli, A. Imberty, P. Dumy, O. Renaudet, *Bioconjugate Chem.* **2013**, *24*, 1598.

[261] K. S. Bücher, N. Babic, T. Freichel, F. Kovacic, L. Hartmann, *Macromol. Biosci.* **2018**, *18*, e1800337.

[262] E. M. V. Johansson, S. A. Crusz, E. Kolomiets, L. Buts, R. U. Kadam, M. Cacciarini, K.-M. Bartels, S. P. Diggle, M. Cámara, P. Williams et al., *Chem. Biol.* **2008**, *15*, 1249.

[263] G. Michaud, R. Visini, M. Bergmann, G. Salerno, R. Bosco, E. Gillon, B. Richichi, C. Nativi, A. Imberty, A. Stocker et al., *Chem. Sci.* **2016**, *7*, 166.

[264] B. Blanchard, A. Imberty, A. Varrot, *Proteins: Struct. Funct. Genet.* **2014**, *82*, 1060.

[265] N. Gilboa-Garber, D. J. Katcoff, N. C. Garber, *FEMS Immunol. Med. Microbiol.* **2000**, *29*, 53.

[266] N. Garber, U. Guempel, N. Gilboa-Garber, R. J. Royle, *FEMS Microbiol. Lett.* **1987**, *48*, 331.

[267] K. von Nessen, M. Karg, T. Hellweg, *Polymer* **2013**, *54*, 5499.

[268] M. Rey, X. Hou, J. S. J. Tang, N. Vogel, *Soft Matter* **2017**, *13*, 8717.

[269] Y. BOURNE, C. H. ASTOUL, V. ZAMBONI, W. J. PEUMANS, L. MENU-BOUAOUICHE, E. J. M. van Damme, A. BARRE, P. ROUGÉ, *Biochem. J.* **2002**, *364*, 173.

[270] A. M. Wu, J. H. Wu, M.-S. Tsai, Z. Yang, N. Sharon, A. Herp, *Glycoconj. J.* **2007**, *24*, 591.

[271] H. J. Allen, E. A. Johnson, K. L. Matta, *Immunol. Commun.* **1977**, *6*, 585.

[272] E. Miceli, B. Kuropka, C. Rosenauer, E. R. Osorio Blanco, L. E. Theune, M. Kar, C. Weise, S. Morsbach, C. Freund, M. Calderón, *Nanomedicine* **2018**, *13*, 2657.

[273] K. Kratz, A. Lapp, W. Eimer, T. Hellweg, *Colloids Surf. A Physicochem. Eng. Asp.* **2002**, *197*, 55.

[274] E. Ruffet, N. Paquet, S. Frutiger, G. J. Hughes, J. C. Jaton, *Biochem. J.* **1992**, *286 (Pt 1)*, 131.

[275] R. Sankaranarayanan, K. Sekar, R. Banerjee, V. Sharma, A. Surolia, M. Vijayan, *Nat. Struct. Mol. Biol.* **1996**, *3*, 596.

[276] B. Ma, J. L. Simala-Grant, D. E. Taylor, *Glycobiology* **2006**, *16*, 158R-184R.

[277] J. M. Meyer, A. Neely, A. Stintzi, C. Georges, I. A. Holder, *Infect. Immun.* **1996**, *64*, 518.

[278] D. Kang, D. R. Kirienko, P. Webster, A. L. Fisher, N. V. Kirienko, *Virulence* **2018**, *9*, 804.

[279] I. L. Lamont, P. A. Beare, U. Ochsner, A. I. Vasil, M. L. Vasil, *Proc. Natl. Acad. Sci. U S A* **2002**, *99*, 7072.

[280] T. Masuko, A. Minami, N. Iwasaki, T. Majima, S.-I. Nishimura, Y. C. Lee, *Anal. Biochem.* **2005**, *339*, 69.

[281] Y. van Kooyk, G. A. Rabinovich, *Nat. Immunol.* **2008**, *9*, 593.

[282] M. E. Taylor, K. Drickamer, *Curr. Opin. Cell Biol.* **2007**, *19*, 572.

[283] B. E. Collins, J. C. Paulson, *Curr. Opin. Chem. Biol.* **2004**, *8*, 617.

[284] G. A. Rabinovich, M. A. Toscano, *Nat. Rev. Immunol.* **2009**, *9*, 338.

[285] R. C. Davicino, R. J. Eliçabe, M. S. Di Genaro, G. A. Rabinovich, *Int. Immunopharmacol.* **2011**, *11*, 1457.

[286] J. J. Lundquist, E. J. Toone, *Chem. Rev.* **2002**, *102*, 555.

[287] V. Ladmiral, E. Melia, D. M. Haddleton, *Eur. Polym. J.* **2004**, *40*, 431.

[288] S. M. Dimick, S. C. Powell, S. A. McMahon, D. N. Moothoo, J. H. Naismith, E. J. Toone, *J. Am. Chem. Soc.* **1999**, *121*, 10286.

[289] R. T. Lee, Y. C. Lee, *Glycoconj. J.* **2000**, *17*, 543.

[290] T. Fujita, *Nat. Rev. Immunol.* **2002**, *2*, 346.

[291] M. Hartmann, T. K. Lindhorst, *Eur. J. Org. Chem.* **2011**, *2011*, 3583.

[292] G. Hester, C. S. Wright, *J. Mol. Biol.* **1996**, *262*, 516.

[293] K. Kawai, S. Terada, O. Yokota, D. Fujita, H. Ishizu, S. Kuroda, *Virchows Arch.* **2002**, *441*, 584.

[294] F. P. Schwarz, K. D. Puri, R. G. Bhat, A. Surolia, *J. Biol. Chem.* **1993**, *268*, 7668.

[295] M. Mammen, S.-K. Choi, G. M. Whitesides, *Angew. Chem. Int. Ed.* **1998**, *37*, 2754.

[296] S. N. Raju Kutcherlapati, N. Yeole, M. R. Gadi, R. S. Perali, T. Jana, *Polym. Chem.* **2017**, *8*, 1371.

[297] L. Albertin, M. H. Stenzel, C. Barner-Kowollik, L. J. R. Foster, T. P. Davis, *Macromolecules* **2004**, *37*, 7530.

[298] D.-W. Park, S. Haam, I.-S. Ahn, T. G. Lee, H.-S. Kim, W.-S. Kim, *J. Biotechnol.* **2004**, *107*, 151.

[299] A. M. Granville, D. Quémener, T. P. Davis, C. Barner-Kowollik, M. H. Stenzel, *Macromol. Symp.* **2007**, *255*, 81.

[300] A. Bianchi, A. Bernardi, *J. Org. Chem.* **2006**, *71*, 4565.

[301] F. Nisic, A. Bernardi, *Carbohydr. Res.* **2008**, *343*, 1636.

[302] Q. Li, Z. Li, *Acc. Chem. Res.* **2020**, *53*, 962.

[303] N. V. Medhekar, A. Ramasubramaniam, R. S. Ruoff, V. B. Shenoy, *ACS Nano* **2010**, *4*, 2300.

[304] F. Jiang, S. Cui, N. Song, L. Shi, P. Ding, *ACS Appl. Mater. Interfaces* **2018**, *10*, 16812.

[305] Y. Feng, L. B. Luo, J. Huang, K. Li, B. Li, H. Wang, X. Liu, *J. Appl. Polym. Sci.* **2016**, *133*, 1.

[306] R. McHale, R. K. O'Reilly, *Macromolecules* **2012**, *45*, 7665.

[307] J.-F. Lutz, A. F. Thünemann, K. Rurack, *Macromolecules* **2005**, *38*, 8124.

[308] O. Moukha-chafiq, R. C. Reynolds, J. C. Wilson, T. S. Snowden, *ACS Comb. Sci.* **2019**, *21*, 628.

[309] M. Dyba, B. da Silva, H. Coia, Y. Hou, S. Noguchi, J. Pan, D. Berry, K. Creswell, J. Krzeminski, D. Desai et al., *Chem. Res. Toxicol.* **2018**, *31*, 772.

[310] L. P. Conway, R. J. Delley, J. Neville, G. R. Freeman, H. J. Maple, V. Chan, A. J. Hall, D. R. W. Hodgson, *RSC Adv.* **2014**, *4*, 38663.

[311] J. García, S. Fernández, M. Ferrero, Y. S. Sanghvi, V. Gotor, *Tetrahedron Lett.* **2004**, *45*, 1709.

[312] C. Ortiz, M. L. Ferreira, O. Barbosa, J. C. S. dos Santos, R. C. Rodrigues, Á. Berenguer-Murcia, L. E. Briand, R. Fernandez-Lafuente, *Catal. Sci. Technol.* **2019**, *9*, 2380.

[313] P. Choudhury, B. Bhunia, *Biopharm J.* **2015**, *1*, 41.

[314] N. N. Gandhi, *J. Am. Oil Chem. Soc.* **1997**, *74*, 621.

[315] A. Marsh, A. Khan, D. M. Haddleton, M. J. Hannon, *Macromolecules* **1999**, *32*, 8725.

[316] E. Calce, V. Bugatti, V. Vittoria, S. de Luca, *Molecules* **2012**, *17*, 12234.

[317] M. Schmidlehner, P.-S. Kuhn, C. M. Hackl, A. Roller, W. Kandioller, B. K. Keppler, *J. Organ. Chem.* **2014**, *772-773*, 93.

[318] H. M. A. Hassan, V. Abdelsayed, A. E. R. S. Khder, K. M. AbouZeid, J. Terner, M. S. El-Shall, S. I. Al-Resayes, A. A. El-Azhary, *J. Mater. Chem.* **2009**, *19*, 3832.

[319] S. L. Pedersen, A. P. Tofteng, L. Malik, K. J. Jensen, *Chem. Soc. Rev.* **2012**, *41*, 1826.

[320] A. Kokel, C. Schäfer, B. Török, *Green Chem.* **2017**, *19*, 3729.

[321] F. Wiesbrock, R. Hoogenboom, U. S. Schubert, *Macromol. Rapid Commun.* **2004**, *25*, 1739.

[322] A. Pellis, G. M. Guebitz, T. J. Farmer, *Molecules* **2016**, *21*, 1245.

[323] A. Delavault, K. Ochs, O. Gorte, C. Syldatk, E. Durand, K. Ochsenreither, *Molecules* **2021**, *26*, 470.

[324] M. Henze, D. Merker, L. Elling, *Int. J. Mol. Sci.* **2016**, *17*, 210.

[325] M. Gelo-Pujic, E. Guibé-Jampel, A. Loupy, S. A. Galema, D. Mathé, *J. Chem. Soc., Perkin Trans. 1* **1996**, 2777.

[326] G.-T. Jeong, K.-Y. Byun, W.-T. Lee, H.-W. Ryu, C. Sunwoo, H.-S. Kim, D.-H. Park, *Biochem. Eng. J.* **2006**, *29*, 69.

[327] M. Garcia, K. Kempe, D. M. Haddleton, A. Khan, A. Marsh, *Polym. Chem.* **2015**, *6*, 1944.

[328] A. R. M. Yahya, W. A. Anderson, M. Moo-Young, *Enzyme Microb. Technol.* **1998**, *23*, 438.

[329] X.-F. Li, M.-H. Zong, G.-L. Zhao, Y.-G. Yu, H. Wu, *Biotechnol. Bioproc. E.* **2010**, *15*, 608.

[330] S. Ogawa, A. Endo, N. Kitahara, T. Yamagishi, S. Aoyagi, S. Hara, *Carbohydr. Res.* **2019**, *482*, 107739.

[331] V. Athawale, N. Manjrekar, M. Athawale, *Tetrahedron Lett.* **2002**, *43*, 4797.

[332] M. Sayed, Y. Gaber, A. Bornadel, S.-H. Pyo, *Biotechnol. Prog.* **2016**, *32*, 83.

[333] J. E. Puskas, C. K. Chiang, M. Y. Sen, *Green Polymerization Methods: Renewable Starting Materials, Catalysis and Waste Reduction*. *Green Cationic Polymerizations and Polymer Functionalization for Biotechnology*, Wiley-VCH Verlag, Weinheim Germany, **2011**.

[334] M. P. Mingos, D. R. Baghurst, *Chem. Soc. Rev.* **1991**, 1.

[335] G. D. Yadav, I. V. Borkar, *Ind. Eng. Chem. Res.* **2009**, *48*, 7915.

[336] R. Sharma, *Enzyme Inhibition and bioapplications* **2012**, 3.

[337] C. S. Sarap, P. Partovi-Azar, M. Fyta, *ACS Appl. Bio Mater.* **2018**, *1*, 59.

[338] P. Song, Z. Xu, Q. Guo, *ACS Macro Lett.* **2013**, *2*, 1100.

[339] M. Meot-Ner, *Chem. Rev.* **2005**, *105*, 213.

[340] S. Sivakova, S. J. Rowan, *Chem. Sci.* **2005**, *34*, 9.

[341] H. Yang, W. Xi, *Polymers* **2017**, *9*.

[342] H.-W. Yang, A.-W. Lee, C.-H. Huang, J.-K. Chen, *Soft Matter* **2014**, *10*, 8330.

[343] J. Li, Z. Wang, Z. Hua, C. Tang, *J. Mater. Chem. B* **2020**, *8*, 1576.

[344] M. Garcia, M. P. Beecham, K. Kempe, D. M. Haddleton, A. Khan, A. Marsh, *Eur. Polym. J.* **2015**, *66*, 444.

[345] H. J. Spijker, A. J. Dirks, J. C. M. van Hest, *J. Polym. Sci. Part A: Polym. Chem.* **2006**, *44*, 4242.

[346] P. Amo-Ochoa, F. Zamora, *Coord. Chem. Rev.* **2014**, *276*, 34.

[347] M. Wang, B. Choi, X. Wei, A. Feng, S. H. Thang, *Polym. Chem.* **2018**, *9*, 5086.

[348] G. Moad, Y. K. Chong, A. Postma, E. Rizzardo, S. H. Thang, *Polymer* **2005**, *46*, 8458.

[349] Y. Kang, A. Lu, A. Ellington, M. C. Jewett, R. K. O'Reilly, *ACS Macro Lett.* **2013**, *2*, 581.

[350] Y. Kang, A. Pitto-Barry, H. Willcock, W.-D. Quan, N. Kirby, A. M. Sanchez, R. K. O'Reilly, *Polym. Chem.* **2015**, *6*, 106.

[351] J. Ulbricht, R. Jordan, R. Luxenhofer, *Biomaterials* **2014**, *35*, 4848.

[352] T. T. Hoang Thi, E. H. Pilkington, D. H. Nguyen, J. S. Lee, K. D. Park, N. P. Truong, *Polymers* **2020**, *12*.

[353] M. Talelli, C. J. F. Rijcken, C. F. van Nostrum, G. Storm, W. E. Hennink, *Adv. Drug Deliv. Rev.* **2010**, *62*, 231.

[354] B. S. Tucker, B. S. Sumerlin, *Polym. Chem.* **2014**, *5*, 1566.

[355] J. B. Epp, T. S. Widlanski, *J. Org. Chem.* **1999**, *64*, 293.

[356] K. Ulbrich, V. Šubr, J. Strohalm, D. Plocová, M. Jelínková, B. Říhová, *J. Control. Release* **2000**, *64*, 63.

[357] S. Perrier, *Macromolecules* **2017**, *50*, 7433.

[358] K. Zhang, M. Aiba, G. B. Fahs, A. G. Hudson, W. D. Chiang, R. B. Moore, M. Ueda, T. E. Long, *Polym. Chem.* **2015**, *6*, 2434.

[359] K. Zhang, S. J. Talley, Y. P. Yu, R. B. Moore, M. Murayama, T. E. Long, *Chem. Commun.* **2016**, *52*, 7564.

[360] K. Hatanaka, H. Takeshige, T. Akaike, *J. Carbohyd. Chem.* **1994**, *13*, 603.

[361] X. Pan, F. Zhang, B. Choi, Y. Luo, X. Guo, A. Feng, S. H. Thang, *Eur. Polym. J.* **2019**, *115*, 166.

[362] M. Sponchioni, L. Morosi, M. Lupi, U. Capasso Palmiero, *RSC Adv.* **2017**, *7*, 50981.

[363] I. Lacík, A. Chovancová, L. Uhelská, C. Preusser, R. A. Hutchinson, M. Buback, *Macromolecules* **2016**, *49*, 3244.

[364] L. Peng, Y. Luo, Y. Zheng, W. Zhang, G. Chen, *ACS Appl. Nano Mater.* **2018**, *1*, 2219.

[365] X. Li, M. Bao, Y. Weng, K. Yang, W. Zhang, G. Chen, *J. Mater. Chem. B* **2014**, *2*, 5569.

[366] I. J. Goldstein, C. E. Hollermann, E. E. Smith, *Biochemistry* **1965**, *4*.

[367] Y. Chen, W. Wang, Di Wu, M. Nagao, D. G. Hall, T. Thundat, R. Narain, *Biomacromolecules* **2018**, *19*, 596.

[368] M. Ahmed, R. Narain, *Biomaterials* **2011**, *32*, 5279.

[369] X. Jiang, M. Ahmed, Z. Deng, R. Narain, *Bioconjugate Chem.* **2009**, *20*, 994.

[370] J. S. J. Tang, A. D. Smaczniak, L. Tepper, S. Rosencrantz, M. Aleksanyan, L. Dähne, R. R. Rosencrantz, *Macromol. Biosci.* **2022**, *22*, 2100461.

[371] P. Singhsa, D. Diaz-Dussan, H. Manuspiya, R. Narain, *Biomacromolecules* **2018**, *19*, 209.

[372] J. P. Lorand, J. O. Edwards, *J. Org. Chem.* **1959**.

[373] J. Wang, W. Qi, G. Chen, *Chin. Chem. Lett.* **2019**, *30*, 587.

[374] M. Grymel, G. Pastuch-Gawołek, A. Lalik, M. Zawojak, S. Boczek, M. Krawczyk, K. Erfurt, *Molecules* **2020**, *25*.

[375] L. M. Likhosherstov, O. S. Novikova, V. N. Shibaev, *Dokl. Chem.* **2002**, *383*, 89.

[376] M. A. Brun, M. D. Disney, P. H. Seeberger, *Chembiochem* **2006**, *7*, 421.

[377] J. Li, S. Zacharek, X. Chen, J. Wang, W. Zhang, A. Janczuk, P. G. Wang, *Bioorg. Med. Chem.* **1999**, *7*, 1549.

[378] K. Yu, J. N. Kizhakkedathu, *Biomacromolecules* **2010**, *11*, 3073.

[379] J. Geng, J. Lindqvist, G. Mantovani, G. Chen, C. T. Sayers, G. J. Clarkson, D. M. Haddleton, *QSAR Comb. Sci.* **2007**, *26*, 1220.

[380] H. Charville, J. Jin, C. W. Evans, M. A. Brimble, D. E. Williams, *RSC Adv.* **2013**, *3*, 15435.

[381] V. Percec, P. Leowanawat, H.-J. Sun, O. Kulikov, C. D. Nusbaum, T. M. Tran, A. Bertin, D. A. Wilson, M. Peterca, S. Zhang et al., *J. Am. Chem. Soc.* **2013**, *135*, 9055.

[382] B. Kang, P. Okwieka, S. Schöttler, S. Winzen, J. Langhanki, K. Mohr, T. Opatz, V. Mailänder, K. Landfester, F. R. Wurm, *Angew. Chem. Int. Ed.* **2015**, *54*, 7436.

[383] R. Wodtke, J. König, A. Pigorsch, M. Köckerling, C. Mamat, *Dyes Pigm.* **2015**, *113*, 263.

[384] J. Garcia Lopez, E. V. Piletska, M. J. Whitcombe, J. Czulak, S. A. Piletsky, *Chem. Commun.* **2019**, *55*, 2664.

[385] C. A. Flemming, J. T. Trevors, *Water Air Soil Pollut.* **1989**, *44*, 143.

[386] Z. L. Harris, J. D. Gitlin, *Am. J. Clin. Nutr.* **1996**, *63*, 836S-41S.

[387] Z. Deng, H. Bouchékif, K. Babooram, A. Housni, N. Choytun, R. Narain, *J. Polym. Sci. Part A: Polym. Chem.* **2008**, *46*, 4984.

[388] P. K. Das, D. N. Dean, A. L. Fogel, F. Liu, B. A. Abel, C. L. McCormick, E. Kharlampieva, V. Rangachari, S. E. Morgan, *Biomacromolecules* **2017**, *18*, 3359.

[389] L. Albertin, M. H. Stenzel, C. Barner-Kowollik, L. J. R. Foster, T. P. Davis, *Macromolecules* **2005**, *38*, 9075.

[390] J. Seuring, S. Agarwal, *ACS Macro Lett.* **2013**, *2*, 597.

[391] A. Bordat, T. Boissenot, J. Nicolas, N. Tsapis, *Adv. Drug Deliv. Rev.* **2019**, *138*, 167.

[392] J. Niskanen, H. Tenhu, *Polym. Chem.* **2017**, *8*, 220.

[393] K. K. Bansal, P. K. Upadhyay, G. K. Saraogi, A. Rosling, J. M. Rosenholm, *Express Polym. Lett.* **2019**, *13*, 974.

16 Appendix

16.1 Supporting Information to Chapter 7: Optimization of the Microwave Assisted Glycosylamines Synthesis Based on a Statistical Design of Experiments Approach

1-Amino-1-deoxy-β-D-N-acetylgalactoside (**Am-I-01**). ^{1}H-NMR (D_2O, 400 MHz): δ 5.21 (d, *J* = 3.6 Hz, 0.04H α-H1 (starting material)), 4.60 (d, *J* = 7.6 Hz, 0.05 H, β-H1 (starting material)), 4.30-3.51 (m, 6 H), 4.06 (d, *J* = 9.2 Hz, 0.64 β-H1), 2.03 (s, 3 H); ESI MS, calcd. for $C_8H_{16}N_2O_5$: $[M + H]^+$ 221.11, found 221.45 $[M + H]^+$.

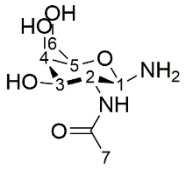

Am-I

1-Amino-1-deoxy-β-D-lactoside (**Am-II-01**). ^{1}H-NMR (D_2O, 400 MHz): δ 5.21 (d, *J* = 3.6 Hz, 0.05 H, α-H1 (starting material)), 4.65 (d, *J* = 8.0 Hz, 0.06 H, β-H1 (starting material)), 4.43 (d, *J* = 7.8 Hz, 1 H, β-H7), 4.10 (d, *J* = 8.8 Hz, 0.84 H, β-H1), 3.97-3.48 (m, 11 H), 3.19 (m, 0.82 H); ESI MS, calcd. for $C_{12}H_{24}NO_{10}$: $[M + H]^+$ 342.14, found 342.46 $[M + H]^+$.

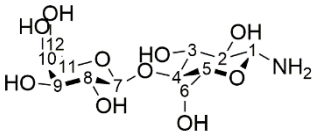

Am-II

1-Amino-1-deoxy-β-D-glucopyranuronoside (**Am-III**). ^{1}H-NMR (D_2O, 400 MHz): δ 5.24 (d, *J* = 3.7 Hz,4 H, α-H1 (starting material)), 4.64 (d, *J* = 7.9 Hz, β-H1 (starting material), 4.09 (d, *J* = 8.8 Hz, 0.82 H, β-H1), 3.12-4.34 (m, 4 H); ESI MS, calcd. for $C_6H_{12}NO_6$: $[M + H]^+$ 194.07, found 194.43 $[M + H]^+$.

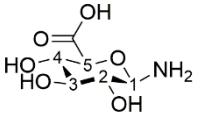

Am-III

1-Amino-1-deoxy-β-L-fucose (**Am-IV**). ^{1}H-NMR (D_2O, 400 MHz): δ 4.15-4.03 (m, 0.26 H), 3.99 (d, *J* = 8.8 Hz, 0.70 H, β-H1), 3.36-3.94 (m, 3.20 H), 3.32 (t, *J* = 8.8 Hz, 0.58 H) 1.20 (d, *J* = 6.4 Hz, 3 H); ESI MS, calcd. for $C_6H_{14}NO_4$: $[M + H]^+$ 164.09, found 164.38 $[M + H]^+$.

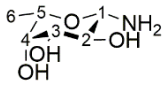

Am-IV

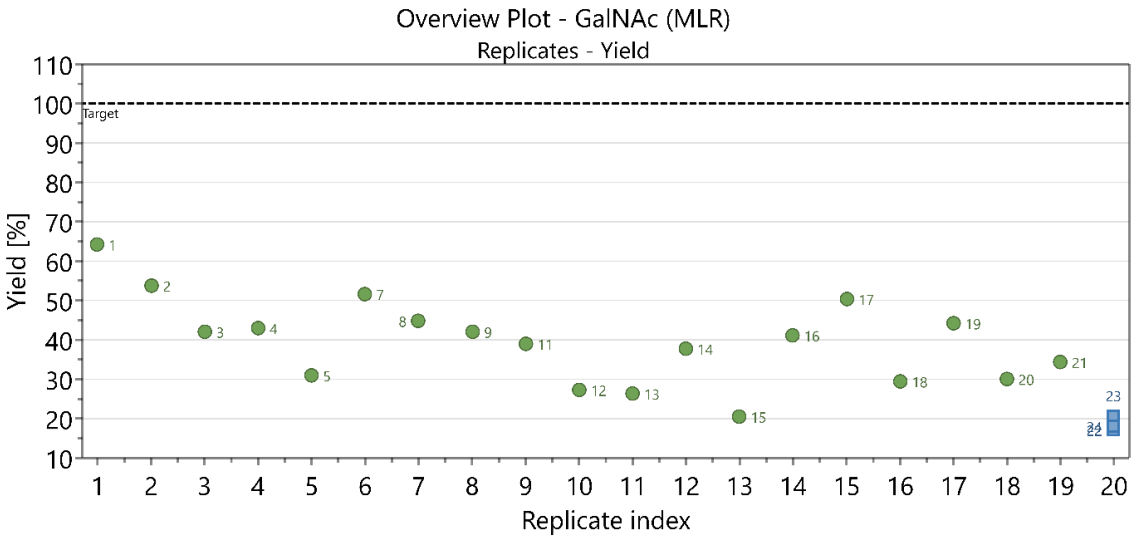

Figure 39. Overview plot of yields of $GalNAcNH_2$. Replicates are indicated in blue.

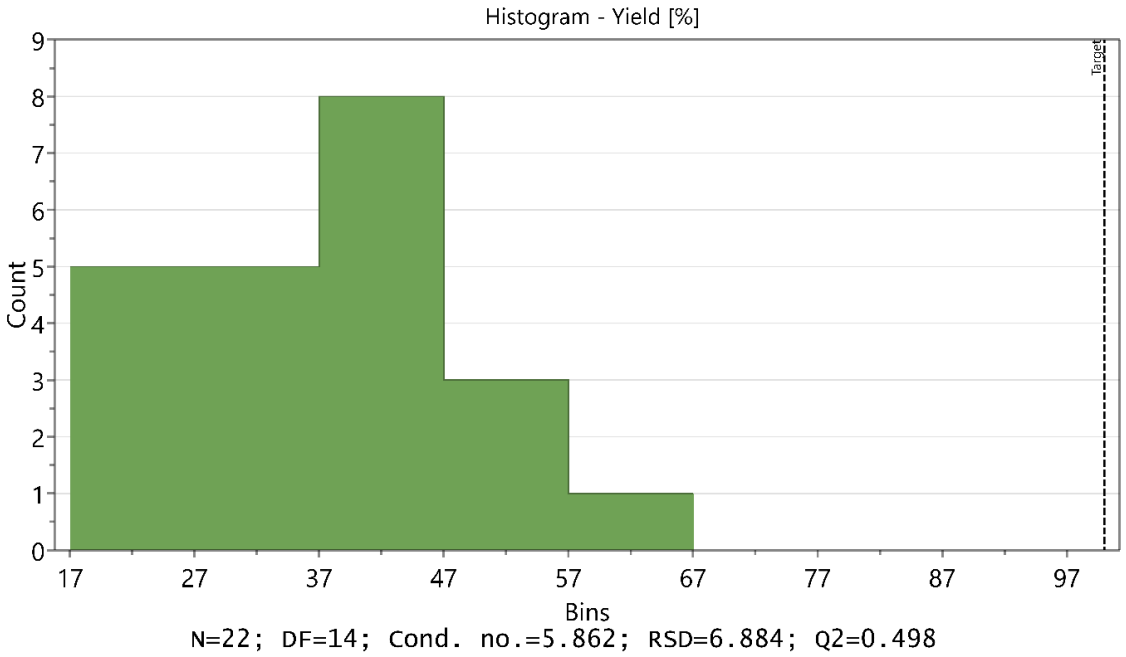

Figure 40. Histogram of yields of $GalNAcNH_2$. Skewness test not triggered.

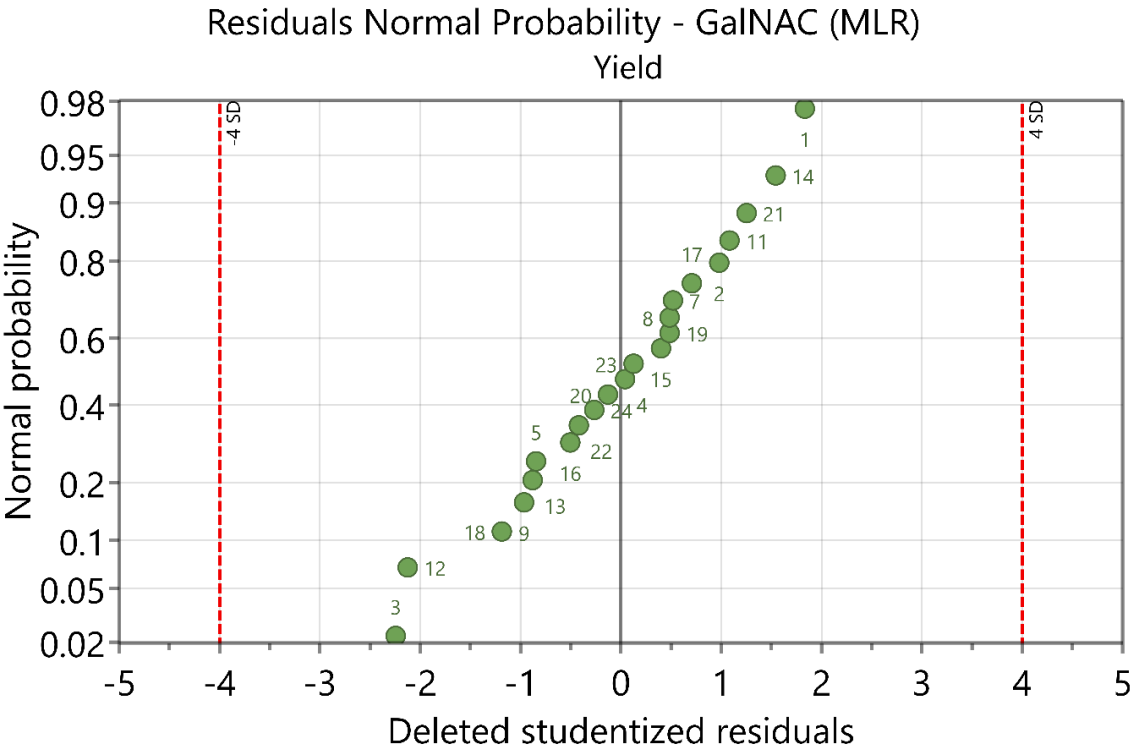

Figure 41. Plot of $GalNAcNH_2$ with residuals of yields versus the normal probability of the distribution.

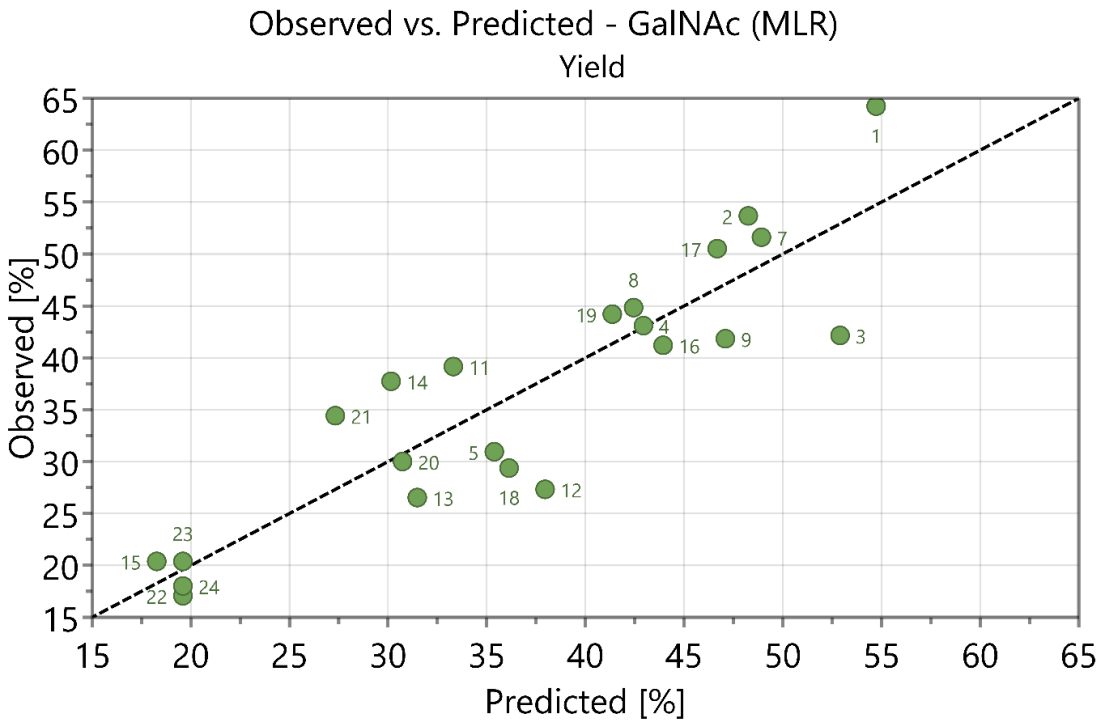

Figure 42. Plot of observed values versus predicted values for yields of GalNAcNH$_2$.

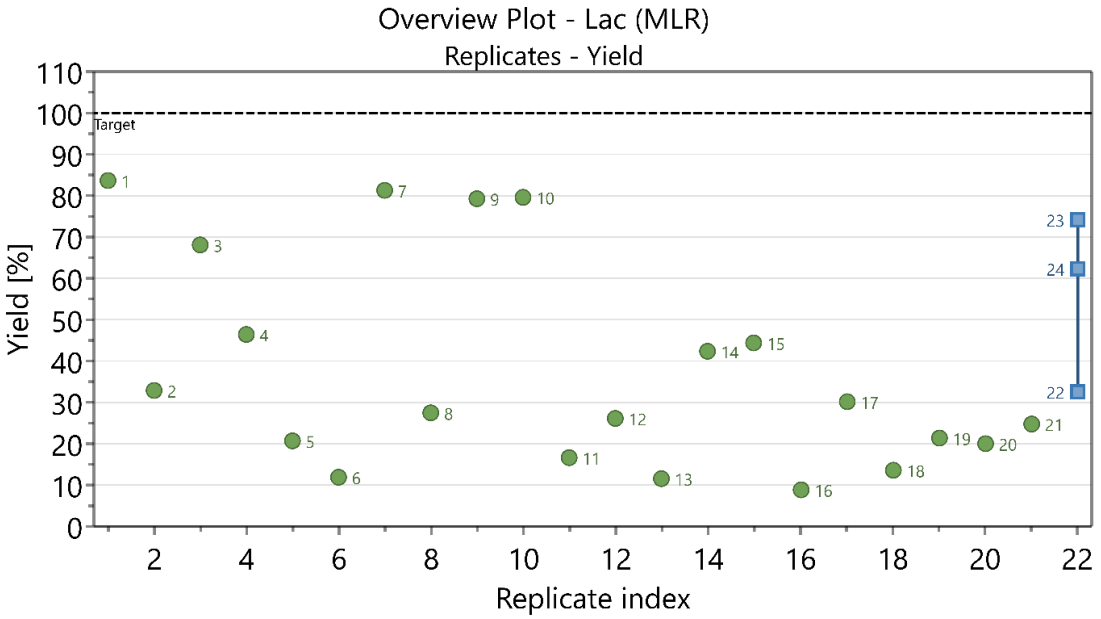

Figure 43. Overview plot of yields of LacNH$_2$. Replicates are indicated in blue.

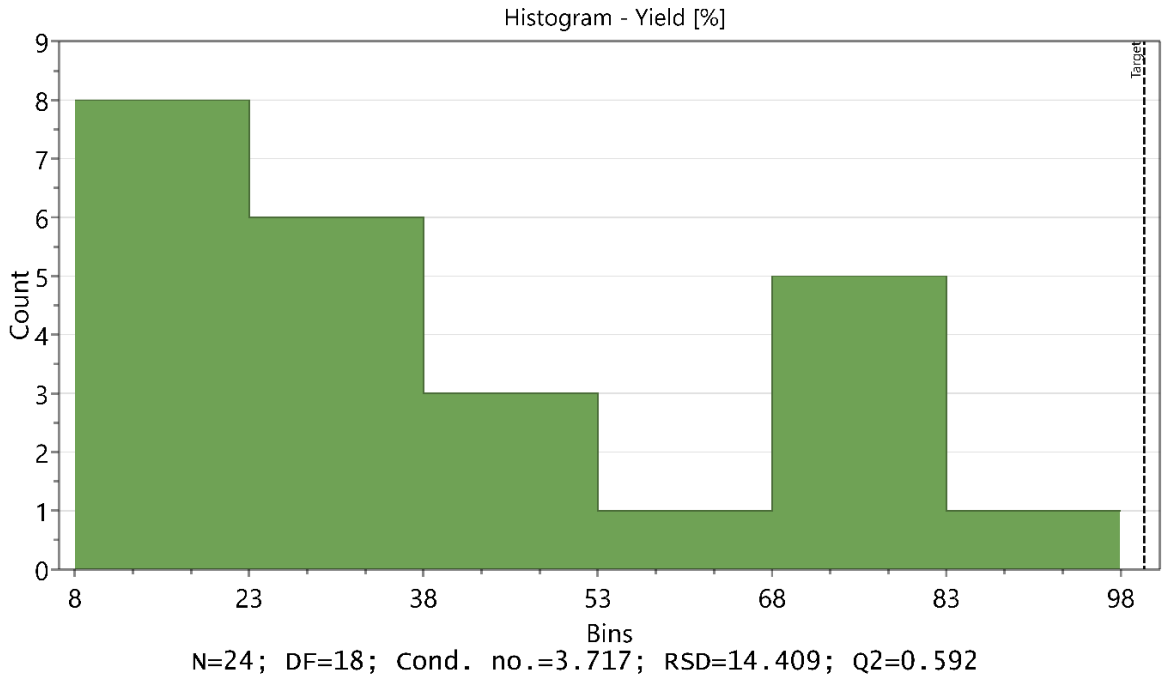

Figure 44. Histogram of yields of $LacNH_2$. Skewness test not triggered.

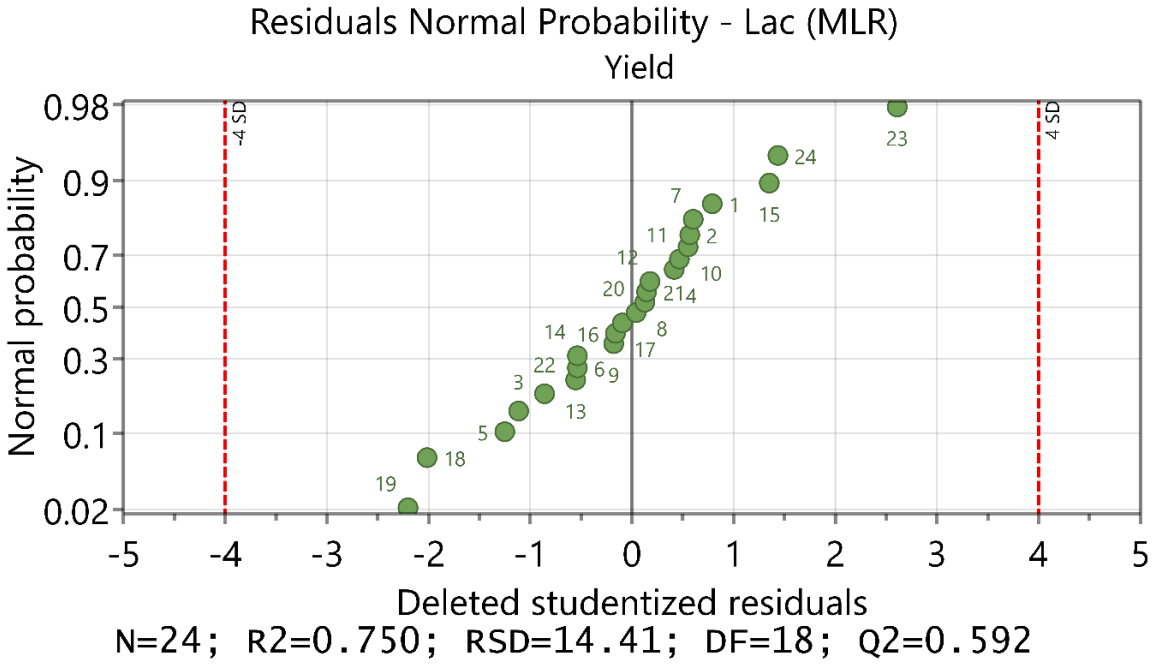

Figure 45. Plot of $LacNH_2$ with residuals of yields versus the normal probability of the distribution.

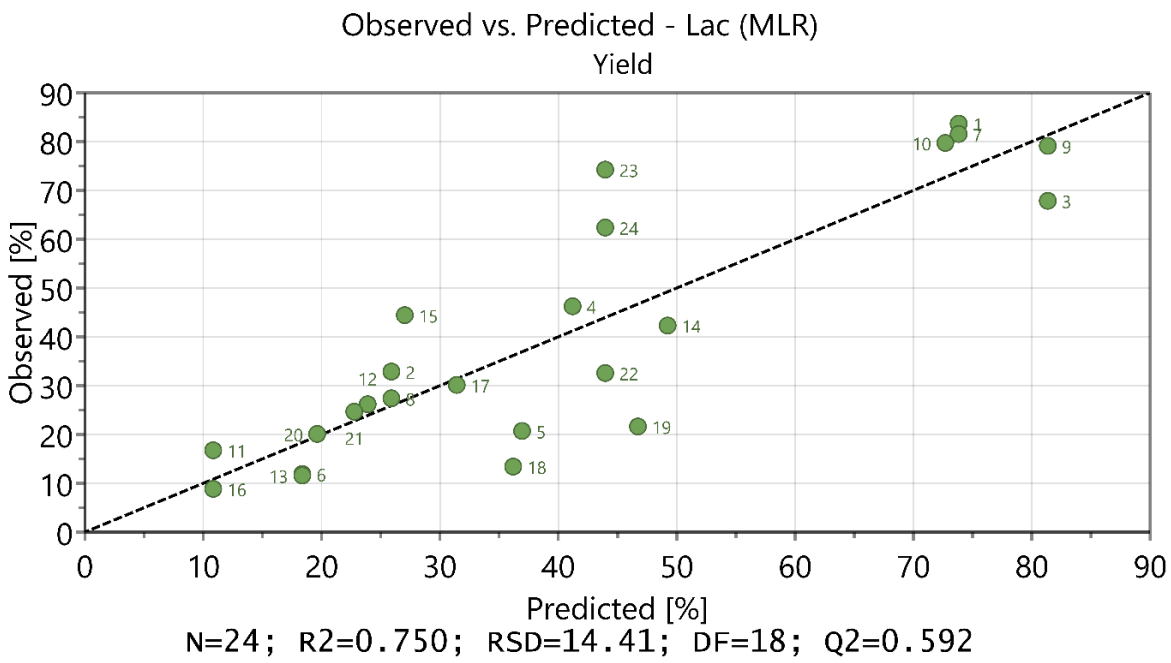

Figure 46. Plot of observed values versus predicted values for yields of $LacNH_2$.

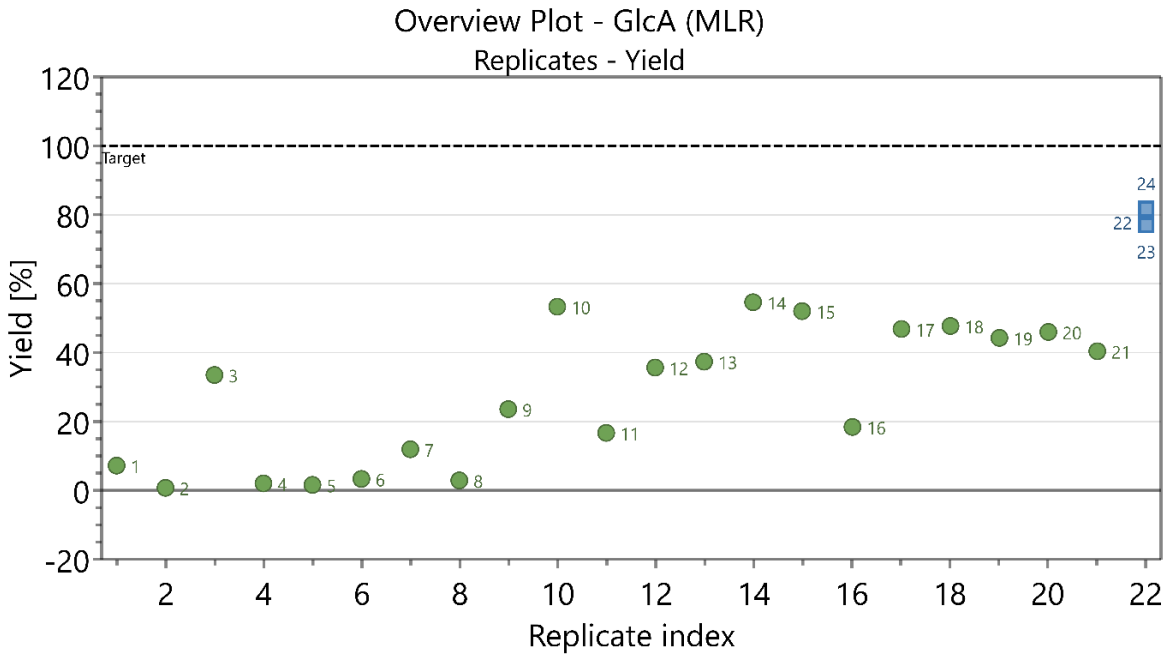

Figure 47. Overview plot of yields of $GlcANH_2$. Replicates are indicated in blue.

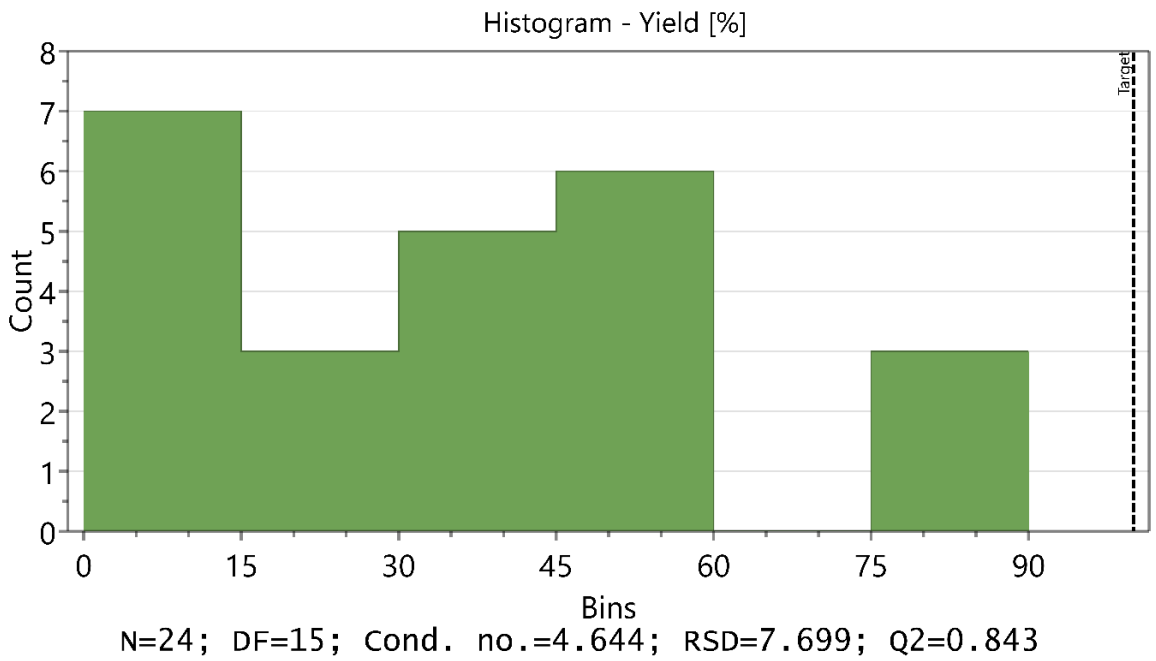

Figure 48. Histogram of yields of $GlcANH_2$. Skewness test not triggered.

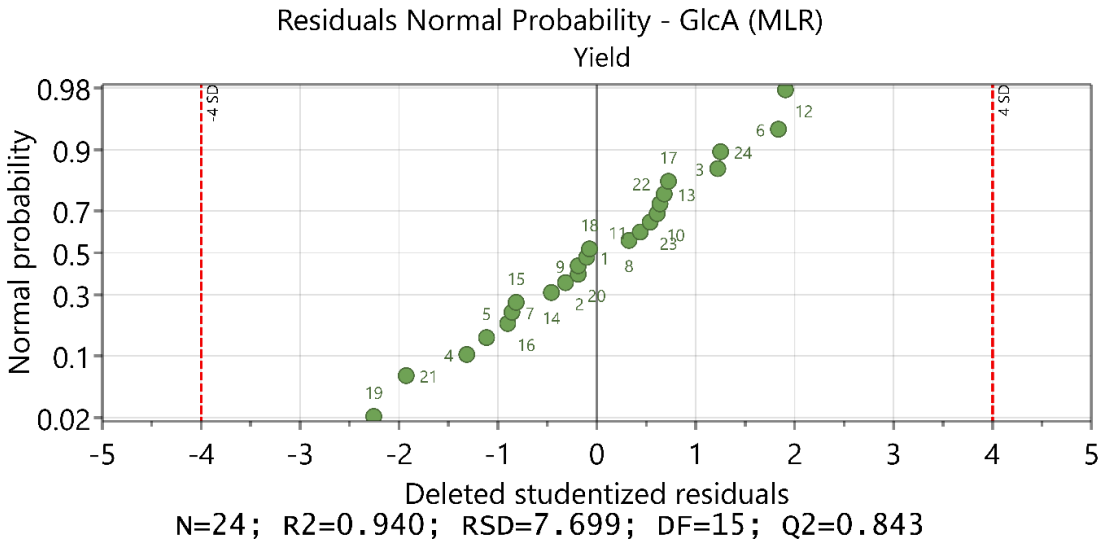

Figure 49. Plot of $GlcANH_2$ with residuals of yields versus the normal probability of the distribution.

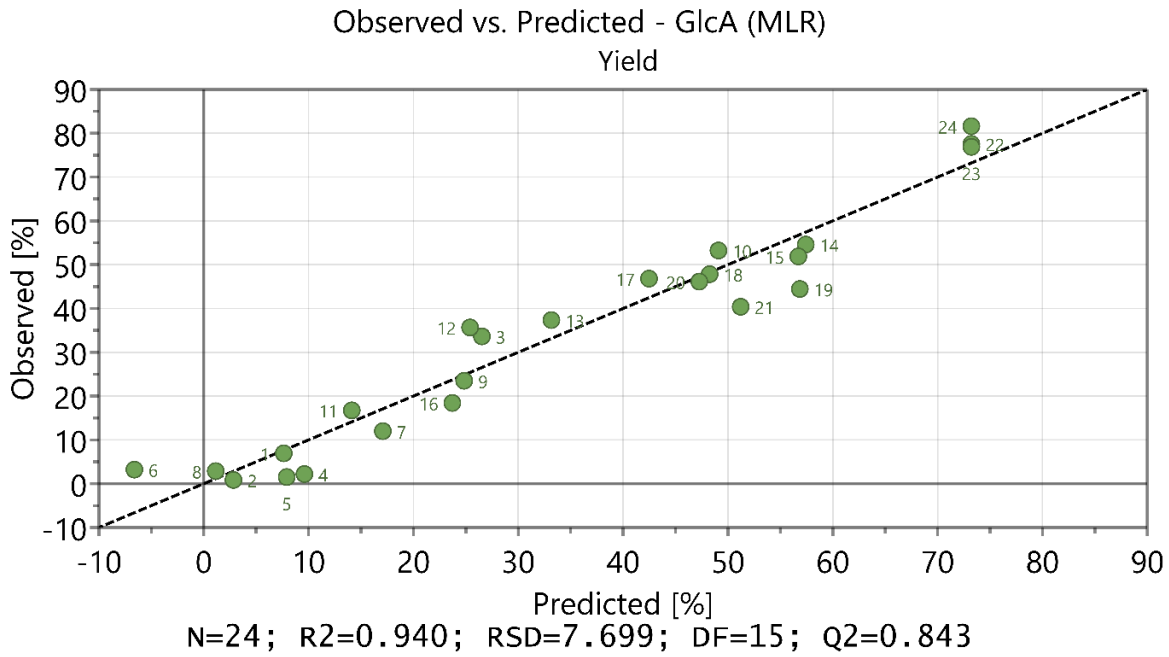

Figure 50. Plot of observed values versus predicted values for yields of $GlcANH_2$.

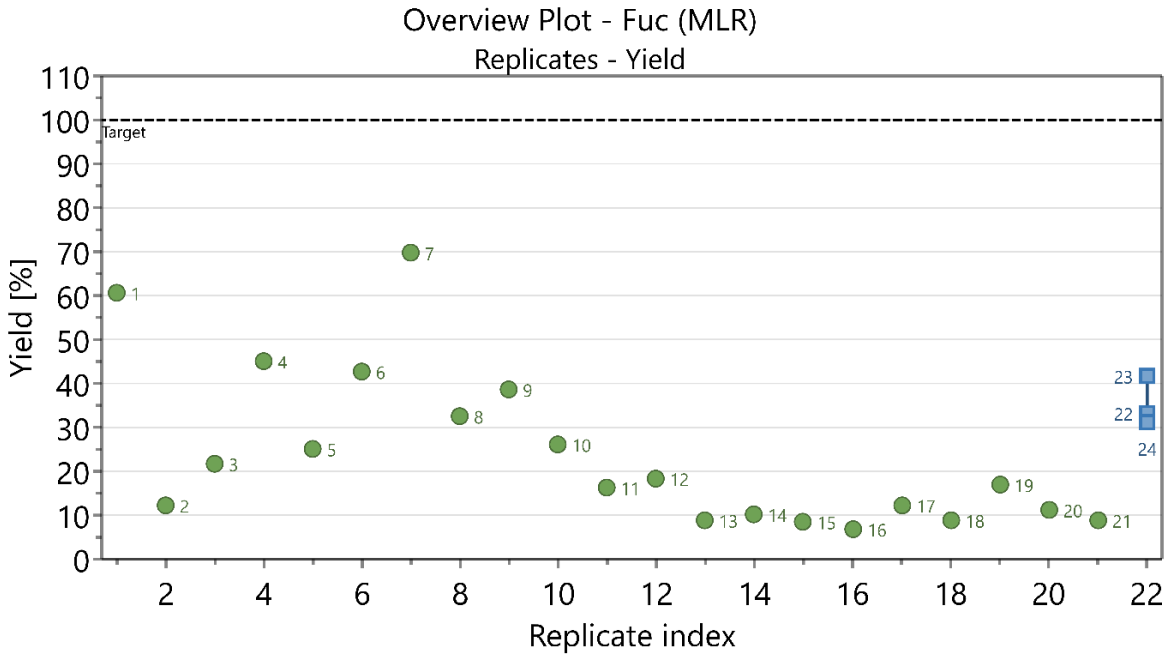

Figure 51. Overview plot of yields of $FucNH_2$. Replicates are indicated in blue.

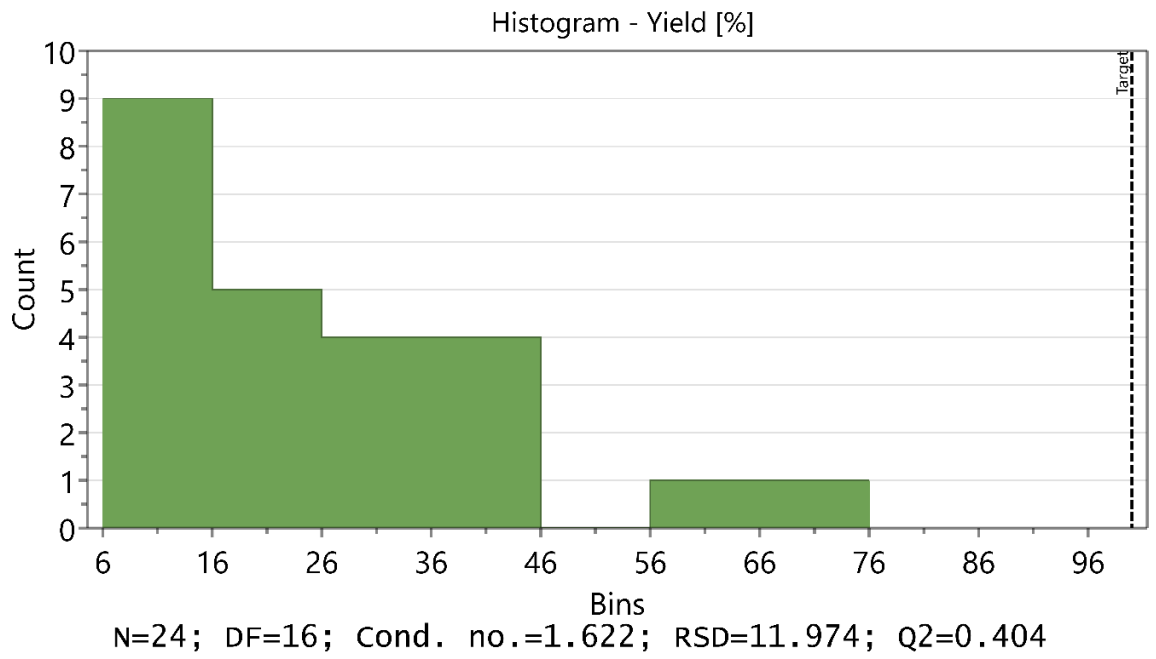

Figure 52. Histogram of yields of $FucNH_2$. Skewness test triggered. No transformation performed.

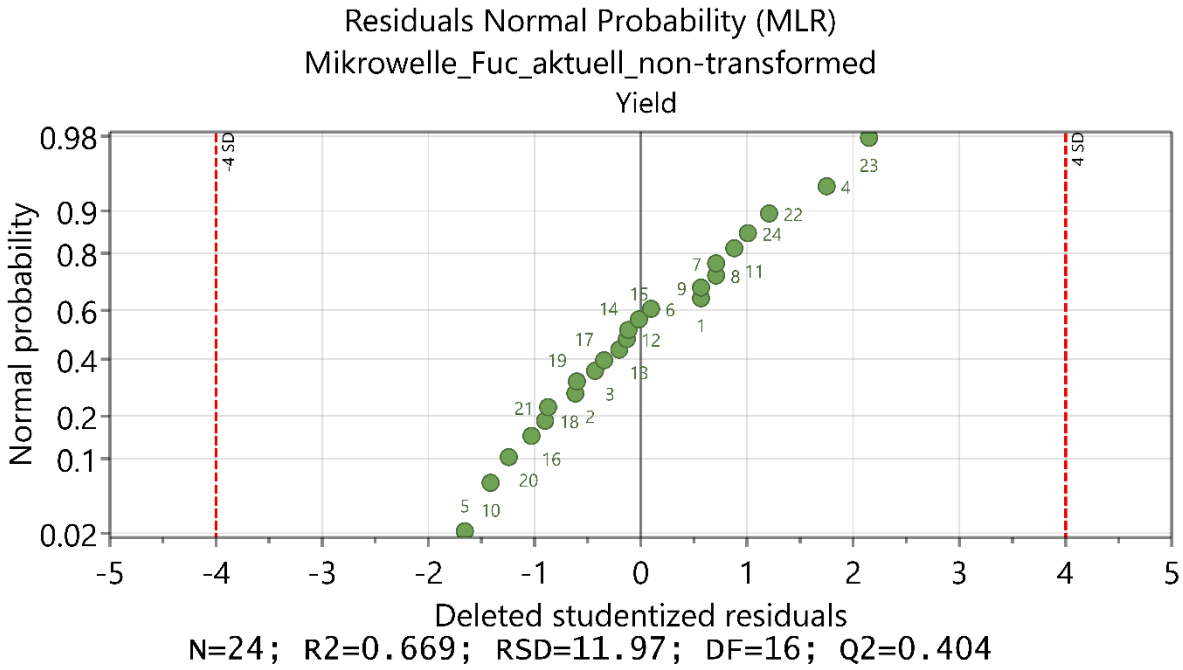

Figure 53. Plot of $FucNH_2$ with residuals of yields versus the normal probability of the distribution.

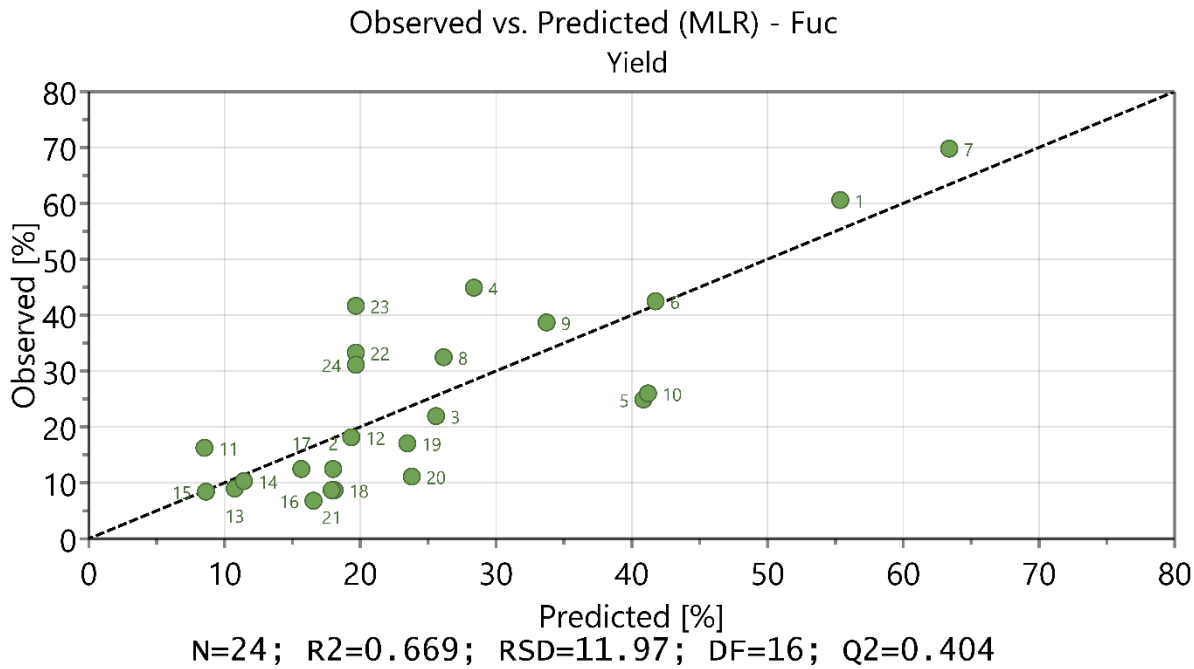

Figure 54. Plot of observed values versus predicted values for yields of $FucNH_2$.

16.2 Supporting Information of Chapter 8: Functional Glyco-Nanogels for Multivalent Interaction with Lectins

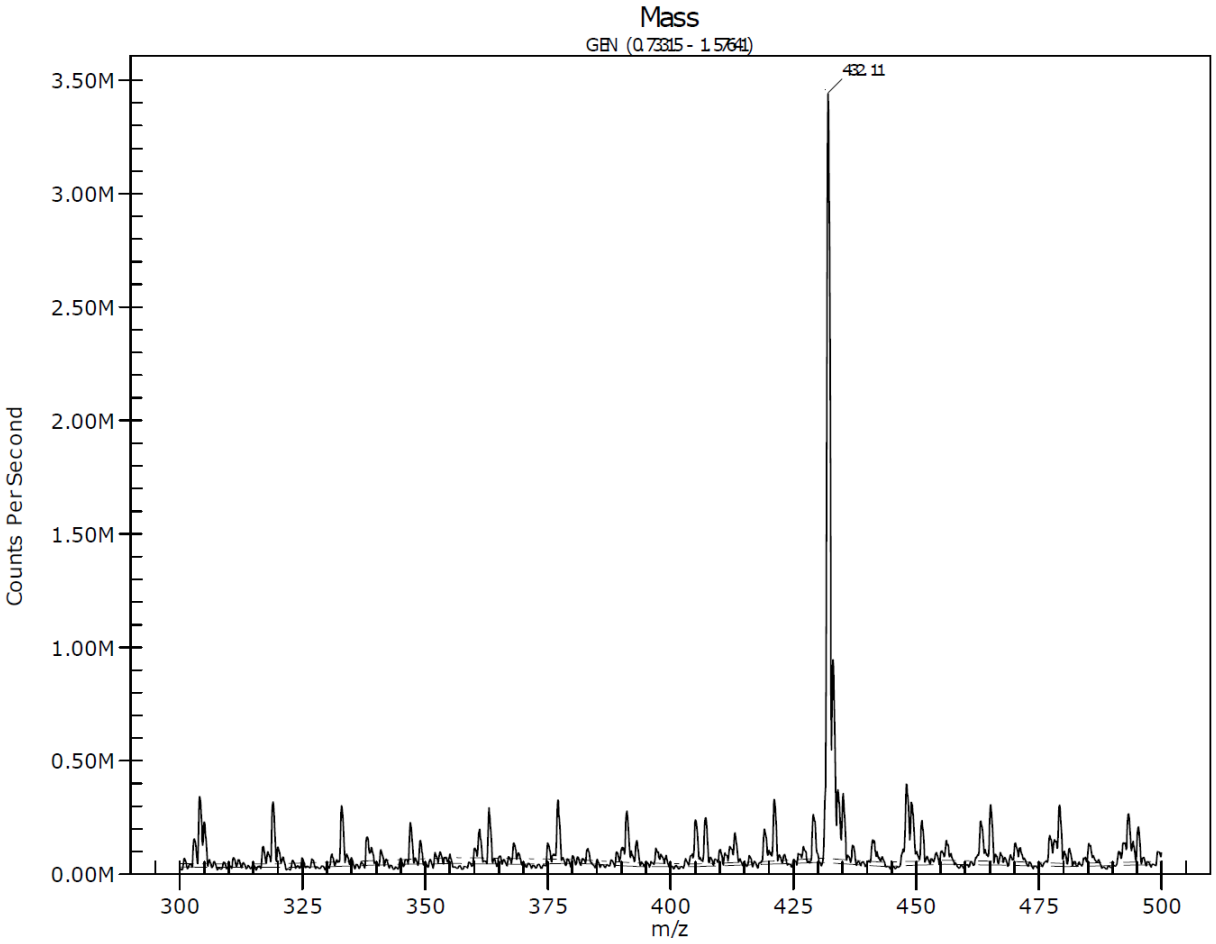

Figure 55. ESI-MS spectrum of LacMAm.

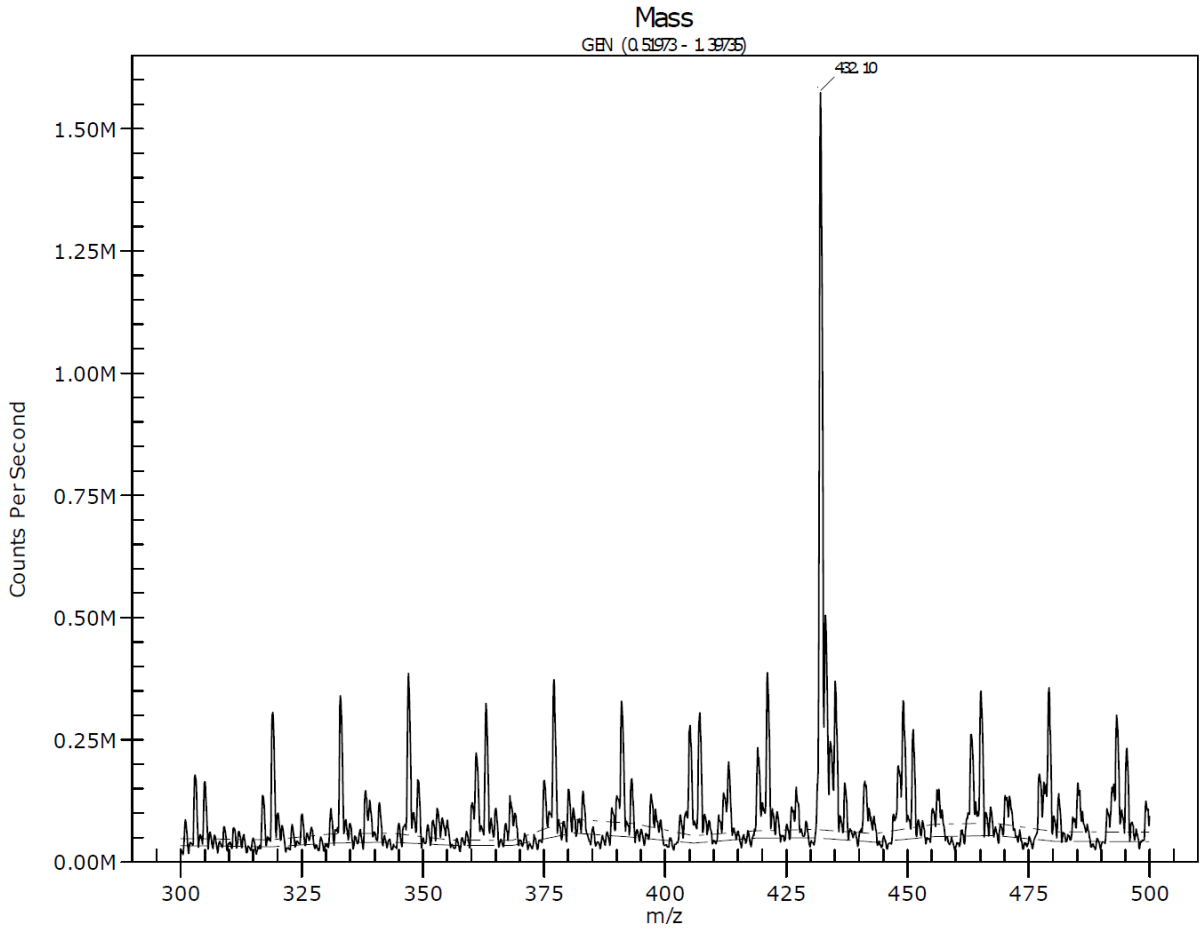

Figure 56. ESI-MS spectrum of MelMAm.

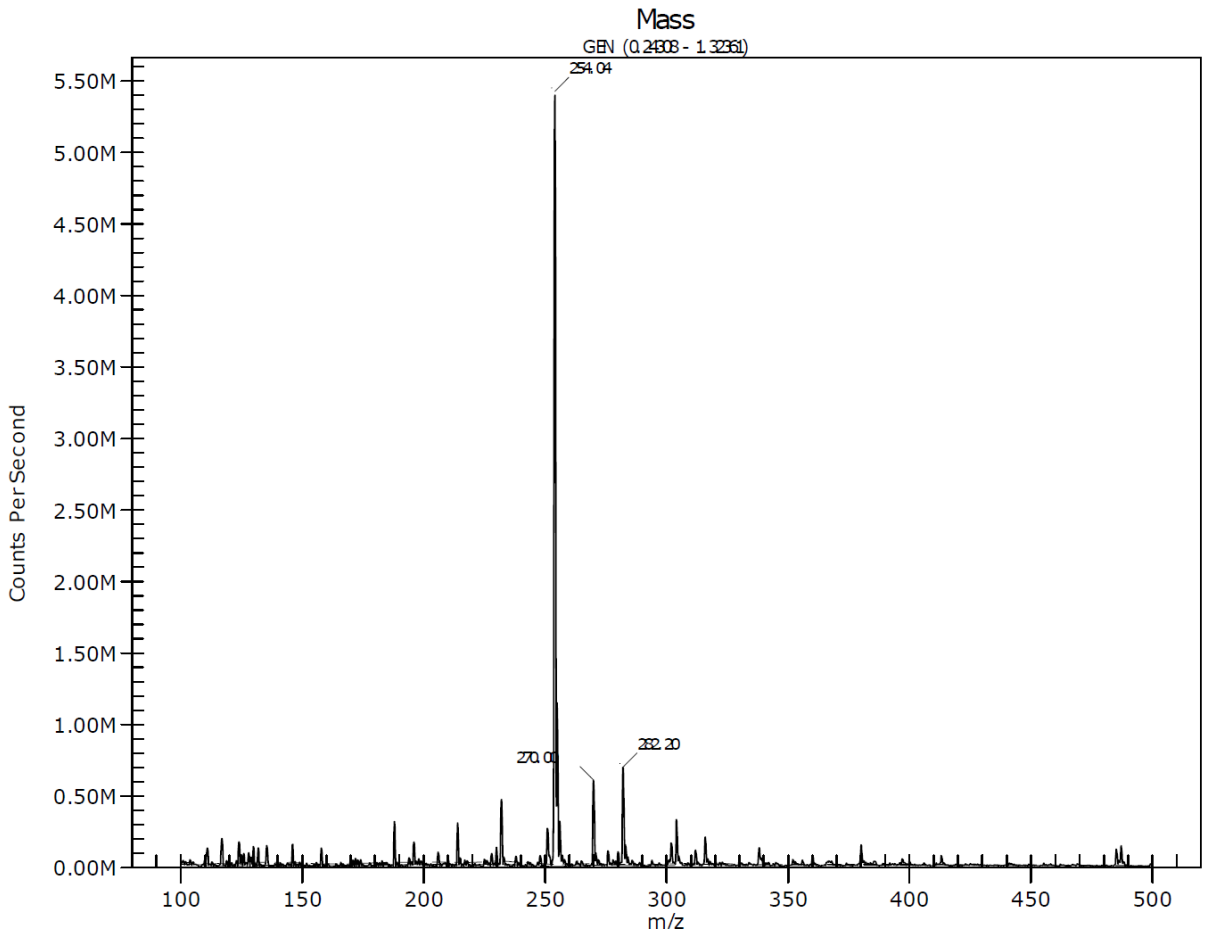

Figure 57. ESI-MS spectrum of FucMAm.

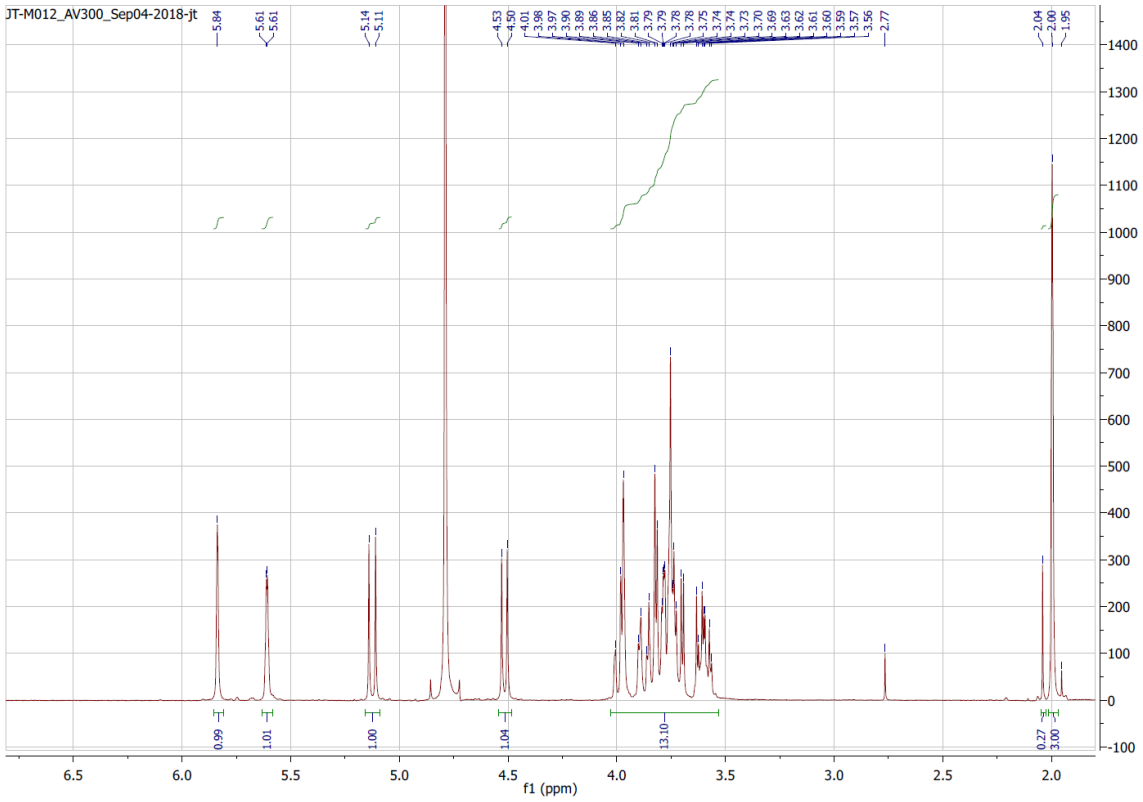

Figure 58. ^{1}H NMR spectrum of LacMAm.

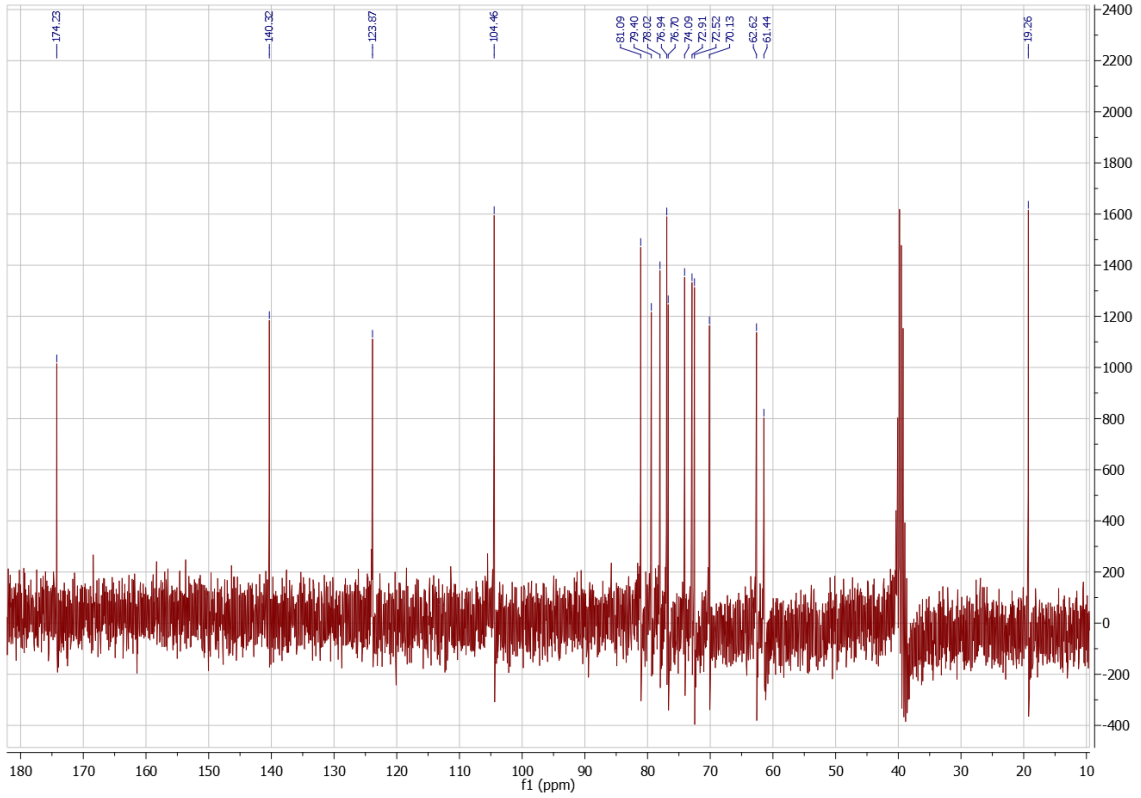

Figure 59. ^{13}C NMR spectrum of LacMAm.

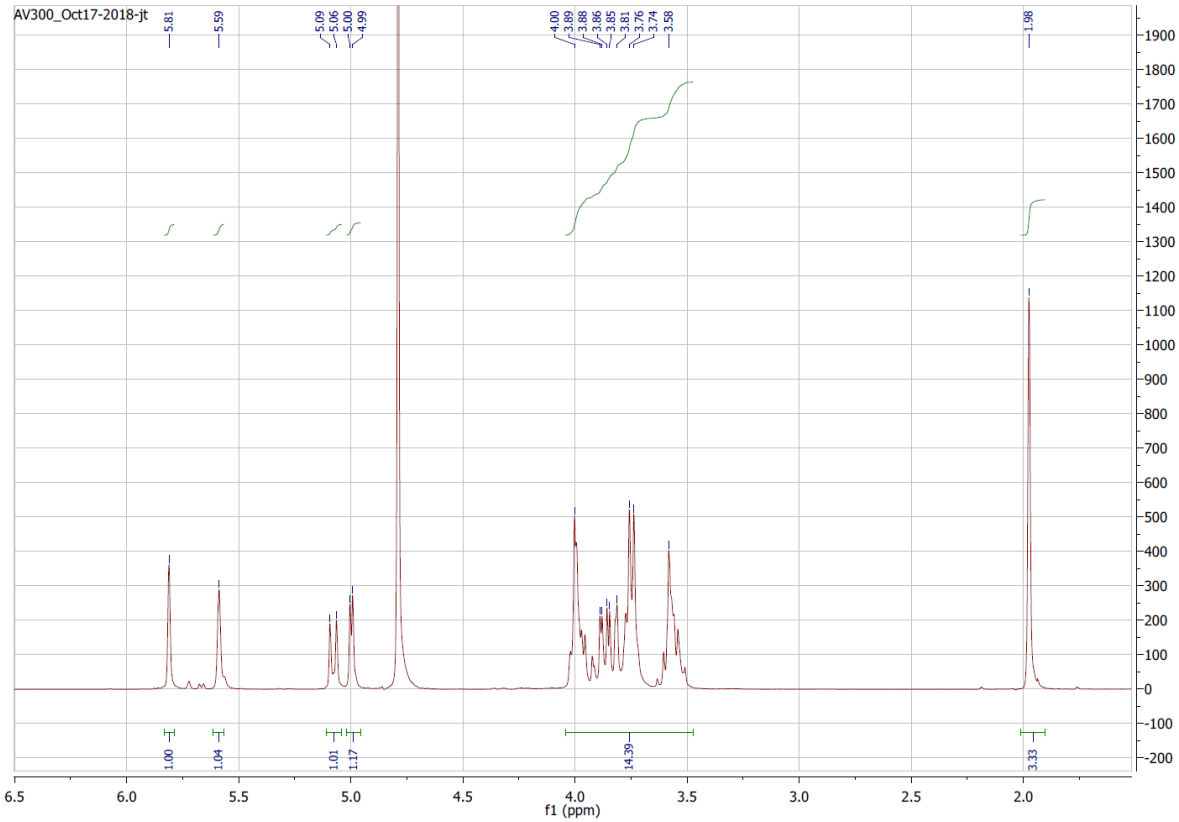

Figure 60. ^{1}H NMR spectrum of MelMAm.

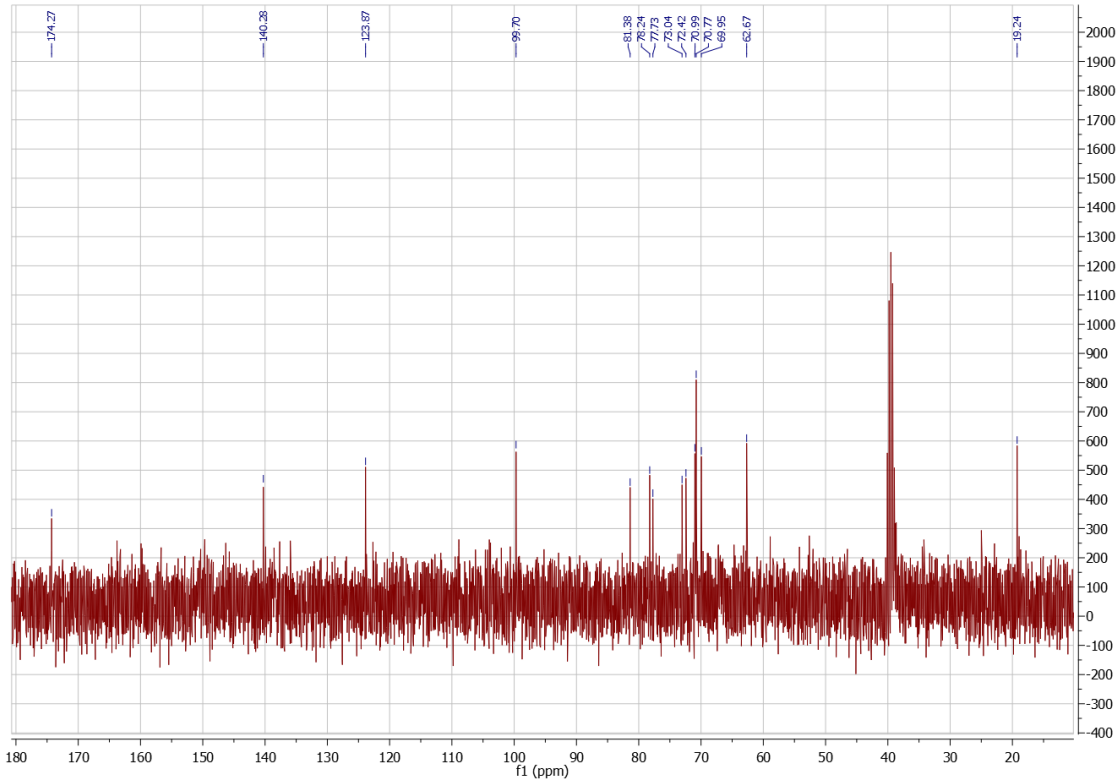

Figure 61. ^{13}C NMR spectrum of MelMAm.

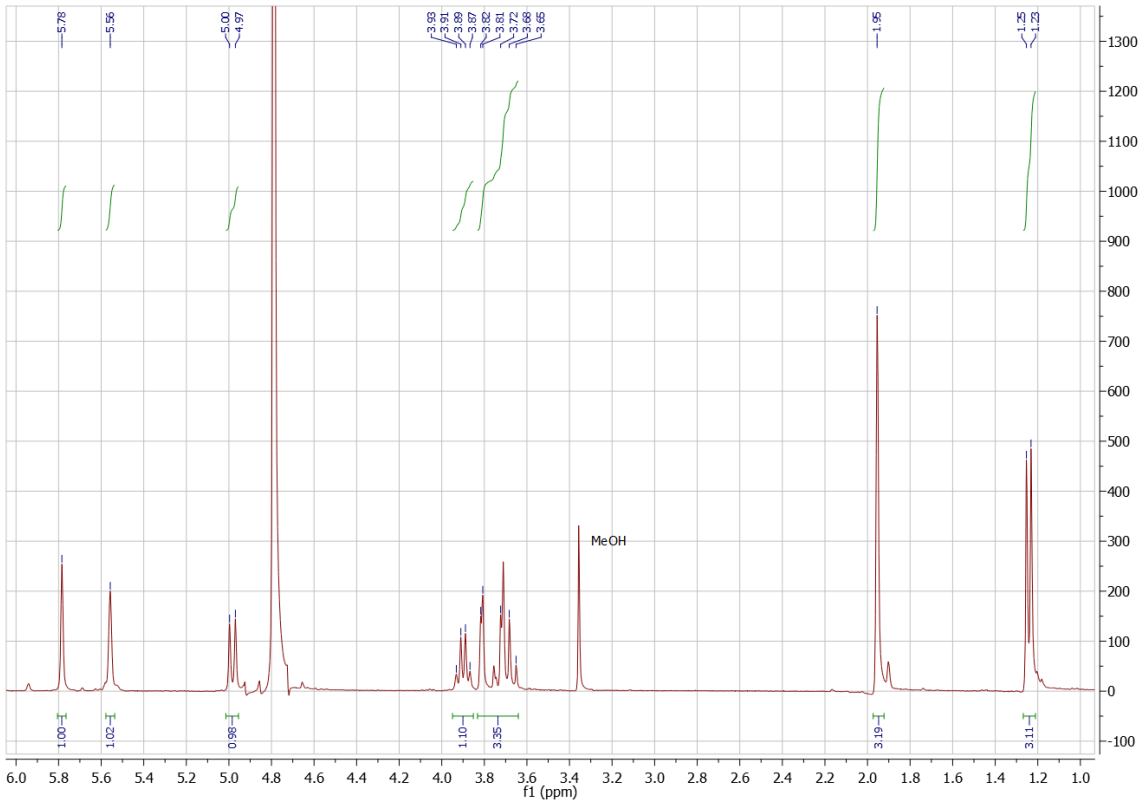

Figure 62. ^{1}H NMR spectrum of FucMAm.

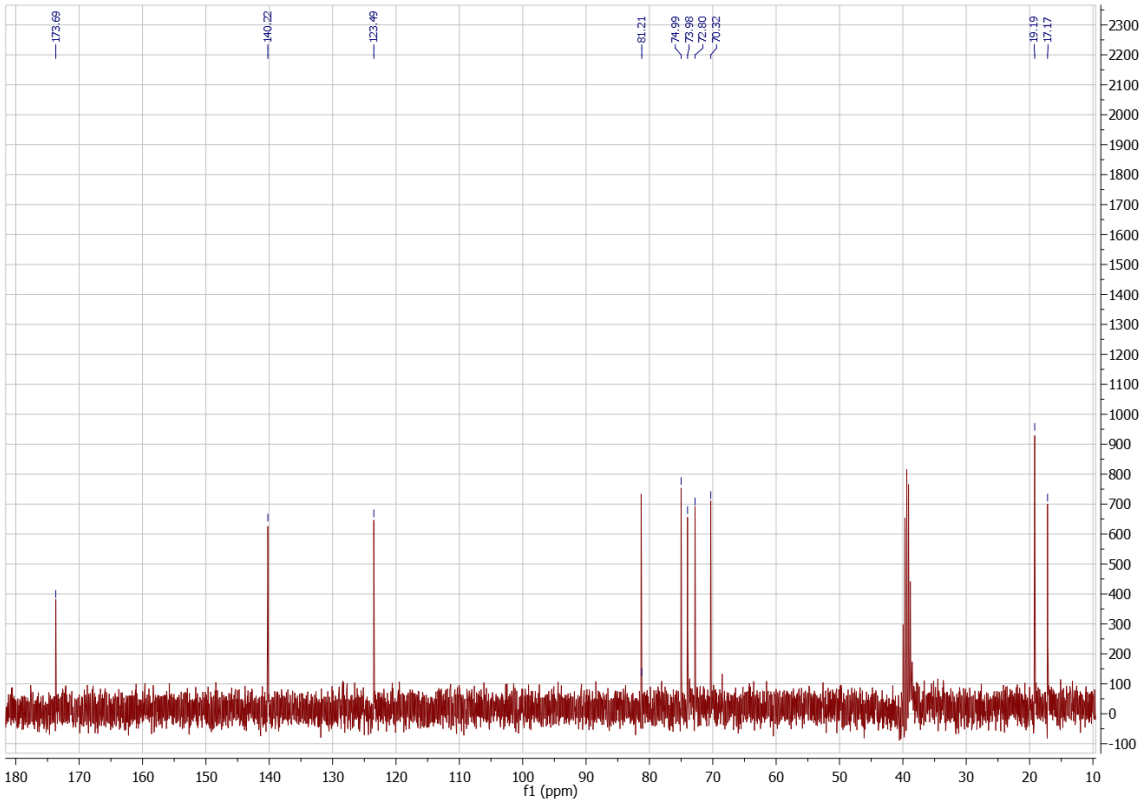

Figure 63. ^{13}C NMR spectrum of FucMAm.

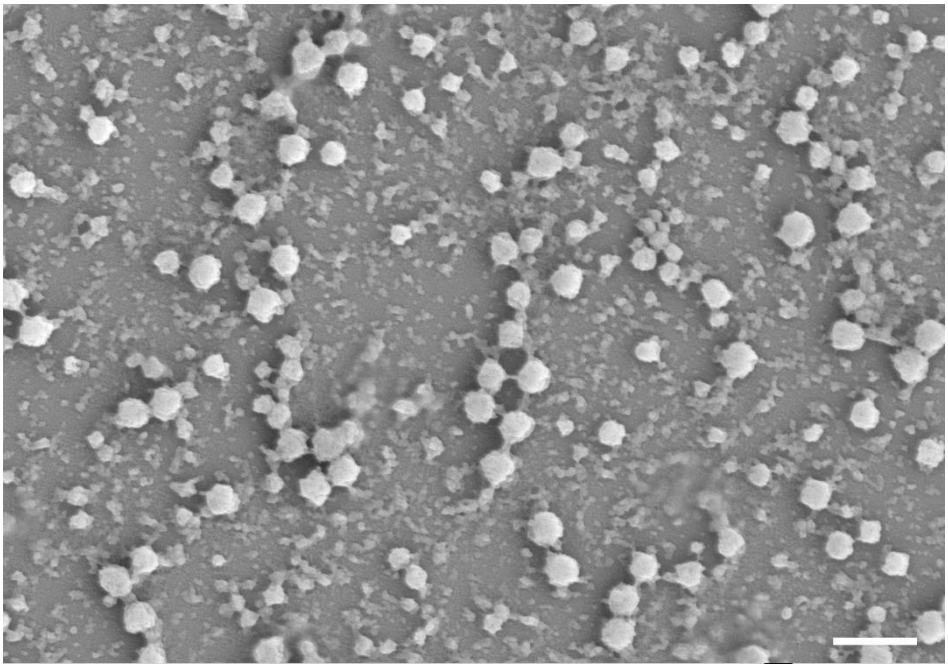

Figure 64. SEM image of MG-4. Scale bar: 1 µm.

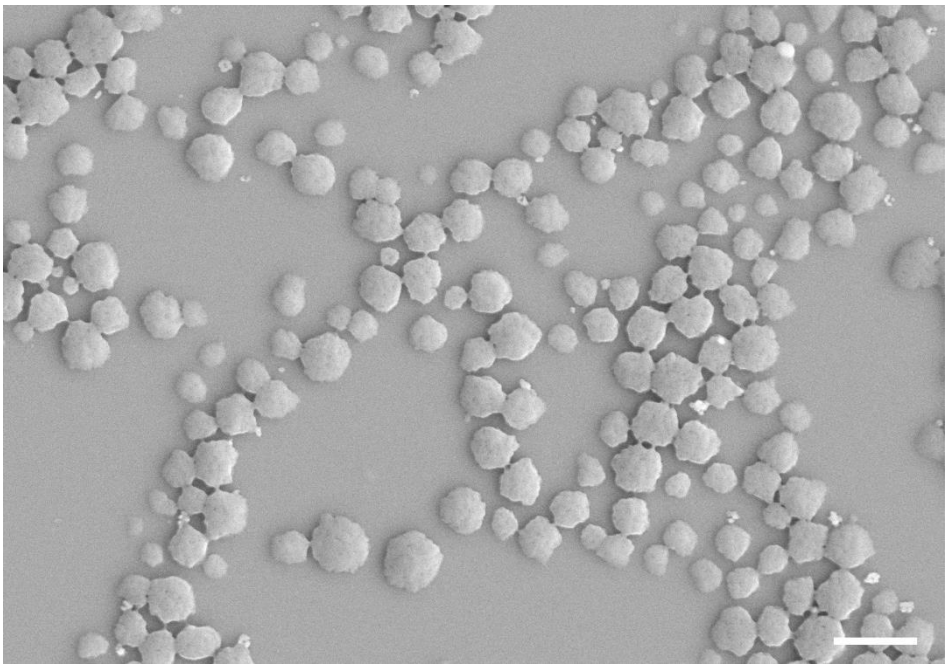

Figure 65. SEM image of MG-5. Scale bar: 1 µm.

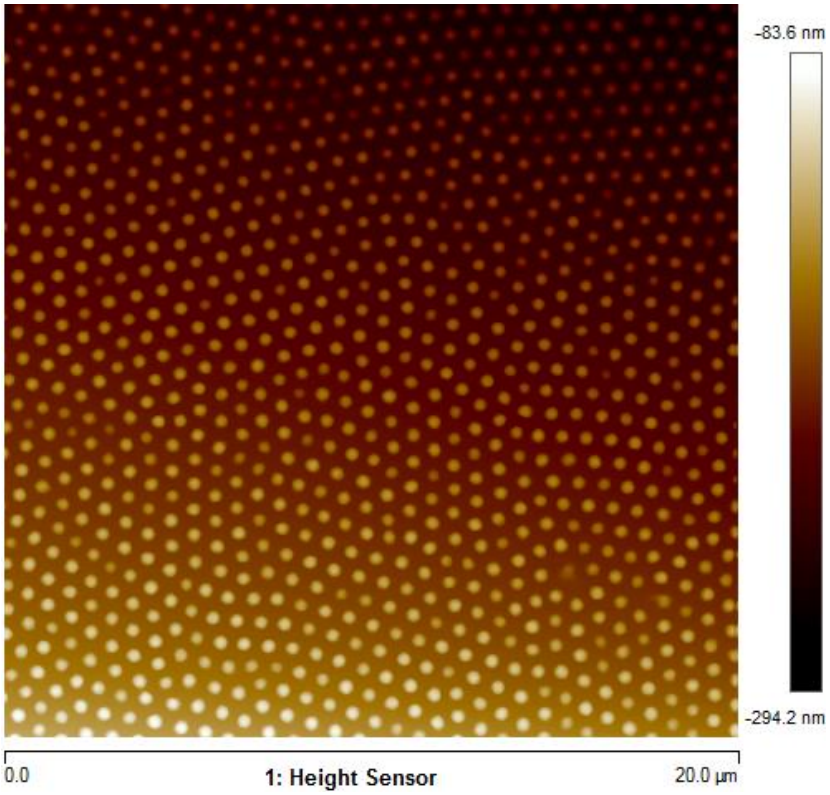

Figure 66. AFM image of G-1.

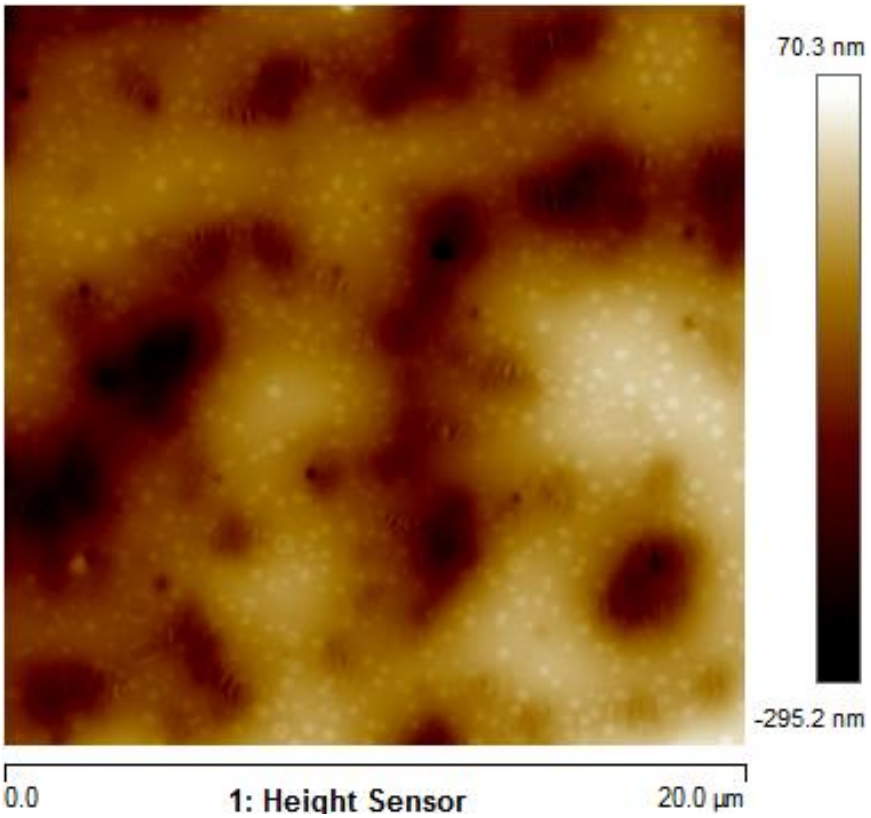

Figure 67. AFM image of MG-0.

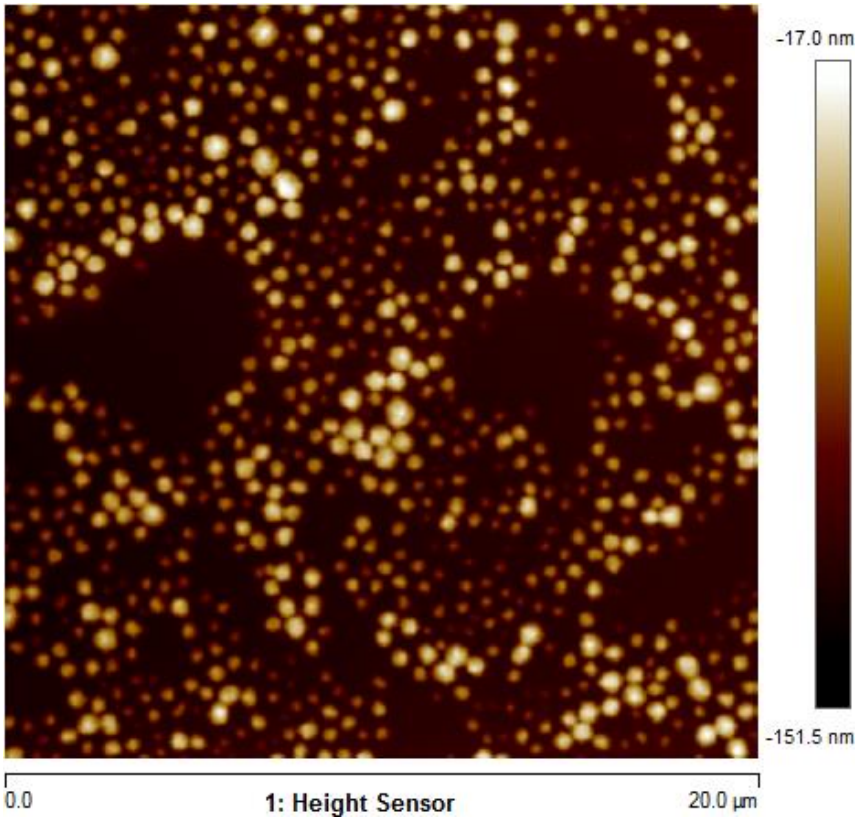

Figure 68. AFM image of MG-1.

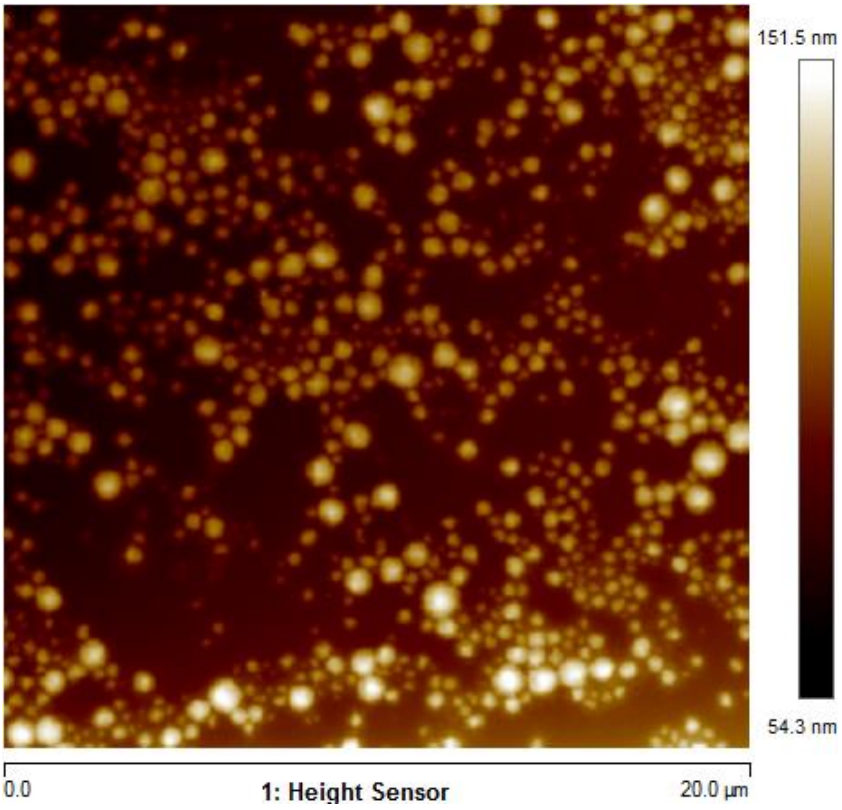

Figure 69. AFM image of MG-2.

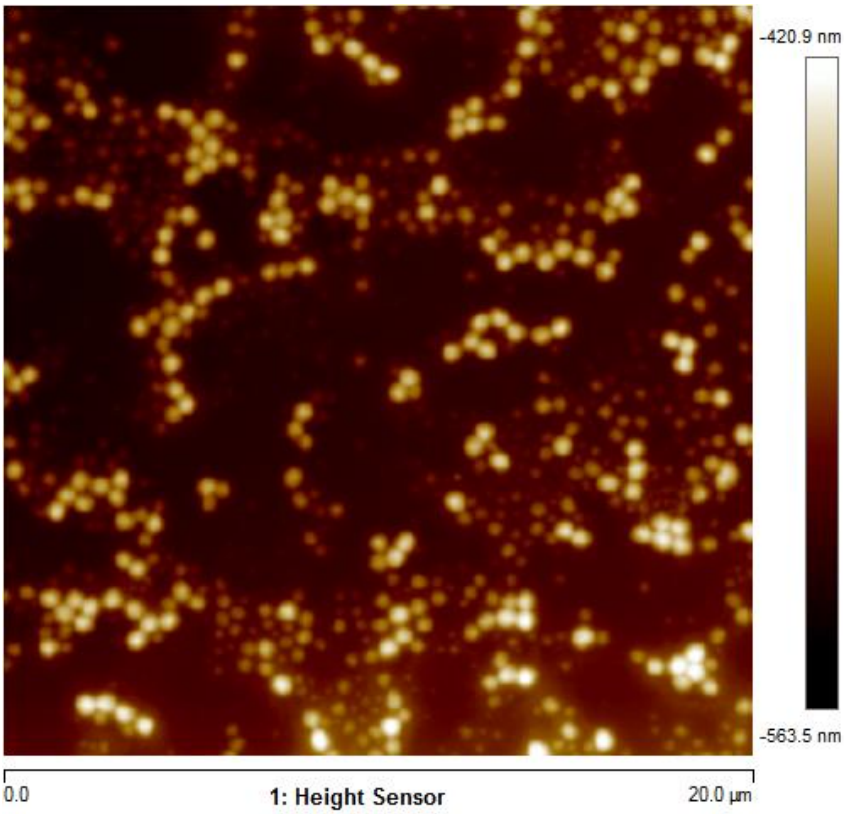

Figure 70. AFM image of MG-4.

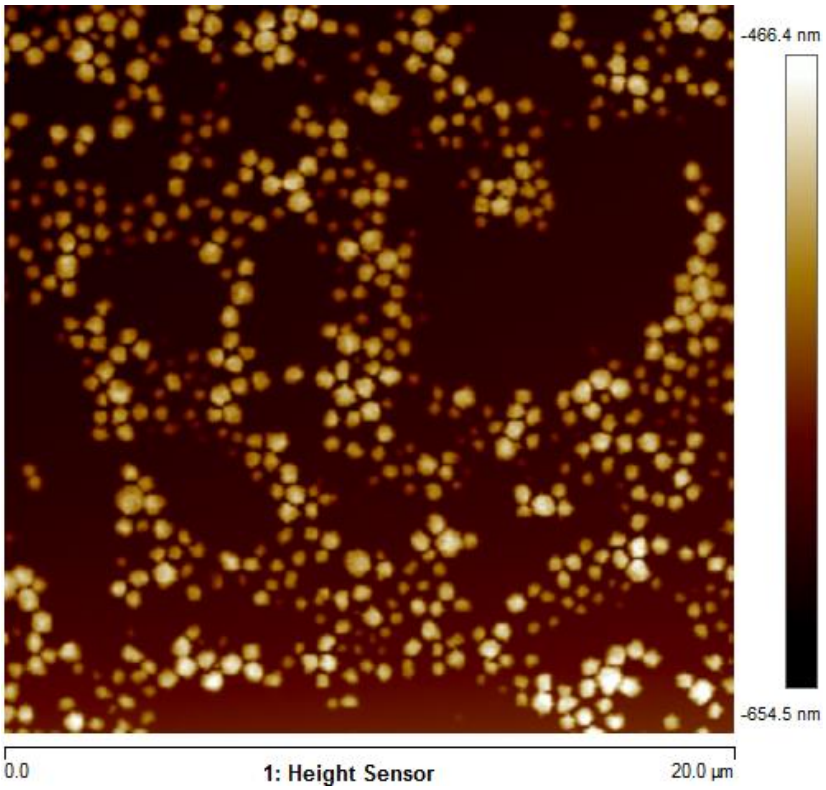

Figure 71. AFM image of MG-5.

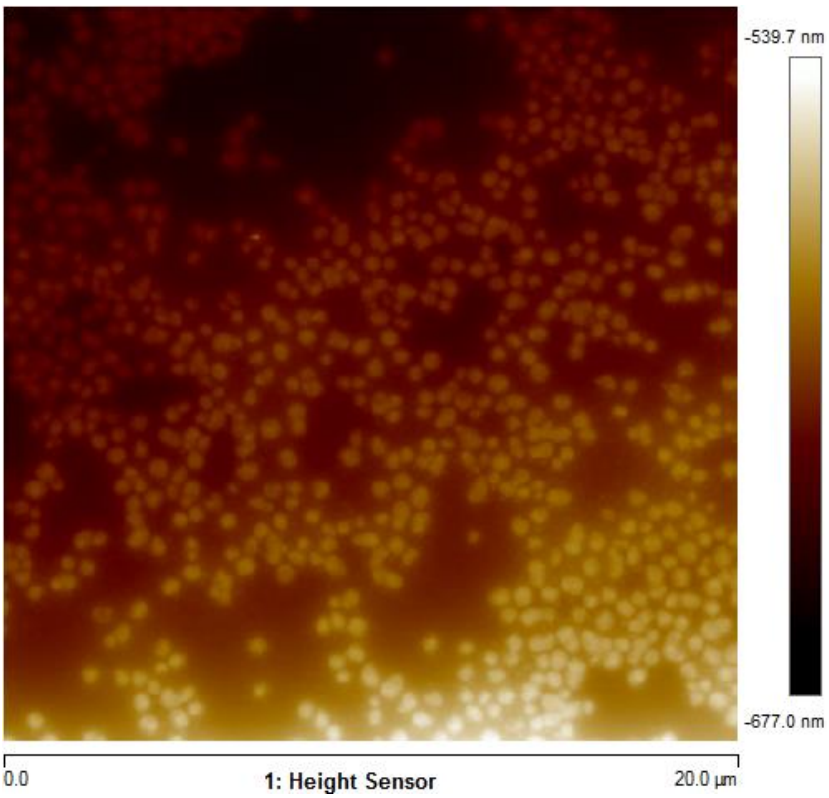

Figure 72. AFM image of FG-1.

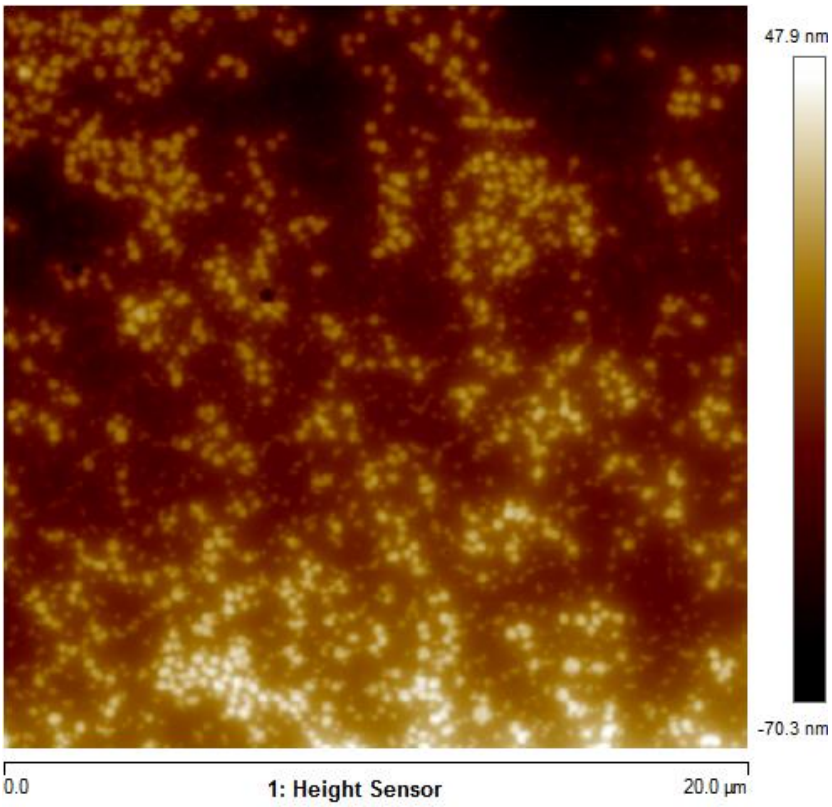

Figure 73. AFM image of FG-2.

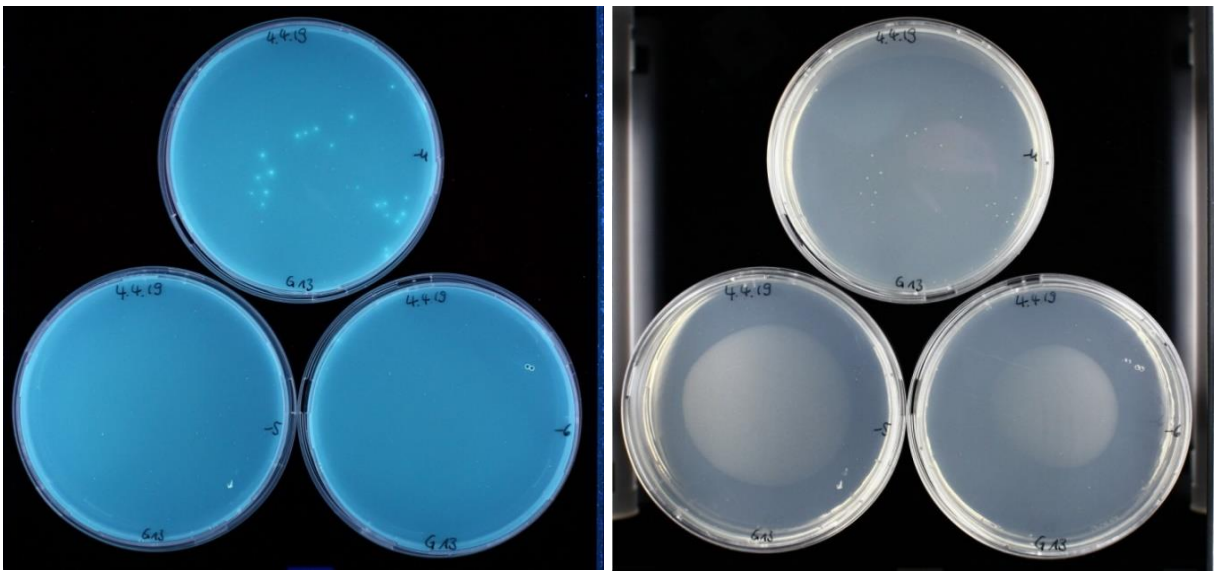

(**a**) (**b**)

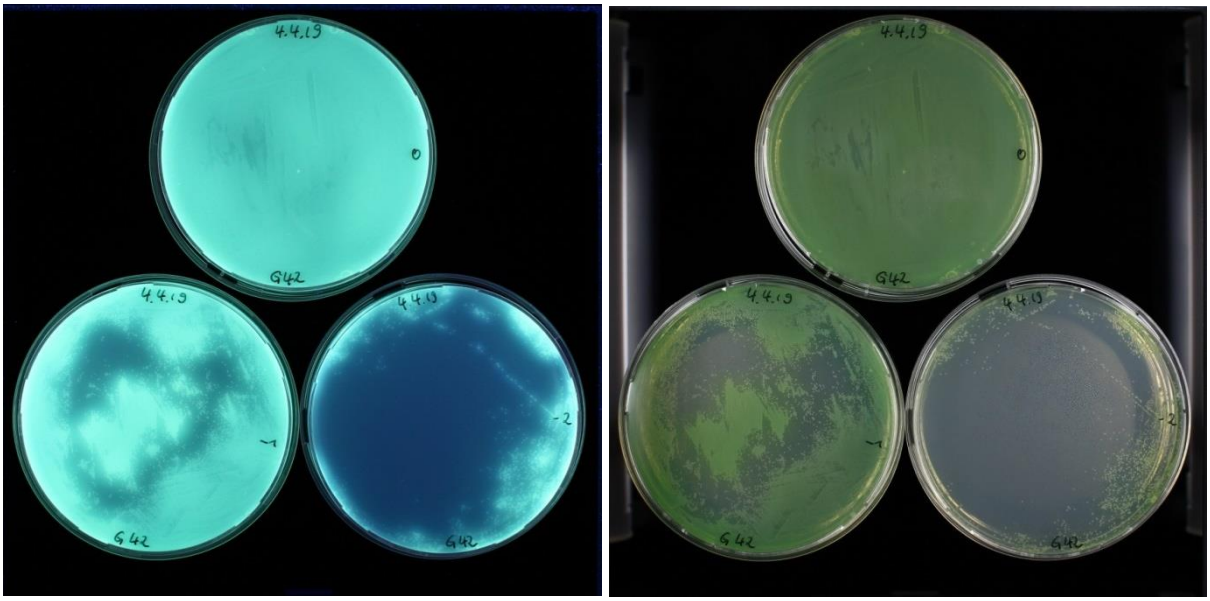

(**c**) (**d**)

Figure 74. Cetrimid Agar plates of PA incubated with MG-1 (a and b) FG-1 (c and d). (a) and (c) fluorescence image, (b) and (d) white light image. FG-1 inhibits pyoverdine, but is not acting antimicrobial. Less colonies are found with MG-1 due to higher dilution. 10^{-4} to 10^{-6} for MG-1 and undiluted to 10^{-2} for FG-1.

16.3 Supporting Information of Chapter 9: Protection group- free synthesis of α- mannopyranosyl methacrylamide

16.3.1 ^{1}H NMR spectroscopic data

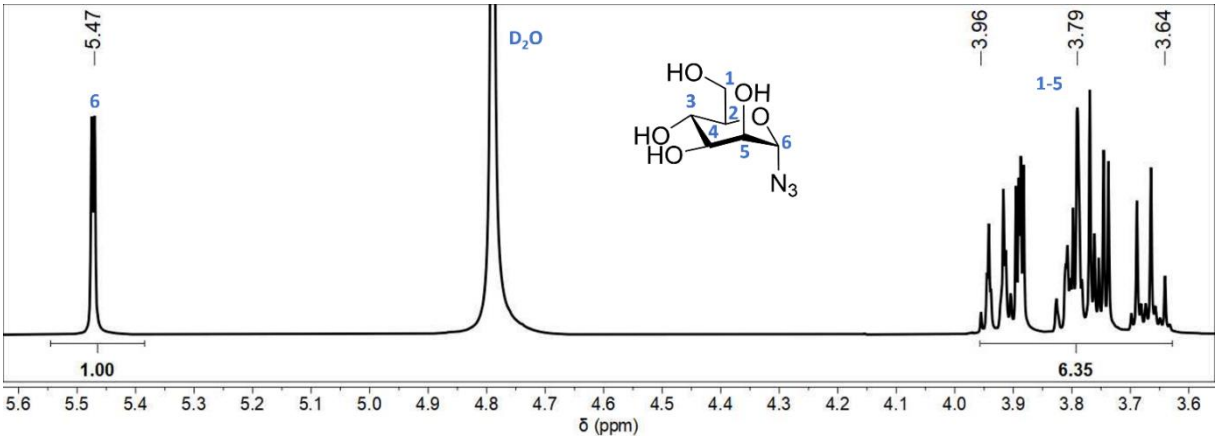

Figure 75. ^{1}H NMR spectrum of α-mannopyranosyl azide **2**.

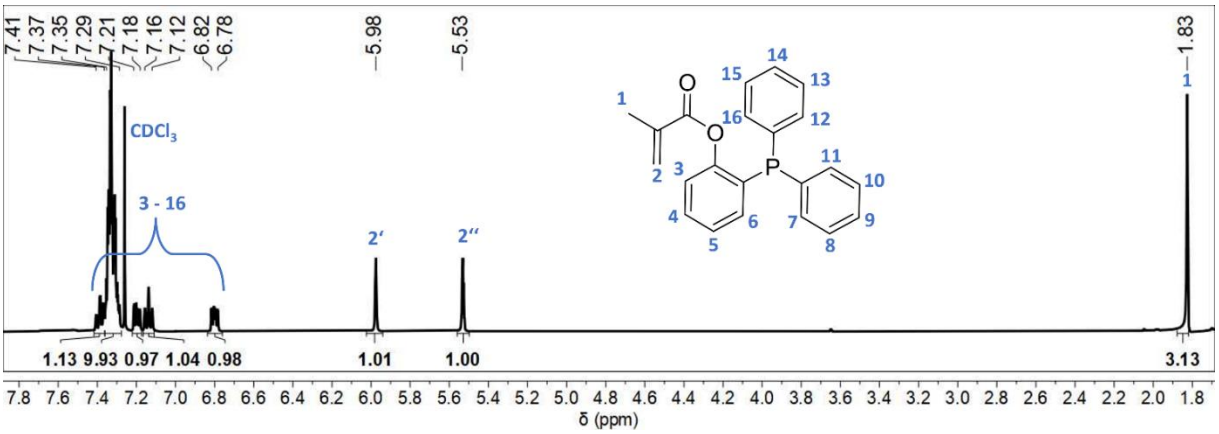

Figure 76. ^{1}H NMR spectrum of 2-(diphenylphosphonyl)phenyl methacrylate **4**.

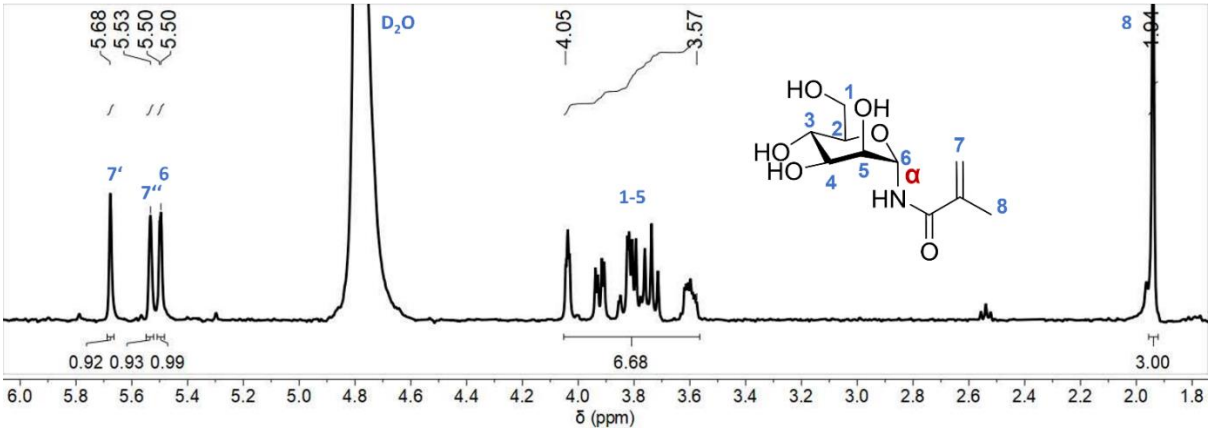

Figure 77. [1]H NMR spectrum of α-mannopyranosyl methacrylamide **5**.

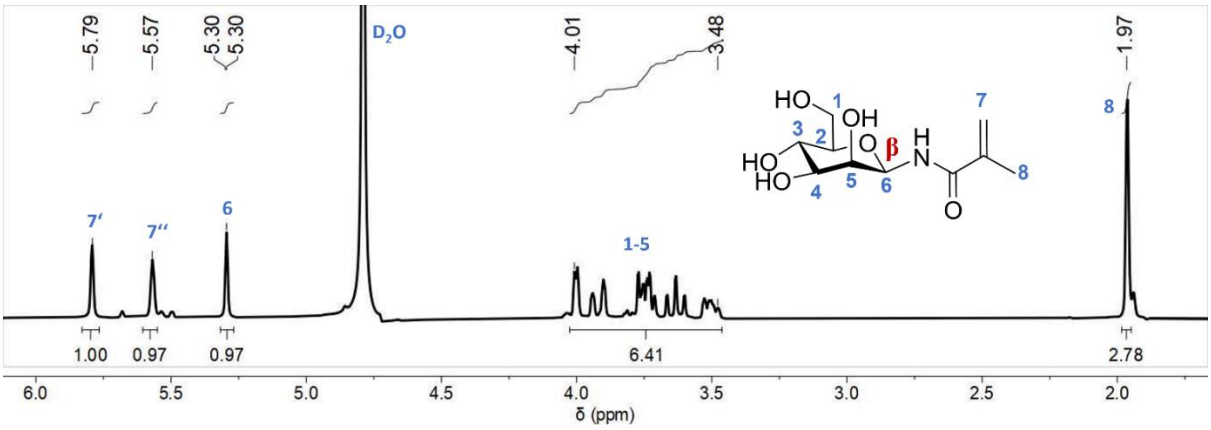

Figure 78. [1]H NMR spectrum of β-mannopyranosyl methacrylamide **5**.

16.3.2 ESI-MS data

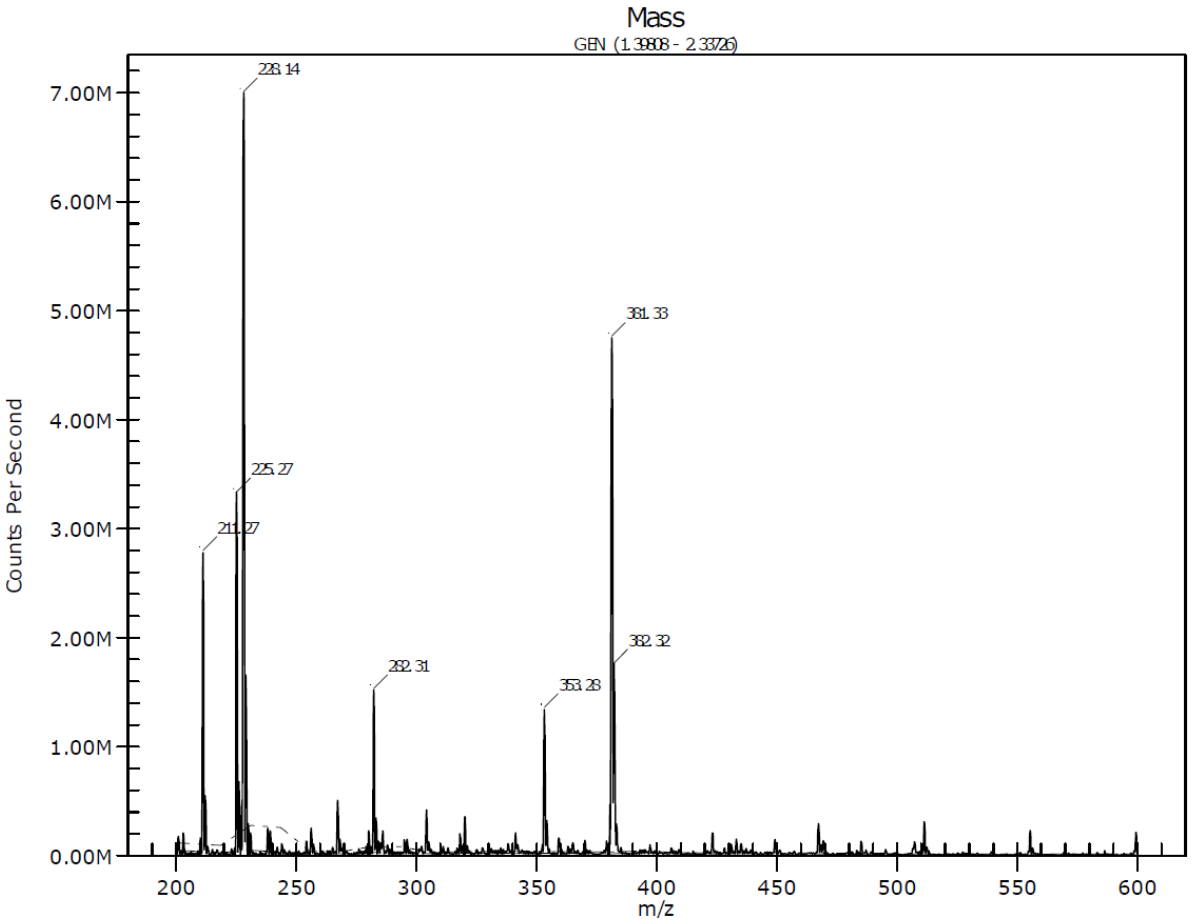

Figure 79. ESI-MS spectrum of α-mannopyranosyl azide **2**.

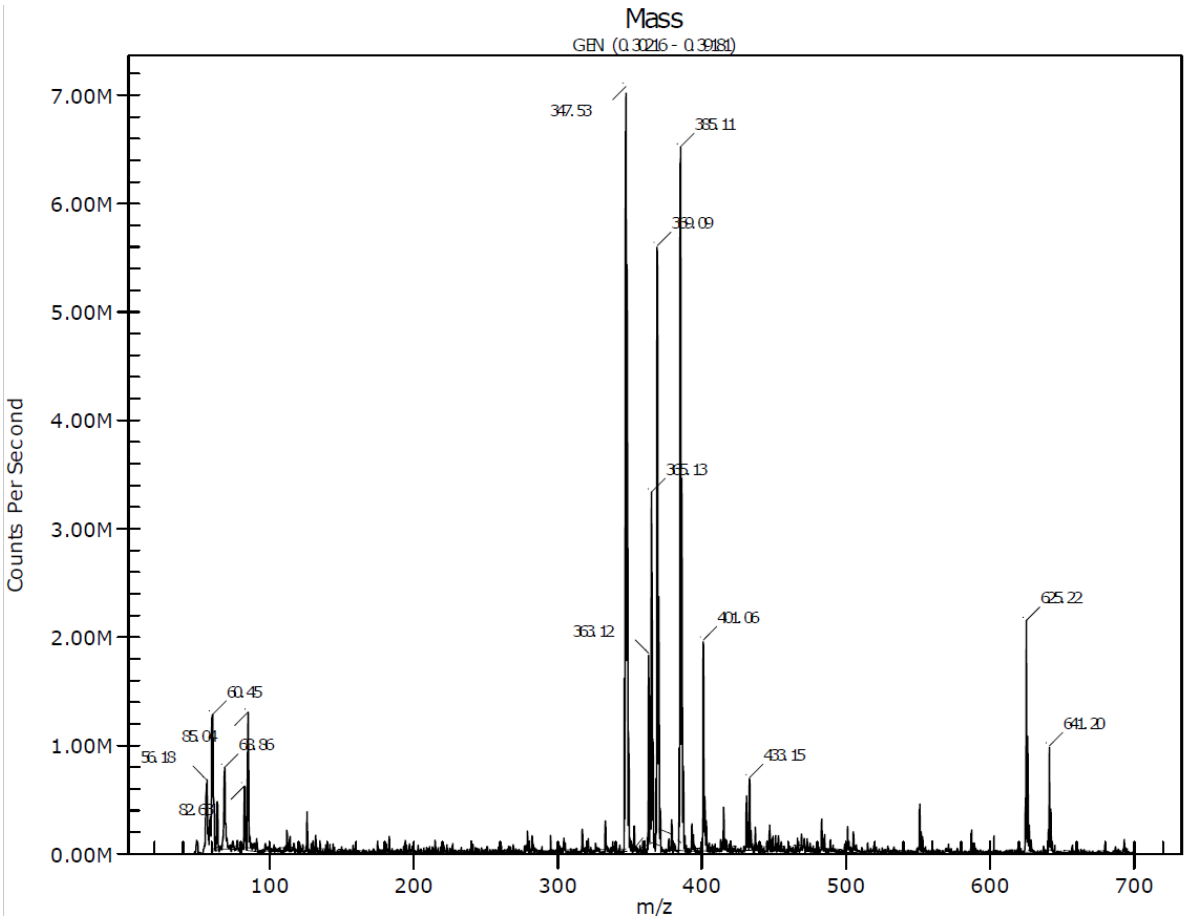

Figure 80. ESI-MS spectrum of 2-(diphenylphosphonyl)phenyl methacrylate **4**.

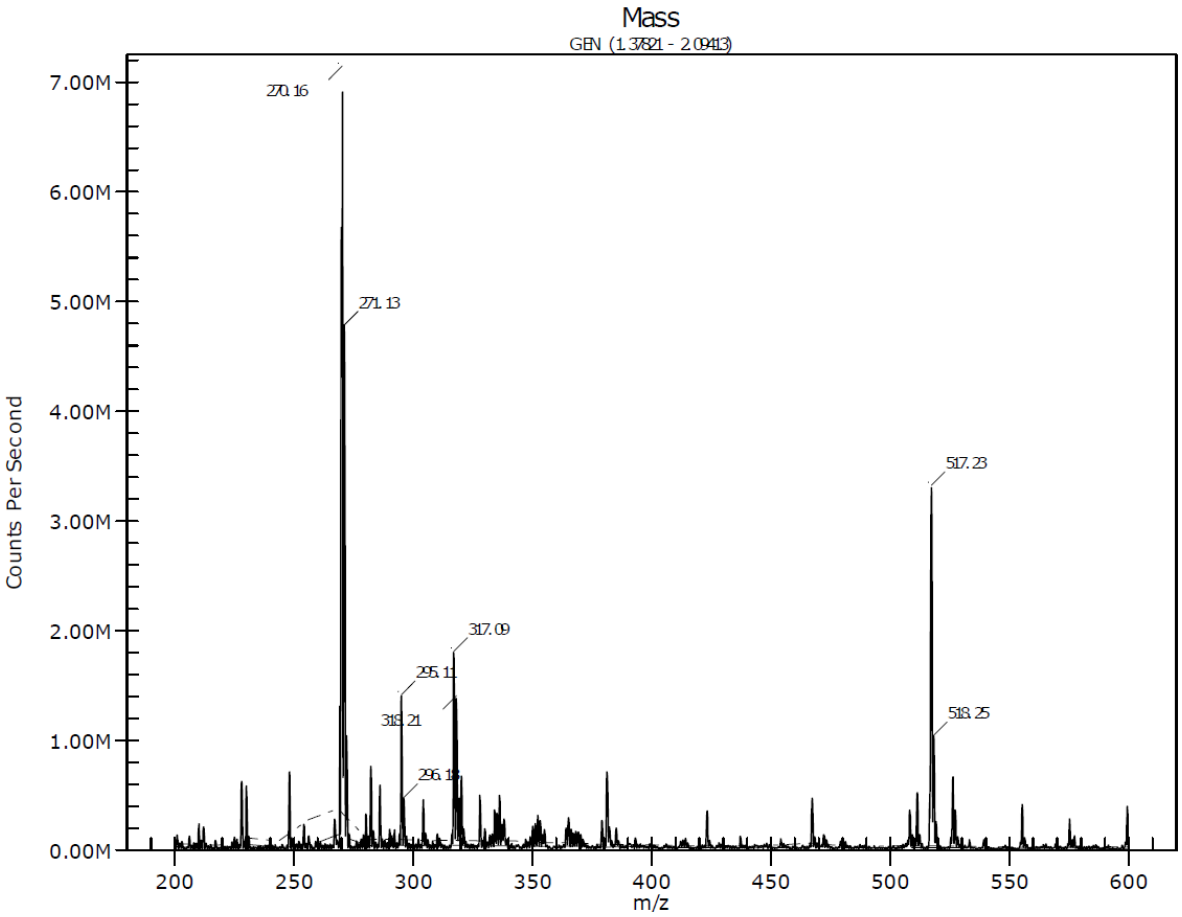

Figure 81. ESI-MS spectrum of α-mannopyranosyl methacrylamide **5**.

16.3.3 HPLC elugrams

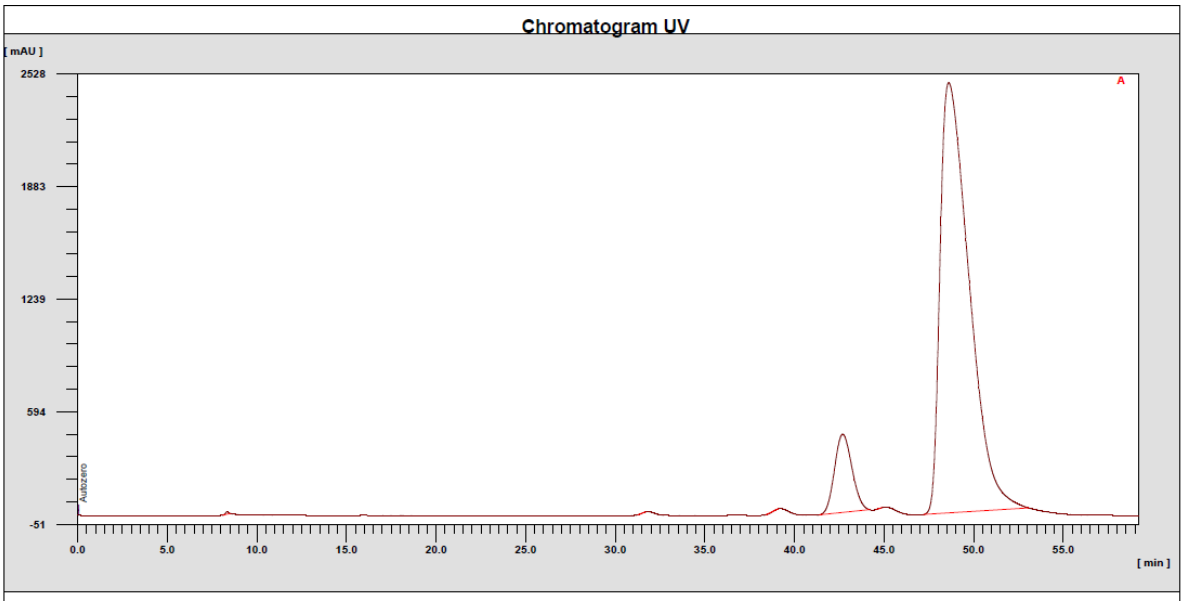

Figure 82. HPLC elugram of reaction entry 1.

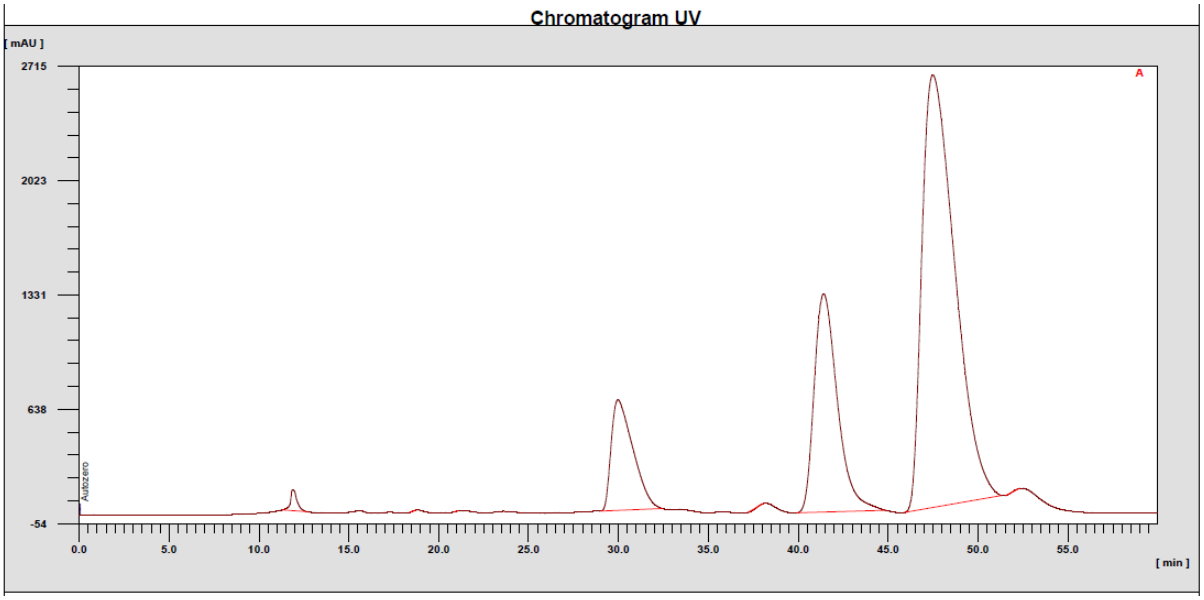

Figure 83. HPLC elugram of reaction entry 2.

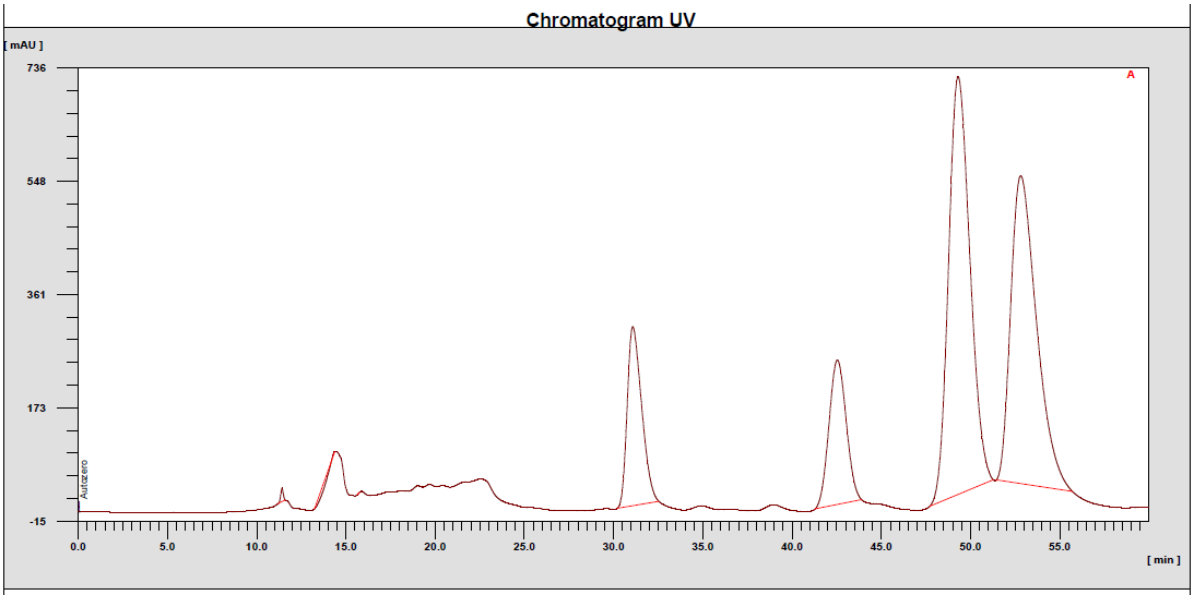

Figure 84. HPLC elugram of reaction entry 3.

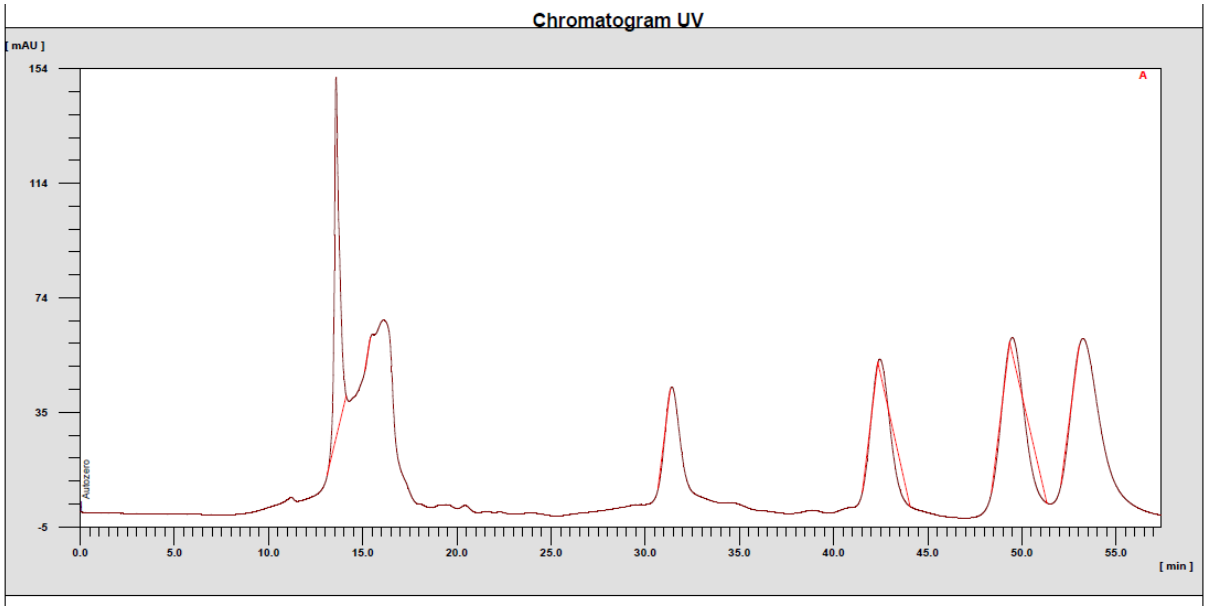

Figure 85. HPLC elugram of reaction entry 4.

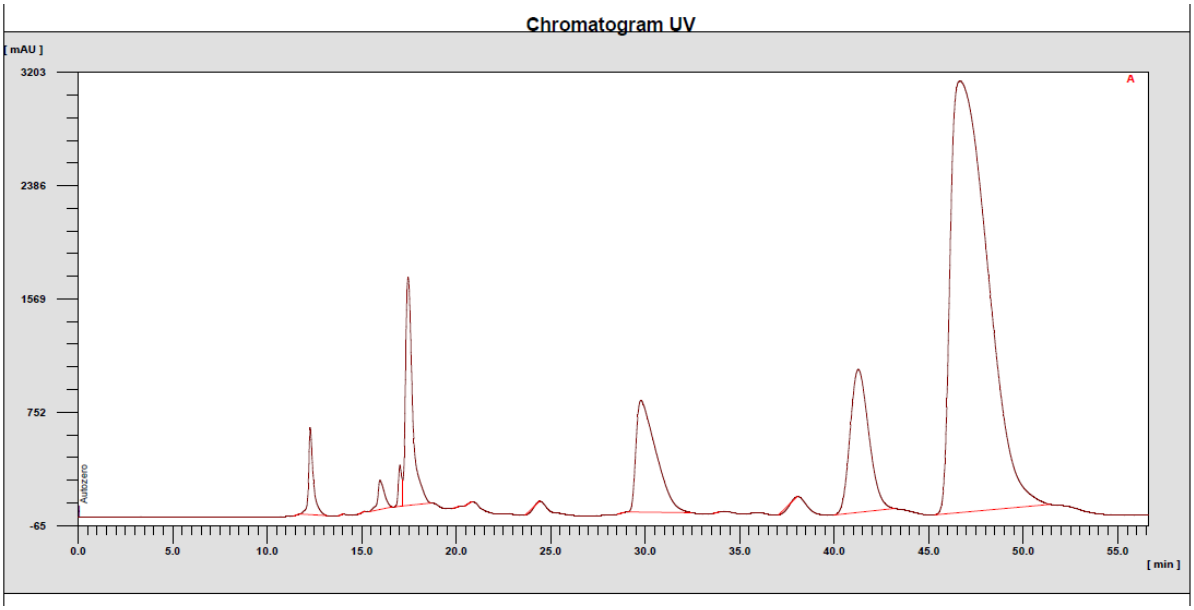

Figure 86. HPLC elugram of reaction entry 5.

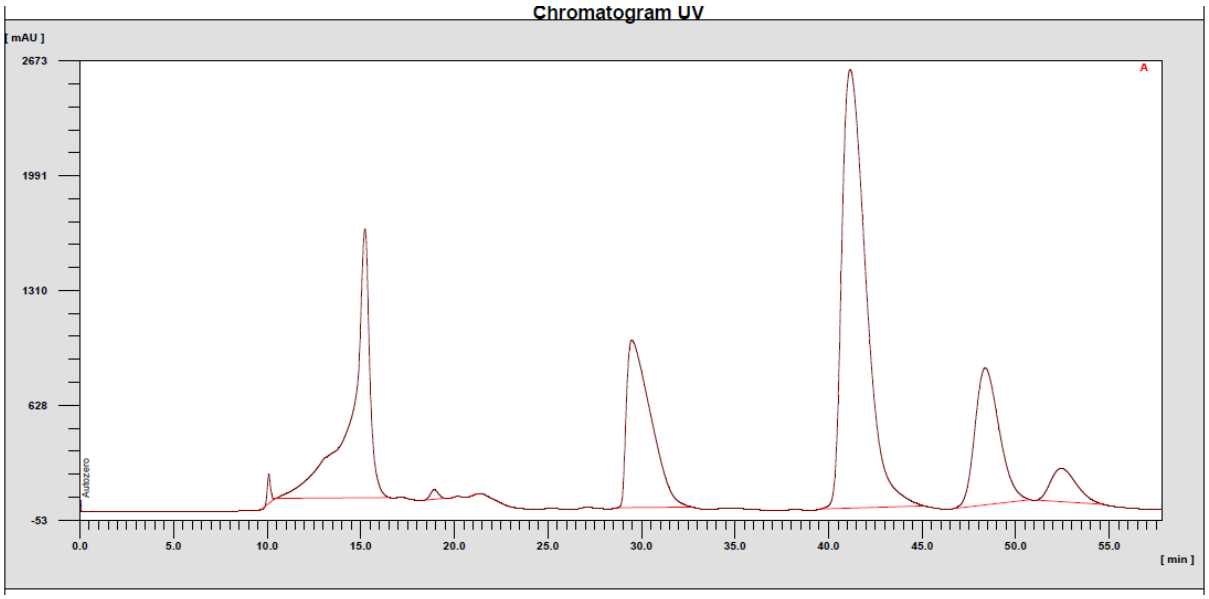

Figure 87. HPLC elugram of reaction entry 6.

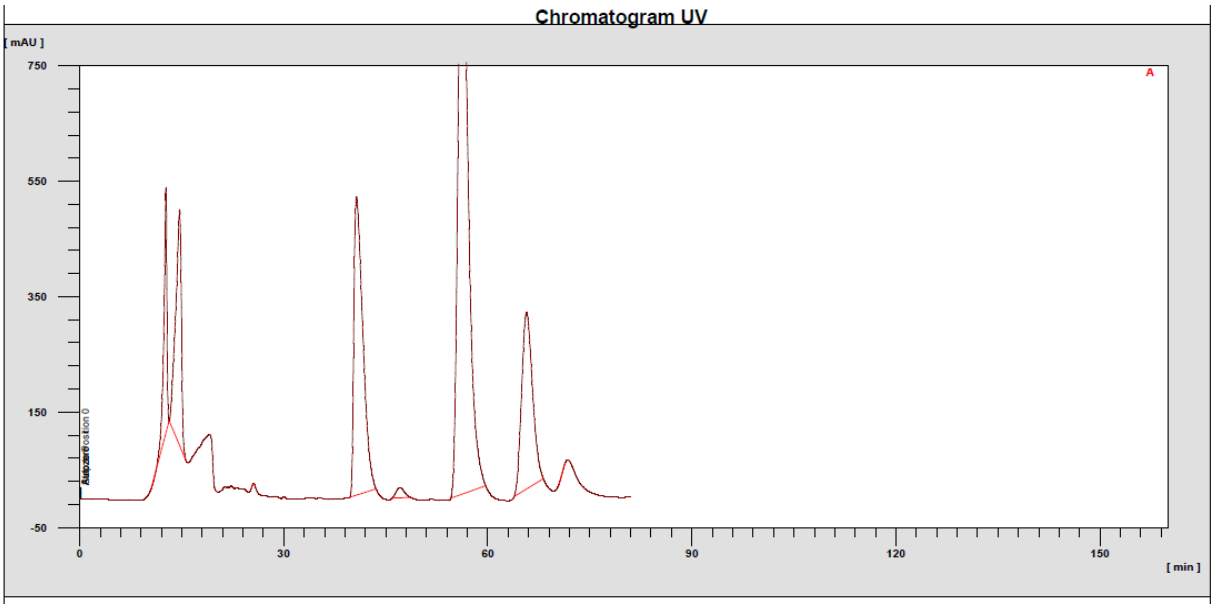

Figure 88. HPLC elugram of reaction entry 7.

16.4 Supporting Information of Chapter 10: Microwave-assisted synthesis of 5'-*O*-methacryloylcytidine using the immobilized lipase Novozym 435

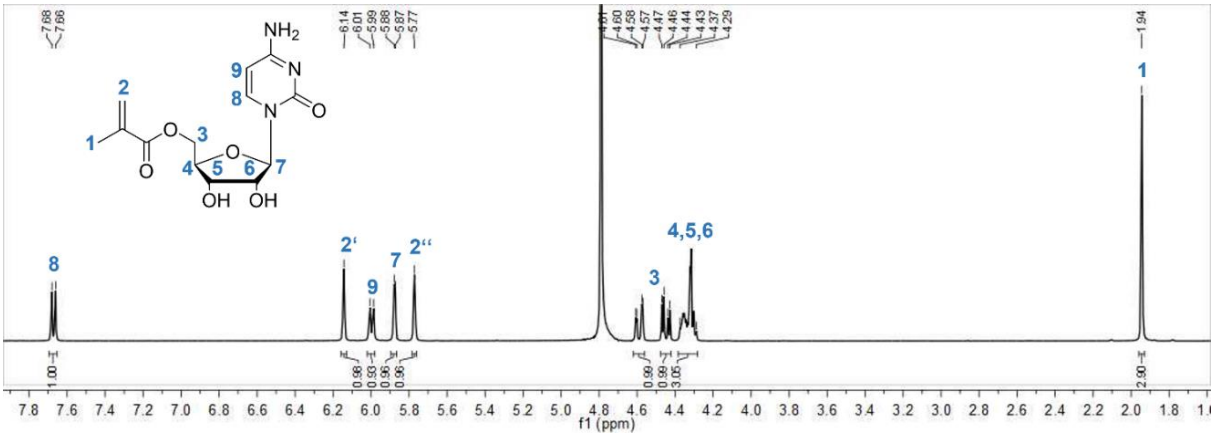

Figure 89. ^{1}H NMR of 5'-*O*-methacryloylcytidine.

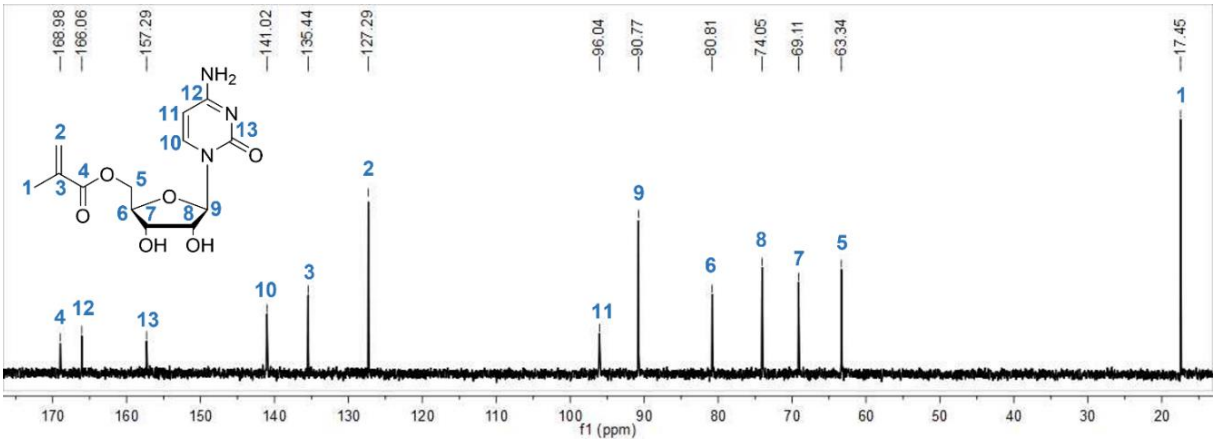

Figure 90. ^{13}C NMR of 5'-*O*-methacryloylcytidine.

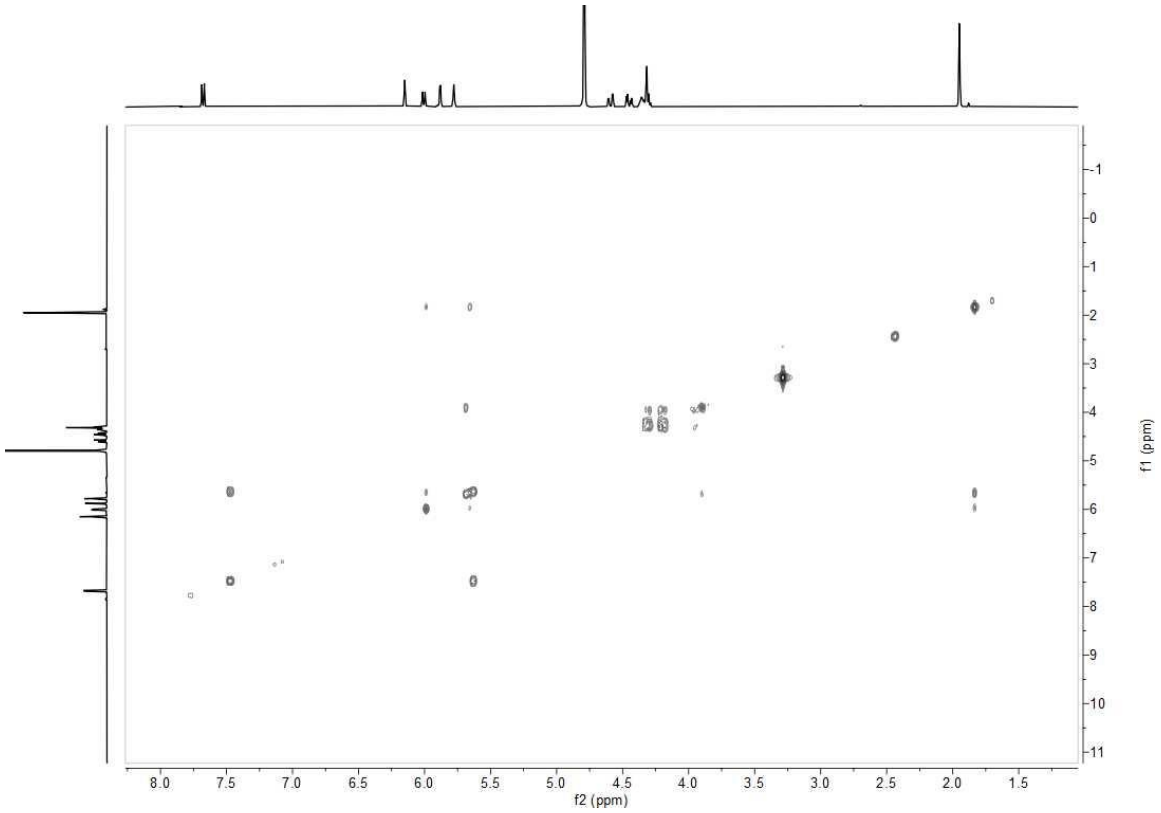

Figure 91. 2D COSY NMR of 5'-*O*-methacryloylcytidine.

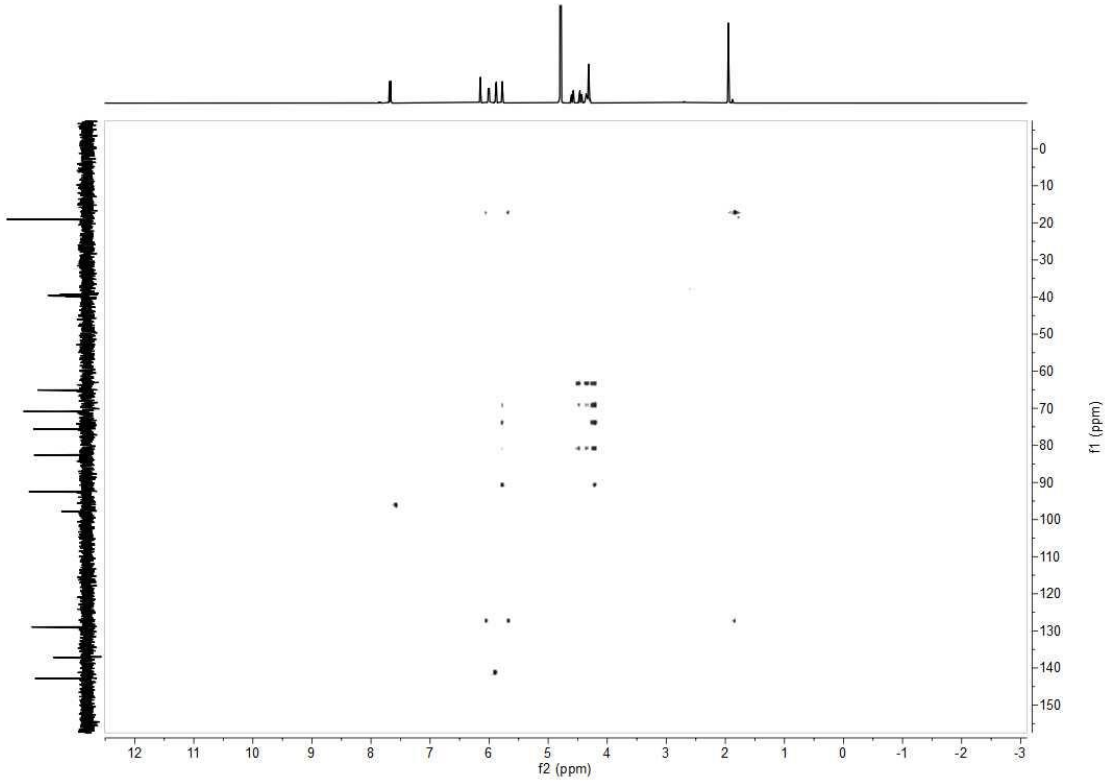

Figure 92. 2D HSQC NMR of 5'-*O*-methacryloylcytidine.

Table 15. Effect of the substrate choice. Reaction conditions: 12.7 wt% Novozym 435, 95 °C, 1:35 cytidine to substrate molar ratio.

Substrate	Time (min)	Yield (%)
Methyl methacrylate	30	9,4
	60	14,1
	120	7,2
Vinyl methacrylate	30	36,2
	60	13,1
	120	7,5

Table 16. Effect of enzyme concentration with 1:35 molar ratio vinyl methacrylate.

Concentration of lipase (wt%)	Time (min)	Temperature (°C)	Yield (%)
5.5	30	95	7.2
		60	2.8
		45	2.4
	60	95	7.8
	120	95	4.2
12.7	30	95	36.2
		60	28.4
		45	11.4
	60	95	13.1
	120	95	7.5
22.5	30	95	21.2
	60	95	11.0
	120	95	9.9

Table 17. Effect of reaction temperature with a vinyl methacrylate molar ratio of 1:35.

Temperature (°C)	Concentration of lipase (wt%)	Time (min)	Yield (%)
45	5.5	30	2.4
	12.7	30	11.4
		60	6.6
		120	9.8
60	5.5	30	2.8
	12.7	30	28.4
		60	19.4
		120	9.1
95	5.5	30	7.2
	12.7	30	36.2
		60	13.1
		120	7.5
120	12.7	30	9.5
		60	4.1
		120	3.6

Table 18. Effect of reaction time with a 1:35 molar ratio of vinyl methacrylate.

Time (min)	Concentration of lipase (wt%)	Reaction temperature (°C)	Yield (%)
10	12.7	95	11.6
20	12.7	95	19.9
30	5.5	95	7.2
	12.7	45	11.4
		60	28.4
		95	36.2
		120	9.5
	22.5	95	21.2
45	12.7	95	17.2
60	5.5	95	7.8
	12.7	45	6.6
		60	19.4
		95	13.1
		120	4.1
	22.5	95	9.9
120	5.5	95	4.2
	12.7	45	9.8
		60	9.1
		95	7.5
		120	3.6
	22.5	95	7.5
300	12.7	95	6.4

Table 19. Effect of molar ratio at a reaction temperature of 95 °C.

Substrate molar ratio	Enzyme concentration (wt%)	Time (min)	Yield (%)
1:35	12.7	30	36.2
		60	13.1
		120	7.5
		300	6.4
1:76	12.7	30	7.8
		60	15
		120	12.6
	22.5	120	17.3
		300	4.8

16.5 Supporting Information of Chapter 11: Synthesis and self-assembly of cytidine- and guanosine-based copolymers

Calculation methods

Monomer conversion was calculated following eq. 2 from the crude reaction mixture. $\int_{H(polymer)}$ equals the integration of the polymer backbone peak, $\int_{H(monomer)}$ the peak integration of the vinyl proton of the monomer.

$$conversion = \frac{\int_{H(polymer)}}{\int_{H(monomer)} + \int_{H(polymer)}} \times 100\ \% \quad (2)$$

The calculation of the theoretical molecular weight ($M_{n,\ theory,\ NMR}$) is based on the conversion using eq. 3:

$$\boldsymbol{M_{n,theory,NMR}} = \left(\frac{\boldsymbol{c_{monomer}}}{\boldsymbol{c_{CTA}}} \times \boldsymbol{conversion} \times \boldsymbol{M_{monomer}}\right) + \boldsymbol{M_{CTA}} \quad (3)$$

where $c_{monomer}$ and c_{CTA} are the initial concentrations of monomer and CTA. $M_{monomer}$ and M_{CTA} indicate the molecular masses of monomer and CTA. “Livingness” was determined with following eq. 4:

$$L = \frac{c_{CTA}}{c_{CTA} + 2 f c_I (1 - e^{-k_d t})(1 - \frac{f_c}{2})} \times 100 \quad (4)$$

where c_{CTA} and c_I are the initial concentrations of CTA and initiator. The expression "2" refers to the formation of two primary radicals with a certain efficiency f from one initiator molecule. The expression "2" refers to the formation of two primary radicals from one initiator molecule with a certain efficiency f, which is typically 0.5 for diazo-initiators. The resulting chain number at radical termination is given as "1-f_c/2", where f_c is the coupling factor. k_d describes the decomposition coefficient of the initiator, while t is the reaction time.

$M_{n,UV\text{-}Vis}$ was determined using a Specord 210 spectrophotometer. by using Beer-Lambert eq. 5:

$$A = \frac{\varepsilon d c_{mass}}{M_{n,UV-Vis}} \quad (5)$$

where A is the absorption, ε the extinction coefficient, d the optical path length and c_{mass} the concentration. $\frac{\varepsilon d}{M_{n,UV-Vis}}$ represents the slope, which results in the calculation of $M_{n,\,UV\text{-}Vis}$ with the following eq. 6:

$$M_{n,UV-Vis} = \frac{\varepsilon \times d}{slope} \quad (6)$$

The average hydrodynamic radius and therefore the diameter of the formed aggregates were derived from the Stokes-Einstein eq. 1:

$$r = k_B T / 6\pi\eta D \quad (1)$$

where k_B is the Boltzmann's constant, T the absolute temperature, η the dynamic viscosity and D the diffusion coefficient.

Table 20. Analytical data of pHPMA **10**.

Monomer	Conversion	Polymer	$M_{n,\,theory,\,NMR}$	$M_{n,\,NMR}$	$M_{n,\,UV\text{-}Vis}$	$M_{n,\,SEC}$[a]	PDI
10	75 %	**9**	7.8 kDa	38.7 kDa (DP: 267)	38.2 kDa (DP: 263)	9.1 kDa	1.66

[a]DMF, PMMA standard.

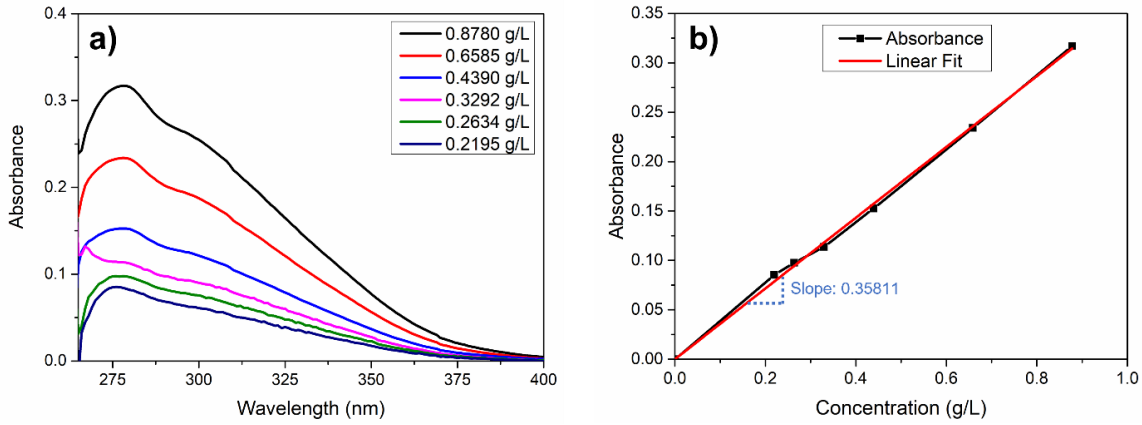

Figure 93. a) UV-Vis spectrum of pHPMA **10** at different concentrations and b) linear fit of absorbance maximum to concentration.

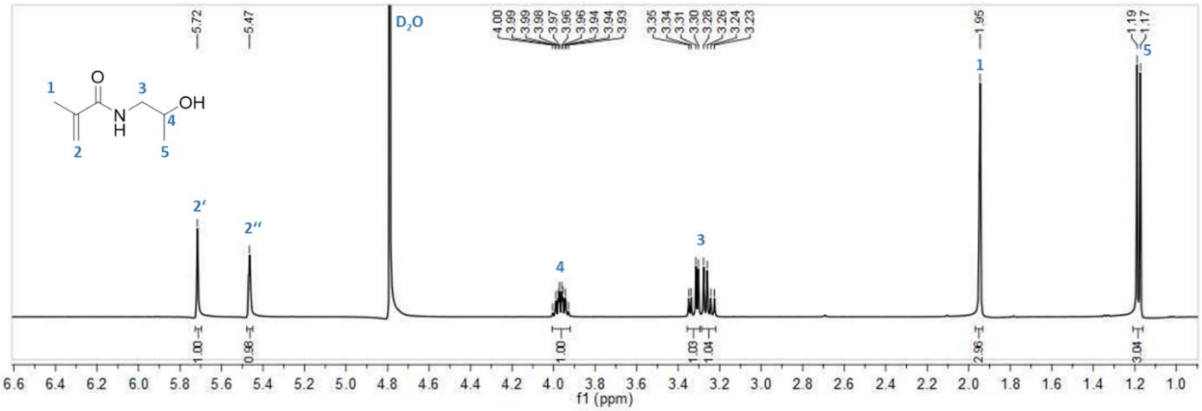

Figure 94. ^{1}H NMR spectrum of HPMA **10** in D_2O.

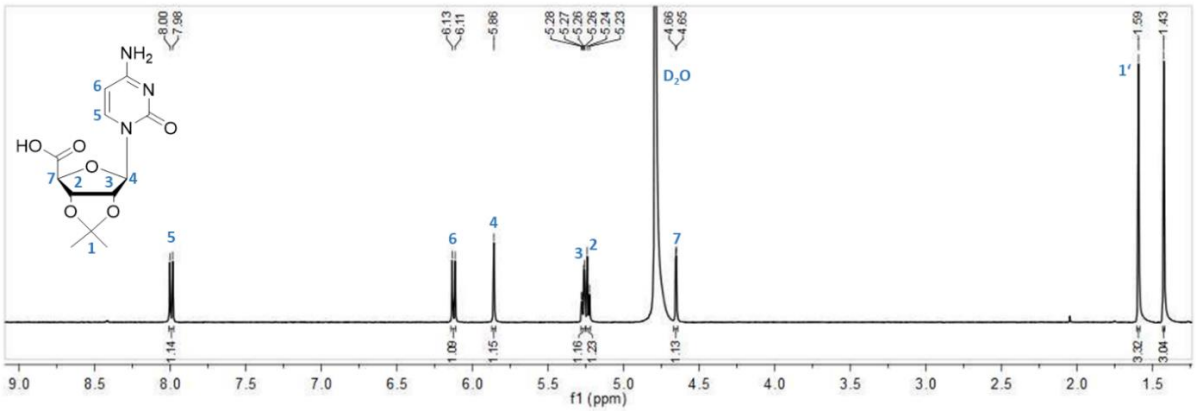

Figure 95. ^{1}H NMR spectrum of iC-COOH **3** in D_2O.

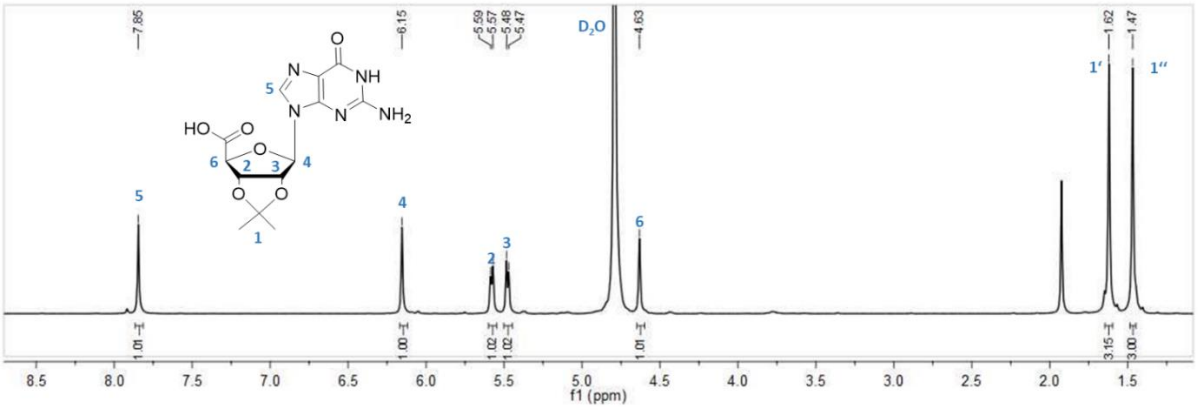

Figure 96. ^{1}H NMR spectrum of iG-COOH **4** in D_2O.

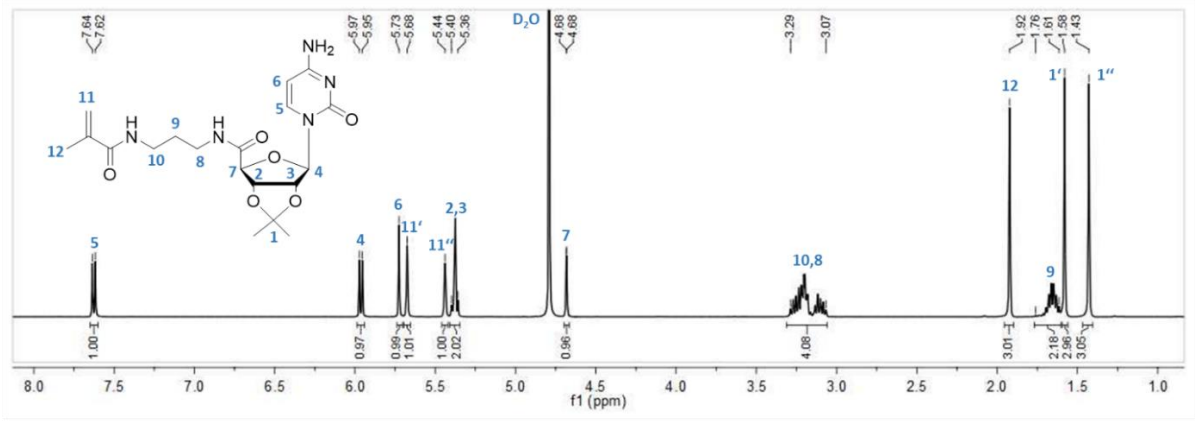

Figure 97. ^{1}H NMR spectrum of monomer iCPMA **1** in D_2O.

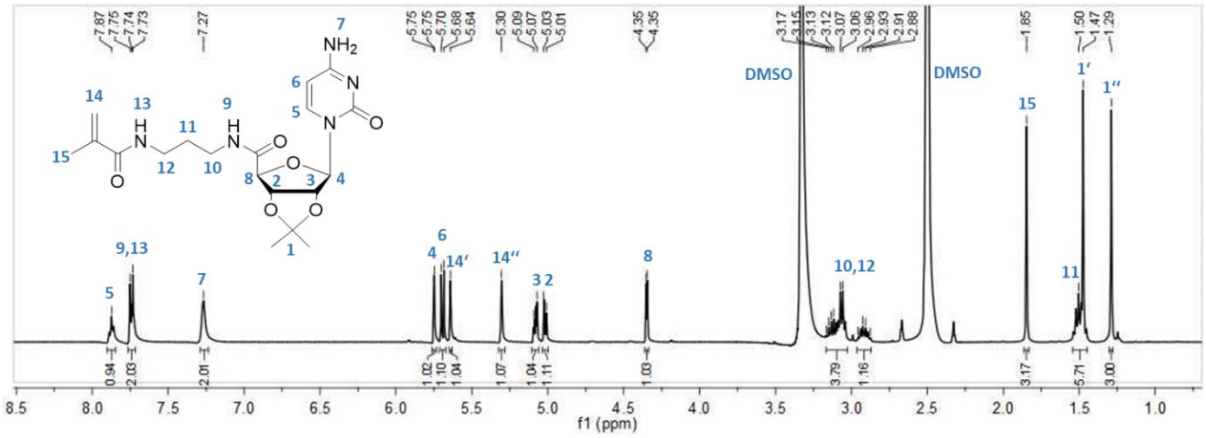

Figure 98. ^{1}H NMR spectrum of monomer iCPMA **1** in DMSO-d_6.

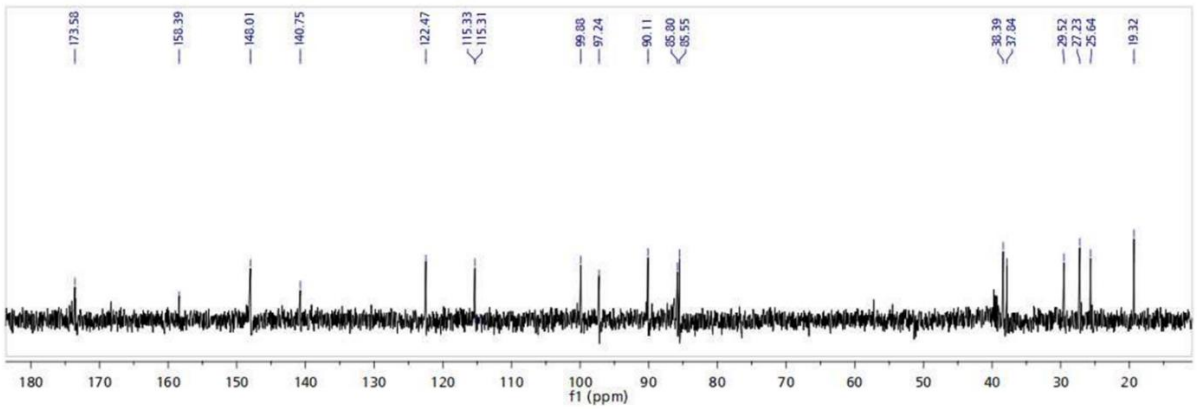

Figure 99. ^{13}C NMR spectrum of monomer iCPMA **1** in D_2O + DMSO-d_6.

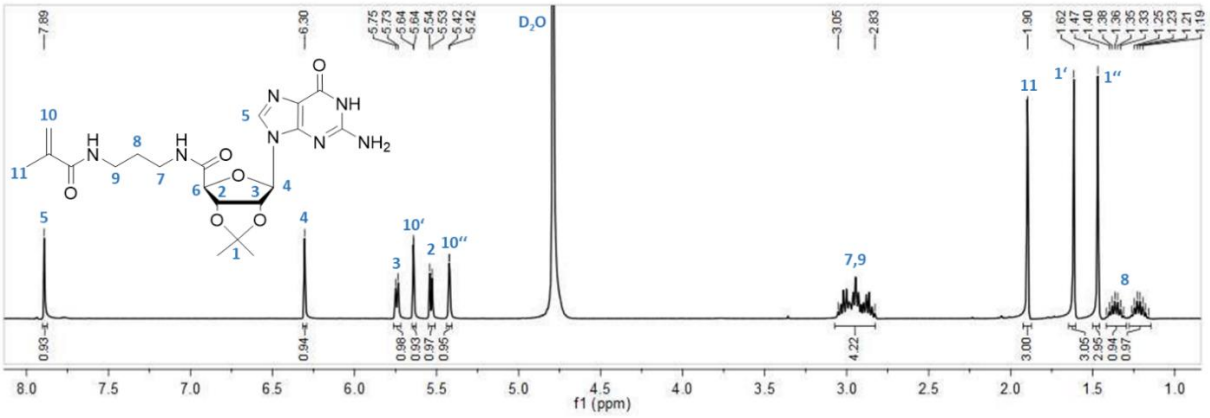

Figure 100. ^{1}H NMR spectrum of monomer iGPMA **2** in D_2O.

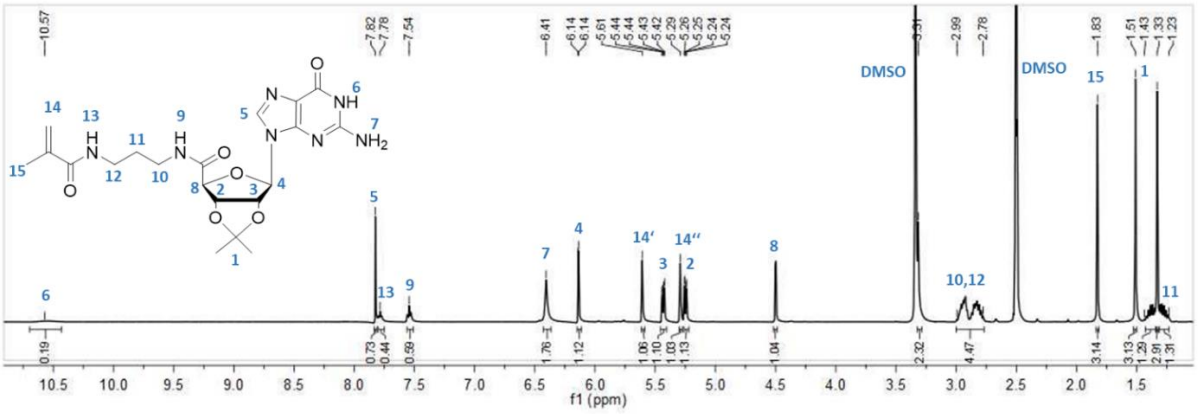

Figure 101. ^{1}H NMR spectrum of monomer iGPMA **2** in DMSO-d_6.

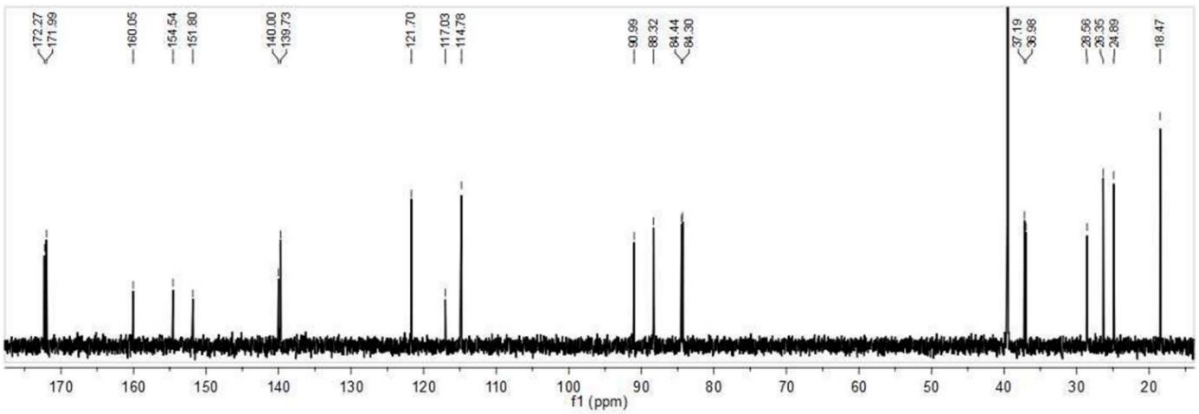

Figure 102. ^{13}C NMR spectrum of monomer iGPMA **2** in D_2O + DMSO-d_6.

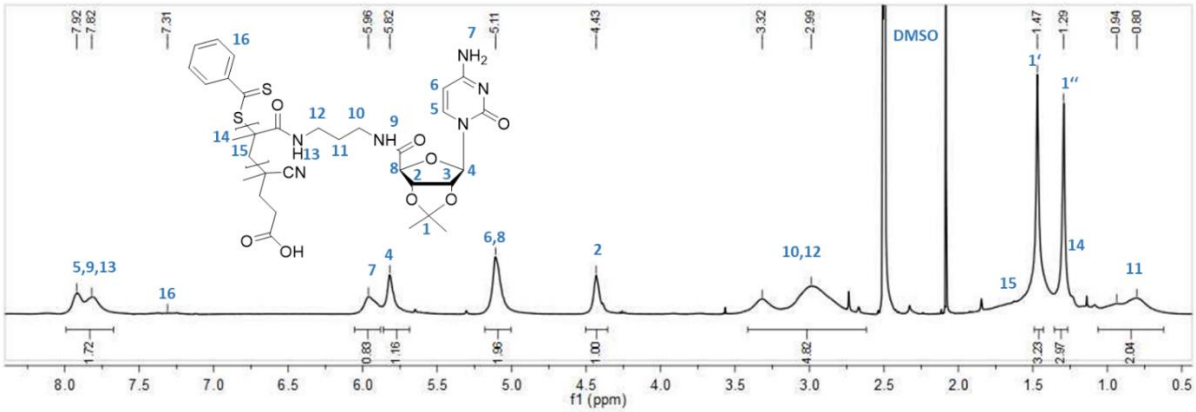

Figure 103. ^{1}H NMR spectrum of homopolymer piCPMA **5** in DMSO-d_6.

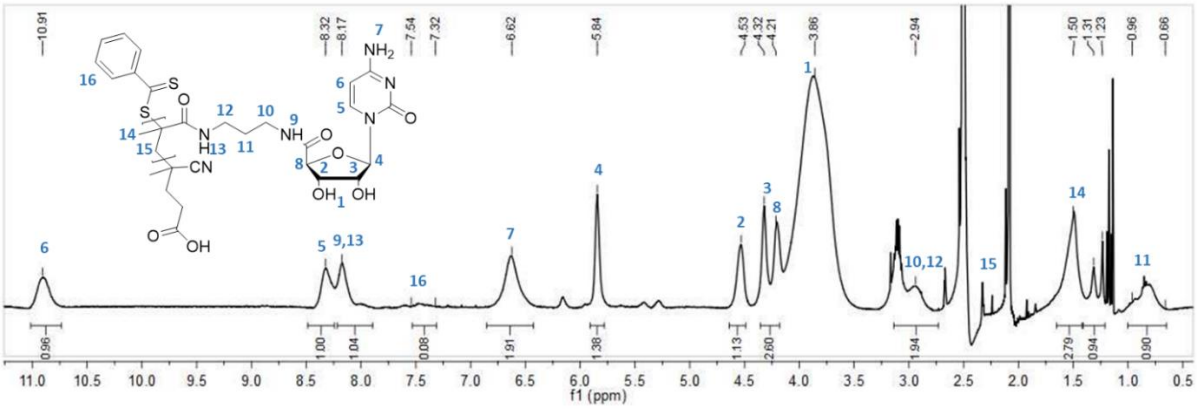

Figure 104. ^{1}H NMR spectrum of deprotected homopolymer pCPMA **7** in DMSO-d_6.

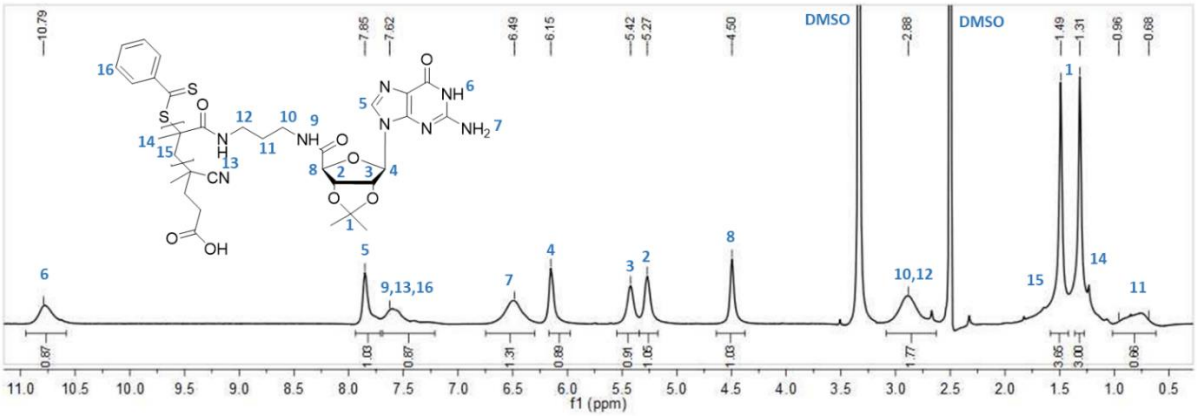

Figure 105. ^{1}H NMR spectrum of homopolymer piGPMA **6** in DMSO-d_6.

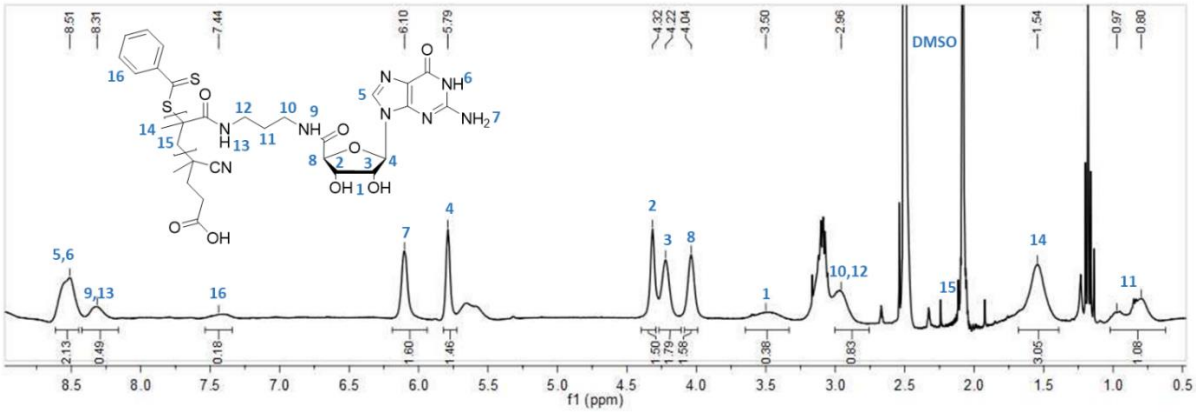

Figure 106. ^{1}H NMR spectrum of deprotected homopolymer pGPMA **8** in DMSO-d_6.

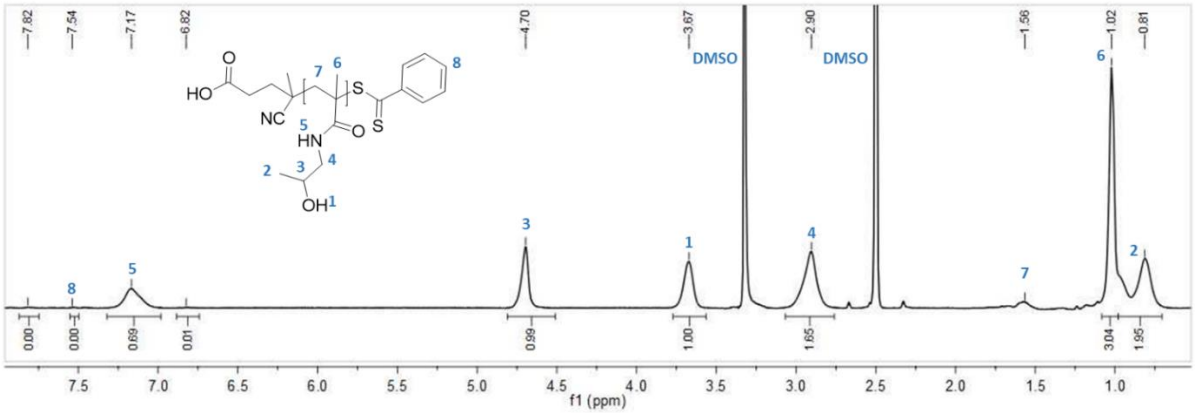

Figure 107. ^{1}H NMR spectrum of pHPMA **9** in DMSO-d_6.

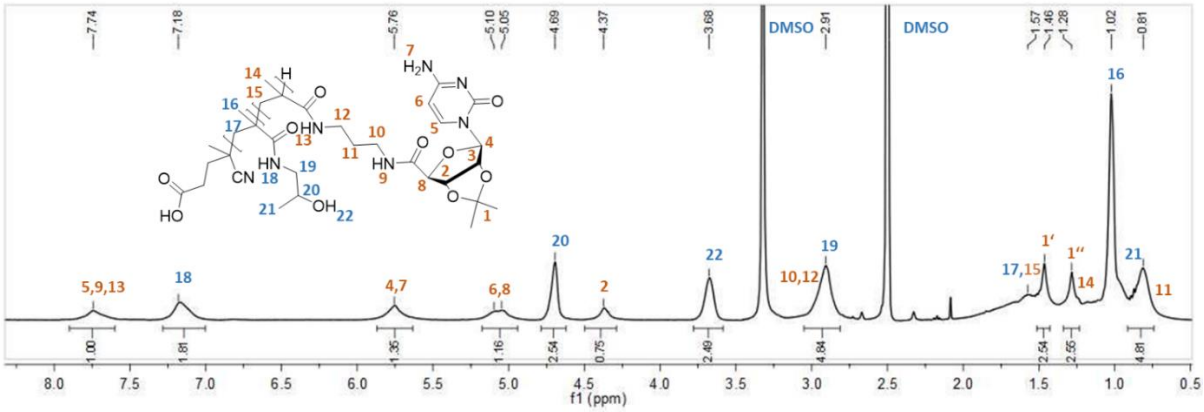

Figure 108. ^{1}H NMR spectrum of blockcopolymer pHPMA-b-piCPMA **11** in DMSO-d_6.

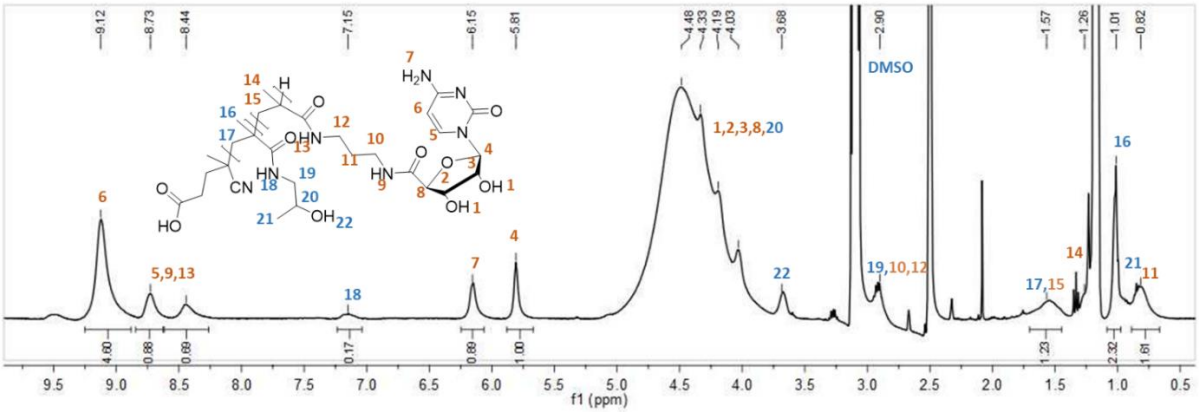

Figure 109. ^{1}H NMR spectrum of deprotected pHPMA-*b*-CPMA **13** in DMSO-d$_6$.

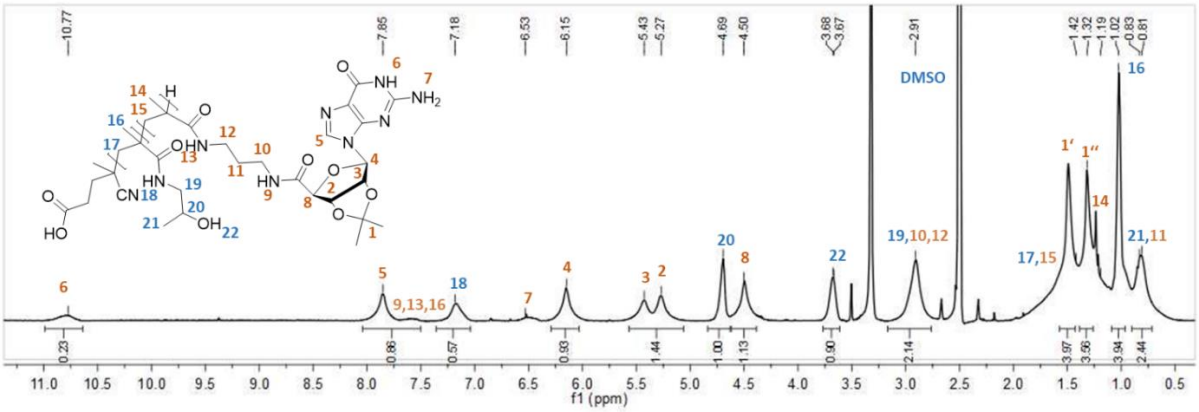

Figure 110. ^{1}H NMR of blockcopolymer pHPMA-*b*-piGPMA **12** in DMSO-d$_6$.

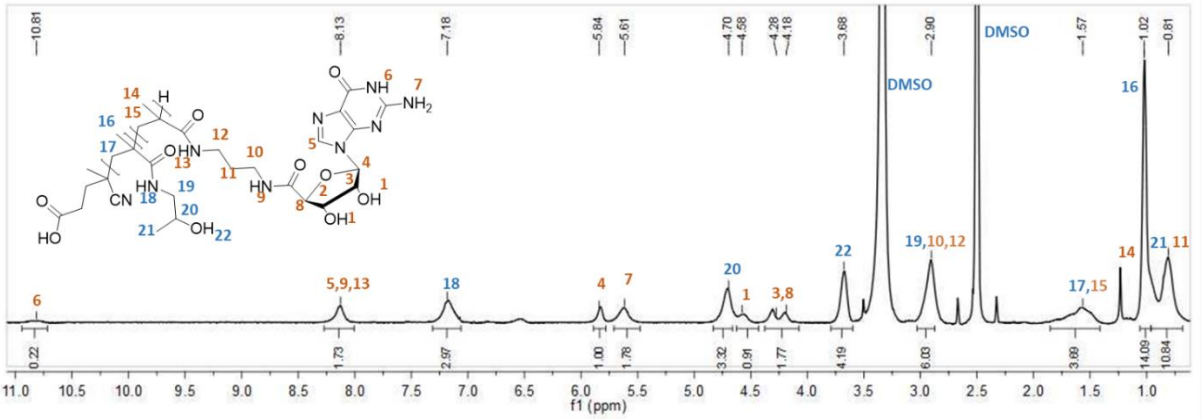

Figure 111. ^{1}H NMR spectrum of depreotected pHPMA-*b*-pGPMA **14** in DMSO-d$_6$.

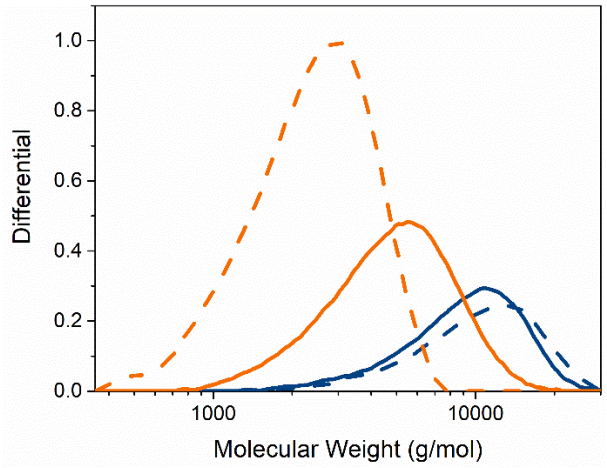

Figure 112. SEC analysis of piCPMA **5** (orange) and piGPMA **6** (blue) synthesized in DMF/H_2O (straight) or 1,4-dioxane/H_2O (dashed), respectively.

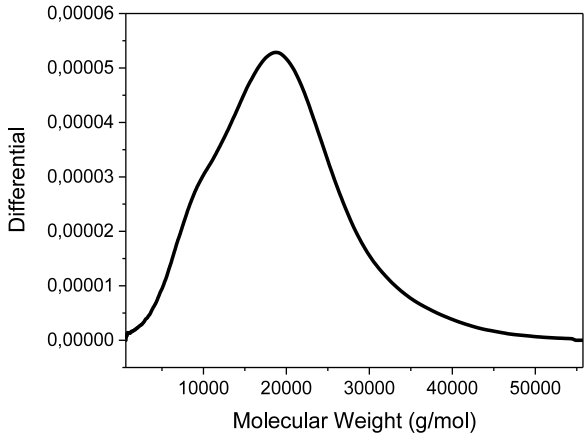

Figure 113. SEC analysis of pHPMA **9**.

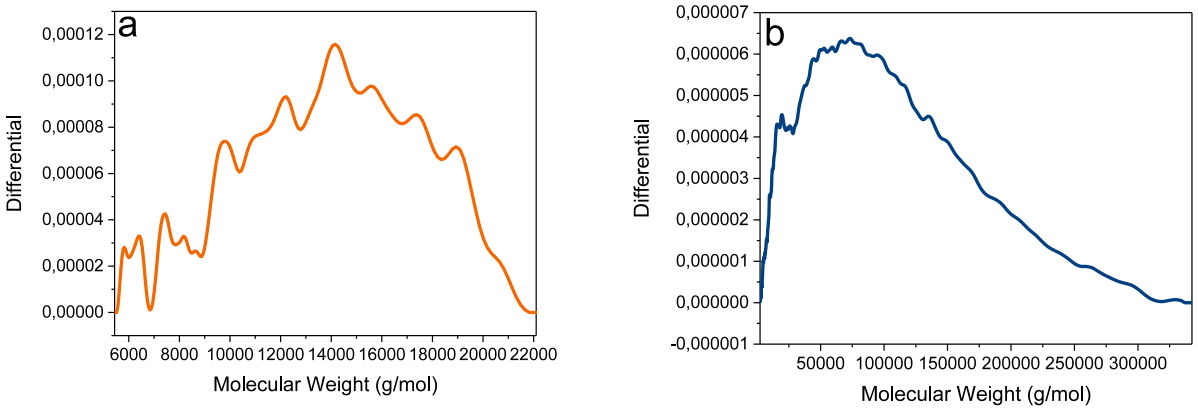

Figure 114. SEC analysis of a) pHPMA-*b*-piCPMA **11** and b) pHPMA-*b*-piGPMA **12**.

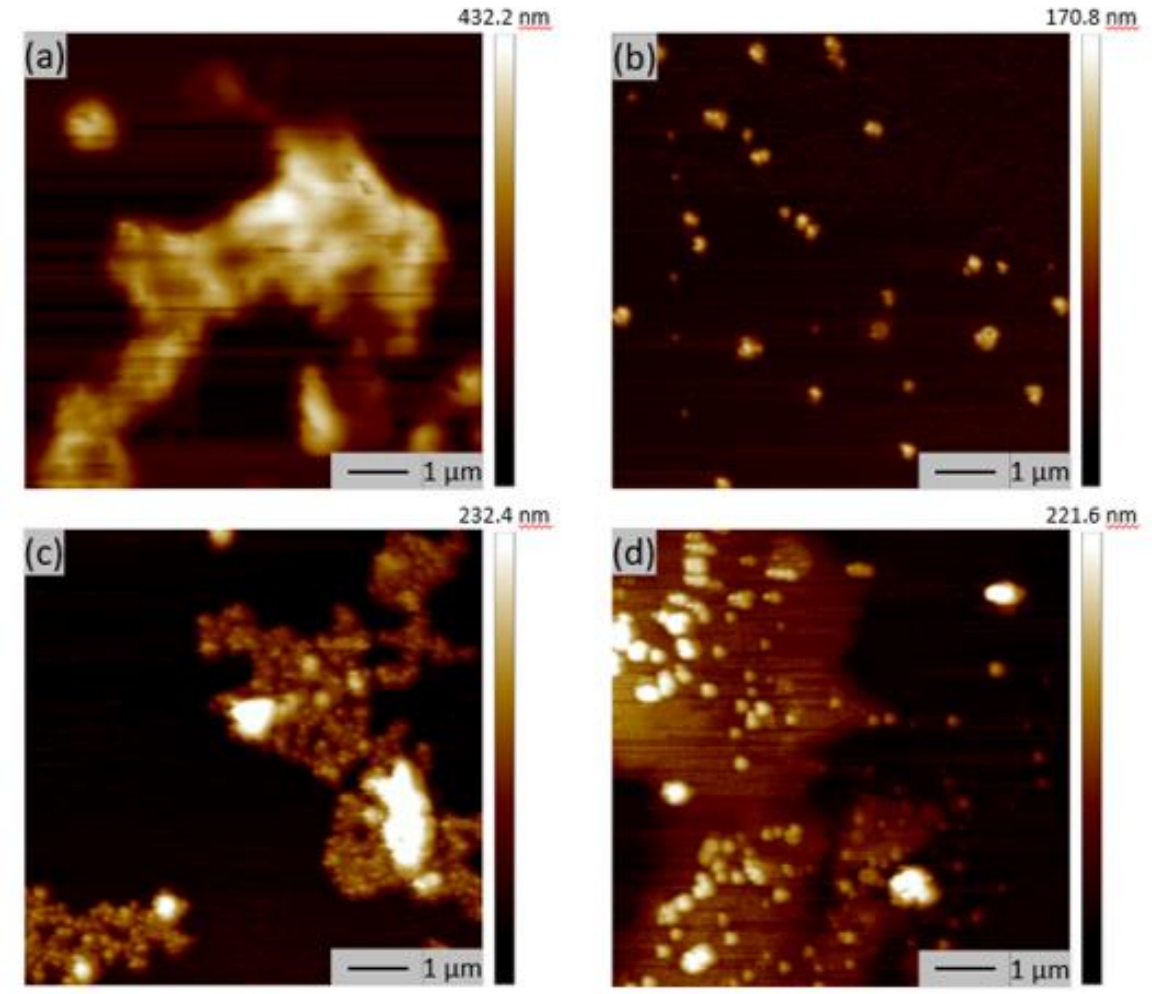

Figure 115. AFM images of (a) pHPMA-*b*-pCPMA **13**, (b) pHPMA-*b*-pGPMA **14**, (c) mixture of **13** and **14** before heating and (d) mixture of **13** and **14** after heating.